The *Fat* Gene Cooperates With the Hippo Pathway to Prevent Neuronal Degeneration

Thesis

UNRESTRICTED

Simona Occhi

The *fat* gene cooperates with the Hippo pathway to prevent neuronal degeneration

PhD in Molecular and Cellular Biology

June 2010

DATE OF SUBMISSION: 5 MAY 2010
DATE OF AWARD: 30 JUN 2010

DIBIT, Department of Biological and Technological Research. Milan, Italy

DECLARATION

This thesis has been submitted in partial fulfillment of the requirements of the Open University for the Degree of Doctor of Philosophy in Molecular and Cellular Biology.

This thesis has been written by myself and has not been used in any previous application for a degree. All the results presented here were obtained by myself. Exclusively EM sections and pictures were prepaired and observed in Marseille, at IBDML, Campus de Luminy Case, in collaboration with Dr. Bernard Chaurrox.

Part of the work contained in this thesis is under review at *Embo Journal*:

Simona Occhi*, Francesco Napoletano*, Piera Calamita, Vera Volpi, Eric Blanc, Bernard Charroux, Julien Royet and Manolis Fanto.

Polyglutamine Atrophin provokes neurodegeneration by repressing *fat.*

*These authors contributed equally

LIST OF CONTENTS

LIST OF ABBREVIATIONS

App= Approximated

Atg= Autophagy related genes

D= Dachs

Dally= Division abnormally delayed

Diap1= *Drosophila* inhibitor of apoptosis

Dpp= Decapentaplegic

DRPLA= Dentatorubral-pallidoluysian Atrophy

Ex= Expanded

Ey= Eyeless

Eya= Eyes-absent

Flp= Flippase

Fmi= Flamingo

FRT= Flp recombinase target

Ft= Fat

Fz= Frizzled

GMR= *glass* multiple reporter

GOF= Gain of Function

HD= Huntington Disease

Hh= Hedgehog

Hpo= Hippo

Hth= Homothorax

IOC= Interommatidial cell

LOF= Loss of Function

Lst= Lats

MARCM= Mosaic analysis with a repressible cell marker

Mer= Merlin

Mst= Mats

MTA= Metastatis-Associated Proteins

NDR= Nuclear Dbf2 related

NES= Nuclear Export Signal

NF2= Neurofibromin 2

NLS= Nuclear Localization Signal

ORF= Open Reading Frame

PAS= Phagophore-assembly site

PCP= Planar Cell Polarity

PE= Phosphatidyl Ethanolamine

PFC= Posterior follicle cell

PI3K= Phospho-Inositide-3-Kinase

PKD= Polycystic kidney disease

PolyQ= Polyglutamine

RT= Room Temperature

Sav= Salvador

SARAH= Sav-RASSF-Hpo

SBMA= Spinobulbar Muscular Atrophy

SCA= Spinocerebellar Ataxia

Sd= Scalloped

So= Sine oculis

Tll= Tailless

Tsh= Teashirt

Vg= Vestigial

Wnt= Wingless

Wts= Warts

YAP= Yes Associated Protein

Yki= Yorkie

UAS= Upstream Activating Sequence

LIST OF FIGURES

Chapter 1

Chapter 3

Chapter 4

Chapter 5

Chapter 6

Chapter 7

ABSTRACT

Fat is a cadherin that regulates planar polarity and acts as a tumor suppressor both in vertebrates and invertebrates. *Drosophila fat* recessive mutations have been shown to induce an excessive cell proliferation and a hyperplastic tissue overgrowth during larval development.

Fat has recently been described to be part of a signaling cascade, the Hippo tumor suppressor pathway, which regulates organ size and cell proliferation to prevent tumorigenesis.

A further known interactor of Fat is the transcriptional co-factor Atrophin. This connection is highly relevant to neuronal homeostasis, because expansion of polyglutamine tracts in human Atrophins lead to a neurodegenerative disorder, the Dentatorubral-pallidoluysian Atrophy (DRPLA). Microarrays analysis in *Drosophila* models for DRPLA disorder has shown that *fat* transcription is downregulated by wt and polyQ mutant Atrophins.

We thus tested the hypothesis that *Drosophila* Fat is involved in neuronal homeostasis and cell survival. The phenotypic analysis of the *Drosophila* nervous system in *fat* mutant fly eyes showed that *fat*, when mutated, leads to a progressive neurodegenerative phenotype. Interestingly the Hippo Pathway is involved in retinal degeneration and it is partially required for the *fat* induced phenotype.

My morphologic and genetic studies suggest a deregulation of the autophagic signaling in mutants of both Fat and the Hippo pathway as the cell mechanism leading to cell degeneration.

In conclusion my data indicate that Fat cooperates with the Hippo Pathway to maintain cellular homeostasis and protect neuronal cells from degeneration.

Chapter 1

INTRODUCTION

Homeostatic processes in biology are necessary to guarantee the maintenance of tissue architecture and functionality and consequently organism survival. Pathologic situations, like cancer and ageing, arise from the loss of the correct balance between intrinsic signals that normally regulate cellular differentiation, proliferation and protein turnover. The inbalance of the processes destined to preserve cellular homeostasis leads to nutrient deprivation, excessive cellular stress and tissue damage that, at a certain point, cannot be compensated and cause death at the cell and organismal level.

Here I describe how the Fat (Ft) cadherin and its associated pathways regulate neuronal homeostasis in the *Drosophila* eye.

1.1 FT IS AN ATYPICAL CADHERIN

Cadherins are transmembrane glycoproteins and represent one of the major families of adhesion molecules fundamental for the organization of cells into tissues and responsible for the achievement of multicellular architecture (Gallin et al, 1983; Yoshida & Takeichi, 1982). Their expression appears to be tightly regulated during development and each tissue or cell type shows a characteristic pattern of cadherin molecules (Yagi & Takeichi, 2000). They are important in both simple and complex organisms, not only for their mechanical contribution but also as signaling molecules during multiple aspects of tissue morphogenesis (Yagi & Takeichi, 2000).

Cadherins form a superfamily with several subfamilies, which can be

distinguished on the basis of protein domain composition, genomic structure and phylogenetic analysis of the protein sequences (Fig. 1.1). Classical cadherins, protocadherins, Fat, Dachsous, Flamingo and desmosomal cadherins are among the known vertebrate cadherin subfamilies (Gumbiner, 2000; Tepass et al, 2000).

The classic cadherins are by far the best understood in terms of both mechanism and function within the context of animal development (Anastasiadis & Reynolds, 2000; Daugherty & Gottardi, 2007; Scott & Yap, 2006). Classic cadherins are conserved from flies to mammals. Shotgun, or *Drosophila* E-cadherin, is the best known homolog of the classic vertebrate cadherins. The primary role of Shotgun is to preserve the *Drosophila* epithelium integrity and to recruit other proteins to the region of cell-cell contact, where adherens junctions are organized (Tepass et al, 1996).

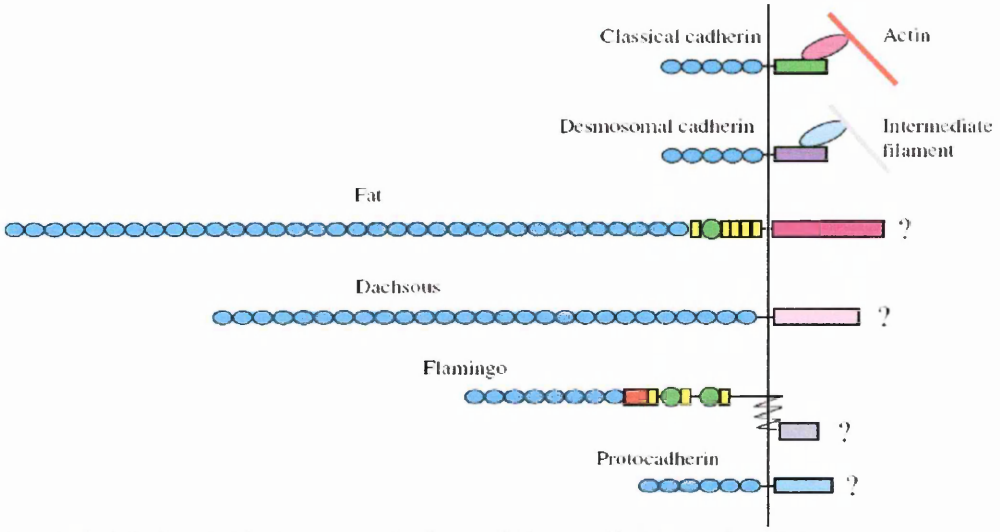

Figure 1.1 Schematic representation of the cadherins structure
All cadherins possess calcium-binding extra-cellular repeats of varying number (blue dots). Non-classical cadherins also have additional extracellular motifs including laminin A-G (green circles), EGF domains (yellow boxes) and flamingo box (red one). Cadherins are single membrane-spanning proteins with the exception of Flamingo, a seven-pass membrane protein. Classical cadherins are described to bind the actin cytoskeleton through the β and α-catenin complex (pink oval) whereas desmosomal subfamily associate with the intermediate filaments. Under debate is the linkage of non-classical cadherins to the cytoskeleton (Tanoue & Takeichi, 2005).

The Ft-like or atypical cadherin subfamily is conserved across species (Tanoue & Takeichi, 2005). Ft was the first cadherin to be identified in *Drosophila* and it is one of the largest transmembrane proteins in the fruit fly (Bryant et al, 1988). Molecular studies revealed that the *ft* gene is localized on the left arm of the second chromosome (24D in the cytological map). The sequence encodes an enormous protein of more than 5000 aminoacids with a predicted molecular weight of around 500 kDa (Mahoney et al, 1991). This was surprising since the sequence of the vertebrate cadherins typically codes for polypeptides of around 1000 aminoacids.

The protein is composed of 34 cadherin repeats at the N-terminal portion, all of which contain aminoacids highly conserved among cadherins. The extracellular region also includes five EGF-like repeats followed by a cysteine rich sequence. A hydrophobic putative transmembrane domain links the extracellular to the cytoplasmic portion. Interestingly, the intracellular region does not show any homology to the cytoplasmic domain of the vertebrate cadherins (Mahoney et al, 1991).

For many years, the way by which Ft was activated has remained obscure since it was not clear whether the entire Open Reading Frame (ORF) was translated into a single polypeptide and to what degree the protein was further processed. Very recently, the groups of Helen McNeill and Kenneth Irvine have nicely characterized post-translational modifications undergone by the Fat protein (Feng & Irvine, 2009; Sopko et al, 2009a). Biochemical *in vivo* assays on imaginal discs from *Drosophila* larvae demonstrated that Ft is synthesized as a transient, 560 kDa precursor which, after maturation, is proteolytically processed. The endogenous Ft exists as 450-470 kDa and 90-110 kDa forms. Additionally, both *in vivo* and *in vitro* studies demonstrated that Ft is phosphorylated in its

intracellular domain. The authors suggested that Dachsous (Ds), the Ft putative ligand, increases the local concentration of Ft at cell contacts inducing its *cis*-dimerization that, in its turn, promotes the *trans*-phosphorylation of Ft by Disc Overgrown (Dco), a kinase already shown to be part of the Ft signaling (Cho et al, 2006). However the functional activities of the two distinct Ft forms have not been clarified yet.

1.1.2 PCP signaling in *Drosophila*

The coordination of cellular polarization is an important feature of development and critical for organ function. In addition to the apical-basolateral polarity, many tissues, especially the epithelium, organize the cells in a plane that is orthogonal to the classic apical-basal axis. This form of polarity is referred to as planar cell polarity (PCP). Originally studied during genetic screens and functional analyses of *Drosophila* wings, eyes and sensory bristles (Adler, 2002; Lawrence et al, 2007; Mlodzik, 1999). PCP has been recently described as an evolutionary conserved process (Keller, 2002; Wallingford, 2004).

In *Drosophila,* the wings arrange their actin-rich extensions, called hairs. Each of them is part of a single cell, and each wing cell is polarized within the plane of the epithelium. A single developing hair extends from the distal portion of each cell in the wing (Fig. 1.2) and grow outward from the cell leading to distal hair polarity (Wong & Adler, 1993). In the fly eye, PCP provides for the organization of the main retinal structures, the ommatidia. Ommatidia are composed of eight photoreceptors and additional accessory cells, which, in section, form a trapezoidal shape. Normally, all ommatidia in the dorsal half of the eye point dorsally, and those in the ventral half point

ventrally (Fig. 1.2). Mutations in PCP genes lead to a loss of planar organization in both the eye and the wing, leaving cell identity and apical-basal cell polarity unaffected (Fanto & McNeill, 2004; Simons & Mlodzik, 2008).

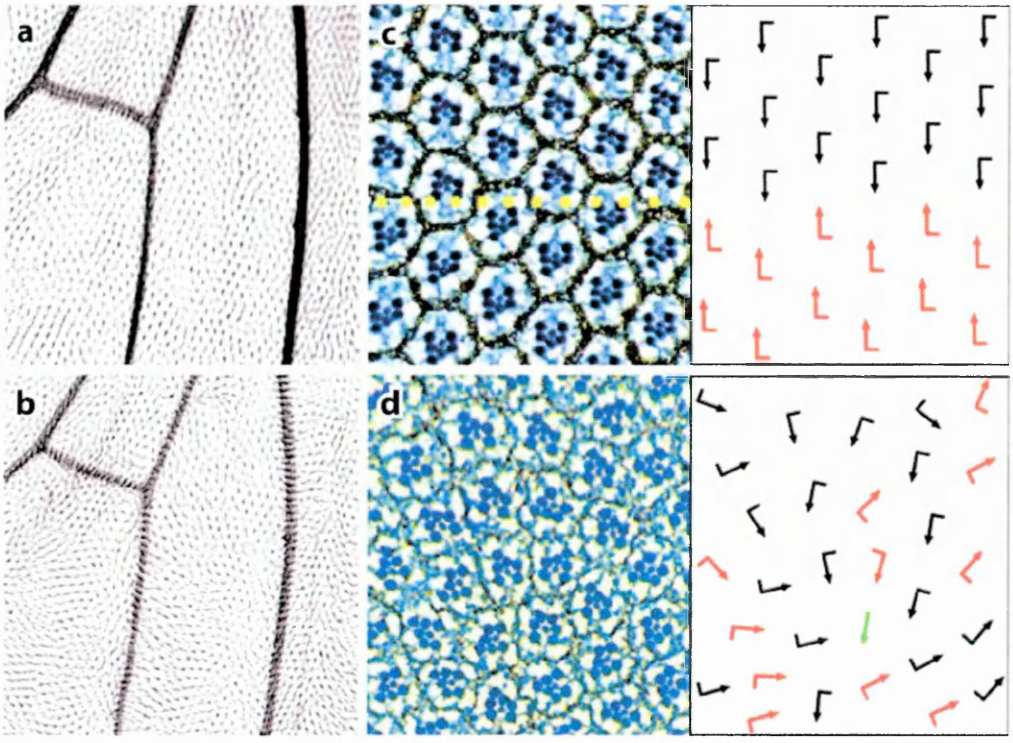

Figure 1.2 PCP features in *Drosophila*.
PCP effects in the wing (a,b) and eye (c,d). In normal flies, wing hairs (a) and photoreceptors clusters (c), called ommatidia show a regular arrangements in the plane of the epithelium. In PCP mutants, the correct cell organization is lost. Mutant hair wings point in all directions (b) and ommatidia result randomly oriented (d). Black and red arrows represent the dorsal and ventral orientations of the ommatidia that are lost in the mutant scenario. Occasional symmetrical ommatida (*green arrow*) are also found in the mutants (Simons & Mlodzik, 2008).

Genetic studies described three major groups of PCP regulating genes, two of them considered to be canonical, the Frizzled(Fz)/Flamingo(Fmi) group and the Ft/Ds PCP system. The third one, the *wingless* related gene signaling (Wnt), has been described as a non-canonical PCP pathway, although none of the genetic experiments performed has revealed a direct role for Wnts in PCP signaling (Casal et al, 2006; Chen et al, 2008a).

1.1.3 The Ft/Ds PCP group

The Ft/Ds PCP group is composed of *ft, ds, four-jointed (fj)* and *atrophin (atro)* genes (Casal et al, 2002; Fanto et al, 2003; Rawls et al, 2002).

Ft and Ds are gigantic atypical cadherins that bind each other. They are supposed to act as receptor and ligand, even though the nature of their relationship is still under debate (Casal et al, 2006; Matakatsu & Blair, 2006). The Ft cytoplasmic domain is thought to be responsible for its PCP activity and it has been shown to interact with the transcriptional co-factor Atro, suggesting a possible role in transcriptional regulation (Fanto et al, 2003). Ft is localized in the apico-lateral membrane, above adherens junctions (Ma et al, 2003), where it displays heterophilic binding with another atypical cadherin, Ds (Clark et al, 1995).

As previously described, Ft/ Ds intercellular signaling is implicated in the regulation of a specific form of polarity, the PCP (Fanto & McNeill, 2004). Loss of Ft or Ds leads to disorganization of the cells inside the mutant tissue. Interestingly, it has been shown that PCP defects by *ft* or *ds* are generally non-autonomous since *wild-type* cells adjacent to the mutant clones are altered in their PCP organization (Rawls et al, 2002; Yang et al, 2002). Moreover, *ft* and *ds* mutants in the fly eye have opposite and non-autonomous effects, since loss of *ft* leads to disruptions of PCP in cells on the polar side of the mutant clone, while loss of *ds* disrupts PCP on cells on the equatorial side of the clone, suggesting that Ds binding may inhibit Ft activity in PCP (Matakatsu & Blair, 2004; Simon, 2004).

At the moment, the best known target of Ft/Ds required for PCP signaling is Fj (Zeidler et al, 1999). Fj is a Golgi transmembrane glycoprotein that, when mutated, induces mild PCP defects (Strutt et al,

2004). Fj and Ds are expressed in opposing gradients in antero-posterior axis, both in eyes and wings, suggesting that their activity is reciprocal to each other (Casal et al, 2002). The heterodimeric bridges formed by Ds and Ft from cell to cell ensure that the amounts of Ft and Ds on the surface of one cell can affect the distribution of Ds and Ft on the neighbouring cells (Ma et al, 2003). Very recently, Fj has been demonstrated to modify Ft and Ds post-translationally by phosphorylating their cadherin repeats as they transit through the Golgi, potentially modulating their activity (Ishikawa et al, 2008). The current model provides for the idea that Ft PCP activity is regulated by gradients of Ds and Fj expression (McNeill, 2009).

The functional relationship of the Fz/Fmi group versus the Ft/Ds group remains an open question. Initially Ft/Ds group has been suggested to work upstream of Fz/Fmi group, largely based on data in the fly eye (Ma et al, 2003; Yang et al, 2002). However, more recent studies strongly suggest that the two signalings act in parallel and that they regulate PCP independently one from the other, thus being sometimes redundant (Casal et al, 2006; Lawrence et al, 2007).

Although *Drosophila* has been the best genetic model to unravel the PCP signaling, recent results from vertebrates argue that the PCP mechanism is strongly conserved and possibly linked to human diseases. It has been shown that PCP plays a crucial role during kidney development, and defects in the mechanism induce a serious disease, the polycystic kidney disease (PKD) (Bisceglia et al, 2006). Although many of the genes that are mutated in PKDs have been identified, the pathogenetic mechanisms initiating cyst formation are still unclear. Recent work shows that cystic kidney disease associates with defective oriented cell divisions and proposes a model in which oriented cell division is essential for the

normally thin elongated tubes that make up much of the nephron (Fischer et al, 2006). In this context, among the four homologs of Ft isolated in vertebrates, Fat4 is considered the most similar to *Drosophila* Ft (Katoh & Katoh, 2006; Rock et al, 2005; Tanoue & Takeichi, 2005) and loss of the protein has been shown to display many PCP defects, including dilation of renal tubules and formation of cysts in the kidney (Saburi et al, 2008).

1.1.4 Ft regulates proximal-distal patterning

Another important process regulated by Ft/Ds signaling is proximal-distal patterning (Cho & Irvine, 2004). The adult *Drosophila* wing, as the other appendages, is subdivided into anterior and posterior compartments that exhibit characteristic patterns. The patterning and growth of wing imaginal discs is governed by a series of regulatory interactions including components of the Hedgehog (Hh), Notch, Wnt and Decapentaplegic (Dpp) signaling pathways (Klein, 2001; Klein & Arias, 1998). Ft, Ds and Fj are all required to regulate the proximal–distal patterning of spacing crossveins in the wings and the segmentation of the leg (Cho & Irvine, 2004).

Interestingly, recent data argue for a link between the regulation of PCP signaling and proximal-distal patterning by Ft (Matakatsu & Blair, 2008). The Approximated (App) protein, a member of the DHHC family, responsible for palmitoylation of selected cytoplasmic proteins (Linder & Deschenes, 2007), was originally identified because of defects in proximal–distal patterning. However, it has been recently found that null alleles of *app* cause alterations also in PCP. Surprisingly, *app* null alleles partially rescue most of the *ft* phenotypes: viability, tissue patterning, overgrowth and PCP

defects, suggesting that App is a novel negative regulator of Ft signalings (Matakatsu & Blair, 2008).

1.1.5 Ft is a tumor suppressor and prevents excessive tissue growth

The *ft* locus has its name from the phenotype observed in flies carrying recessive viable mutations: they cause minor defects in adult morphology such as changes in the body shape, increase in the dimensions of thorax and abdomen and wing vein pattern (Mohr, 1923).

Nevertheless many *ft* mutant alleles of different origins have been isolated and most of them are lethal at the pupal stage. Studies on some of these lethal mutations showed an excessive cell proliferation and a hyperplastic overgrowth of imaginal discs cells during larval development (Bryant et al, 1988). A delayed entry in pupation has been observed due to a great extension of the larval stage, during which an autonomous increase in the rate of cell division and a failure to properly arrest discs growth occur. It has been demonstrated that *ft* mutant cells fail to undergo the correct differentiation due to defects in cell adhesiveness and recognition, and these defects, together with the over-proliferative phenotype, lead *ft* mutant tissues to contain a higher number of mutant cells (Garoia et al, 2000). Therefore all these data make Ft one of the *Drosophila* tumor suppressor genes (Mahoney et al, 1991).

Among the signaling pathways required by Ft to regulate tissue growth, components of the EGFR pathway have been found to genetically interact with Ft (Garoia et al, 2005; Garoia et al, 2000). In *Drosophila*, the EGFR signaling plays a pivotal role in several processes such as differentiation, proliferation and during wing and eye imaginal discs growth

(Baker & Yu, 2001; Schweitzer & Shilo, 1997; Shilo, 2003). Once EGFR signaling was raised, *ft* mutant eyes and wings were shown to display a much more severe phenotype concerning both the outgrowth number and the tissue size. In addition, the transcription of genes involved in EGFR signaling appeared to be regulated by *ft,* suggesting that *ft* controls also the imaginal discs morphogenesis (Garoia et al, 2005). However, the mechanism explaining this genetic interaction has not been clarified yet.

A further molecule described to be part of the Ft growth control signaling is the unconventional myosin Dachs (D) (Cho & Irvine, 2004; Mao et al, 2006). Hypomorphic mutations of *d* were shown to suppress the phenotype due to the loss of *ft,* both in imaginal discs overgrowth and in proximal-distal patterning. Furthermore, overexpression of Ft decreased D staining at the membrane, suggesting an antagonistic influence of Ft on D localization and stability (Mao et al, 2006). The model proposed puts D as a downstream negative regulator of the Ft growth signaling.

Finally, the very recent discovery of a novel signaling mechanism, the Hippo tumour suppressor pathway, links Ft tissue growth control to a new network (Cho et al, 2006).

1.2 FT IS CONNECTED TO THE HIPPO PATHWAY

The Hippo (Hpo) pathway was firstly described as a kinase cascade that negatively regulates cell growth (Edgar, 2006). The protein complex is composed of tumor suppressors that ultimately inactivate Yorkie (Yki), a transcriptional co-factor that in some tissues, like wings, interacts with the transcription factor Scalloped (Sd) to regulate the transcription of genes

required for cell growth, survival and differentiation (Goulev et al, 2008; Wu et al, 2008; Zhang et al, 2008).

The activity of the Hpo signaling is coupled to organ size and cell differentiation through inhibition of cell proliferation and promotion of apoptosis (Pan, 2007; Yin & Pan, 2007). Adult tissues from flies mutants for components of the Hpo pathway have proportionately larger tissue size than respective *wt* tissues. This was linked to a faster proliferation of the mutant cells and has been well clarified by studying both larval imaginal discs and pupal retinal phenotypes (Harvey & Tapon, 2007; Harvey et al, 2003; Tapon et al, 2002; Wu et al, 2003).

Retinae isolated from the mutant pupae exhibited an excessive higher number of interommatidial cells (IOCs), that has become a hallmark of the downregulation of the normal Hpo pathway function (Kango-Singh et al, 2002; Tapon et al, 2002). IOCs are the cells that during differentiation give rise to the pigment cells which surround the ommatidia. Systematic analyses have revealed that this phenotype was due to an excessive proliferation and a block of the pupal apoptosis that would normally induce the death of extra-IOCs. These effects were observed not only in the fly eye but in all the other structures derived from the larval imaginal discs, indicating an ubiquitous role of the Hpo network (Harvey & Tapon, 2007).

1.2.1 The central cassette of the Hpo pathway

Four molecules, Hpo,Salvador (Sav),Warts (Wts) and Mats (Mst) form a protein complex described as the central core of the Hpo kinase cascade (Fig. 1.3). Most of these genes were identified by genetic screens

for *Drosophila* tumour suppressors, since mutants alleles limited tissue growth during the fly development (Pan, 2007; Edgar, 2006).

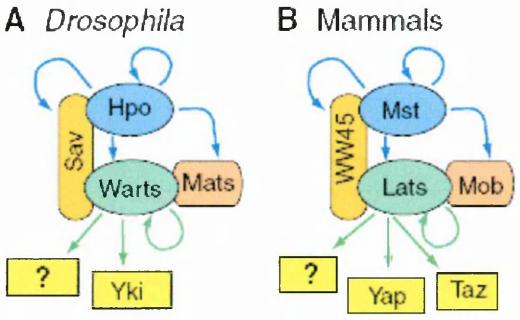

Figure 1.3 The Hpo pathway core Schematic view of the centrale kinase cascade in *Drosophila*(A) and vertebrates(B). Blue arrows point to the proteins phosphorylated by Hpo/Mst and green arrows those proteins phosphorylated by Wts/Lst (Reddy & Irvine, 2008).

Hpo and Wts are both Ser/Thr kinases. Hpo belongs to the nuclear Dbf2 related (NDR) family of protein kinases whereas Wts is a member of the Sterile-20 superfamily (Harvey et al, 2003; Wu et al, 2003). Hpo acts upstream of Wts and activates the kinase by direct phosphorylation without affecting the levels of Wts expression.

Wts post–translational modification, carried out by Hpo, is facilitated by Sav, described as a scaffold protein, since its main function is a direct binding of both Hpo and Wts (Pantalacci et al, 2003; Wu et al, 2003). Sav, also called *shar-pei*, encodes a WW domain-containing protein and its mutations give rise to an overgrowth phenotype similar to, although weaker than, *wts* mutant clones, suggesting that Sav belongs to the Hippo network (Kango-Singh et al, 2002; Tapon et al, 2002).

Interestingly, results from *in vitro* and *in vivo* studies have indicated the existence of an inhibitor of Hpo activation, the tumour suppressor dRASSF, a member of the Ras association family (Polesello et al, 2006). Hpo, Sav and dRASSF proteins are characterized by the presence of a common domain called SARAH (Sav-RASSF-Hpo), that mediates the binding between Hpo and Sav on one hand, and Hpo and dRASSF on the

other hand. dRASSF has been demonstrated to act as a negative regulator of the Hpo pathway, since it can antagonize Sav-mediated Hpo activation (Polesello et al, 2006).

One of the first tumor-suppressor genes identified by the above genetic screens was named *large tumor suppressor* (*lats*) by the Gerald Rubin's group (Xu et al, 1995), and independently identified and named *warts* (*wts*) by the Peter Bryant's group (Justice et al, 1995). Wts phosphorylation is facilitated by Sav that, in turn, needs to be phosphorylated by Hpo to become active. Complete activation of Wts requires interaction with Mst, a *Drosophila* Mob-1-related tumour suppressor protein, that potentiates Wts kinase activity (Lai et al, 2005). The phosphorylation of Mst by Hpo contributes to Mst-Wts binding (Wei et al, 2007). Once activated, Wts can phosphorylate and block the activity of Yki, a transcriptional co-activator that is the final output of the Hpo signaling cascade (Huang et al, 2005).

1.2.2 Upstream modulators of the Hpo central cassette

Following the discovery of the molecules belonging to the Hpo core, the obvious next question was to find whether this pathway was regulated by extracellular signals, and several candidate genes were tested for their ability to induce Hpo target genes. These efforts led to the discovery of three related genes, *expanded (ex), merlin (mer)* and *ft* (Bennett & Harvey, 2006; Cho et al, 2006; Hamaratoglu et al, 2006; Silva et al, 2006).

ex and *mer* both encode members of the Band 4.1 super family, a group of cytoplasmic proteins, characterized by the presence of a FERM (4.1, Ezrin, Radixin, Moesin) domain, that generally act as protein adaptors.

They are localized at the adherens junctions where they are thought to transduce a signal from transmembrane receptors to the cytoskeleton or intracellular downstream molecules (LaJeunesse et al, 1998; McCartney et al, 2000; McClatchey, 2003). *ex* was firstly identified as a *Drosophila* tumour suppressor (Boedigheimer et al, 1993a). Later, *mer* was demonstrated to be the *Drosophila* ortholog of the human NF2, a tumour suppressor gene that, when mutated, causes a congenital neuronal disease with the formation of tumours in the central nervous system (McCartney et al, 2000).

Genetic epistasis experiments have suggested that *mer* and *ex* act upstream of *hpo* and are partially redundant in regulating cell proliferation and apoptosis through the Hpo pathway (Cho et al, 2006; Hamaratoglu et al, 2006). Altough *mer;ex* double mutants resulted in an impaired endocytic trafficking of transmembrane receptors, like EGFr, Ft and Notch (Maitra et al, 2006), later studies demonstrated the rescue of *ex* mutants by the over-expression of Wts, suggesting a model in which the reported effects on other pathways were likely mediated downstream of Wts (Feng & Irvine, 2007).

In parallel, distinct functional requirements of *Drosophila* Mer and Ex in the Hpo pathway were reported, supporting a different spatial and temporal expression and function of Ex with respect to Mer (Pellock et al, 2007).

Very recent experiments have introduced a new perspective on the Hpo regulation and raised the possibility of a more complex signaling involving different feedback loops (Badouel et al, 2009). The group of Hellen McNeill demonstrated that Ex directly binds and contribute to the inactivation of Yki, suggesting that Ex can regulate the Hpo pathway activity

not only upstream but also downstream or even independently of Wts (Badouel et al, 2009).

Also very recently, a new gene, *kibra,* has been linked to the upstream modulation of the Hpo pathway (Baumgartner et al, 2010; Genevet et al, 2010; Yu et al, 2010). Kibra has already been studied in vertebrates where it has been detected mainly in kidney and brain (Kremerskothen et al, 2003). Flies mutants for *kibra* displayed many features, such as tissue overgrowth and apoptotic block, similar to, although weaker, than the phenotype observed in mutants of the Hpo pathway. The Kibra protein was found to be faintly expressed in wing and eye imaginal discs but present at much higher levels in the ovarian follicle cells. Notch signaling, oocyte polarity and ectopic cell division resulted misregulated in the ovarian posterior follicle cells (PFCs) mutants for *kibra,* as already reported for other components of the Hippo signaling (Polesello, 2007; Meignin, 2007; Yu et al, 2008; Genevet et al, 2010; Yu et al, 2010; Baumgartner et al, 2010).

Genetic epistatic experiments placed *kibra* upstream of the *hpo-sav-wts* core to function in cooperation and in part redundantly with both *ex* and *mer* (Baumgartner et al, 2010; Genevet et al, 2010; Yu et al, 2010). In addition, it was demonstrated that *kibra* is a Yki transcriptional target gene like *ex*, *diap1* and *cycE* (Genevet et al, 2010).

1.2.3 The transmembrane protein Ft is connected to the Hpo pathway

The Hpo pathway has been linked to the tumour suppressor Ft since they regulate a common set of target genes (Bennett & Harvey, 2006; Cho et al, 2006; Willecke et al, 2006; Silva et al, 2006). Ft has actually been

proposed to act upstream of the Hpo pathway as a potential cell surface receptor, but the molecules that link Ft to this network are still under debate (Bennett & Harvey, 2006; Cho et al, 2006; Willecke et al, 2006; Silva et al, 2006).

ft has been shown to influence Yki phosphorylation and its subcellular localization (Oh & Irvine, 2008), and in addition to be partially rescued by the over-expression of Wts (Feng & Irvine, 2007). This was the first evidence that directly linked the Hpo signaling to a transmembrane protein.

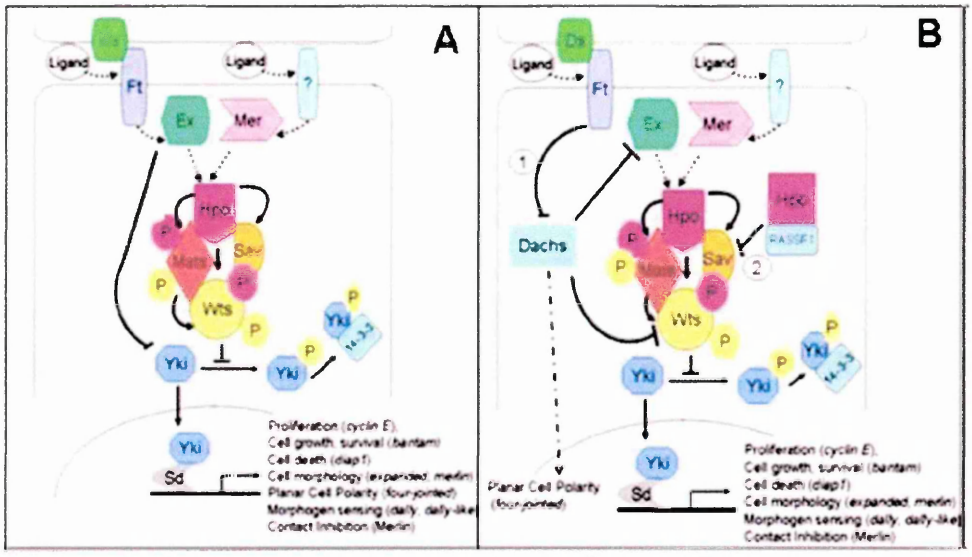

Figure 1.4 Models of the Hpo signaling in *Drosophila*
In A, the Ft/Ex complex upstreamly regulates the Hpo core to finally inactivate the transcription of target genes by retaining the transcriptional co-factor Yki in the nucleus. Ex by itself can directly phosphorylate and inactivate Yki. In B, the Ft/D/Wts model proposes that Ft interacts with D to regulate the abundance of Wts and inactivate Yki in a parallel way to Hpo/Sav/Wts. In both the models Ds interaction with Ft seems to be required (rev. from Kango-Singh & Singh, 2009).

Two models have been proposed to explain how Ft controls this pathway (Fig. 1.4). The first has placed Ft and Ex in a linear pathway with the Hpo complex (Bennett & Harvey, 2006; Willecke et al, 2006; Silva et al, 2006). In contrast, the second model argued for a central role of the unconventional myosin D which, downstream of Ft, was supposed to control

the abundance of another intermediate of the cascade, Wts, rather than Ex or Hpo (Cho et al, 2006; Feng & Irvine, 2007). Ft/D, on one hand, and Hpo, on the other hand, would regulate Wts in a parallel manner, the former affecting the quantity, the latter controlling its activity (Yin & Pan, 2007; Reddy & Irvine, 2008).

In addition to D, Ds and Fj have been linked to Ft in the Hpo pathway regulation, although the molecular mechanism by which Ds-Ft binding could regulate growth has not been elucidated (Cho et al, 2006; Rogulja et al, 2008; Willecke et al, 2008). Subsequent relevant discoveries have demonstrated that Ds regulates Dco-dependent phosphorylation of Ft and Ft-associated proteins to control Ft signaling in growth and PCP, thus supporting the model in which Ft/Ds and Ft/Hpo signalings cross-talk to monitor the intracellular events that regulate tissue growth (Feng & Irvine, 2009; Sopko & McNeill, 2009b).

However, as Ft is not required to promote apoptosis through the Hpo pathway, other upstream regulators of this signaling probably exist.

1.2.4 Yki is the downstream target of the Hpo pathway

Yki, the *Drosophila* ortholog of the mammalian transcriptional coactivator Yes-Associated Protein (YAP), was described as the missing link between Wts and transcriptional regulation in the Hpo pathway (Huang et al, 2005). It was identified in a yeast two-hybrid screen using a domain of Wts as bait. Activation of Yki was shown to recapitulate all the phenotypes caused by mutants of the Hpo core, and genetic epistasis placed *yki* downstream of *hpo*, *sav* and *wts*. Biochemical studies actually demonstrated that Wts interacts with and inactivates Yki function by

phosphorylating a specific WW domain common to other components of the Hippo pathway (Huang et al, 2005). Once phosphorylated, Yki is sequestered from the nucleus to the cytoplasm, where the maintenance of its inactive form is guaranteed both by the interaction with the 14-3-3 cytoplasmic protein (Dong et al, 2007; Oh & Irvine, 2008) but also by an independent mechanism that goes directly from Ex to Yki (Badouel et al, 2009; Baumgartner et al, 2010; Ren et al, 2010).

Like other transcriptional coactivators, Yki does not bind to DNA directly but it interacts with several DNA-binding transcription factors. The identification of its direct DNA-binding partner has been a key issue for many years. Recent studies have identified Scalloped (Sd), the only transcription factor of the *Drosophila* TEAD/TEF family, as a cognate factor that binds with the N-terminal region of Yki to regulate Hpo target genes (Goulev, 2008; Wu, 2008; Zhang, 2008). Sd belongs to a family of evolutionarily conserved proteins characterized by the presence of a TEA/ATTS DNA-binding domain (Campbell et al, 1992). Sd is known to physically interact with the product of the *vestigial* (*vg*) gene and has been extensively characterized for its role in wing development and formation (Halder et al, 1998; Simmonds et al, 1998). Genetic and biochemical studies have demonstrated that *sd* is required for the tissue overgrowth induced by *hpo* core mutants or Yki over-expression. However, the role of Sd in other tissues than wings has not been clarified yet and, the fact that Sd is not expressed in all imaginal discs like Yki suggests that Yki-Sd act in a tissue specific manner and others Yki partners should exist (Goulev et al, 2008; Wu et al, 2008; Zhang et al, 2008).

This idea was supported by the discovery of new Yki DNA-binding partners, the trascription factors Homothorax (Hth), a TALE-homeodomain

protein, and Teashirt (Tsh), a zinc finger transcription factor (Peng et al, 2009). Hth and Tsh interact physically with each other and are involved in several developmental processes. In the fly eye, they function together to repress the later-acting retinal differentiation genes, such as *eyes absent* (*eya*) and *sine oculis* (*so*), thus maintaining anterior eye disc cells in an undifferentiated state (Bessa et al, 2002). In this context, recent genetic experiments indicated that Hth and Tsh work through the Hpo signaling to promote cell proliferation and survival in the anterior eye discs by directly up-regulating the *bantam* mi-RNA, one of the Hpo cascade target genes (Peng et al, 2009).

1.2.5 Transcriptional targets of Hippo signaling

Originally, the first transcriptional targets found to be regulated by the Hpo pathway were *diap1*, the *Drosophila* inhibitor of apoptosis, *cycE*, involved in cell-cycle progression (Harvey et al, 2003; Pantalacci et al, 2003; Tapon et al, 2002; Wu et al, 2003) and, more recently, the micro-RNA molecule *bantam*, a positive regulator of imaginal disc growth (Nolo et al, 2006; Thompson & Cohen, 2006).

Another important class of Yki target genes are some upstream components of the Hippo network such as *ex, mer, kibra* and *fj*. Ex, Mer and also the new regulator Kibra are shown to be all upregulated in clones mutants for components of the Hpo pathway, suggesting a possible negative feedback loop regulating their expression (Cho et al, 2006; Genevet et al, 2010; Hamaratoglu et al, 2006). Fj is involved in the Ft/Ds PCP regulation and its expression was also found to increase after the inhibition of the Hpo signaling (Cho et al, 2006; Willecke et al, 2006). It was

suggested that Fj is necessary to increase the ability of Ds to bind Ft and activate the downstream signaling and this model was supported by the discovery that Ds regulates Dco dependent phosphorylation of Ft (Feng & Irvine, 2009; Sopko & McNeill, 2009b).

The last class of target genes regulated by the Hpo pathway are involved in cell fate and patterning decisions, such as Wnt in the wing imaginal discs, Notch signaling in the leg discs (Cho et al, 2006; Cho & Irvine, 2004; Mao et al, 2006), and the proteoglycans Dally (division abnormally delayed) and Dally-like, required for the regulation of diffusible ligands such as Wnt, Dpp and Hh (Baena-Lopez et al, 2008).

1.2.6 Ft and Hpo network are conserved in vertebrates

Most of the known components of the Hpo network seem to be evolutionarily conserved and have more than one orthologue in vertebrates, most of them being implicated in mammalian tumorigenesis (Harvey & Tapon, 2007).

Lats1/2, the homologues of *Drosophila* Wts, have been described to cause sarcomas, ovarian and renal tumours and human Mats has been linked to skin melanoma and mammary gland carcinoma (Lai et al, 2005; St John et al, 1999; Tapon et al, 2002). The phosphorylation sites important for the activation of Hpo (whose vertebrate orthologue is called Mst) and Wts/Lst kinases, together with the inactivation of Yki/YAP, have been mapped both in flies and mammalian systems and are highly similar, not only for their structure, but also for their function {Dong, 2007; Zhao, 2007; Oh & Irvine, 2008; Zhang, 2008).

Drosophila melanogaster	Human orthologs	Protein	Role in Hippo Signaling Pathway	Role in Human Cancer (Reference)
Fat	Fat4	Proto-Cadherin	Hippo Pathway Receptor (?)	Mutated in breast cancer (Qi et al., 2009)
Dachsous	DCHS1	Proto-Cadherin	Ligand for the Fat receptor (?)	Unknown
Expanded	FMRD6 (Willin)/ EX2	4.1 Superfamily FERM domain protein	Upstream regulators of the Hippo kinase cascade	Unknown
Merlin	NF2	4.1 Super-family FERM domain protein	Upstream regulators of the Hippo kinase cascade	Mutated in familial and sporadic schwanomas (Evans et al., 2000)
Hippo	MST1/2	Ste-20 family Protein Kinase	Bind Salvador and Mats, and phosphorylate Mats and Warts in response to upstream signals	Hypermethylated in soft tissue sarcoma (Seidel et al., 2007)
Salvador	hWW45	WW domain Adaptor protein	Binds Hpo, the Sav-Hpo complex more efficiently regulates the activity of the Warts kinase	Mutated in cancer cell lines (Tapon et al., 2002)
Mats	MOBK1B	Mob superfamily coactivator of protein kinases	Phosphorylated by Hpo and Wts, and binds Hpo, and Wts, to regulate Wts activity	Mutated in cancer cell lines (Lai et al., 2005)
Warts	Lat1/2	NDR family Protein Kinase	Phosphorylates Mats, Wts and Yki to regulate Hippo pathway activity	Silenced in breast tumors (Turenchalk et al., 1999; Zeng and Hong, 2008)
Yorkie	YAP TAZ	Transcriptional Coactivator	Unphosphorylated form binds Sd, and translocates to the nucleus to regulate expression of transcriptional targets of Hippo signaling	Amplified (overexpressed) in breast tumors, colorectal cancer and several other solid tumors (Overholtzer et al., 2006; Zender et al., 2006)
Scalloped	TEAD	Transcription factor	Binds with Yki to regulate target gene expression.	Unknown
dRASSF1	RASSF1	RA domain containing RAS effector protein	Binds Hippo. complex may be disrupted by Sav in response to pathway activation	Hypermethylated in Lung and kidney cancers
Dachs	Unknown	Unconventional Myosin	Binds with Warts	Unknown

Table1. Genes involved in *Drosophila* and mammalian Hpo pathway

Human orthologues of Sd, the TEAD/TEF transcription factors, had been discovered previously and described to be mediators of YAP functions in mammalian cells, although they interact with other transcription factors not isolated in *Drosophila* (Strano et al, 2005; Zhao et al, 2008).

Among the upstream regulators of the Hpo pathway, the mammalian othologue of Mer, the tumour suppressor Neurofibromin 2 (NF2), has been well described. By contrast for Ex and Ds the homology is more uncertain (Hamaratoglu et al, 2006). Examination of the mammalian genome has revealed the presence of four Ft homologues; the most similar to the fly protein seems to be Fat4 (Katoh & Katoh, 2006; Tanoue & Takeichi, 2005). The regulation of PCP signaling and cell division by Fat4 appears to be conserved, both in the function and in the molecules required for the signaling (Saburi et al, 2008). In addition, very recent studies linked loss of

vertebrate Fat4 to breast cancer, like mutants for the Hpo pathway, suggesting Fat4 as a regulator of the Hpo network in mammals (Qi et al, 2009).

Altough information about the roles of the other vertebrate Fat proteins is relatively limited, Fat1 has been described to display no obvious effects on PCP but to be critically involved in vascular smooth muscle cells migration and growth (Hou et al, 2006). Intriguingly, recent studies have demonstrated that vertebrate transcriptional co-factors Atrophins, like Fat1, are induced after arterial injury and they regulate migration and orientation by physically interacting with Fat1, suggesting Atrophin as a potential interactor of vertebrate Fat (Hou & Sibinga, 2009).

1.3 ATROPHINS AS FT INTERACTORS

The above described results about a cooperation among mammalian Fat and Atrophin, strengthen previous models of a link between *Drosophila* Ft and Atro. As already mentioned, from yeast-two hybrid screens and studies on genetic interactions, Atro has been shown to bind Ft cytoplasmic domain and to be involved in the same Ft/Ds PCP signaling (Fanto et al, 2003). These findings suggest that Ft and Atro are part of a conserved signaling important for the regulation of PCP and perhaps also for other processes.

Atrophins are a widely expressed family of transcriptional co-factors, conserved across species. The main interest on Atrophin genes came first from the relationship between Atrophin1 and the DRPLA neurodegenerative disease (Nagafuchi et al, 1994a; Yazawa et al, 1995). It has been actually

demonstrated that the disorder is caused by the expansion of a highly polymorphic CAG repeat within the coding region of Atrophin-1 gene (Koide et al, 1994), which leads to neuronal death in the dentate nucleus of cerebellum, globus pallidus, caudate and putamen in the brain (Igarashi et al, 1998).

The *Atrophin1* gene was initially cloned while performing genetic screens for human genes containing CTG/CAG or CCG/CGG triplet repeats (Li et al, 1993). Subsequent studies assigned the *Atrophin1* gene to the short arm of chromosome 12, and further reports placed Atrophin1 as the causative factor for the DRPLA disease (Koide et al, 1994; Nagafuchi et al, 1994a). In search of potential Atrophin1 homologues, one molecule was identified and called RERE, because of the presence of two arginine-glutamic acid dipeptide-like repeats (RE-repeats) at the C-terminus of the protein. Owing to its resemblance with Atrophin1, RERE has also been referred to as Atrophin2 (Yanagisawa et al, 2000).

In 2002, *Drosophila* Atrophin (Atro), the unique homolog of human Atrophins, was independently discovered by two groups: the group of Xu, in the USA, identified *Atro* during a search for lethal mutations that affect growth and patterning (Zhang et al, 2002), and the group of Kerridge, in France, isolated *Atro* (called also *Grunge*) through an EMS mutagenesis, during a screening for possible *tsh* interactors (Erkner et al, 2002). Both the groups have reported *Atro* as being involved in several developmental processes.

Atrophin1 is a smaller protein (1191 amino acids), compared to Atrophin2 (1566 amino acids) and to *Drosophila* Atro (1966 aa) (Erkner et al, 2002; Koide et al, 1994; Nagafuchi et al, 1994a; Yanagisawa et al, 2000; Zhang et al, 2002). Unlike Atrophin1 and *Drosophila* Atro, Atrophin2 does

not contain any long glutamine-repeat tract. *Atrophin2*, on chromosome 1p, encodes two isoforms, Atrophin2-L and Atrophin2-S (Shen et al, 2007; Zoltewicz et al, 2004). Studies on the Atrophin2-S isoform (990 amino acids) has revealed a domain structure that is co-linear with Atrophin1, with which it shares high similarity, although without any poly-glutamine repeat (Yanagisawa et al, 2000). Differently from Atrophin1, the amino-terminal portion of Atrophin2-L isoform (1566 amino acids) has a significant homology to the MTA (Metastasis-associated Proteins) family of proteins. The domain structure of Atrophin2 was demonstrated to be conserved from *Drosophila* (Zhang et al, 2002) to humans (Zoltewicz et al, 2004), although Atrophin1 can only be found in the genome of higher vertebrates. This suggests that the *Atrophin1* gene arose during evolution as a truncated duplication of a primordial *Atrophin2* type gene.

Drosophila Atro, located on chromosome 3L, encodes a protein of 1966 amino acids wich shares high levels of identity with the human proteins, being more similar to the human Atrophin2. Interestingly, Atro contains two different poly glutamine stretches, one more N-terminal and named Q11, and one more C-terminal named Q14 (Zhang et al, 2002).

1.3.1 Structure and expression pattern of Atrophins

The function of Atrophins has been related to the two distinct domains present in the full length Atrophin2: the MTA homologous N-terminal domain and the Atrophin-like C-terminal domain (Fig. 1.5). The Atrophin domain is bipartite, with conserved amino terminal (Atr-N) and carboxy terminal (Atr-C) portions, interrupted by a simple sequence. Atrophin1 has been defined as the truncated version of Atrophin2, because

it lacks the entire MTA homologous N-terminal domain but it contains two arginine-glutamic acid dipeptide (RE) repeats and one putative Nuclear Export Signal (NES) within the Atr-C segment, whereas the Atr-N segment carries a putative Nuclear Localisation Signal (NLS) (Nucifora et al, 2003). Unfortunately, the function of the Atr-N and Atr-C regions has not been well clarified yet.

The N-terminal region of Atrophin-2 contains several motifs such as BAH, involved in DNA methylation, replication, and transcription regulation (Callebaut et al, 1999), ELM2, that mediates association with histone deacetylase (Wang et al, 2006), SANT, which recruits histone methylation activity (Wang, 2008a; Rice, 2003), GATA, a DNA binding module (Sanchez-Garcia & Rabbitts, 1994) and two NLS. These motifs often appear in proteins that function as transcription co-repressors or that are predicted to directly interact with other transcription regulators that have DNA-binding activity. Northern blot analysis has revealed that Atrophin1 transcripts are ubiquitously expressed in a variety of neuronal and non-neuronal tissues (Kanazawa, 1998; Knight et al, 1997).

The *Atrophin2* gene codifies for two transcripts that give rise to the long and short form of the protein. Their expression varies considerably in different tissues, but they are predominantly detected in the nucleus (Shen et al, 2007; Yanagisawa et al, 2000).

Studies performed to find the localization of *Drosophila* Atro have revealed an ubiquitous distribution during the early stages of embryogenesis, whereas at later stages it becomes more enriched at the ventral nerve cord region (Erkner et al, 2002; Zhang et al, 2002). Throughout larval development phase, Atro mainly localises to the nucleus

of the cells maintaining an ubiquitous pattern in most of the imaginal discs observed.

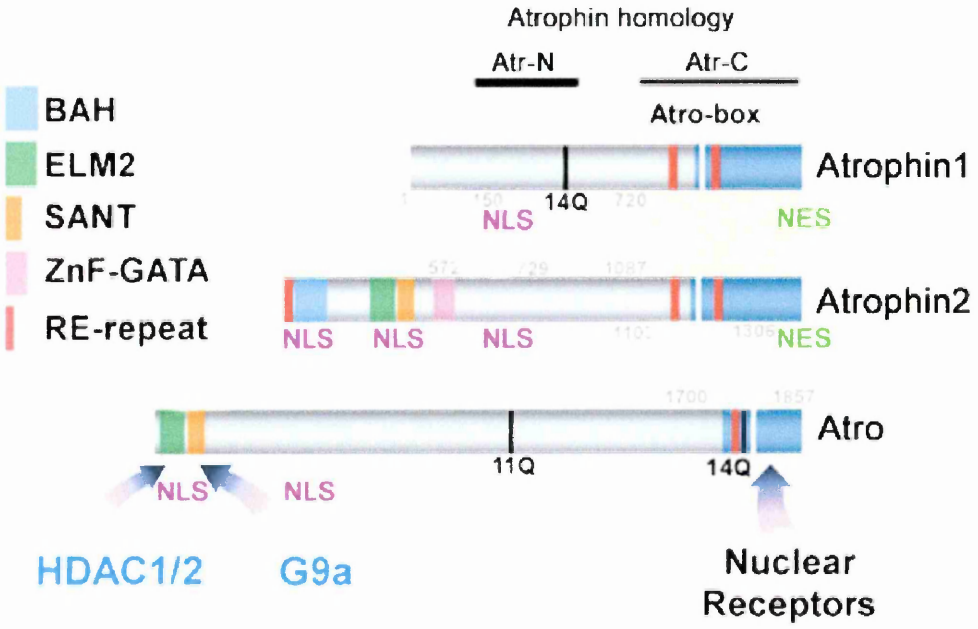

Figure 1.5 Structure and domains of human and *Drosophila* Atrophins
The Atrophin domain contains two conserved regions: an amino terminal (Atr-N) and a carboxy terminal (Atr-C) portion. Atr-N contains one NLS, Atr-C contains one putative NES and two RE repeats. Atr-N of Atrophin1 also contains a glutamine repeat (14Q). The N-terminus of Atrophin2 contains BAH, ELM2, SANT and ZnF-GATA domains. It also carries two NLS and one more RE-repeat. Atro (*Drosophila* Atrophin) shares an overall 38% homology to human Atrophin2, carrying the ELM2 and SANT domains. Atro contains two different poly glutamine stretches, 11Q and 14Q, two putative NLS and a RE-repeat at the C-terminus of the protein. The mapped nuclear receptor interacting domains, at the C-terminus of each protein, are marked in dark blue. The ELM2 domain and SANT domain are docking sites where HDAC1/2 (Histone Deacetylase 1, 2) and G9a (H3-K9 histone methyltransferase) bind, respectively.

1.3.2 Atrophins functions

Atrophin1 is not an essential gene during mouse development (Shen et al, 2007). By contrast, both *Atrophin2* and *Drosophila Atro* genes are required for both mice and flies to develop and to survive (Plaster et al, 2007; Zoltewicz et al, 2004; Zhang et al, 2002). One of the functions exerted by Atrophins during development is the regulation of the EGFR signalling. Mutation or reduced expression of *Drosophila Atro* resulted in

ectopic wing vein formation in the intervein regions (Charroux et al, 2006; Kankel et al, 2004). The possibility that Atro negatively regulates EGFR signalling has been further supported by genetic interactions with several key components of the EGFR signalling pathways, in both *Drosophila* wing and eye (Charroux et al, 2006).

Atrophins have a function in nuclear receptor signalling. They have been recently demonstrated to interact with transcriptional repressors such as Tlx, in vertebrates, and Tailless (Tll) in *Drosophila* (Moran & Jimenez, 2006; Pankratz et al, 1992; Yu et al, 1994) and also with nuclear proteins, such as Brakeless (Haecker et al, 2007).

Regarding their involvement in transcriptional repression, it has been demonstrated that Atrophins, especially Atrophin2, are involved in histone deacetylation and methylation. Chromatin, at regions where Atrophin2 binds, has been shown to become compact and favour gene silencing (Wang, 2006; Chen, 2008a; Wang, 2008b). This evidence prompted reasearchers to view Atrophin proteins primarily as dedicated corepressors (Shen et al, 2007). However, considerable evidence suggested that Atro can regulate gene transcription in a positive manner as well (Kankel et al, 2004). A recent report has proposed that Atrophin2 can switch from a transcriptional repressive form to a transcriptional activating form (Wang et al, 2008b).

1.4 POLYGLUTAMINE NEURODEGENERATIVE DISORDERS

Polyglutamine expansion within human Atrophin1 causes the DRPLA, one of the late-onset polyglutamine (polyQ) neurodegenerative diseases

(Zoghbi & Orr, 2000), that represent a relevant cause of heritable neurodegeneration. These disorders are at least nine: Huntington disease (HD), spinocerebellar ataxia (SCA) 1, 2, 3, 6, 7, and 17, DRPLA and spinobulbar muscular atrophy (SBMA), the first to be reported in the literature (La Spada et al, 1991). They result from the expansion of a CAG repeat along the respective disease genes, encoding an abnormally long glutamine tract that confers toxic properties to the resident proteins (Gusella & MacDonald, 2000). This shared mutation suggests a common pathogenic mechanism, notwithstanding the fact that the pathogenic proteins are evolutionarily and functionally unrelated.

Among the factors leading to these diseases, an important component is the toxic gain of function caused by the disorder-causing proteins, even though in some cases it has been suggested that the loss of function of the normal gene might also contribute to the pathology (Cattaneo et al, 2005; Gatchel & Zoghbi, 2005; Zoghbi & Botas, 2002).

1.4.1 The DRPLA neurodegenerative disorder

The DRPLA exhibits clinical symptoms such as dementia, choreoathetosis, myoclonus epilepsy and cerebellar ataxia. The pathogenic mechanism is still not clear (Tsuji, 1999). It has been shown that the expansion of CAG tracts induces a significant loss of neurons in several brain regions such as globus pallidus, subthalamic nucleus, dentate nucleus and spinal cord (Nagafuchi et al, 1994a).

The polyQ expansion in Atrophin1 had been suggested to compromise the function of the protein. However, recent findings on mutant mice indicated that *atrophin1*$^{-/-}$ animals do not display any defect,

neurological or of other phenotypes (Shen et al, 2007). Therefore, it is likely that the polyQ expansion along Atrophin1 causes a dominant negative effect.

Several models have been proposed to explain the neurotoxicity caused by mutant Atrophin1, including protein cleavage of Atrophin1 by caspases, (Ellerby et al, 1999; Nucifora et al, 2003; Schilling et al, 1999), the formation of aggregates or inclusions in the nucleus, a hallmark of polyglutamine diseases (Ross, 1995), and the phosphorylation of Atrophin1 (Okamura-Oho et al, 2003). Unfortunately, the exact significance of these modifications in the pathogenesis of the DRPLA has not yet been established.

1.4.2 Factors causing polyglutamine disorders

Despite the shared nature of the genetic mutation causing the pathology, polyQ diseases differ clinically and neuropathologically. For example, a preferential loss of specific neuronal populations has been observed, although there is a considerable overlap in basal ganglia, brainstem nuclei, cerebellum and spinal motor nuclei degeneration (Fernandez-Funez et al, 2000; Ross, 1995). In addition, although the commonly accepted treshold for glutamine repeats is 37-40AA, there are three examples, SCA6, SCA3 and SCA17, whose CAG expansions are smaller, suggesting a different mechanism from the other disorders (Shao & Diamond, 2007).

Many hypotheses have been put forward to explain polyQ disease pathogenesis and all of them are not mutually exclusive. For any given

polyQ disease, more than one mechanism likely contributes to neuronal dysfunction and eventual cell death.

A decade ago, a clue to pathogenesis has come from the discovery that expanded polyQ proteins accumulate within intraneuronal inclusions in selected brain regions, suggesting that polyQ protein aggregation mediated neurodegeneration by affecting gene expression or by disrupting nuclear organisation and function (Orr, 2001; Peters et al, 1999; Saudou et al, 1998; Zoghbi & Orr, 2000).

The role of nuclear inclusions in the pathogenesis has been a matter of debate. Although the original idea was that nuclear inclusions are pathogenic, later evidence has led to the alternative view that inclusions might be protective, by sequestering toxic oligomeric forms of the mutant protein (Gatchel & Zoghbi, 2005; Sisodia, 1998; Zoghbi & Botas, 2002). Additional evidence has suggested that neurotoxicity of the polyQ proteins is influenced not only by their altered function (Orr, 2001; Gatchel & Zoghbi, 2005; Zoghbi & Botas, 2002), but also by a proteolytic cleavage and post-translational modifications of the mutant proteins (Muchowski, 2002; Pennuto et al, 2009).

Other mechanisms like mitochondrial dysfunction, impaired axonal transport and aberrant neuronal signaling, including excitotoxicity and cellular protein homeostasis impairment, have all been implicated in the pathogenesis of one or more polyQ disorders (Bennett et al, 2007; Gatchel & Zoghbi, 2005; Li et al, 2008; Pandey et al, 2007; Riley & Orr, 2006).

1.5 *Drosophila* AS A MODEL TO MIMIC NEURODEGENERATIVE DISEASES

Neurodegenerative diseases represent a subgroup once considered among the most obscure and intractable of all human illnesses.

One of the powerful approaches for studying disease mechanisms is the establishment of animal models. The model organism *Drosophila* has been successfully used to study a wide range of human neurodegenerative diseases, contributing to the understanding of the molecular basis of these diseases (Bonini & Fortini, 2003; Lu & Vogel, 2009; Muqit & Feany, 2002). Since around 75% of human genes implicated in genetic diseases have at least one ortholog in *Drosophila* (Reiter et al, 2001), flies allow excellent genetic manipulation and *in vivo* readouts of a studied pathology. In general, fundamental aspects of cell biology relevant to processes such as cell cycle, synaptogenesis, membrane trafficking and cell death, are similar in *Drosophila* and humans.

Four approaches have been employed successfully to study neurodegeneration in *Drosophila*. First, forward genetic screens have been carried out to identify genes that, when mutated, can cause degeneration of the brain (Kretzschmar et al, 1997; Rogina et al, 1997). Second, transgenic overexpression approach has been used to model disease caused by a toxic gain of function (GOF) mechanism, such as Alzheimer, Parkinson and polyQ diseases (Feany & Bender, 2000; Fernandez-Funez et al, 2000; Jackson et al, 1998). Third, a genetic inhibition of endogenous gene approach has been used to model the subset of familial diseases transmitted in a recessive fashion, which are likely caused by a loss of function (LOF) mechanism (Bilen & Bonini, 2005; Yang et al, 2003; Rong & Golic, 2000). Fourth, a pharmacological approach can be used to model

neurodegenerative diseases and to test candidate therapeutics in animals (Chaudhuri et al, 2007; Coulom & Birman, 2004).

1.5.1 Approaches to model human diseases in flies

Reverse genetics can be used to target the fly homolog of a specific gene implicated in a human disease. The phenotypes that resulted from the altered gene expression are then studied. The most common mean of expressing human neurodegenerative genes in *Drosophila* makes use of the binary GAL4-dependent upstream activating sequence (UAS), the Gal4/UAS system (Brand & Perrimon, 1993). In this system, a human disease-related gene is subcloned into the UAS expression construct and then microinjected into fly embryos to establish transgenic lines.

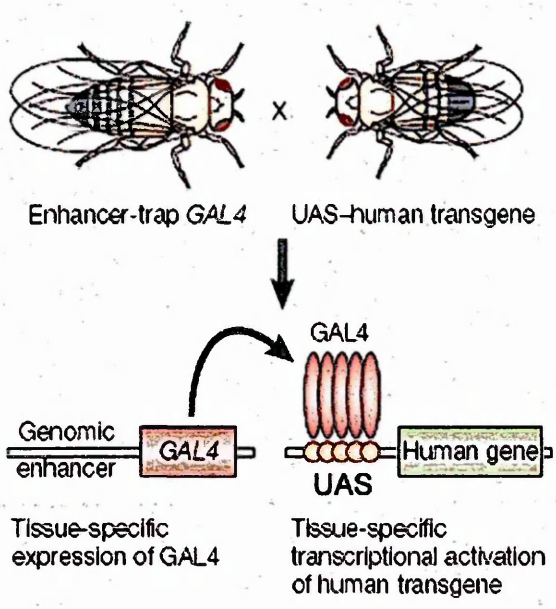

Figure 1.6 Schematic view of the GAL4/UAS system
Transgenic flies, expressing the yeast transcriptional activator GAL4 under a specific promoter, are crossed with transgenic flies carrying a human disease-related gene under the control of the UAS sequence. In the absence of ectopically expressed GAL4, the UAS-transgene is inactive. Once the protein GAL4 is expressed and recognizes the UAS sequence, the transgene trascription is activated and mutant flies express the transgene exclusively in the tissue where GAL4 is expressed (Muqit & Feany, 2002).

The expression of the transgene is placed under the control of the yeast transcriptional activator GAL4. In the absence of GAL4, the transgene is inactive. When flies that carry the human transgene, under the control of the UAS sequence, are crossed to flies that express GAL4 in a specific

tissue or cell type, the human protein is made only in the tissues that have GAL4 (Fig. 1.6).

One of the most useful driver lines expresses GAL4 in all cells of the eye under the control of the *glass* transcription factor promoter, called GMR (*glass* multiple reporter). As a consequence, the study of neurodegenerative diseases, and in particular of polyglutamine ones, has found in the *Drosophila* compound eye a successful model of these pathologies. In almost all cases, expression of expanded polyQ containing protein has induced a phenomenon of retinal degeneration. Remarkably, studies in *Drosophila* have revealed that also the expression of expanded polyQ-containing proteins in glial cells confers toxicity, suggesting that degeneration or dysfunction of these cells may contribute to the disease process (Lievens et al, 2008; Tamura et al, 2009).

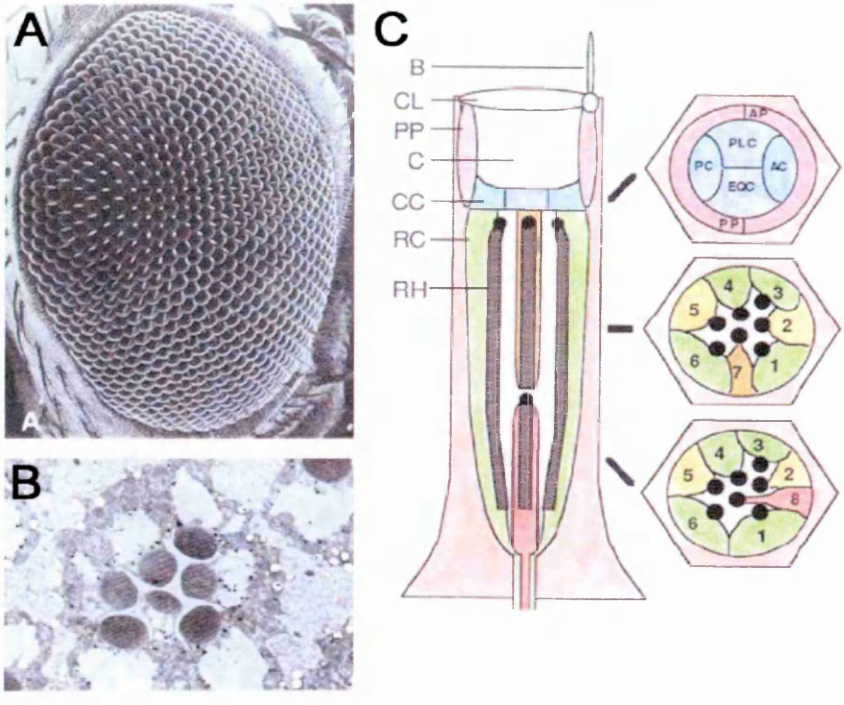

Figure 1.7 *Wild-type* eye structure
(A) Scanning electron micrograph of a *Drosophila* compound eye. Each facet represents a single ommatidium. Mechanosensory bristles project between ommatidia. (B) Tangential EM section through an ommatidium. The cells are arranged with crystal-like accuracy, as evidenced from the precision of the asymmetrical arrangement of the rhabdomeres. The rhabdomeres of the outer

photoreceptors (R1-6) are arranged in an asymmetrical trapezoid surrounding the central rhabdomere. (C) A schematic ommatidium. The lens system consists of a fluid-filled pseudocone (C) bordered laterally by the primary pigment cells (PP), basally by the cone cells (CC), and apically by the corneal lens (CL). This unit collects and focuses light onto the underlying photoreceptors (RC). Each photoreceptor carries apically a rhabdomere (RH), that contains the photosensitive pigments. The rhabdomeres of R1-R6 extend the depth of the ommatidium and are arranged in an asymmetrical trapezoid pattern. R7 provides a central rhabdomere to this arrangement in the apical part of the ommatidium and R8 provides this function basally. The ommatidium has a hexagonal profile in cross section and, at alternate vertices, a mechanosensory bristle (B) projects to the exterior (Tomlinson, 1988).

The compound eye of *Drosophila*, the most accessible and life-dispensable system to study neuronal tissue, is a precisely organized structure composed of 800 repeated subunits called ommatidia (Fig. 1.7). Each ommatidium is made of eight light-capturing photoreceptor neurons, R1-R8, together with a number of accessory cells. Only seven of the eight photoreceptors are visible in tangential sections taken towards the external surface of the eye. Photoreceptors elaborate an apical membranous structure, the rhabdomere, which is fundamental for these neuronal cells to capture light stimuli and transmit the impulse to the brain. Neurodegeneration and neurotoxicity are monitored by measuring the loss of visible photoreceptor neurons in the eye; lethality of the organism, or behavioural phenotypes, although many other measures of degeneration can be used (Jackson et al, 1998).

1.5.2 *Drosophila* models for the DRPLA polyglutamine disease

Drosophila Atro encodes for a large ubiquitous protein, containing all functional domains of human Atrophins, including two polyQ stretches (Erkner et al, 2002; Zhang et al, 2002). In the laboratory, a model for the study of DRPLA in *Drosophila* has been established by generating three transgenes expressing Atro Wt, Atro75QN or Atro66QC proteins, the last

two carrying the expansion of one of the two polyQ tracts. Over-expression of one of the three in the eye, including Atro Wt, causes the classical neurodegenerative phenotypes observed in other models of polyglutamine disorders: progressive retinal collapse and depigmentation, with Atro75QN being most severe (Nisoli et al., 2010). In addition to the typical polyQ toxicity, the results obtained have also suggested that protein-specific effects modulate the phenotypes, as observed for other polyQ models like Huntington disease.

PolyQ Atrophins promote neurodegeneration with autophagic hallmarks, both in neuronal photoreceptors and glial cells. So far, however, the contribution of autophagy to the pathogenesis of the DRPLA has not been fully understood (Nisoli et al., 2010). Although endogenous autophagy plays a crucial role in moderating polyQ Atrophin toxicity, further induction of autophagy does not rescue neurodegeneration of the DRPLA fly models, differently from what has been reported for other *Drosophila* neurodegenerative models (Ravikumar et al, 2004; Wang & Levine, 2010). Further evidence suggests that neurodegeneration induced in the DRPLA flies results from partial inhibition or delay of autophagic digestion, sharing many similarities with another group of human diseases, called lysosomal storage disorders (Settembre et al, 2008; Venkatachalam et al, 2008).

1.6 AUTOPHAGY

Autophagy is a general term that refers to a cellular degradative pathway involving the delivery of cellular components, like organelles or portion of cytosol, to the lysosomes, for final breakdown by resident

hydrolases (Levine & Kroemer, 2008; Mizushima et al, 2008; Rubinsztein, 2006). Three types of autophagy have been described which share a common destiny of lysosomal degradation but are mechanistically different from one another: macroautophagy, the most extensively studied, microautophagy and chaperone-mediated autophagy (Klionsky, 2005; Massey et al, 2006). Microautophagy involves inward invagination of lysosomal membrane, which delivers a small portion of cytoplasm into the lysosomal lumen. Chaperone-mediated autophagy involves the direct translocation across the lysosomal membrane of cytosolic proteins, that require unfolding by chaperone proteins.

Macroautophagy (or autophagy) is conserved from yeast to mammals, and the molecular and cellular network mediating this process has been nicely described in the literature (Klionsky, 2007). Upon induction, a small vesicular organelle, called the isolation membrane or phagophore, was shown to elongate and then enclose a portion of the cytoplasm. This results in the formation of a double-membrane structure, the autophagosome. Subsequently, the outer membrane of the autophagosome fuses with a lysosome to form an organelle called autophagolysosome, which leads to the degradation of the enclosed materials together with the inner autophagosomal membrane. Endosomes can also fuse with the autophagosome to form an organelle, called amphisome, that subsequently fuses with the lysosome. Amino acids and other small molecules, that are generated by autophagic degradation, are delivered back to the cytoplasm for recycling or energy production (Klionsky, 2007; Levine & Kroemer, 2008; Mizushima & Klionsky, 2007a).

1.6.1 Molecular machinery of autophagy

Although autophagy was firstly identified by electron microscopy in mammalians by observing autophagosomes, the molecular understanding of autophagy began little more than a decade ago, starting primarily from genetic screens in the budding yeast *Saccharomyces cerevisiae* and then leading to the identification of 32 autophagy-related (*Atg*) genes (Klionsky, 2007).

The autophagy process is composed of mechanistically distinct steps starting with induction, which requires cargo recognition and packaging, vesicle formation and autophagosome-vacuole fusion, and finally breakdown of the content and subsequent release of the degraded products to the cytosol (Fig. 1.8). Different sets of Atg proteins are involved in these steps and orchestrate the vast majority of the process. Many *Atg* homologs have subsequently been identified and characterized in higher eukaryotes, suggesting that autophagy is a highly conserved pathway through the evolution (Xie & Klionsky, 2007).

1.6.2 Autophagosome formation and elongation

The nucleation and assembly of the initial phagophore membrane appears to start at the phagophore-assembly sites (PAS), where multiple proteins, besides Atg ones, are recruited (Cheong et al, 2008; Kawamata et al, 2008; Suzuki et al, 2007a). The source of the phagophore membrane has not been clarified yet, although recent data support a contribution from both mitochondria and also the endoplasmic reticulum and Golgi network (Axe et al, 2008; Juhasz & Neufeld, 2006; Reggiori et al, 2005; Yen et al, 2010).

It has been demonstrated that the formation of the phagophore requires the activity of the class-III phosphoinositide 3-kinase (PI3K) Vps34, which is part of a large macromolecular complex, specific for autophagy, that contains the proteins Atg6 (also called Beclin 1), Atg14 and Vps15 (Itakura et al, 2008; Kihara et al, 2001; Liang et al, 1999). This complex activates a series of Atg proteins, the most relevant of which is Atg1 (also called ULK1), a kinase described to exert a crucial and indispensable role in autophagy induction by binding Atg13 and Atg17 (Chan et al, 2009; Jung et al, 2009; Kamada et al, 2000).

Two other proteins have been discovered to be involved in the stage of autophagosome initiation, Atg5 and Atg12, that undergo the first of the two ubiquitylation-like reactions that control autophagy. Atg12 is conjugated to Atg5 in a reaction that requires Atg7 [ubiquitin-activating-enzyme (E1)-like] and Atg10 [ubiquitin-conjugating-enzyme (E2)-like]. Atg5-Atg12 conjugates are localized onto the PAS and dissociate when autophagosome formation is completed (Suzuki et al, 2001; Suzuki et al, 2007a).

The second ubiquitylation-like reaction, described in literature in the context of autophagosome formation, is the conjugation of microtubule associated protein 1 light chain 3 (LC3 also known as Atg8 in yeast and *Drosophila*) to the lipid phosphatidyl ethanolamine (PE). LC3 has been extensively studied and found to be firstly processed by Atg4, to expose its C-terminus glycine residue and form the cytosolic LC3-I form, which is then covalently conjugated to PE to form the membrane associated LC3-II form. This process requires the activities of Atg7 (E1-like) and Atg3 (E2-like) and specifically targets LC3 to the Atg5-Atg12-associated membranes (Ohsumi & Mizushima, 2004).

In physiological conditions, the basal level of autophagy is very low and the majority of Atg8/LC3 is cytosolic. Experiments performed to find factors that influence autophagy activation have shown that, upon autophagy induction, Atg8 increases in its lipid-conjugated form and is localized to both sides of the phagophore, where it controls the size of the autophagosomes. Interestingly, Atg8 levels correlate with autophagic vacuole numbers, which can be assessed by quantifying Atg8 positive vesicles inside the cells' cytoplasm (Kabeya et al, 2000).

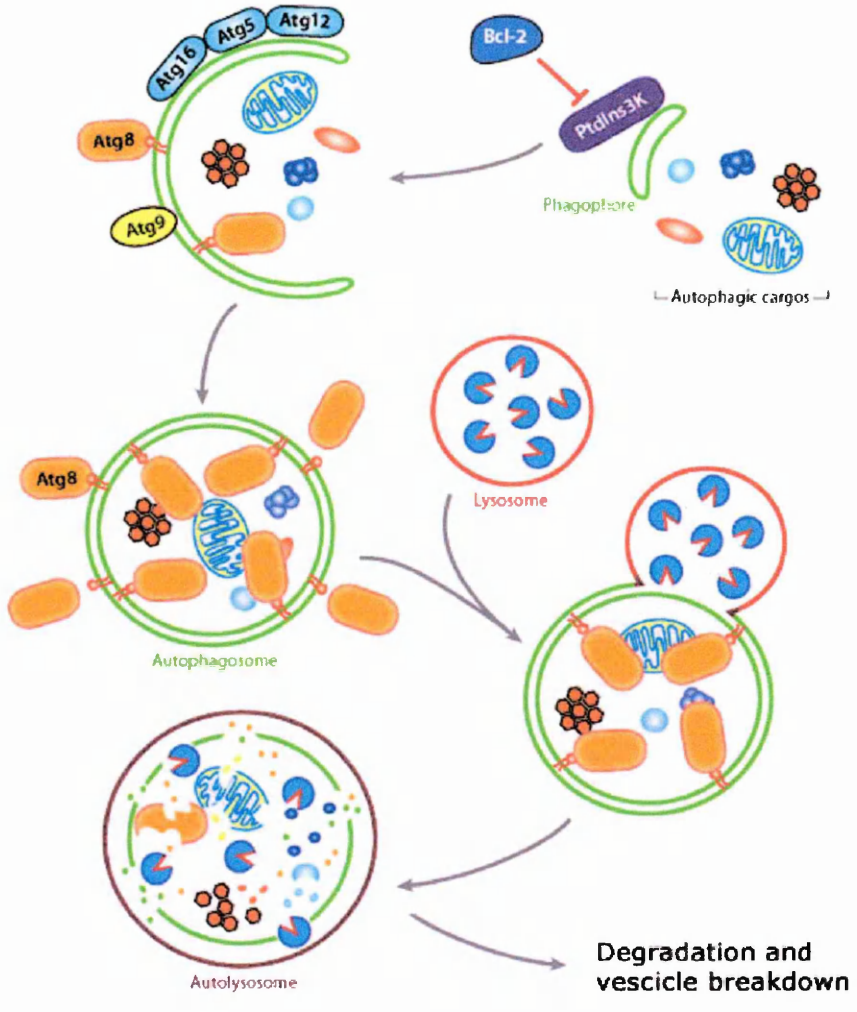

Figure 1.8 Schematic model of the autophagy machinery
A portion of the cytoplasm, including organelles, is enclosed by a phagophore or isolation membrane, to form an autophagosome. Pagophore nucleation is facilitated by the class III Ptdins3K that mediates enwrapping of cytosolic proteins and organelles like mitochondria. Atg12-Atg5-Atg16 and Atg8-PE are recruited to the phagophore to help for the phagophore expansion and the elongation of the double membrane. Upon autophagosome completion most of the Atgs are dissociated, allowing the fusion of the autophagosome with the lysosome. Finally

the material inside the autolysosome is degraded by lysosomal proteases and released to the cytosol (from He & Klionsky, 2009).

1.6.3 Autophagosome maturation and fusion with the lysosome

Autophagosomes form randomly in the cytoplasm and, when their formation is completed, the Atg8 attached to the outer membrane is cleaved from PE by Atg4 and released back to the cytosol. Microtubules have been described as being crucial for driving the trafficking of autophagosomes to lysosomes, which are clustered around the microtubule-organising centre near the nucleus, and subsequently tether, dock and fuse together to form the so called autolysosome, where the contents of the two vesicles are mixed (Jahreiss et al, 2008).

One of the main methods discovered to measure autophagic flux is the monitoring of Atg8/LC3 turnover, since LC3-II is degraded when autolysosomes have been formed. In addition, as Atg8/LC3 is degraded by autophagy, the decrease or disapperance of total LC3 protein amount, or immunofluorescent staining, is paradoxically a second good indicator of autophagic flux (Kabeya et al, 2000; Mizushima & Klionsky, 2007a; Rusten et al, 2004).

Besides Atg8/LC3, levels of other autophagy substrates can be used to monitor the network. Classically, autophagy was considered to be a random degradation system, but recent studies have revealed that several specific substrates are preferentially degraded by autophagy, of which the best studied example is p62 (also known as SQSTM1/sequestome 1). p62 is selectively incorporated into autophagosomes through direct binding to LC3 (Bjorkoy et al, 2005); thus, total cellular expression or immunofluorescent levels of p62 inversely correlate with autophagic activity. When autophagy

is blocked or deregulated, p62 has been observed to accumulate (Mizushima & Klionsky, 2007a). P62 protein is not only a direct interactor of Atg8. Originally it had been described as a scaffolding protein commonly found in inclusion bodies containing polyubiquitinated aggregates, destined to be degraded by autophagy in several neurodegenerative disorders, such as Parkinson (Kuusisto et al, 2001; Nagaoka et al, 2004; Zatloukal et al, 2002).

1.6.4 Vescicle breakdown and final degradation

After autophagosome fusion with the lysosome, degradation of the inner vesicle has been described to depend on a series of lysosomal/vacuolar acid hydrolases, including in yeast proteinases A, B and the lipase Atg15 (Teter et al, 2001) and in mammalian cells cathepsin B, D (a homolog of proteinase A) and L (Tanida et al, 2005).

One of the most traditional methods to evaluate the efficiency of this last step is the measurement of bulk degradation of long-lived proteins (Cuervo et al, 1997). In this assay, cells are cultured with isotope-labeled amino acids for a long time, to label long-lived proteins, followed by a short incubation period without isotope-labeled amino acids, to wash out radiolabeled short-lived proteins, which are primarily degraded by the proteasome. The cellular release of degraded proteins can be quantified after the treatment with an autophagy-inducing stimulus.

This has been considered an excellent quantitative assay, and the comparison of the degradation rates between samples cultured in the presence or absence of an autophagy inhibitor has been adopted as a

standard to ensure that what was being measured correlated with the real contribution of autophagic degradation (Mizushima et al, 2010).

1.6.5 Regulation of autophagy activation

Under physiological conditions, autophagy has a number of vital roles such as maintenance of the amino acid pool during starvation, prevention of neurodegeneration, anti-aging, tumor suppression, preimplantation development, clearance of intracellular microbes, and regulation of innate and adaptive immunity (Cecconi & Levine, 2008; Deretic & Levine, 2009; Levine & Kroemer, 2008; Rubinsztein, 2006).

One of the characteristic features of autophagy is its dynamic regulation; the activity is markedly upregulated by numerous stimuli. The best known inducer of autophagy is nutrient starvation, ranging from yeast to mammals (Kim et al, 2008; Igarashi et al, 1998). Besides starvation, autophagy can also be activated by several physiological stress stimuli such as hypoxia (Azad et al, 2008; Papandreou et al, 2008), energy depletion (Inoki et al, 2003), endoplasmic reticulum stress (Yorimitsu et al, 2006), high temperature, hormonal stimulation or pharmacological agents,such as rapamycin (Noda & Ohsumi, 1998; Lum et al, 2005a). The lysosomal degradative network is also stimulated by pathological circumstances such as bacterial or viral infections and protein aggregopathies (Xu et al, 2007).

Conversely, autophagy suppression is also often associated with certain diseases, including a subset of cancers, neurodegenerative disorders, infectious diseases. A decline in autophagy function is also a common feature of aging (Cuervo, 2004; Martinez-Vicente & Cuervo, 2007).

1.6.6 Signaling pathways regulating autophagy

Nutrient starvation induces autophagy in eukaryotic cells through inhibition of TOR (target of rapamycin), an evolutionarily-conserved serine/threonine kinase. TOR, as a central sensor of cell growth, plays a key role at the interface of the pathways that coordinately regulate the balance between cell growth,cell division and autophagy in response to nutritional status, stress signals and energy status. The activation of TOR signaling provokes the inhibition of autophagy induction (Codogno et al., 2005).

In *Drosophila* and mammalian cells, the pathways through which hormones regulate autophagy are different from those of nutrients, however both converge on TOR (Lum et al, 2005a). Insulin and insulin-like growth factors regulate TOR through the class I PtdIns3K PKB/Akt pathway. Upon association with growth factors, receptor tyrosine kinases undergo autophosphorylation and become activated, increasing membrane recruitment of both PKB/Akt and its activator PKD1. PKB/Akt, in turn, inhibits a downstream protein complex, called the tuberous sclerosis complex 1/2 (TSC1/TSC2).

TSC1/TSC2 heterodimer is a stable complex which senses the upstream inputs from various kinases, not only PKB/Akt, but also ERK1/2 (Ma et al, 2005; Inoki et al, 2002). Moreover, it acts as the GAP for Rheb (the Ras homology enriched in brain protein), a small GTPase that binds and finally stimulates TOR activity. Besides TOR, Rheb homologues also play a role in autophagy regulation by growth factors, inducing the signaling via the Raf-1–MEK1/2–ERK1/2 pathway (Furuta et al, 2004; Pattingre et al, 2003).

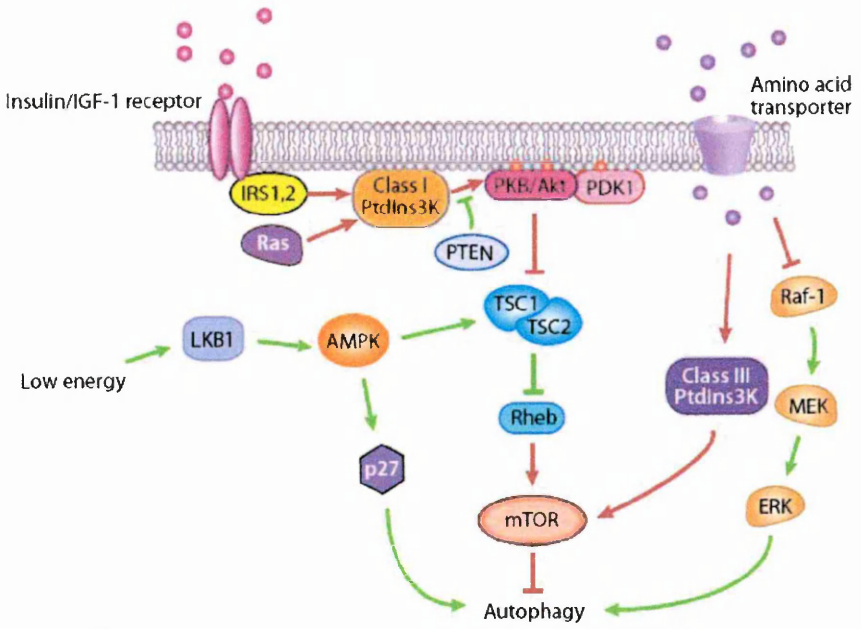

Figure 1.9 Signalings regulating the autophagy activation
(from He & Klionsky, 2009)

TOR has been described as belonging to two distinct complexes, TORC1 and TORC2. They are structurally and functionally distinct protein complexes that share the same catalytic subunit, TOR, which are both conserved from yeast to mammals. TORC1 has a primary function in regulating autophagy (Kamada et al, 2004; Lum et al, 2005a). Direct inhibition of the TORC1 complex with the rapamycin treatment stimulates autophagy, suggesting that TOR downregulates the lysosomal degradative pathway (Noda & Ohsumi, 1998; Yang & Klionsky, 2009). However, a recent report challenged this view by showing that rapamycin and siRNA knockdown of one of the key downstream effectors of the TORC1, S6 kinase 1 (S6K1), inhibit autophagy in cancer cells (Zeng & Kinsella, 2008). In addition, a more recent finding shows that mTORC1 regulates autophagy through an unknown mechanism that is insensitive to rapamycin (Thoreen et al, 2009).

During periods of intracellular metabolic stress, activation of autophagy has been descrided as a crucial process for cell viability. Both in

Drosophila and in mammalian cells, a reduced cellular energy level is sensed by AMPK (5'-AMP-activated protein kinase), which is activated by a decreased ATP/AMP ratio. Active AMPK leads to phosphorylation and activation of the TSC1/TSC2 complex, which inhibits mTOR activity through Rheb (Inoki et al, 2003).

Autophagy, stimulated by mTOR downregulation, results in elevated ATP production via recycling of nutrients. In addition, the AMPK pathway phosphorylates and activates p27kip1, a cyclin-dependent kinase inhibitor, leading to cell cycle arrest. The latter is essential to prevent cells from undergoing apoptotic death and to induce autophagy for survival, in response to bioenergetic stress during growth factor withdrawal and nutrient deprivation (Liang et al, 2007).

1.6.7 Autophagy in neurodegenerative diseases

Growing evidence has recently linked autophagy to numerous intracellular functions such as development, differentiation, cell defense against pathogens, and cell death (Cuervo, 2004; Mizushima & Klionsky, 2007a; Shintani & Klionsky, 2004). Connections have also been established between malfunctioning of autophagy and different human disorders (Fig. 1.10) such as cancer, muscular and metabolic diseases, and neurodegenerative disorders (Cuervo, 2004; Martinez-Vicente & Cuervo, 2007).

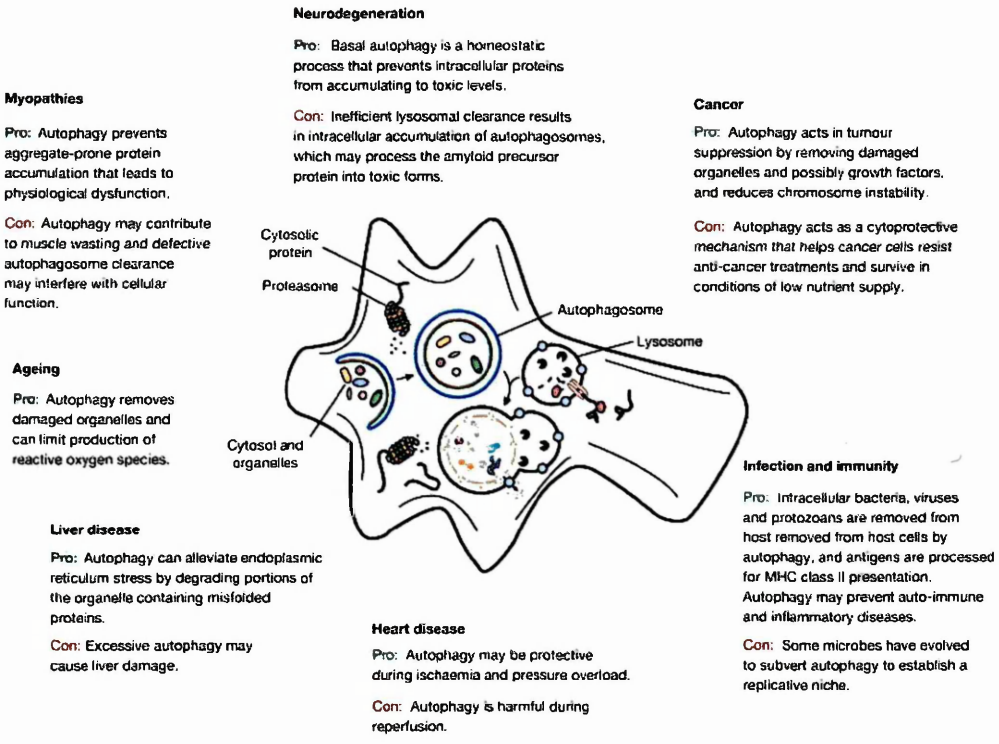

Figure 1.10 Autophagy in human diseases
Degradation is fundamental to maintain cellular homeostasis. Autophagy can act as a cytoprotective mechanism to prevent various diseases like cancer, neurodegeneration, myophaties, metabolic diseases and infections although in some cases it could also be deleterious (from Mizushima et al, 2008).

Several reports have demonstrated that autophagosomes accumulate in the brain of patients with diverse disorders such as Alzheimer's, Parkinson's and Huntington's disease, leading to the hypothesis that, in addition to the ubiquitin-proteasome system, the degradation of disease-related mutant proteins is highly dependent on autophagy, (Rubinsztein, 2006; Rubinsztein et al, 2007; Williams et al, 2006). Consistent with this idea, autophagy has been implicated in regulating the turnover of mutant polyglutamine forms of Huntingtin, that accumulate in affected neurons (DiFiglia et al, 1997) but although highly ubiquitinated are poor substrates for proteasome (Venkatraman et al, 2004). The presence of many undegraded ubiquitinated polyQ-aggregates suggested that the proteasome is attempting at clearing the mutant proteins without any success (Ross & Poirier, 2004). The autophagic signaling has

been found to compensate for the impairment in the proteasome system in a fly model of spinobulbar muscle atrophy (Pandey et al, 2007).

An age-related decline of nervous system function has been described in several Atg knockout mice, like Atg5 or Atg7, and also in *Drosophila* mutants, suggesting that the loss of autophagy induces a neurodegenerative phenotype (Hara et al, 2006; Juhasz et al, 2007; Komatsu et al, 2006).

Pharmacological activation of autophagy has been shown to alleviate the toxicity associated with aggregate-prone proteins, both in cultured cells and in mouse or *Drosophila* models (Ravikumar et al, 2004; Rubinsztein et al, 2007). Rapamycin, a pharmacologic inducer of autophagy, reduces the aggregation of expanded polyQ in transfected cells (Ravikumar et al, 2002), protects against neurodegeneration in a fly model of Huntington disease and improves performance on behavioral tests by decreasing aggregate formation, in a mouse model of Huntington disease (Ravikumar et al, 2004). In conclusion, it is reasonable to assume that proper functioning of autophagy is necessary for maintenance of neuronal homeostasis and for the removal of pathogenic proteins unsuitable for degradation through other proteolytic pathways.

However, as this system becomes overloaded during this compensatory stage, and other aggravating factors, such as aging and oxidative stress, contribute, autophagy failure becomes evident, leading to functional cellular decline and eventual cellular death. Decrease with age in the activity of both the lysosomal and the proteasome system, has been reported in almost every tissue in old organisms (Cuervo et al, 2005). Declining protein degradation could be responsible in part for the failure of the intracellular quality control systems observed in the neurodegenerative

disorders with age. Poor degradation of autophagosome cargo, together with an impaired ability to upregulate autophagy, have also been described in aged organisms. The subsequent intracellular accumulation of protein aggregates and autophagic vacuoles containing undigested materials, have been proposed as mainly responsible for cellular failure and onset of symptoms, thus accelerating cellular death (Cuervo et al., 2010).

2. AIM OF THE PROJECT

It has been suggested that polyQ diseases are transcriptionopathies, in which toxicity first arises from large scale alterations of transcription. In addition, because of the molecular function of Atrophins, DRPLA is a disease with a straightforward link to transcriptional activity.

Several *Drosophila* models for DRPLA have been generated in the lab, identifying both typical polyQ toxicity and atrophin-specific events that modulate cell and organism toxicity (Nisoli et al., 2010).

To understand how transcriptional alterations cause neurodegeneration and are linked to the normal functions of Atrophin, a genome wide transcription profiling has been performed in the lab on the DRPLA *Drosophila* models, focusing on primary events that precede neurodegeneration.

The most fascinating result that emerged from the microarray analysis was the repression of the *ft* tumour suppressor gene transcription. *ft* transcription is significantly dowregulated not only by the two polyQ Atrophin forms but also by the *wt* Atrophin, albeit at a much lower degree. This suggests that *ft* transcriptional regulation is an Atrophin specific function which is altered by the polyQ expansion. The analysis also denotes that polyQ Atrophins stimulate the transcription of genes regulating stress responses, cell cycle and homeostasis of the photoreceptors neurons, outcomes already observed for other polyQ proteins.

The functional significance of *ft* downregulation induced by Atrophins has been addressed through *Drosophila* genetics revealing a strong genetic interaction between *atrophin* and *ft* in neurodegeneration.

In light of these findings my PhD project focuses on the hypothesis that *ft* is required *per se* to prevent neuronal degeneration.

I have thus designed a series of experiments to unravel the biological relevance of Ft and whether it affects neuronal homeostasis independently of any mutation in Atrophin.

Subsequently, to draw a more complete model of the *ft* biological function I have deemed it necessary to start to define the molecular signaling *ft* belongs to and finally the cellular mechanism through which this tumor suppressor and its signaling pathway control homeostasis and degeneration.

Chapter 3

METHODS

3.1 *Drosophila* strains

The following mutant fly stocks have been used for the analysis of the retinal phenotype in homozygous mitotic clones:

yw,eyflp/w;ft^{fd},FRT40/P[w^+],FRT40

yw,eyflp/w;ft^{fd},FRT40/GFP,FRT40

yw,eyflp/w;ft^{82},FRT40/P[w^+],FRT40

yw,eyflp/w;FRT40/P[w^+],FRT40

yw,eyflp/w;FRT82B,sav^3/FRT82B,P[w^+]

yw,eyflp/w;hpo^{BF33},FRT42D/GFP,FRT42D

yw,eyflp/w;hpo^{42-47},FRT42D/GFP,FRT42D

yw,eyflp/w;FRT82B, wts^{X1}/FRT82B,P[w^+]

yw,eyflp/w;FRT82B, wts^{MGH1}/FRT82B,P[w^+]

yw,eyflp/w;ex^{e1},FRT40/P[w^+],FRT40

yw,mer^4,FRT19A/FRT19A,TubGal80,hsflp

yw,eyflp/w;d^{GC13},FRT40/P[w^+],FRT40

yw,eyflp/w;ft^{fd},d^{GC13},FRT40/P[w^+],FRT40

yw,eyflp/w;ft^{fd},FRT40, yki^{B5}/P[w^+],FRT40

yw,eyflp/w;ds^{38},FRT40/P[w^+],FRT40

yw,eyflp/w;ds^{38},d^{GC13},FRT40/P[w^+],FRT40

yw,eyflp/w;ds^{38},FRT40, yki^{B5}/P[w^+],FRT40

yw,eyflp;$atro^{e46-2}$,FRT2A/GFP,FRT2A

yw,eyflp;$atro^{e46-2}$,FRT80/P[w^+],FRT80

yw,eyflp;gug^{35},FRT2A/GFP,FRT2A

yw,eyflp;gug^{35},FRT80/ P[w^+],FRT80

yw,eyflp/yw;Tor$^{\Delta P}$,FRT40/P[w^{+}],FRT40

yw,eyflp/yw;ft^{fd}, Tor$^{\Delta P}$,FRT40/P[w^{+}],FRT40

yw,eyflp/yw;ft^{fd},FRT40/GFP,FRT40;atg1$^{\Delta 3D}$,FRT80/FRT80,M,armLacZ

The following stocks have been used for the phenotypic analysis of mutant retinae expressing exogenous transgenes that carry *wt*, mutant or RNAi constructs. Expression of transgenes have been driven taking advantage of the Gal4-dependent upstream activating sequence Gal4/UAS system (Brand & Perrimon, 1993).

- *ft^{IR}* (#9396 from VDRC): *UASft^{IR}/GMRGal4;Ubi-Gal80^{ts}*
- *shotgun^{IR}* (#103962 from VDRC): *UASshotgun^{IR}/GMRGal4;Ubi-Gal80^{ts}*
- *yw,eyflp;GMR,FRT,P[w+],FRT,Gal4/+;UASYki/+*
- *yw,eyflp/yw;ft^{fd},FRT40/armLacZ,FRT40;UAS-GFP::Atg8a/TubGal4*
- *yw,eyflp; ft^{fd},FRT40/TubGal80,FRT40;TubGal4/+*
- *yw,eyflp; ft^{fd},UASTor^{TED},FRT40/TubGal80,FRT40;TubGal4/+*
- *yw,eyflp; ft^{fd},FRT40/TubGal80,FRT40;UASTsc1^{IR}/TubGal4*
- *yw,eyflp; ft^{fd},FRT40/TubGal80,FRT40; UASAtg1^{GS10797}/TubGal4*

Standard methods have been used for fly handling. Flies were raised at 25°C or 29°C as specified in the text.

3.2 Generation of mitotic clones with Flp/FRT system

Mitotic clones have been generated by the *flp/FRT* technique either with *ey-flp* or *hs-flp* as recombination source (Xu & Rubin, 1993). The *flippase* recombinase gene (*flp*) is placed under the control of the *eyeless* (*ey*) enhancer, to drive the expression of the enzyme specifically in the eye-antennal imaginal discs during the larval stage. Alternatively, for *hs-flp*, two pulses of heat-shock at 37°C of 90 min at 24 and 36 hours after egg laying

have been used to induce a FLP ubiquitous expression. The FLP recombinase recognises and mediates site-specific recombination between *FRT* (Flp recombinase target) sites placed at identical position on homologous chromosomes (Golic & Lindquist, 1989). If the site-specific recombination between homologues occurs after DNA replication, and the daughter chromatids segregate appropriately, the region of the chromosome arm that lies distal to the *FRT* site will be made homozygous and each daughter cell will inherit two copies of this region from one of the parental chromosomes (Fig. 3.1). We used this system to make a mutagenized chromosome arm homozygous in clones of cells in the eye of flies that are otherwise heterozygous for the mutation of our interest.

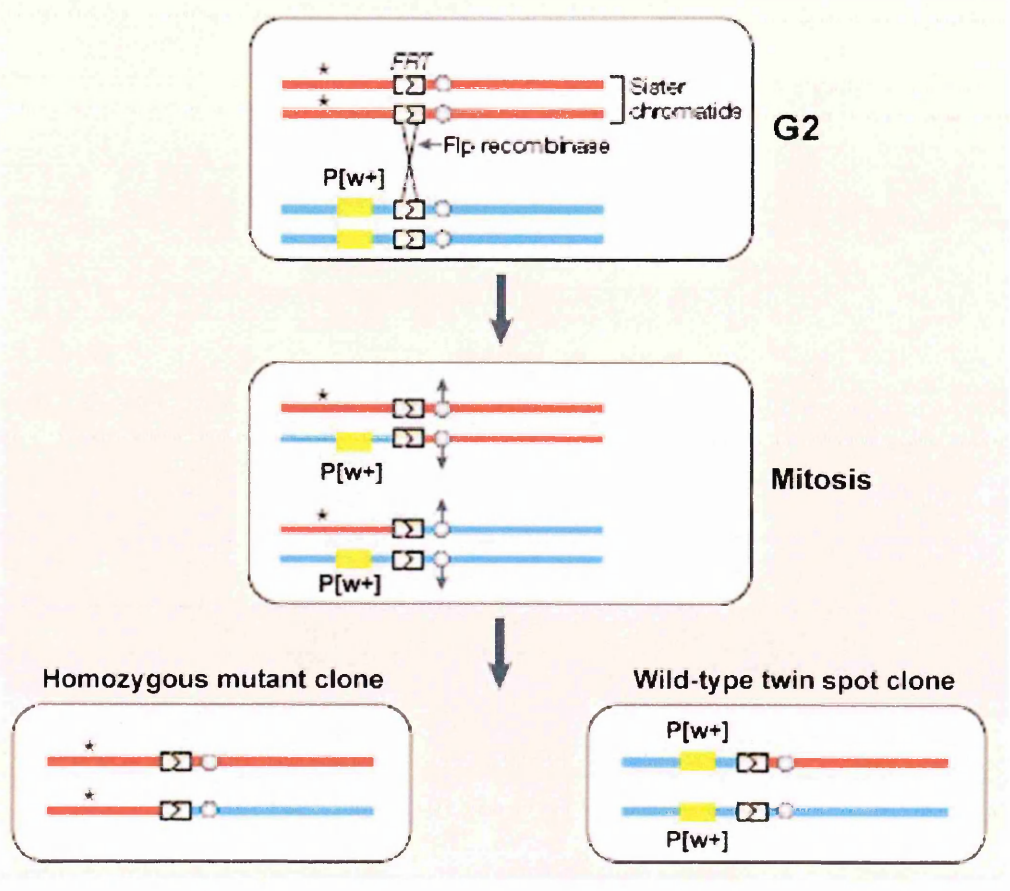

Figure 3.1 The Flp-FRT mitotic recombination (adapted from Johnston et al., 2002)

3.3 The MARCM genetic system

The MARCM (Mosaic analysis with a repressible cell marker) system has been used to induce the expression of specific transgenes exclusively inside homozygous mutant clones in the fly eye (Lai & Lee, 2006; Lee & Luo, 1999). The peculiarity is that the MARCM system combines the GAL80 repressor protein with the *Drosophila* Gal4-UAS binary system and the Flp/FRT system, in order to genetically label clones (Lai & Lee, 2006; Lee & Luo, 1999) (Fig. 3.2). In parental cells, the activity of GAL4 is repressed by the GAL80 protein. After Flp/FRT-dependent mitotic recombination, homozygous mutant cells lack GAL80 and hence possess an active GAL4. GAL4 driver can activate the transcription of reporter genes, like *GFP*, placed under the crontrol of the UAS sequence (*UAS-GFP*), specifically inside homozygous mutant cells (Lee & Luo, 1999).

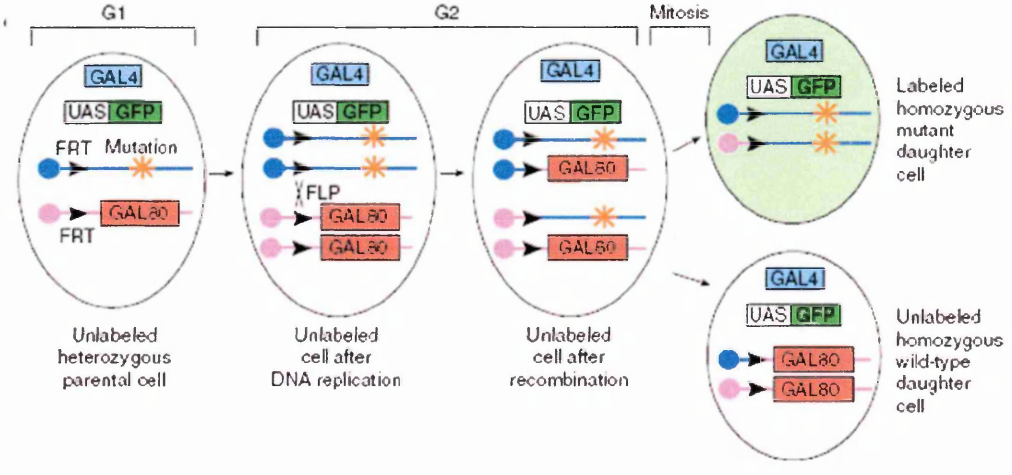

Figure 3.2 Model of the MARCM genetic system (from (Lee & Luo, 1999))

3.4 Light microscopy

Adult eyes containing homozygous mutant clones were fixed in 0.1M Na-phosphate buffer, 1% glutaraldehyde, 1% OsO4 on ice for 30 min, then incubated with 2% OsO4 in 0.1M Sodium-phosphate buffer for 2 hrs on ice,

dehydrated in ethanol washes (30%, 50%, 70%, 90% and 100%), washed twice in propylene oxide and incubated overnight in a 1:1 mix of propylene oxide and epoxy resin (Fluka). Finally eyes were embedded in pure epoxy resin and polymerized over-night at 80°C. The embedded heads were cut on a Leica UltraCut microtome using a diamond Diatome Histo knife. Retinal sections (1μm) were analysed with a Zeiss AxioplanII microscope at the ALEMBIC facility at San Raffaele Institute.

3.5 Electron microscopy

For the electron microscopy, adult heads were dissected and fixed at room temperature (RT) in 4% Paraformaldehyde (PFA); 2% glutaraldehyde in 0.12M sodium cacodylate buffer at pH 7.4 for 1 hr. The heads were then washed 3 x 10 min in 0.12M sodium cacodylate buffer, post-fixed in 2% OsO4 in 0.12M sodium cacodylate buffer for 1 hr and washed again 3 x 10 min. Afterwards, samples were dehydrated in ethanol series and infiltrated with propylene oxide, infiltrated with increasing percentages of epoxy resin series (from 30% to 100%) and finally polymerized at 80°C.

The retinal sections for the electron microscopy (80 nm) were cut on a Leica UltraCut microtome using a diamond Diatome Histo knife. Ultrathin sections were post stained with 2% uranyl acetate, followed by Reynolds' lead citrate, and stabilized for transmission electron microscopy by carbon coating. Finally sections were analysed with a Zeiss LEO912 microscope at 100 kV. Images were captured with a Gatan 792 Bioscan camera using Digital Micrograph as software.

3.6 Immunohistochemistry

Immunostainings of adult retina were performed with whole-mount preparation. Staged eyes were dissected and fixed in 4% formaldehyde in Phosphate Buffer Saline (PBS) for 1 hr. The brain was removed approximately 30 min into fixation. Fixed eyes were then given 3 x 10 min washes in PBS-T (PBS plus 0.3% Triton X-100). Washed eyes were incubated in primary antibody in PBS-T with 5% goat serum overnight at 4°C. Eyes were given 3 x 10 min washes in PBS-T and incubated for 4 hrs at RT in secondary antibody followed by an overnight staining in 2 μg/ml rhodamine-conjugated phalloidin (Sigma). After incubation, eyes were given 3 x 10 min PBS-T washes and mounted in Vectashield.

Antibodies used: mouse anti-β-galactosidase (1:1000, Promega), rabbit anti-GFP (1:500, Molecular Probe), rabbit anti-p62 (1:2000, a gift from Didier Contamine) Secondary fluorescence-conjugated antibodies from Molecular Probes or Jackson Laboratories were used at 1:200 dilutions. Samples were viewed with BioRad and Zeiss LSM confocal microscopes.

Chapter 4-7

RESULTS and DISCUSSIONS

Chapter 4

AN UNEXPECTED PHENOTYPE IN THE *Drosophila ft* MUTANT FLY EYE

The *Drosophila* Ft was first identified at the beginning of the last century because of the broad shape of weak *ft* mutants (Mohr, 1923). *ft* mutant imaginal discs, the organs that form during larval development and give rise to all the adult fly organs, could grow eight times larger than normal discs. Due to its role in cell proliferation and organ size, *ft* was considered to be a tumour suppressor gene (Bryant et al, 1988). Ft was also found to control PCP together with the cadherin Ds and the transcriptional co-factor Atro (Casal et al, 2002; Yang et al, 2002; Fanto et al, 2003).

Very recently, experiments performed in the lab demonstrated that *ft* gene transcription is downregulated by *Drosophila* Atro (F. Napoletano, unpublished), that in humans is linked to a polyQ neurodegenerative disorder (Nisoli et al, 2010). This new outcome led us to investigate the phenotype of *ft* mutants in the nervous system.

4.1 Mutations of the *Drosophila ft* gene give rise to a progressive degeneration of the adult retina

To test whether *Drosophila* Ft by itself plays a role in neuronal degeneration we started our investigation by studying age-related phenotypes in *ft* mutant neuronal tissue.

We took advantage of the fly retina to analyse the phenotype induced by *ft* mutations, since the fly eye is the most accessible and life-dispensable system to explore any possible alteration in the physiology of the nervous system. The retina of flies heterozygous for the loss of function allele, ft^{fd} is normal and all the neuronal cells that compose the fly eye, the photoreceptors, are preserved in their structure and correctly incorporated in an ommatidium (Fig. 4.1B, top left).

We crossed flies heterozygous for ft^{fd} allele, localized on the right arm of the second chromosome near to a transgenic *FRT* site, with flies whose homologous chromosome carries a *FRT* site placed at identical position and is also marked by a *mini-white* transgene, commonly used as a selectable marker because its expression is necessary for eye pigmentation (Pirrotta, 1988). Taking advantage of the *flp/FRT* genetic system, the site-specific recombination between homologues occurs after DNA-replication exclusively in the retinal tissue because of the *eyeless* specific promoter (Golic & Lindquist, 1989). Then, if the daughter chromatids segregate appropriately, the region of the chromosome arm that lies distal to the *FRT* site is made homozygous and each daughter cell inherits two copies of the same region. Thus, two groups of cells are generated: clones of cells homozygous for ft^{fd} and *wt* twin-spot clones. The genotype results heterozygous for *ft* in those part of the retina where the recombination did not occur and in all the rest of the fly's organism. Semithin sections of mosaic ft^{fd} retinae dissected from adult flies visibly showed a difference between *wt* ommatidia (Fig. 4.1B,D, top left) and those belonging to the homozygous mutant clone (Fig. 4.1B,D, right side of the section). Both *wt* twin-spot clones and ft^{fd} heterozygous cells carried the *mini-white* transgene

thus expressing pigments cells that surround each ommatidium (Fig. 4.1B,D top left).

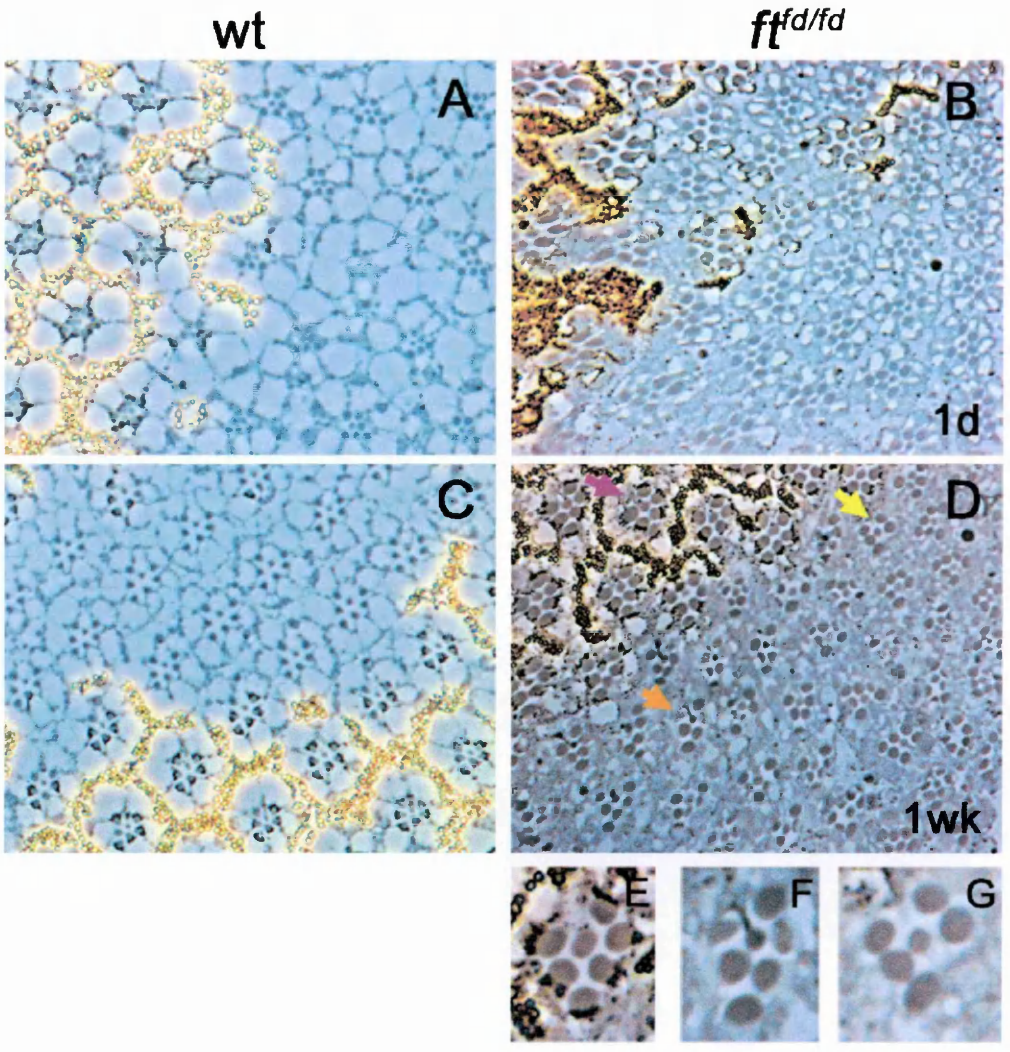

Figure 4.1 Retinal phenotype in *wt* and *ft* mutant clones of the adult fly eyes
All the flies were aged at 29°C. **A,C**- Tangential sections from one day (A) and one week old retinae (C) containing *wt* clones on a background heterozygous for a P(w+) inserted element. In both the cases the shape of the ommatidia and the number of photoreceptor cells per ommatidium is conserved and the tissue is correctly organized both in the background (presence of pigmented cells) and also inside the homozygous clone (absence of pigmented cells). **B,D**- Tangential sections of ft^{fd} mutant clones from retinae of flies aged one day (B) and one week (D) at 29°C. In both the cases retinal tissue is composed of homozygous ft^{fd} mutant clones (bottom right) inside a *wt* tissue (top left). One day old homozygous ft^{fd} tissue (B) is normal and comparable to the organization of the ommatidia inside *wt* tissue (pigmented region). Semithin section of one week old retinae (D) display an altered organization of the photoreceptors specifically inside the ft^{fd} homozygous clone. Enlargement of a *wt* ommatidium (E, pink arrow in D) shows each of the 7 photoreceptors carrying pigments at the base of the rhabdomere and the whole ommatidium surrounded by pigment cells. The majority of the ommatidia inside the clone are normal but occasionally one photoreceptor (at most) shows an abnormal conformation (F, orange arrow in D) or the total number of neuronal cells per ommatidium is reduced (G, yellow arrow in D).

By contrast, ft^{fd} homozygous ommatidia were characterized by the absence of pigments (Fig. 4.1B,D, right side of the section). Furthermore, photoreceptor cells conventionally organized on the apical portion of their cytoplasm a structure dense in microvilli, called the rhabdomere, that contained the photosensitive pigments (Fig 4.1E). Mutant photoreceptors could be distinguished from the *wt* ones by the absence of pigments at the base of their rhabdomeres (Fig. 4.1F,G). Fly crosses were made at room temperature (18°-19°C) and, to exclude a contribution of mis-development on our analysis, the progeny was moved to higher temperatures only after flies eclosion. The developmental period for *Drosophila melanogaster* varies with temperature, as with many ectithermic species. The shortest development time (egg to adult), 7 days, is normally achieved at 28/29°C, when the fly lifespan is about 30 days at 29°C (Ashburner, 1978). The accepted range of temperatures among which *Drosophila* life-cycle correctly occurs without any developmental defect or problem with fertility, is from 17°C to 29°C as maximum. We therefore decided to age flies at 29°C just to make our data analysis more rapid.

Although initially *wt* for morphology (Fig 4.1B), after one week at 29°C adult flies displayed an alteration in the morphology of some *ft* mutant ommatidia specifically inside the clone (Fig. 4.1D), whereas the *wt* tissue was entirely normal. The differences we detected inside *ft* homozygous tissue have been grouped in two main categories: modification in the shape and structure (Fig. 4.1F) and decrease in the total number of photoreceptors per ommatidium (Fig. 4.1G).

Since the abnormalities observed in the one week old *ft* mutant ommatidia could be the manifestation of a gradual cellular process, we wondered whether ft^{fd} retinal phenotype could change with time. Several ft^{fd}

mutant flies were thus collected, aged at 29°C for different time points and the phenotype of the fly eye was examined.

The progressiveness of the phenotype was scored through a blind test in which I did a quantitative analysis of the eye morphology in a number of ft^{fd} flies aged one week at 29°C compared with the same number of older siblings aged two weeks in the same conditions. The results were then checked by a second investigator just to confirm my analysis. The sections were classified in three distinct categories: low, medium and severe.

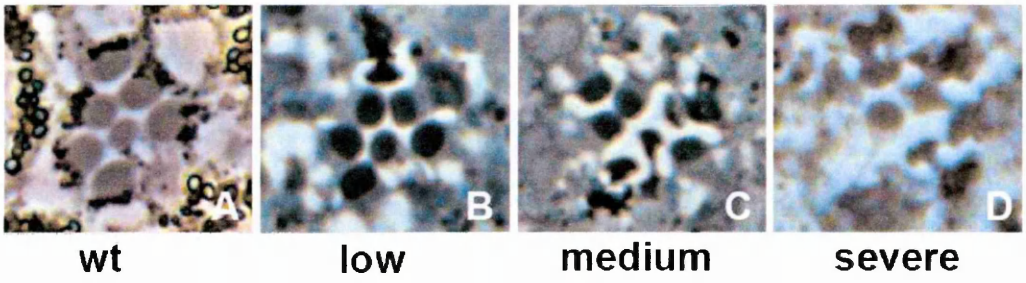

Figure 4.2 Classification of the level of degeneration in $ft^{fd/fd}$ retinal tissue
Sections were classified in distinct categories, low, medium and severe depending on the level of mutant photoreceptors abnormalities with respect to the *wt* (A). Low, when the clone is almost totally normal and only occasionally one photoreceptor is lost or displays an altered morphology (B). Medium, when very few ommatidia are preserved and the majority of them have at least two photoreceptors reduced in size or altered in the conformation (C). Severe, when the tissue inside the homozygous clone presents large gaps and almost all photoreceptors are abnormal (D).

The abnormality was scored as low when the majority of the ommatidia inside the clone appeared normals (Fig. 4.2A) with only a few containing at most one abnormal or missing photoreceptor (Fig. 4.2B). In the medium category were included the sections in which, although the trapezoidal shape was still recognizable, very few mutant ommatidia were totally preserved whereas most of them showed at least two photoreceptors altered (Fig. 4.2C). Sections in which it was rare to find correctly structured photoreceptors inside the clone and where the mutant tissue was collapsed belonged to the severe category (Fig. 4.2D). In very rare cases, distinct

clones within the same eye showed different levels of degeneration; for this reason their contribution has been split to different categories of neurodegeneration.

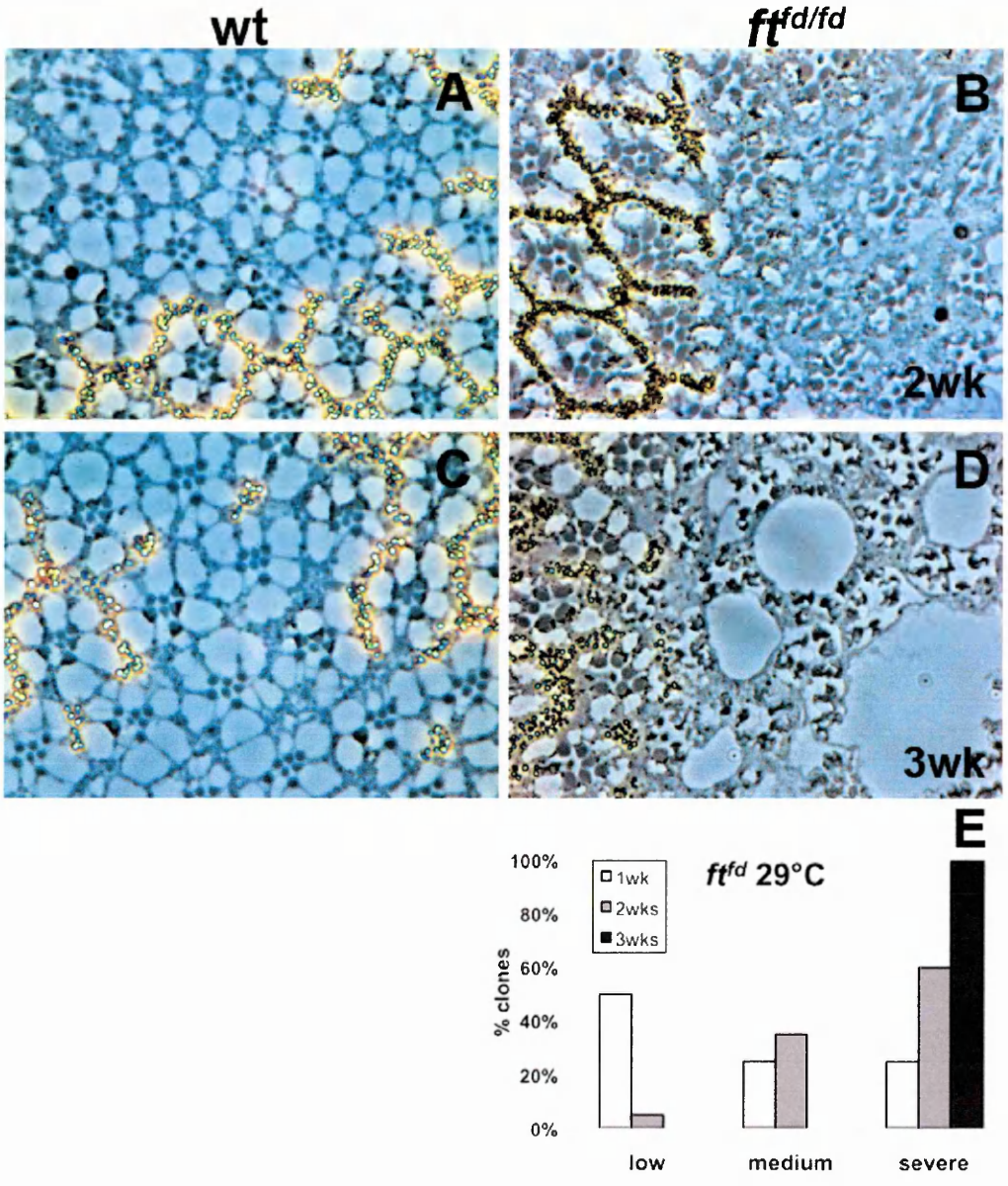

Figure 4.3 Progressive retinal degeneration in *ft*^{fd} mutant clones from flies aged at 29°C

A,C- Semithin sections of *wt* homozygous clones isolated from adult flies aged two (A) and three weeks (C) at 29°C. In both the examples photoreceptors belonging to the homozygous tissue (absence of pigments) are preserved and comparable to the cells of the heterozygous tissue (presence of pigments). **B**- Semtihin section of *ft*^{fd} mutant clones from retinae aged two weeks at 29°C. Degeneration of the cells inside the *ft*^{fd} homozygous clone is evident and the majority of the mutant ommatidia contain at least two abnormal or lost photoreceptor cells. **D**- Semithin section from three weeks old *ft*^{fd} mutant retina. The phenotype is extremely severe, the tissue is full of large gaps and it is very rare to distinguish ommatidial conformation or to find normal photoreceptors. **E**- Quantification of the level of degeneration in *ft*^{fd} mutant clones aged at 29°C for different time points and analyzed in blind. After one week of age, half of the *ft*^{fd} homozygous clones display

a low level of degeneration, 25% medium and 25% are severely degenerated (N=15 clones). After two weeks only 5% of the clones observed is still low degenerated whereas 60% belong to the severe category (N= 15 clones). After three weeks all the ft^{fd} homozygous clones analyzed are severely degenerated (N= 8 clones).

About half of the semithin sections isolated from one week old ft^{fd} mutant clones were scored as low degeneration (Fig. 4.3B), since they contained few ommatidia with one photoreceptor missing or abnormal, the rest being totally normal (Fig. 4.1B). After two weeks the mutant phenotype became more evident and more than half of the sections studied were classified as severely degenerated (Fig. 4.3A,B). The majority of the cells inside the clone were altered and exhibited abnormalities in the shape of both the cytoplasm and the rhabdomere (Fig. 4.3A). However, the trapezoidal form of the mutant ommatidia was mostly conserved.

Taken together, these data indicated that the phenotype of two weeks old *ft* mutant clones was more severely affected when compared with clones from younger flies of the same genotype (Fig. 4.3B).

Older $ft^{fd/fd}$ clones, aged three weeks at 29°C, were also studied but not included in the blind test analysis because very few mutant flies survived until that age. The retinal phenotype was dramatic in almost all the $ft^{fd/fd}$ clones (Fig. 4.3C); the mutant tissue was largely disrupted with a lot of gaps specifically located inside the clone. Mutant photoreceptors had lost their contacts with the neighboring cells. Recognition of the shape of the ommatidia was almost impossible.

In conclusion the experiment revealed a significant and progressive increase in the severity of *Drosophila ft* neuronal degeneration phenotype.

4.2 *ft*^{fd} retinal degeneration also occurs at lower temperatures

When the study of retinal degeneration in *ft* mutants was set up, adult flies were aged at 29°C. Such a high temperature could lead to a stress condition. Consequently, the abnormalities detected in *ft*^{fd} mutant photoreceptors could be due to stress. To check this possibility, we investigated whether the progress in *ft*^{fd} neurodegeneration is influenced by the temperature.

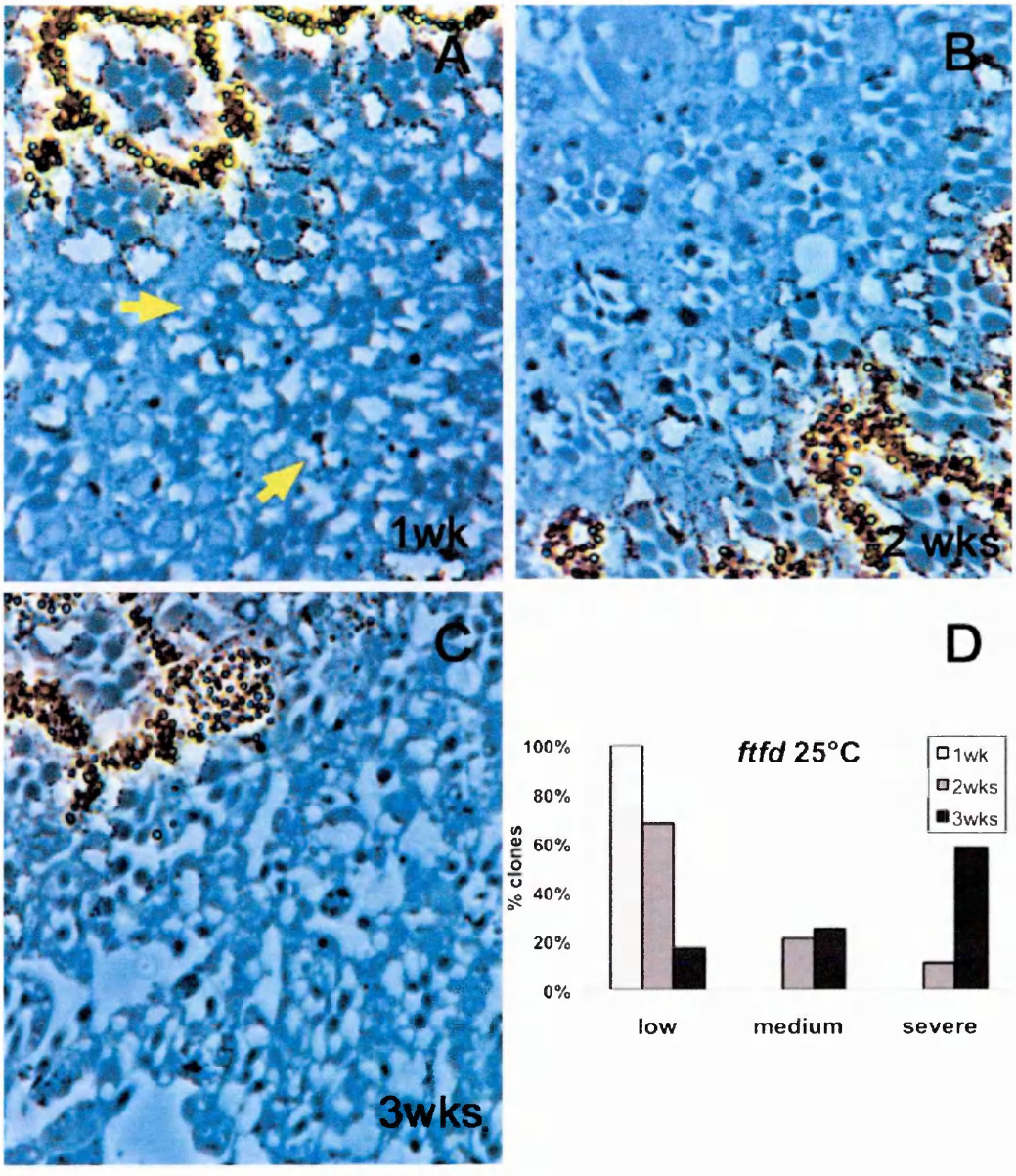

Figure 4.4 Retinal degeneration in *ft*^{fd} mutant clones from flies aged at 25°C
A- Semithin section of one week old fly retina displays a low level of photoreceptor degeneration specifically inside the *ft*^{fd} homozygous clone. The majority of the ommatidia inside the clone are normal but occasionally one photoreceptor (at most) shows an abnormal conformation (bottom yellow arrow) or the total number

of neuronal cells per ommatidium is reduced (top yellow arrow). **B**- Semithin retinal section from flies aged two weeks at 25°C. Degeneration of the cells inside the ft^{fd} homozygous clone is evident but the majority of the mutant ommatidia contain at maximum two abnormal or lost photoreceptor cells. **C**- Semithin section from three weeks old ft^{fd} mutant retina. The phenotype inside the clone is extremely severe, the trapezoidal conformation of mutant ommatidia is not distinguishable and most of the photoreceptors have degenerated. **D**- Quantification of the level of degeneration in ft^{fd} mutant clones aged at 25°C for the same time points chosen for the previous study and analyzed in blind. After one week of age, all the ft^{fd} homozygous clones display a low level of degeneration (N=10 clones). After two weeks more than half of the clones are still low degenerated whereas only 10% belong to the severe category (N=15 clones). After three weeks the number of ft^{fd} clones with a low level of degeneration is strongly reduced (17%) and there is an increase in the number of clones belonging to the medium (25%) and to the severe category (58%) (N=15 clones).

The phenotype of ft^{fd} mutant clones coming from adult flies with the same genetic background, but aged at 25°C, was analysed at the same time points. Almost all semithin sections dissected from one week old flies displayed a low level of degeneration inside the ft^{fd} homozygous clone, with most mutant ommatidia being normal in shape and content (Fig. 4.4A,D). After two weeks at 25°C more than half of the ft^{fd} mutant clones analyzed were still largely normal, although about 20% of the ft^{fd} clones showed a medium level of degeneration (Fig. 4.4B,D) and fewer than 10% of ft^{fd} clones were severely affected. The majority of mutant retinae isolated from three weeks old ft^{fd} flies were severely degenerated (Fig 4.4C).

In conclusion, the data obtained from *ft* retinal phenotype indicated that neurodegeneration was faster when flies were aged at 29°C if compared to *ft* flies aged at 25°C. This is consistent with the general metabolic rate, the duration of the life cycle and life span at these two temperatures.

Thus, the analysis confirmed that *ft* mutation leads to a progressive retinal degeneration which does not depend on the temperature except than for the rapidity through which the severity of *ft* phenotype increases. We can exclude that the 29°C phenotype and time-course are due to speed of

development because the progeny was left at room temperature until the pupation and only adult flies were put at 29°C.

4.3 The retinal phenotype caused by a distinct mutation of the *Drosophila ft* gene, ft^{82}, confirms the ft^{fd} neuronal degeneration

The histological studies previously shown were done by inducing the formation of clones homozygous for a strong loss of function allele against *ft* gene, the ft^{fd} allele. To exclude the possibility that the phenotype depends on that precise mutation or on a secondary mutation induced on the ft^{fd} chromosome arm, we designed a set of experiments using a distinct mutant allele of *ft*.

We decided to leave out ft^{GRV}, the first loss of function *ft* allele to be isolated and characterized (Bryant et al, 1988; Mahoney et al, 1991) because the mutant ommatidia were extremely abnormal. The larger rhabdomeres appeared fused together and the inter-rhabdomeral space was no longer detectable, giving rise to a phenotype that was not time-dependent. Since the distinction of the single photoreceptor cells became impossible, a quantification of the degeneration could not be achieved. This alteration might be the result of an additional mutation present on the ft^{GRV} chromosome.

For this reason, we decided to analyze clones for ft^{82} allele (gift from P.Bryant), although the exact nature of the lesion in ft^{82} is unknown. Comparison of microscopic sections from ft^{82} mutant clones of flies aged one week (Fig. 4.5A) or three weeks at 29°C (Fig. 4.5B), confirmed the ft^{fd} progressive alteration of the neuronal phenotype observed with ft^{fd}. ft^{82} homozygous clones from older flies (3 weeks), displayed a number of abnormal or missing photoreceptors, specifically inside the mutant tissue,

that resulted increased if compared to younger mutants. However, the abnormalities we observed in the ft^{82} mutant photoreceptors were much fewer and weaker than in those of the ft^{fd} mutants at the same time points (Fig. 4.2, Fig. 4.3). No severely affected clones were ever found. This may imply also that the mutation giving rise to the ft^{82} allele is weaker than the ft^{fd} mutation.

However, these results indicate that *ft* induced neurodegeneration is not caused by the nature of the ft^{fd} mutation.

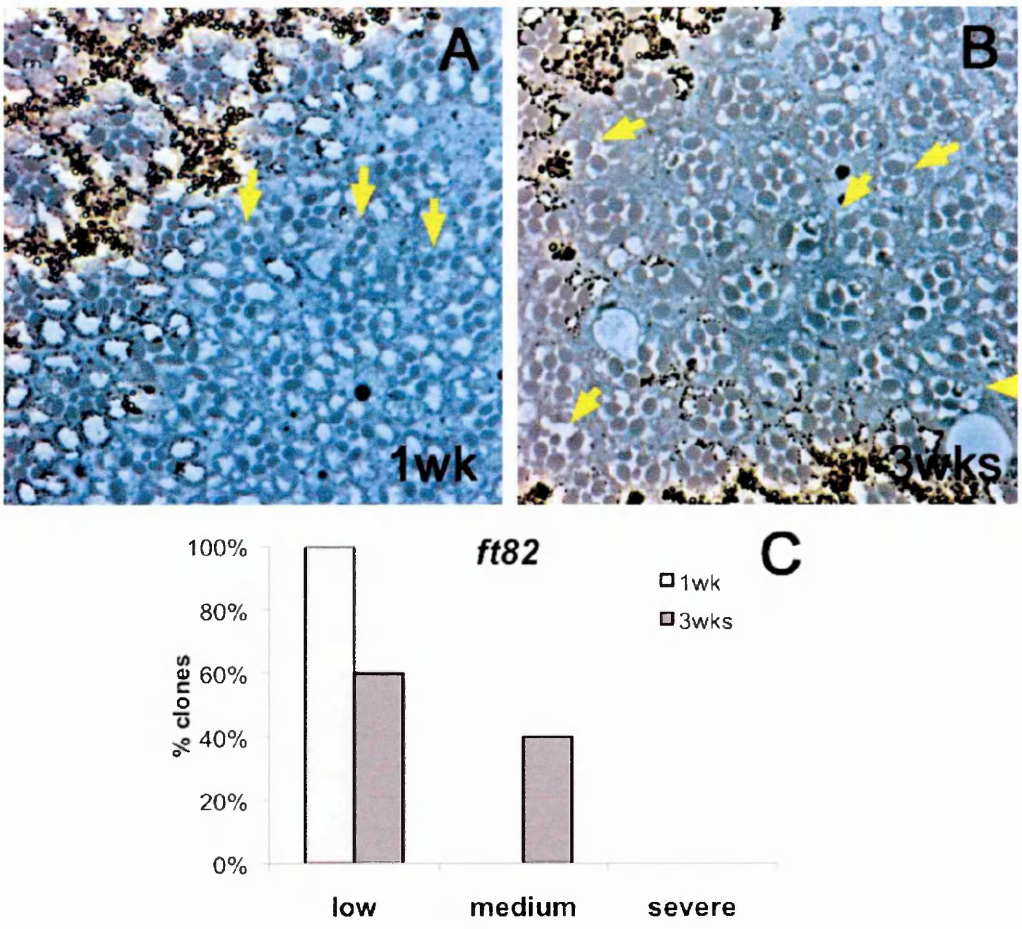

Figure 4.5. Degenerative phenotype in ft^{82} mutant clones of the fly eye
A- Semithin section of ft^{82} mutant tissue from one week old retina. Degeneration is found very rarely and at low levels in few ommatidia (yellow arrows) specifically inside the homozygous clone. **B**- Older ft^{82} mutants, three weeks old, reveal an increase in the severity of retinal phenotype. The majority of ommatida inside the clone contain abnormal or lacking photoreceptors (yellow arrows) and only rarely mutant ommatidia contain the expected number of photoreceptors. **C**- Quantification of the level of degeneration in ft^{82} mutant clones aged at 29°C for different time points and analyzed in blind. After one week of age, all the ft^{82} homozygous clones display a low level of degeneration (N=10 clones). The mutant retinal tissue of older ft^{82} mutant flies,

aged three weeks in the same conditions, results in an increased degenerative phenotype. 60% of the homozygous clones observed are still low degenerated abd 40% of them display a medium level of degeneration (N=10 clones).

4.4 Inhibition of *ft* gene function, by a specific RNA-mediated gene interference, is sufficient to induce a progressive retinal degeneration in adult fly eyes

To confirm *ft* induced retinal degeneration by a different approach and exclude any influence of developmental effects and of the flp/FRT clonal system used so far, we took advantage of commercially available transgenic flies expressing a specific RNA interference (RNAi) against *ft* (ft^{IR}). RNA silencing has proven to be a good alternative to the canonical forward genetics. Therefore, it can be used as a flexible tool to target gene inactivation to any desired cell type at any stage of the *Drosophila*'s lifespan (Dietzl et al.,2007).

To address whether the specific silencing of *ft* in adult post-mitotic cells was sufficient to drive neurodegeneration, the RNAi construct against *ft*, $UASft^{IR}$, was expressed only in the adult photoreceptor neurons. This was possible thanks to the eye-specific *GMR* (glass multiple repeats)-*Gal4* driver, combined with ubiquitous expression of a temperature-sensitive mutant of the *Gal80* repressor that inhibits GAL4-driven transcription at the permissive (low) temperature. With this method, when the flies were raised at 18°C, $UASft^{IR}$ transgene was not expressed. Shifting the flies at 29°C, resulted in *Gal80* inactivation and *Gal4*-dependent transgene expression.

New-born ft^{IR} expressing flies moved from 18°C to 29°C for only one day, were all normal and the retinae contained the correct number of photoreceptors in each mutant ommatidium (Fig. 4.6B,C). They resembled

the retinae of respective control flies (*w*^{1118}*;GMR-Gal4;Gal80/+)* (Fig. 4.6 A,C).

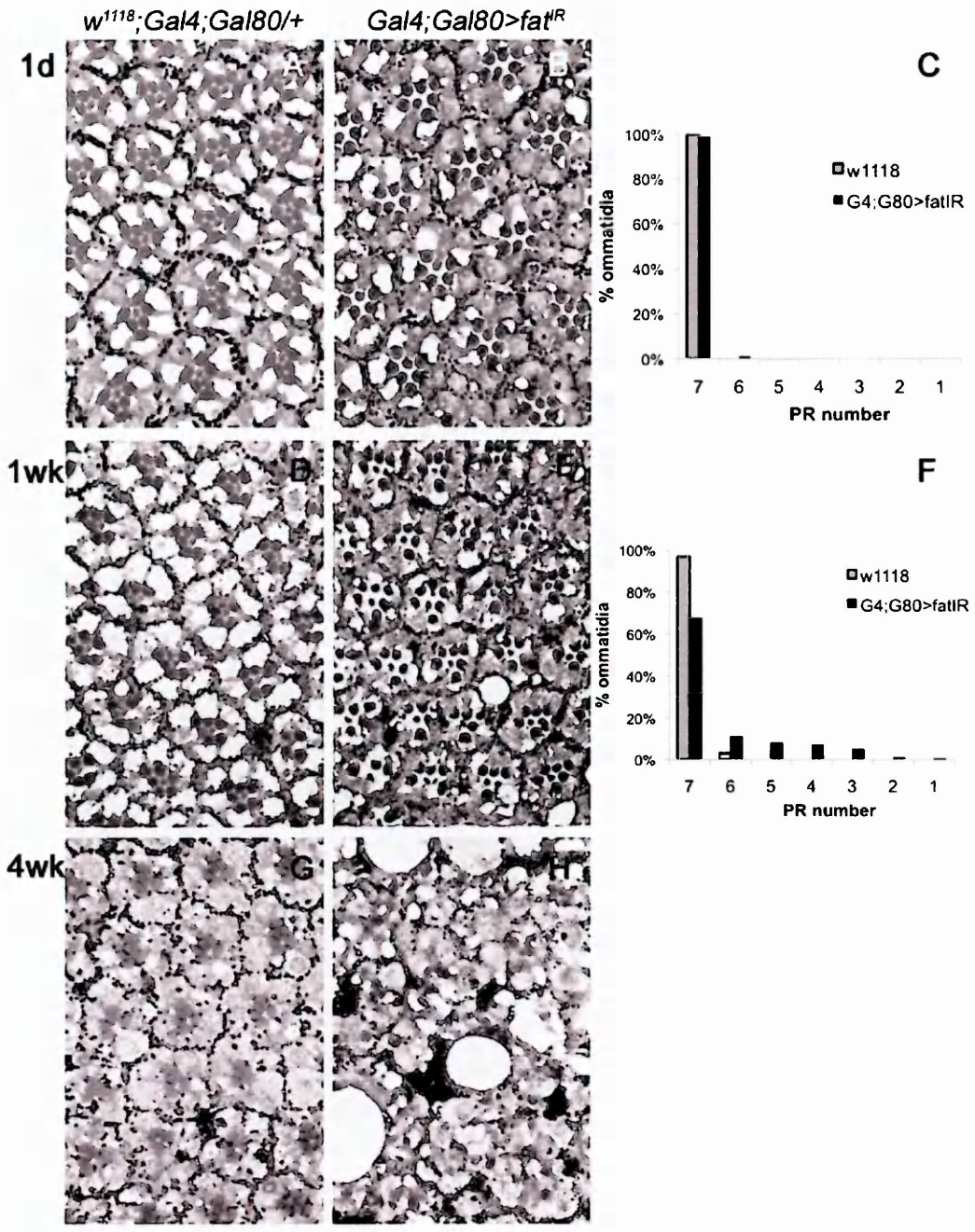

Figure 4.6 RNA interference against *ft*, expressed exclusively in the adult retinal tissue, induces a progressive degeneration
A,B- Semithin sections from *GMR-Gal4>UASft*^{IR}*;Ubi-Gal80*^{ts} retina (B) and its control (A, *w*^{1118}*;GMR-Gal4;Ubi-Gal80*^{ts}*/+)* coming from flies aged one day at 29°C. In both the cases the tissue is almost entirely normal and each ommatidium contains the correct number of photoreceptor cells. **C**- Histogram showing the number of photoreceptors (PR) in *w*^{1118} *;GMR-Gal4;Ubi-Gal80*^{ts} (grey) and *GMR-Gal4>UASft*^{IR}*;Ubi-Gal80*^{ts} (black) flies aged for 1 day at 29°C. Most of *ft*^{IR} mutant ommatidia contain 7PR and a very low number of them (1%) have lost one photoreceptor cell. The chart represents blind counts of 611 ommatidia (10 flies) for the control and 530 ommatidia (10 flies) for *GMR-Gal4>UASft*^{IR}*;Ubi-Gal80*^{ts} from three independent experiments. **D,E**- Semithin sections of *GMR-*

Gal4>UASft^{IR};Ubi-Gal80^{ts} retina (D) and its control (C) coming from flies aged one week at 29°C. The downregulation of *ft* results in a significant loss of PR cells per ommatidium whereas the control retinae are still normal. **F-** The chart at 1week represents blind counts of 300 ommatidia (6 flies) for the control and 564 ommatidia (12 flies) for *GMR-Gal4>UASft^{IR};Ubi-Gal80^{ts}* from three independent experiments. Chi-square 30.18; $p<0.01$ for six degrees of freedom. **G,H-** Semithin sections of *GMR-Gal4>UASft^{IR};Ubi-Gal80^{ts}* retina (H) and its control (G) coming from flies aged four weeks at 29°C. The *ft^{IR}* mutant retinal tissue is increasingly disorganized and under collapse. The number of PR is reduced and mutant cells are difficult to distinguish whereas the control tissue is almost entirely normal with few PR lost.

However, *GMR-Gal4>UASft^{IR}* flies underwent an age-dependent loss of photoreceptors. As a consequence, the number of ommatidia containing a full complement of neuronal cells significantly decreased when flies were aged one week at 29°C (Fig. 4.6 E,F).

Older *ft^{IR}* mutants aged four weeks at 29°C displayed a more severe retinal phenotype, with most of the photoreceptors lost per ommatidium (Fig 4.6H). Since at this latter time-point the shape of ommatidia in *GMR-Gal4>UASft^{IR}* became very difficult to distinguish and the tissue was collapsing, the quantification was not performed. Control retinae were normal at all timepoints (Fig. 4.6 A,D,G).

To summarize, the data obtained by *ft* RNA silencing during the adulthood confirmed the progressive retinal degenerative phenotype observed in *ft^{fd}* and *ft^{82}* mutant fly eyes. These results excluded the possibility that the phenotype was a result of the flp/FRT clonal generation. Interestingly, this outcome also suggested that *ft* retinal degeneration could arise independently of developmental influences, although a contribution of developmental processes to degeneration could not be totally ruled out in the case of *ft* clones.

4.5 Contribution of Ft canonical cell adhesion and planar polarity functions to the retinal degenerative phenotype

Ft is a heterophilic adhesion molecule involved not only in tissue growth but also in cell adhesion and in a specific form of polarity, called planar cell polarity (Yang et al., 2002; Casal et al., 2002). In order to understand the Ft-dependent mechanism that protects neurons from degenerating, the next question was whether the Ft role as a cell adhesion molecule or its regulation of PCP could have any impact on neurodegeneration.

4.5.1 Cadherin functions are not responsible for the neuronal alterations

Ft was the founding member of the Ft-like cadherins subfamily (Tanoue & Takeichi, 2005). To investigate whether *ft* neuronal degeneration could be due to the generic activity of Ft as a cadherin, we targeted one of the classical cadherins and assayed neuronal degeneration.

In *Drosophila*, six cadherin superfamily members have thus far been identified. Shotgun, or DE-cadherin is a homolog of classic vertebrate cadherins and, to date, the best characterized *Drosophila* cadherin. Previous studies had shown Shotgun to be expressed predominantly in epithelial tissues where it was of fundamental importance in assembling the adherens junction (Tepass et al, 1996).

We induced the expression of a specific transgenic RNA interference against *shotgun* cadherin and asked whether it could lead to a phenotype comparable to *ft* degeneration. Because of its relevance during several steps of the fly development, we took advantage of the *GMR-Gal4/Gal80*

inducible system and the RNAi transgene against *shotgun*, *shotgun*^{IR}, was expressed exclusively in the adult fly retina.

One week old *shotgun*^{IR} mutant fly eyes displayed, as expected, some defects due to the loss of the correct junctions among neighboring ommatidia, as shown by the random interruption of sorrounding pigmented cells (Fig. 4.7B).

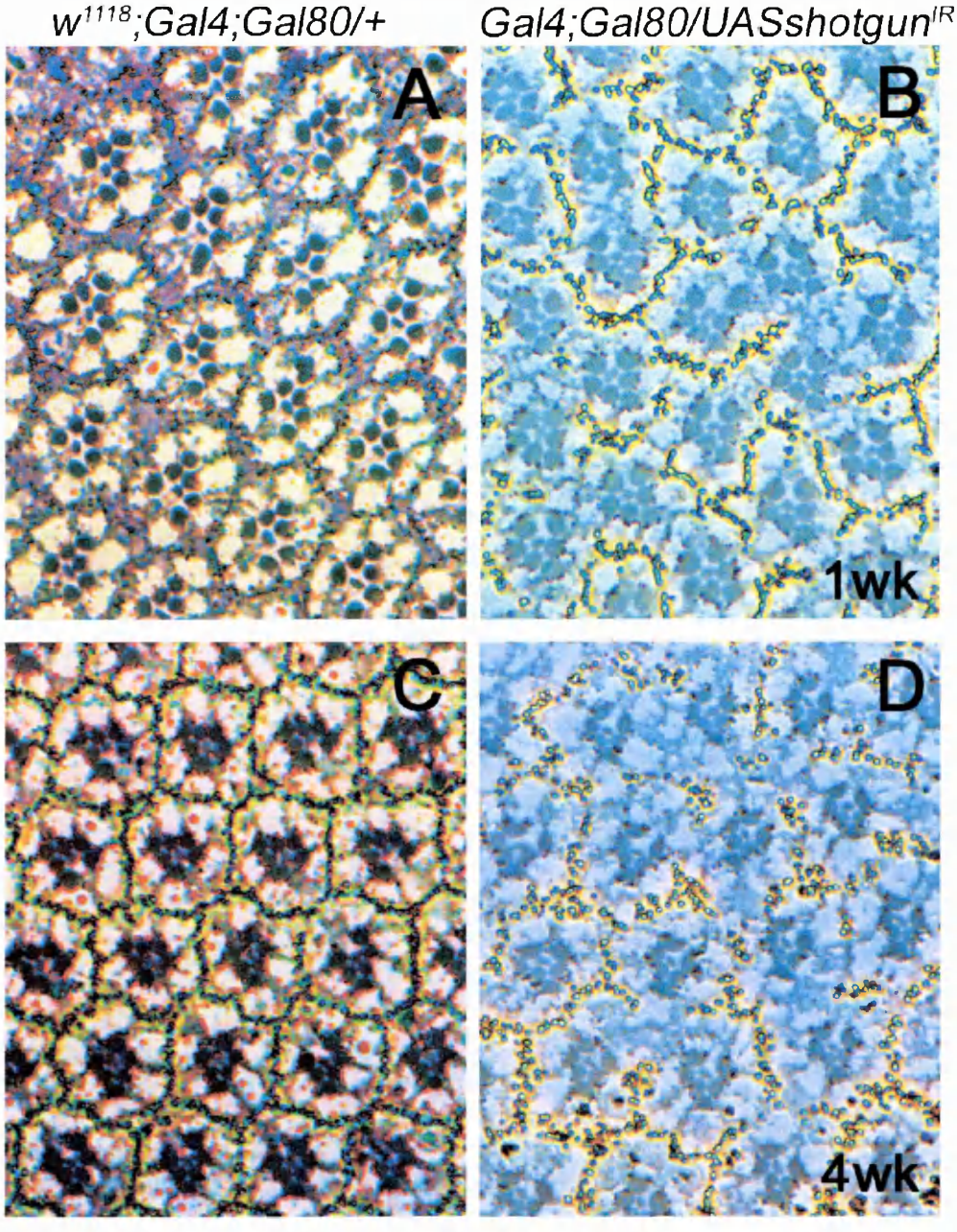

Figure 4.7 RNA interference against *shotgun* cadherin does not cause retinal neurodegeneration
A,B- Semithin sections of *GMR-Gal4> UASshotgun*^{IR}*;UbiGal80*^{ts} retina (B) and its control (A, *w*^{1118}*;GMR-Gal4;UbiGal80*^{ts}*/+)* coming from flies aged one week at 29°C. In both the cases the tissue is almost entirely normal and each

ommatidium contains the correct number of photoreceptor cells. The only defects observed in *shotgun*^{IR} mutant retinae are due to the loss of the correct junctions among neighboring ommatidia, as shown by the random interruption of sorrounding pigmented cells (B). **C,D**- Semithin sections from *GMR-Gal4> UASshotgun*^{IR}*;UbiGal80*^{ts} retina (D) and its control (C) coming from flies aged four weeks at 29°C. In both the cases the tissue is still almost entirely normal and the number of photoreceptor cells per ommatidium is preserved.

Some mutant ommatidia were also misrotated but the number of photoreceptors per ommatidium was conserved both after one week (Fig. 4.7B) and in older mutants aged four week at 29°C (Fig. 4.7D), indicating that downregulating *shotgun* RNA does not lead to a progressive retinal degeneration. Control retinae were normal at both time points (Fig. 4.7A,C).

These analyses suggested that generic cadherin functions are not required for protection against neuronal degeneration and consequently it is unlikely that Ft cadherin activity is responsible for neurodegeneration. However, I cannot exclude that the RNAi downregulation of *shotgun* is not sufficiently effective to unveil its role in adult neuronal protection.

4.5.2 *ft* retinal abnormalities are not initiated by alterations in cell adhesion

Like other cadherins, Ft is a transmembrane protein involved in organizing the adherens junctions, the cellular junctions localized at the apico-lateral boundary of epithelial cells. The role of Ft is thereby critical to maintain cell-cell contact and preserve the integrity of the *Drosophila* epithelium.

To analyze an eventual contribution of adherens junctions in degeneration, we checked whether their architecture was disrupted in *ft* mutant photoreceptors cells, marked by the absence of pigments at the basis of their rhabdomere. Electron microscopy study performed on eleven

day old *ft* mutant retinae indicated that the morphology of adherens junctions was preserved in degenerated photoreceptors (Fig. 4.8B). Their architecture was totally comparable to the *wt* ones (Fig. 4.8A). Accordingly, from the morphologic analysis of *ft* mutant ommatidia it is unlikely that the *ft* degenerative phenotype initiates from the loss of cell-cell contacts.

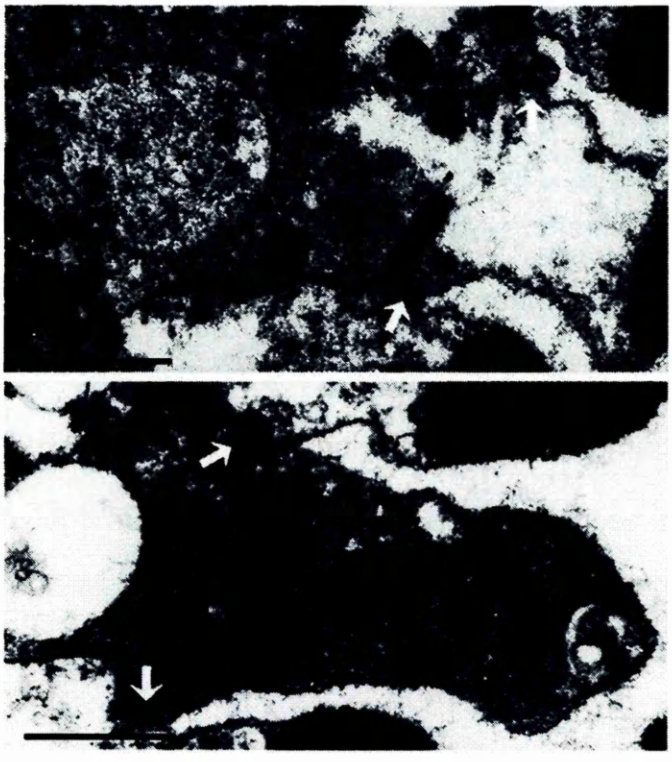

Figure 4.8 Cell adhesion function is maintained in ft^{fd} degenerated photoreceptors
A- EM scan of a *wt* photoreceptor cytoplasm in the surrounding pigmented tissue coming from the *wt* tissue of a ft^{fd} mutant fly eye aged 11 days at 29°C. White arrows indicate adherens junctions.
B- EM scan of a ft^{fd} degenerated photoreceptor from ft^{fd} clone of flies aged 11 days. Arrows point at intact adherens junctions that correctly maintain contacts with neighbouring cells. Scale bars 1μm.

4.5.3 The *ft*-induced neurodegeneration is a cell autonomous event, different from the *ft*-caused planar polarity defect

ft was demonstrated to regulate planar polarity in the eye, and distinct models have been proposed to explain how it could happen (Rawls et al, 2002; Yang et al, 2002). A peculiar feature of clones homozygous for *ft* was that disruption of PCP was restricted to polar regions of the clone. Moreover, genetically *wt* ommatidia located on the border side of the clone were frequently non-autonomously affected and displayed planar polarity defects (Rawls et al, 2002; Yang et al, 2002). By contrast, I could not detect any non autonomous spreading of neurodegeneration outside the *ft* clones.

However it was still possible that *ft* mutant cells influence neighbouring *wt* cells in mixed mosaic ommatidia.

To clarify whether *ft* induced neuronal degeneration was a strictly cell-autonomous event, I analyzed photoreceptor cells from the border of ft^{fd} mutant clones. I examined more than one hundred ommatidia from *ft* mutant fly eyes that resulted severely degenerated and classified as either pigmented (that means derived to the *wt* tissue) or unpigmented (homozygous for ft^{fd}).

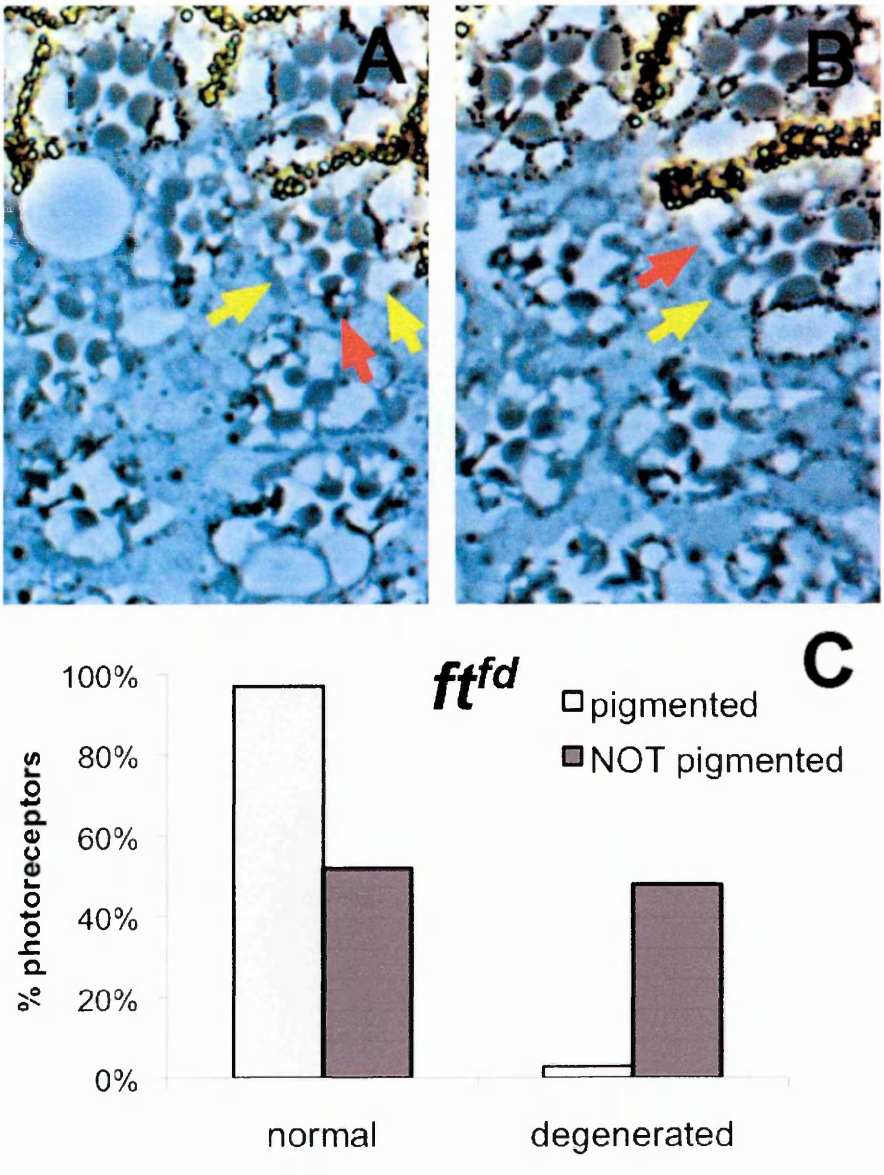

Figure 4.9 *ft*-induced retinal degeneration is a cell-autonomous phenomenon

A,B- Semithin sections of ft^{fd} mutant retinae from severely degenerated ft^{fd} fly eyes. Ommatidia on the border of *wt* tissue (top,

characterized by the presence of pigmented cells) and ft^{fd} homozygous clone (bottom, absence of pigments) contain both normal (yellow arrows) and degenerated ft^{fd} photoreceptors (red arrows). **C**- Quantification of the number of normal cells (first two columns on the left) and degenerated cells (last two columns on the right) among *wt* pigmented cells (light grey columns) and f^{fd} homozygous non pigmented cells (dark grey columns). At this stage of degeneration approximately half of the non pigmented (genotypically mutant) PR cells displays a degenerative phenotype, whereas a very low number (3%) of pigmented cells (genotypically *wt*) were degenerated and most of them were normal in their conformation. The difference among these categories was statistically significant. Chi-square=82.38, $p<0.001$.(N=310 pigmented and N= 317 non pigmented photoreceptors).

Among these two classes, photoreceptors were classified as normal or degenerated (Fig. 4.9C). Most of the ommatidia observed at the clone edge contained both normal ft^{fd} homozygous cells (Fig 4.9A,B yellow arrows) and ft^{fd} cells that have degenerated (Fig 4.9A,B red arrows). Interestingly it was found that almost all photoreceptors with an abnormal morphology lacked their pigment, whereas most of the adjacent contacting pigmented photoreceptors were normal (Fig 4.9A,B).

In conclusion this analysis demonstrated that retinal degeneration caused by *ft* mutations is a cell-autonomous event and that *wt* photoreceptors are not affected by adjacent degenerated cells.

4.6 DISCUSSION

In the first part of my work I have demonstrated that the *Drosophila* tumour suppressor Ft is required to repress retinal neurodegeneration.

Phenotypic analysis of *ft* homozygous mutant tissue revealed abnormalities in the morphology of neuronal cells specifically inside the clones of the fly eye. Strikingly, homozygous mutant clones for *ft* in the eye brought about progressive retinal degeneration. Although *ft* mutant tissue was normal after eclosion from the pupal case, photoreceptors started

degenerating in aged flies and soon the whole *ft* mutant tissue had fallen apart. This phenotype was seen for two distinct *ft* mutant alleles, the stronger ft^{fd} (Fig. 4.1, 4.3, 4.4) and the weaker ft^{82} (Fig. 4.5) alleles, and also following RNAi knockdown of *ft* in the retina (Fig. 4.6).

Flies heterozygous for *ft* were normal and did not display any cellular defect. After inducing recombination inside the retina, we obtained loss of *ft* function in a group of neuronal cells that subsequently showed abnormal morphology of photoreceptors. After one week, fly adult retinae aged at 29°C already show degeneration in a high number of *ft* mutant clones (around 50%).

We currently do not know when this phenomenon starts, but there is evidence in the literature suggesting that cell specification occurs properly in *ft* mutant clones, during fly eye development, and that all cells destined to become photoreceptors differentiate correctly (Fanto et al, 2003). Immunofluorescence previously performed on larval eye imaginal discs of *ft* mutant clones to understand the requirement of Ft in photoreceptor specification revealed that Bar, a marker specific for the R1 and R6 outer photoreceptors, was correctly localized and expressed in *ft* mutant cells (Fanto et al, 2003; Yang et al, 2002). This led us to exclude a linkage between the phenotype we found in mature photoreceptors and defects in their cell fate.

RNAi knockdown of *ft* in the retina also gave rise to a progressive neurodegeneration (Fig. 4.6), showing that also with a distinct genetic approach we obtained a progressive and significant loss of photoreceptor cells lacking *ft*. Tangential sections from *ft* RNAi mutant retinae of one day old flies, showed a normal phenotype, thus supporting our idea that the

main factor causing defects in mutant ommatidia was activated after the pupal stage.

These outcomes suggested an important role of Ft in the maintenance of neuronal homeostasis. We argue that Ft belongs to a signaling pathway that supports cell survival and prevents a progressive degeneration of the adult nervous system.

Ft is a multifunctional protein that was described to take part in several cellular processes. We thus assessed the process through which Ft might affect neuronal homeostasis. Our study on mosaic clonal phenotype revealed that genetically *wt* ommatidia were not susceptible to degeneration (Fig.4.9), demonstrating that degeneration by *ft* was strictly cell autonomous, similar to the effect of polyQ Atrophin and in contrast to the *ft* PCP phenotype (Fanto et al, 2003). Neuronal degeneration did not appear to be linked to the position of the ommatidia or the single cell inside the clone. It is likely to be an intrinsic pathway which starts from inside the cell and does not receive any input, at least initially, from the environment.

So, what might cause *ft* degeneration? Ft was discovered as one of the first *Drosophila* cadherins, for this reason linked to cell adhesion mechanisms (Bryant et al, 1988; Mahoney et al, 1991). It is localized at the apical membrane in the proximity of adherens junctions. Several proteins are required both for polarity and establishment of the photoreceptors' architecture. Among them, Crumbs and DPATJ have been shown to be necessary in the maintenance of the microvilli organization and the stability of photoreceptors (Pellikka et al, 2002). Lack of one of the two proteins leads to a progressive neurodegeneration (Johnson et al, 2002; Richard et al, 2006).

Ft could play a similar role. However, electron microscopic images of *ft* mutant eyes showed a preserved and well organized architecture of rhabdomeres belonging to mutant cells (Fig. 4.8). Even when degeneration was advanced, they continued to maintain contacts with adjacent cells without losing adherens junctions' organization. This argues against a requirement of cell adhesion or planar polarity for *ft* degenerative phenotype, suggesting the hypothesis that the phenomenon arises inside the cellular cytoplasm.

Finally, we cannot exclude that retinal degeneration caused by *ft* mutations is the consequence of an alteration in the metabolism of light inside mutant photoreceptor cells, as we have been unable to assess the contribution of light to neurodegeneration by *ft*. Ft could be part of a protein complex that governs and preserves photoreceptor structure and function. It is however possible that *ft* induced retinal degeneration does not sense light but is due to mis-activation of photoreceptors as a consequence of misfolded rhodopsins.

Chapter 5

INVOLVEMENT OF THE HIPPO TUMOR SUPPRESSOR PATHWAY IN RETINAL DEGENERATION

Drosophila Ft was described as a growth regulator required to restrict the rate of cell proliferation and the size of adult structures (Mahoney et al, 1991). A number of genetic studies has recently revealed that Ft controls growth, at least in part, through the regulation of a new tumor suppressor pathway, the Hpo pathway (Bennett & Harvey, 2006; Cho et al, 2006; Willecke et al, 2006; Silva et al, 2006).

The Hpo pathway regulates the balance between cell proliferation and apoptosis (Harvey & Tapon, 2007). The core of the signaling cascade consists of a complex of tumor suppressors in which Hpo, facilitated by the scaffold protein Sav, phosphorylates and activates the kinase Wts. Cells with mutations in one of these genes *sav*, *hpo* or *wts* exhibited dramatic outgrowths in a variety of fly epithelial tissues but did not manifest changes in cell identity or the ability to differentiate (Harvey et al, 2003; Pantalacci et al, 2003; Tapon et al, 2002; Wu et al, 2003; Xu et al, 1995).

Ft was proposed to act upstream of the Hpo pathway as a potential cell surface receptor of this signaling cascade (Cho et al, 2006), although the phenotype of *ft* mutants does not entirely overlap with those of the other components of the pathway (Harvey & Tapon, 2007). Since one of our main goals was to check the molecular pathway that mediates *ft*-induced neurodegeneration, we decided to explore the relationship between Hpo signaling and *ft*-dependent retinal degeneration. Hence, we examined if ablating components of the Hpo pathway and interacting signaling molecules affect the maintenance of retinal neurons.

5.1 Mutations of the core components of the Hpo pathway induce a progressive degeneration of the fly eye

To check whether the Hpo cascade is required for the maintenance of the *Drosophila* neuronal homeostasis, we induced the formation of clones homozygous for *sav*, *hpo* or *wts* specifically in the eye and performed a time-point phenotypic analysis of the mutant retinal tissue from flies aged at 29°C.

Mutations in the core components of the Hpo pathway have been reported to cause inappropriate proliferation and survival of non-neural IOCs just after differentiation (Udan et al, 2003). Normally, IOCs are produced in excess and most of them are culled in a wave of apoptosis during eye differentiation. In *hpo*, *sav*, or *wts* mutants, these cells fail to die. By contrast they divide several extra times, causing expansion and some disorganization of the eye. The presence of a large excess of IOCs, still present in adult tissues, made our analysis of retinal homozygous clones more difficult.

For *salvador* mutants we used the sav^3 loss of function allele that was described to behave as null allele (Tapon et al, 2002). The mutation causes a frameshift and generates a protein consisting of 406 *sav* amino acids (out of total 608) and an additional C-terminal portion of 84 amino acids derived from the use of an alternative ORF (Tapon et al, 2002). In new-born *sav* homozygous clones the organization of mutant ommatidia was normal and most of them contained the correct number of neuronal cells (Fig. 5.1A).

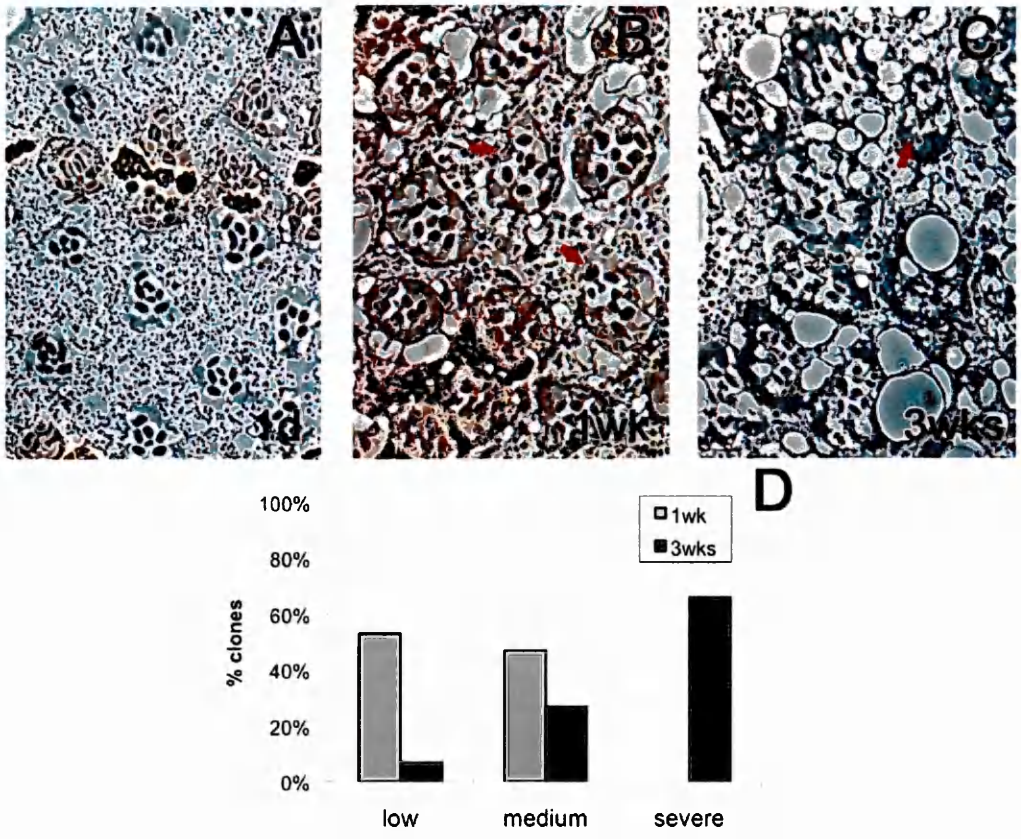

Figure 5.1 *sav* mutant clones display progressive neurodegeneration in the *Drosophila* eye
A,B,C- Semithin tangential sections of sav^3 homozygous clones from mutant flies aged 1 day (A), 1 week (B) and 3 weeks (C) at 29°C. At each time point sav^3 clones display a remarkable increase in interommatidial space as a consequence of failure in lattice programmed cell death. One day after eclosure almost all photoreceptors are intact (A), whereas after one week (B) some cells are lost or have degenerated as indicated by red arrows. After 3 weeks at 29°C (C) most sav^3 homozygous photoreceptors have degenerated (red arrow) and the tissue is collapsed. **D-** Quantification of the level of degeneration in sav^3 mutant clones aged one week (light grey columns) or three weeks (dark grey columns) at 29°C and analyzed in blind. After one week of age, more than half of the sav^3 homozygous clones display a low level of degeneration (53%) whereas all the other clones observed belong to the medium category (N=15 clones). After three weeks there is an increase in the severity of the phenotype and only 8% of the clones observed is still low degenerated, whereas 67% belongs to the severe category (N= 15 clones).

Mutant ommatidia of flies aged one week at 29°C displayed some abnormal photoreceptors (Fig. 5.1B) but in more than half of the homozygous clones observed, the loss of neuronal cells was low (Fig. 5.1D). At this age, some gaps between the mutant cells were already visible, especially inside the inter-ommatidial space, suggesting the beginning of the tissue collapse. In older mutant flies, aged three weeks at

29°C, we could detect an increase in the number of degenerated and lost photoreceptors inside the homozygous clones (Fig. 5.1C,D). The mutant tissue was also extremely collapsed and mutant ommatidia lost their normal shape. Furthermore, it had been already shown that in *sav* clones the inhibition of the correct apoptotis during pupal step lead to an excessive number of IOCs (Udan et al, 2003), differently from what observed in *ft* mutants. This defect was likely to contribute to *sav* retinal phenotype.

Together this study indicated that there is a progressive worsening in the retinal phenotype of *sav* mutant clones even though it is slower and less specific than *ft*-induced neurodegeneration.

To confirm the *sav* results, we also examined the phenotype of flies mutant for its interactor, *hpo*. We induced the formation of *hpo* homozygous clones, exclusively in the retinal tissue, using two distinct *hpo* mutations, hpo^{BF33}, whose mutation introduces a stop codon at aminoacid 174 (out of total 669) and is considered a loss of function allele (Jia et al, 2003), and hpo^{42-47}, whose mutation removes 6 residues inside a kinase subdomain that is actively involved in ATP binding and for this reason described as a null allele (Wu et al, 2003). We performed the two phenotypic analysis in parallel, and, in both the cases young *hpo* homozygous clones displayed a normal organization of mutant ommatidia (Fig. 5.2A).

Unfortunately, the majority of the adult flies, carrying *hpo* mutant clones, did not survive when aged one week at 29°C and most of them died after four days. Presumably, the high mortality rate was due to the severity of the *hpo* alleles used. Overall, the hpo^{42-47} phenotypes were described to be more severe than those of *sav* null alleles (Kango-Singh et al, 2002; Tapon et al, 2002). This was also reflected by the different degrees of pupal lethality caused by removing *hpo* or *sav* function in the eye with the

eyeless-FLP technique, since nearly all *eyeless-FLP-sav*^{3} flies survived to adults whereas only 2% of *eyeless-FLP-hpo*$^{42-47}$ flies survived to adults (Wu et al, 2003). In addition, it has been observed that the eyeless promoter is not expressed exclusively in the eye but also in the fly brain at lower levels (Camilla Larsen personal communication).

Although this factor prevented us from performing an exhaustive quantitative analysis of the retinal phenotype in *hpo* clones, the few *hpo* flies survived after one week showed a low level of degeneration inside the homozygous tissue, with some abnormal or missing photoreceptors (Fig. 5.2B). As found in *sav* mutants, also in *hpo* fly eyes the retinal tissue contained a great number of gaps specifically inside the mutant clones. Our outcomes, although not supported by a quantitative analysis, suggest an involvement of *hpo* in retinal neurodegeneration.

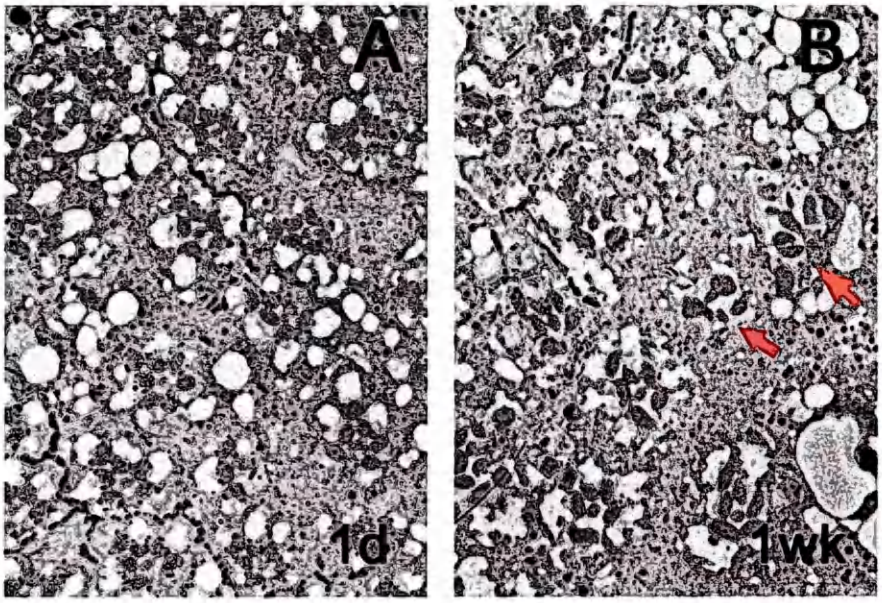

Figure 5.2 Retinal phenotype of the *hpo* mutant clones in the fly eye
A- Semithin tangential section of *hpo*^{BF33} homozygous clones from mutant flies aged one day at 29°C. The ommatidia belonging to the homozygous clone are correctly shaped and each contains 7 normal photoreceptor cells. **B**- Semithin tangential section of *hpo*^{BF33} homozygous clones from mutant flies aged one week at 29°C. Some ommatidia inside the homozygous tissue display a decrease in the total number of photoreceptors (red arrows).

The following experiment was performed to test the retinal phenotype of mutant flies for another component of the Hpo core, the downstream kinase Wts. We induced the formation of clones of cells homozygous for a strong amorph null allele, wts^{X1}, exclusively in the fly eye (Xu et al, 1995). wts^{X1} mutant retinal tissue was normal in new-born flies, whereas littermates aged one week at 29°C displayed few degenerating photoreceptors and some ommatidia with a decreased number of neuronal cells inside the homozygous clones (Fig. 5.3A).

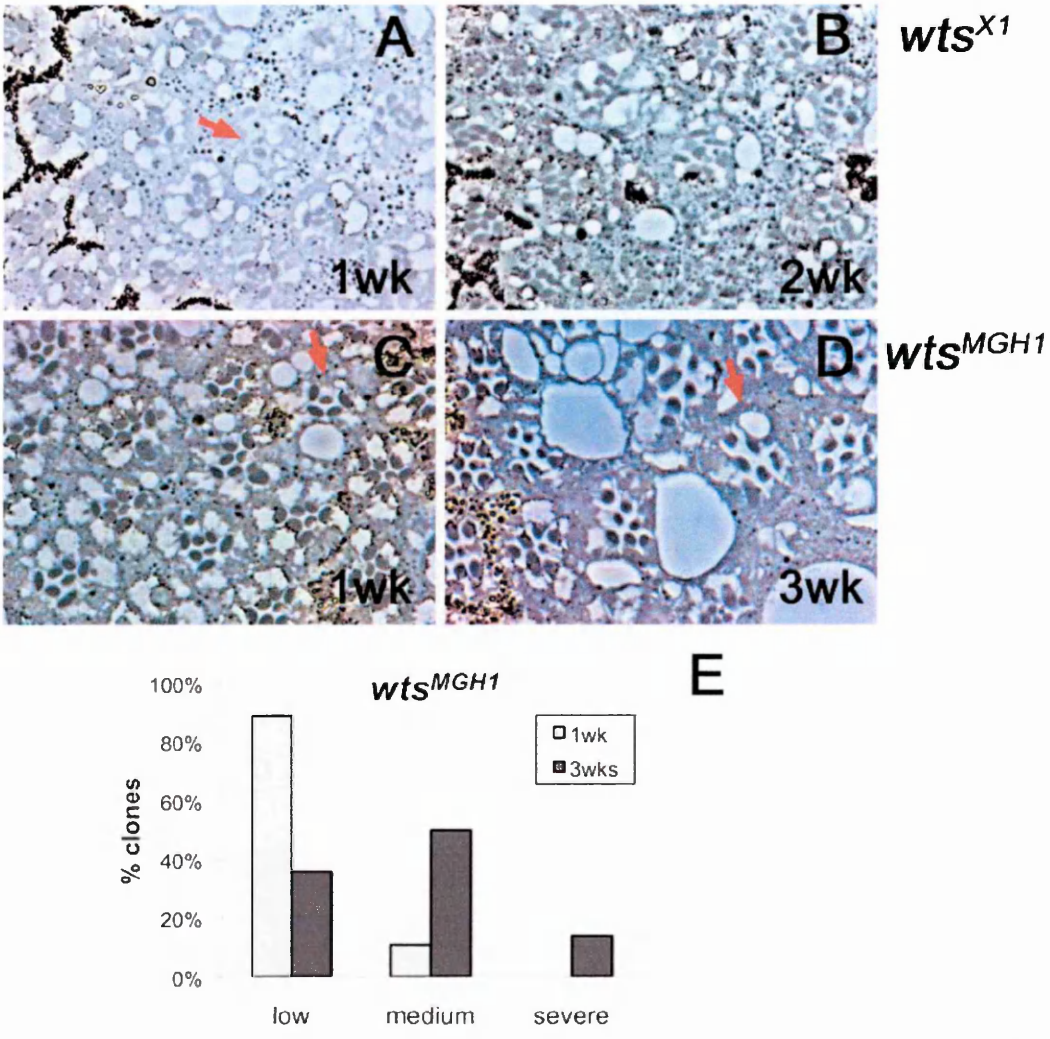

Figure 5.3 *wts* mutant clones in the fly eye display neurodegeneration
A,B- Tangential sections of wts^{X1} homozygous clones from retinae of mutant flies aged 1 week (A) and 2 weeks (B) at 29°C. Most of the one week old wts^{X1} clones observed (A) contain normal ommatidia and only few of them have lost some photoreceptors (red arrow). After three weeks (B) the mutant tissue is evidently disorganized and under collapse and most of the wts^{X1} homozygous cells have degenerated. **C,D**- Tangential sections of wts^{MGH1} homozygous clones from retinae

of mutant flies aged 1 week (C) and 3 weeks (D) at 29°C. After one week some abnormalities inside the clone are found but the mutant ommatidia have lost only few photoreceptors (red arrow). After 3 weeks at 29°C (D) the degeneration of *wts*^{MGH1} homozygous photoreceptors become more evident (red arrow) and the tissue start to collapse. **E**- Quantification of the level of degeneration in *wts*^{MGH1} mutant clones aged one week (with columns) or three weeks (grey columns) at 29°C and analyzed in blind. After one week of age, most of the homozygous clones display a low level of degeneration (90%) whereas only few clones observed belong to the medium category (N=10 clones). After three weeks there is an increase in the severity of the phenotype and only 36% of the clones observed is still low degenerated, whereas half of the *wts*^{MGH1} sections analyzed belong to the medium category and a low number of them (14%) were severely degenerated (N=14 clones).

Both abnormalities increased in older *wts*^{X1} mutant ommatidia when flies were aged two weeks at the same temperature (Fig. 5.3B).

Because most of *wts*^{X1} flies died before reaching three weeks of age, we used another available *wts* allele, *wts*^{MGH1}, even though its exact molecular lesion is unknown (Tapon et al, 2002). *wts*^{MGH1} homozygous clones, from one week old retinae, substantially displayed a low degenerated phenotype with few abnormal or missing neuronal cells (Fig 5.3C,E). Adult flies, aged three weeks at 29°C, showed a more severely affected retina and the tissue inside the homozygous clone was evidently collapsed (Fig. 5.3D,E). Unexpectedly, the *wts*^{MGH1} neuronal phenotype was less severe if compared to *sav*^{3} one at the same time points. This difference from *sav* phenotypes could possibly be explained by the different nature and severity of the alleles used, in particular, if *wts*^{MGH1} retains some activity.

In conclusion, both *sav* and *wts* mutants originated retinal abnormalities inside the homozygous clones that became more severe with the flies' age. However, it is likely that the overgrown interommatidial space and the extra-numerary lattice mutant cells mask the real outcome of *wts* and *sav* mutations in neuronal cells. In this context, the neurodegeneration observed in adult retinae, mutant for the components of the *hpo* core, could

be compared only in part with the degeneration found in *ft* mutants, since excessive IOCs have not been observed in *ft* homozygous clones.

5.2 Over-expression of Yki, the Hpo network output, leads to retinal degeneration in the fly eye

The downstream target of the Hpo cascade is the repression of the transcriptional co-activator Yki, which, together with DNA-binding factors, activates the transcription of the Hippo target genes, such as *diap1* and *cyclinE* (Goulev, 2008; Wu, 2008; Zhang, 2008; Peng, 2009). When the pathway is active, Wts phosphorylates and inactivates Yki by excluding it from the nucleus, preventing the transcription of the Hpo target genes (Huang et al, 2005).

It has been observed that the loss of one of the core components of the Hpo pathway, *sav*, *hpo* or *wts,* induced tissue overgrowth and inhibition of apoptosis, comparable to the modifications caused by the over-expression of Yki (Huang et al, 2005; Oh & Irvine, 2008).

We thus investigated whether the overexpression of Yki in the fly eye could provoke a neurodegenerative phenotype as observed for loss of the upstream regulators Hpo-Sav-Wts. We took advantage of both the Flp/FRT recombination and the Gal4/UAS genetic system to drive the expression of a *UASYki* transgene exclusively in specific regions inside the retinal tissue (Brogiolo et al, 2001). We thus crossed transgenic flies carrying a *UASYki wt* construct with flies expressing a complex transgenic sequence, the *GMR-FRT-P(w$^+$)-FRT-Gal4* cassette, in which a P(w+) insert blocks expression of GAL4 from the GMR promoter. Production of the Flippase enzyme, by heat-shocking an *hs-FLP* transgene, caused recombination

between two *FRT* sites and deletion of the intervening P(w+) sequence. This activated the *GMR-Gal4* driver and led to the overexpression of Yki specifically inside the "flipped-out" clones where mutant cells were marked by the absence of the pigment.

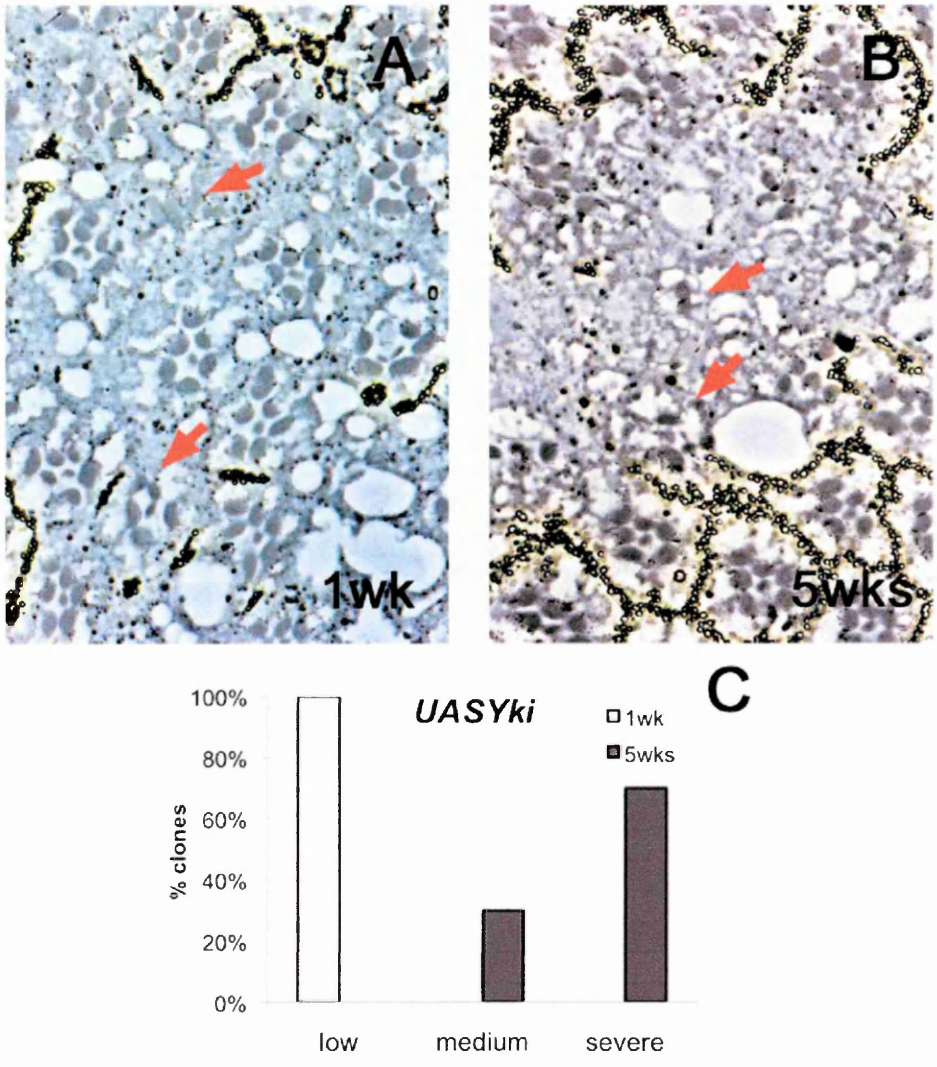

Figure 5.4 *Yki* over-expression in the retinal tissue causes a slow but progressive neurodegeneration
A,B- Semithin sections from *Yki* over-expressing retinae of flies aged one (A) and five weeks (B) at 29°C. After one week (A) the phenotype of the mutant tissue, characterized by the absence of pigmented cells around ommatidia, is low degenerated and only few ommatidia have lost one photoreceptor (red arrows). There is a progressive increase in the degenerative phenotype, although slow, and after five weeks (B) most of the mutant ommatidia contain many degenerated photoreceptors and a strong loss of cells (red arrows). **C-** Quantification of the level of degeneration in *Yki* over-expressing mutants aged one week (white column) or five weeks (grey columns) at 29°C and analyzed in blind. After one week of age, all the mutant retinae observed display a low level of degeneration (N=16 clones). After five weeks there is an increase in the severity of the phenotype, 30% of the clones observed belong to the

medium category, whereas most of them are severely degenerated (N=15 clones).

Our analysis of one week old flies revealed the presence of degenerated or lacking photoreceptors, even though very few, specifically inside Yki-over-expressing clones in one week old flies (Fig. 5.4A,C). This phenotype slowly became worse with time and after five weeks most of the mutant cells in Yki over-expressing ommatidia have degenerated (Fig. 5.4B,C). Thus, the expression of an exogenous form of Yki protein in the fly eye, that should be active and translocate to the nucleus for its transcriptional activity, was likely to mis-regulate the endogenous Hpo target genes. Yki expression gave rise to a retinal neurodegenerative phenotype comparable to the one observed in clones homozygous for *sav* or *wts* loss of function mutant alleles. However, the Yki phenotype was not as strong as *sav* or *wts* in terms of rapidity in the progression.

In conclusion, the data here shown demonstrated that both the core components of the Hpo Pathway and their downstream target Yki, are involved in a signalling that prevents neuronal cells from degenerating.

5.3 Mutations in *ex*, a regulator of the Hpo pathway, result in a neurodegenerative phenotype of the fly retina

The membrane-associated FERM-domain protein Ex was initially proposed to function upstream of the Hpo pathway as a tumour suppressor (Hamaratoglu et al, 2006). Mutations of *ex* gene were demonstrated to influence not only growth and cell survival but also the same downstream target genes of the Hpo pathway (Cho et al, 2006; Hamaratoglu et al, 2006). Ex is normally localized at apical cell-junctions, like Ft. Mutations in

Ft resulted in reduced Ex at apical cell-junctions, suggesting that Ft regulates growth in part through the regulation of Ex (Bennett & Harvey, 2006; Hamaratoglu et al, 2006; Willecke et al, 2006).

In addition, very recent work has indicated that Ex directly binds and favours the inactivation of Yki, suggesting that Ex can regulate the Hippo pathway activity not only upstream but also downstream or even independently of Wts (Badouel et al, 2009).

We thus wondered whether *ex* mutations could mimic the retinal phenotype observed when ablating one of the core components of the Hippo signaling or over-expressing Yki.

We used a loss of function allele, ex^{e1}, classified as genetic null allele (Boedigheimer et al, 1993a). The mutation caused an imprecise excision that removed the 5' end sequence and gave rise to a truncated Ex protein that lacked the first exon (Boedigheimer et al, 1993a). It is unknown whether there is a complete loss of protein expression. We thus induced the formation of ex^{e1} mitotic mutant clones in the fly eye using the Flp/FRT system.

Light microscopic analysis of *ex* mutants revealed a preserved retinal tissue in young adult flies. Mutant ommatidia coming from flies aged one week at 29°C looked well structured without any abnormality in the morphology or number of photoreceptors (Fig. 5.5A). After three weeks the phenotype of ex^{e1} mutant clones was still normal. However, semithin sections of four weeks-old ex^{e1} mutant eyes revealed the presence of some abnormal or missing photoreceptors specifically inside the homozygous tissue (Fig. 5.5B). The phenotype of *ex* clones in the majority of the mutant retinae analyzed was still classifiable as low in our scale and only few mutant ommatidia have more degenerated (Fig. 5.5D).

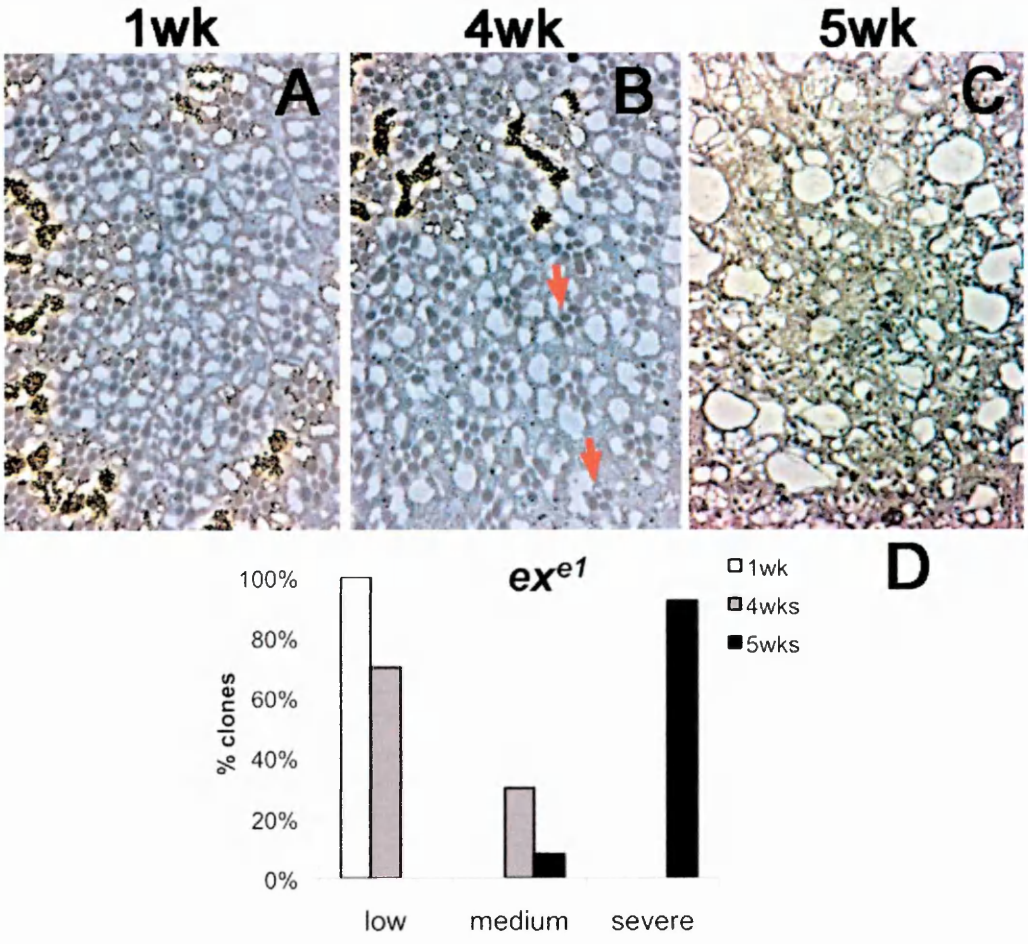

Figure 5.5 *ex* mutant clones display retinal neurodegeneration
A,B,C- Tangential sections of ex^{e1} retinae from homozygous clones of mutant flies aged 1 week (A), 4 weeks (B) and 5 weeks (C) at 29°C. The entire number of one week old ex^{e1} clones observed (A) contain normal ommatidia and only few of them have lost one photoreceptor. After four weeks (B) the mutant tissue is still with low degenerated photoreceptors and very few cells are lost (red arrows). Four weeks old (C) homozygous clones display an increased phenotype,the tissue is evidently collapsing and most of the ex^{e1} homozygous cells have degenerated. **D-** Quantification of the level of degeneration in ex^{e1} mutant clones aged one week (white column), four (grey columns) or five weeks (black columns) at 29°C and analyzed in blind. After one week of age, all the homozygous clones display a low level of degeneration (N=10 clones). After four weeks most of the mutant fly eyes are still low degenerated (70%) and only a minority belongs to the medium category (N=10 clones). After five weeks there is a strong increase in the severity of the phenotype and most of the clones observed are severely degenerated (92%) and the mutant retina is under collapse (N=14 clones).

The abnormalities became more dramatic after five weeks at 29°C (Fig. 5.5C,D). At this time point ex^{e1} homozygous clones were almost totally altered, with large gaps inside the mutant tissue and destroyed ommatidia. Inside the *wt* tissue, pigmented photoreceptors were normal at all time-points.

The data obtained from this experiment demonstrate that *ex* mutations induce retinal neurodegeneration. The rapidity in the progression of the phenotype is slow and more comparable to the degeneration observed in clones over-expressing Yki than in *sav* or *wts* mutants. This difference could be due by the nature of *ex* mutation used on one hand, since, when a mutant protein is expressed, it could retain some function. On the other hand, Ex is not a canonical regulator of the Hippo pathway but was shown to exert a binary and more complex function, monitoring the signaling both upstream of the Hpo-Sav-Wts core and also downstream (Badouel et al, 2009).

5.4 Mutations of *mer* gene, an upstream modulator of the Hpo pathway, cause a weak retinal phenotype

Mer, together with Ex, is a membrane-associated FERM-domain protein, proposed to act upstream and activate the Hpo cascade (Hamaratoglu et al, 2006). Mutation of *Drosophila mer* on its own showed only minor effects on growth, but characterization of *mer*;*ex* double mutants suggested that they acted redundantly at least in part (McCartney et al, 2000).

Related to the phenotype already published on *mer* mutations effect, we thus tested if the same applies during neurodegeneration. If this were the case, we would expect clones mutant for *mer* genes to show a phenotype either qualitatively similar to *ex* clones or weaker than *ex* based to the fact that Mer does not act downstream of the Hpo core as Ex.

In order to understand whether *mer* was involved in the degenerative signaling, we investigated the retinal phenotype in *mer* mutants clones. We

performed a time-point phenotypic analysis of *mer* mutant clones in fly eyes by using a strong null allele, mer^4, whose molecular basis is not known but leads to the expression of a truncated Mer protein (LaJeunesse et al, 1998). One week old mer^4 mutant clones appeared normal (Fig. 5.6A). Adult flies aged three weeks at 29°C still displayed a correct organization of the mutant ommatidia inside the mer^4 homozygous clone and only after five weeks the mutant tissue showed some abnormalities (Fig. 5.6B). Mutant clones contained many gaps, typical of a collapsed tissue, both in the interommatidial space and also inside the cytoplasm of degenerated photoreceptors. Remarkably, the ommatidia shape was conserved and the number of photoreceptors only marginally decreased, even though some of them appeared abnormal (Fig. 5.6B). These phenotypes are much milder than the one of *ex* mutants. This is not surprising since it has been reported that *mer* and *ex* act redundantly and that *ex* appeared to be more involved in the Hippo pathway than *mer* (Boedigheimer et al, 1993a; McCartney et al, 2000). Indeed, in developing imaginal tissues *mer* mutant larvae did not give rise to the hyperplastic discs characteristic of *ex* mutant larvae.

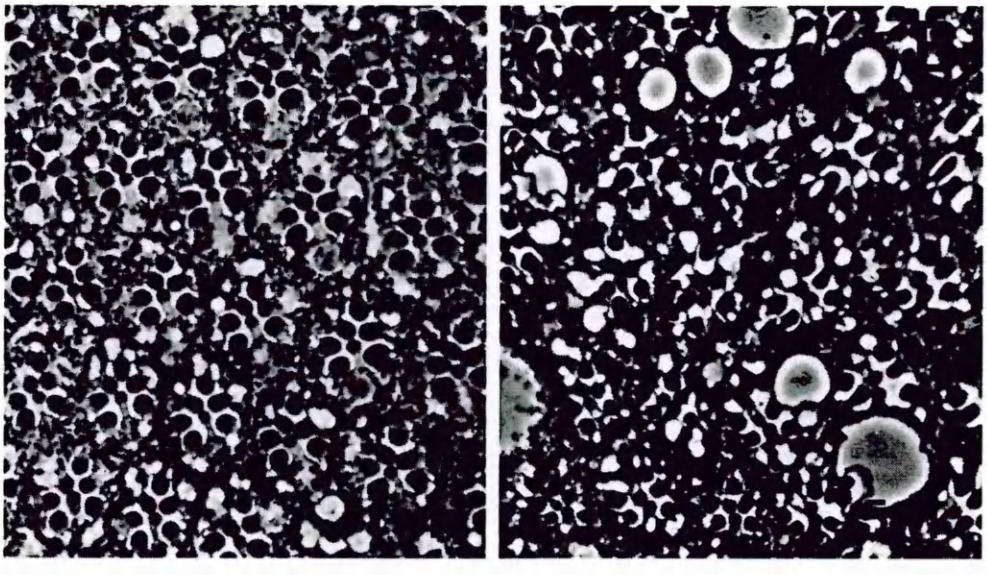

Figure 5.6 *mer* mutations induce only mild abnormalities in the fly eye
A,B- Semithin sections of mer^4 homozygous retinal clones coming from mutant flies aged one (A) and five weeks (B) at 29°C. In both the cases the

number of photoreceptor cells per mutant ommatidium is preserved and only after five weeks the tissue is full of gaps and collapsing.

In conclusion, the neurodegenerative phenotypes observed by mutating the upstream modulators of the Hpo signaling were milder than those of the Hpo core mutants. Nevertheless, we cannot exclude the possibility that other upstream proteins, like the very recently discovered Kibra, participate in the suppression of neurodegeneration.

5.5 Mutations of *d*, a negative regulator of the Hpo pathway, does not induce abnormalities of the *Drosophila* eye

Genetic data has suggested that Wts activity is regulated also by an Ex independent pathway and implicated the unconventional myosin D in growth regulation (Cho et al, 2006). Before the detailed study of the Hpo pathway, D was the only molecule known to be associated with Ft for cell size control (Cho & Irvine, 2004; Mao et al, 2006).

To clarify the role of D in retinal degeneration, we examined semithin sections of *d* mutants for a loss of function allele, d^{GC13}. The ommatidia inside the clones did not display any alteration in the architecture or in the conformation of mutant photoreceptors. The morphology was preserved and comparable between clones aged one week (Fig. 5.7A) and three weeks (Fig. 5.7B) in the same conditions of temperature.

We could not extend our analysis to older flies because most of the mutant did not survive more than three weeks at 29°C. Nevertheless, our results demonstrate that removing *d* in specific neuronal cells does not induce a degenenerative phenotype. This was perhaps not surprising since

D was described as a negative regulator of Wts abundance and D absence activates, rather than blocking, the Hpo pathway.

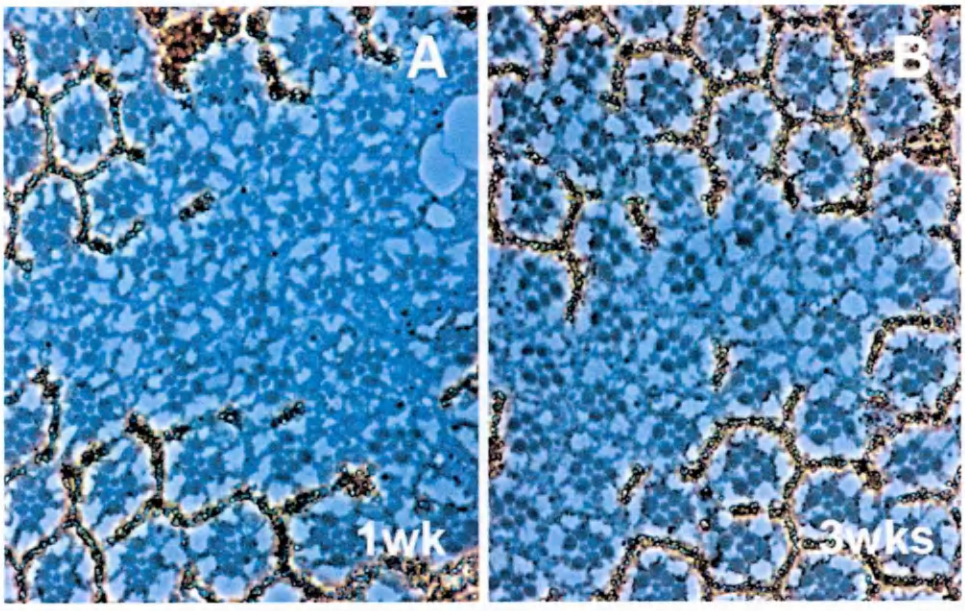

Figure 5.7 Retinal tissue in *d* homozygous mutants is preserved
A,B- Semithin sections of clones homozygous for d^{GC13} allele in a heterozygous background for the allele aged one (A) and three weeks (B) at 29°C.The tissue inside the clones does not show any defect in the shape or photoreceptors' organization. The phenotype in younger and older mutants is comparable.

5.6 Mutations of Ds, the Ft putative ligand, cause strong neuronal degeneration in the *Drosophila* eye

In addition to its effect on growth, the *Drosophila* Ft cadherin also regulates planar polarity in a cell-to-cell signaling process by interacting with Ds, another atypical cadherin, and Fj, a Golgi associated kinase (Lawrence et al, 2007; Strutt & Strutt, 2005). Ft and Ds bind each other and they have been proposed to act as receptor and ligand, respectively (Lawrence et al, 2007; Matakatsu & Blair, 2006; Strutt & Strutt, 2005).

Recently, Ds activity has been linked to the Hpo pathway (Willecke et al, 2008). Loss of *ds* caused overgrowth of *Drosophila* imaginal discs during development and an increased expression of some Yki targets, demonstrating that the activity of the Hpo pathway was lost in the absence

of Ds. On the contrary, Ds overexpression resulted in an increased function of the Hpo network (Rogulja et al, 2008; Willecke et al, 2008).

Since several models have described the involvement of Ds in regulating growth through the interaction with Ft (Rogulja et al, 2008; Willecke et al, 2008), we wondered whether Ds is involved in retinal neurodegeneration.

We therefore induced the formation of *ds* homozygous clones exclusively in the fly eye. We used the ds^{38} mutant allele, which is caused by a spontaneous mutation and is described as a not null allele, since ds^{38} mutant flies eclosed with high efficiency (-40%) in homozygous or transheterozygous combinations, although the escapers were highly deformed and died within a few days after eclosion (Clark et al, 1995).

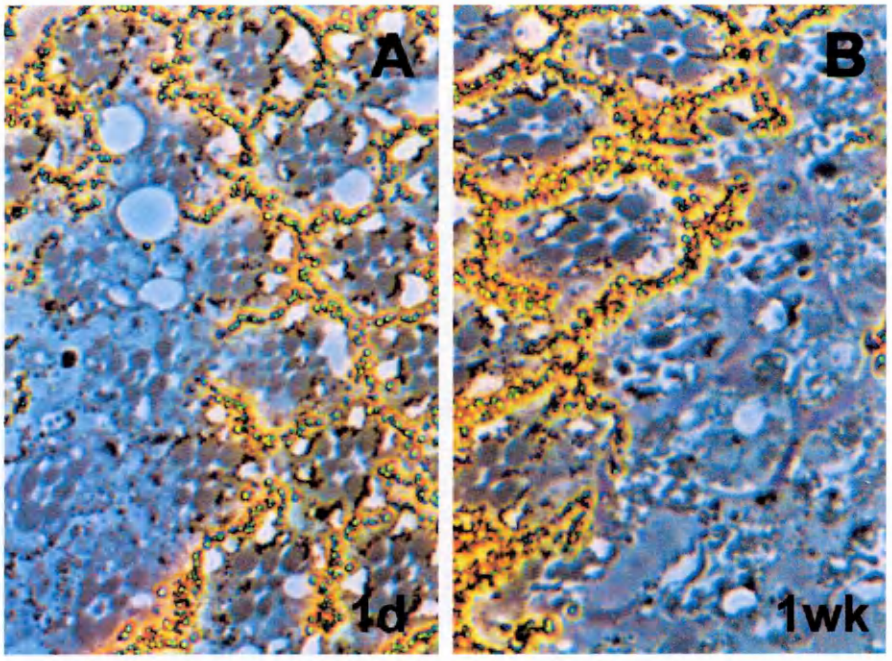

Figure 5.8 Strong retinal degeneration in *ds* homozygous tissue from adult flies aged at 29°
A,B- Semithin sections of ds^{38} mutant clones coming from adult flies aged one day (A) and one week (B) at 29°C. After eclosure *ds* homozygous clones are normal and mutant ommatidia are preserved in shape and content. By contrast, the phenotype in one week old mutant tissue was extremely severe and almost all the homozygous photoreceptors cells have degenerated (B).

The time point phenotypic analysis revealed a very strong degeneration in ds^{38} clones in the retinae of flies aged for one week at 29°C. Photoreceptors were destroyed in all the mutant ommatidia (Fig. 5.8B). By contrast, one day after eclosure, ds^{38} mutant retinae did not show any abnormality (Fig. 5.8A).

Because neurodegeneration proceeded so quickly in *ds* clones, we decided to perform a second analysis at 25°C, as we had already done for ft^{fd} mutants. Soon after eclosion, ds^{38} did not display any defect in ommatidial shape or photoreceptor morphology except some misrotated ommatidia due to the known involvement of Ds in PCP signaling (Fig. 5.9A).

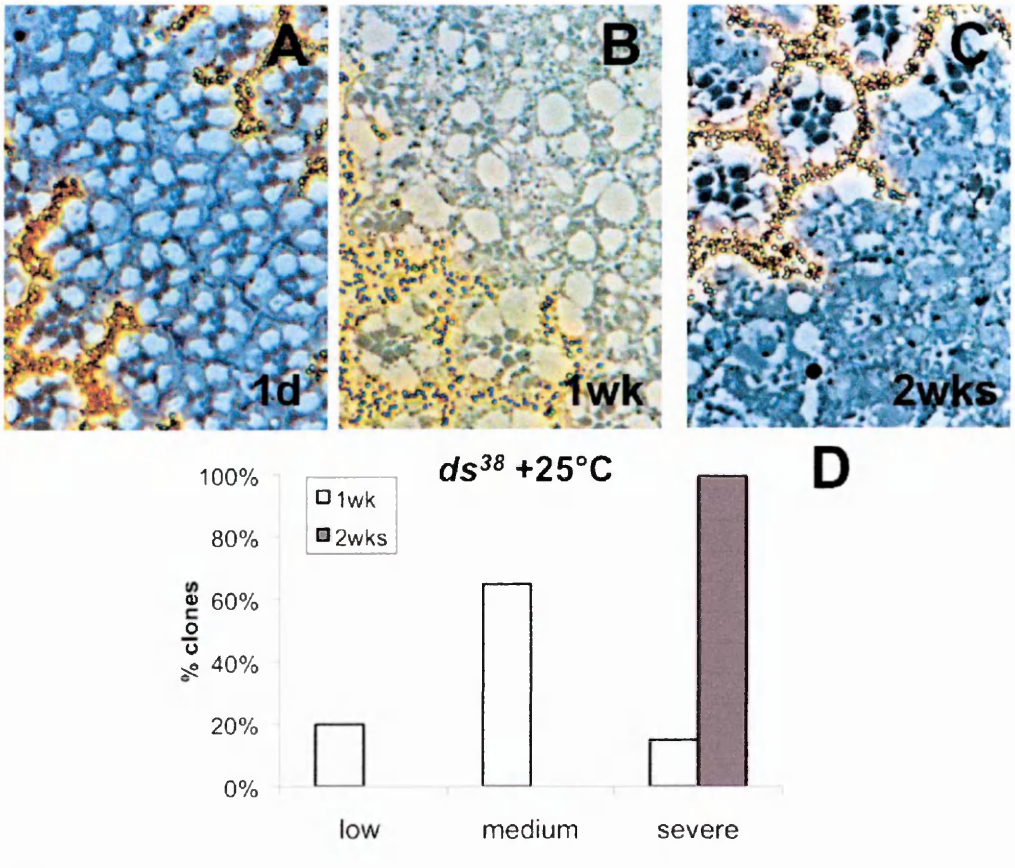

Figure 5.9 Progressive retinal degeneration in *ds* clones from flies aged at 25°

A,B,C- Tangential sections of ds^{38} homozygous clones from retinae of flies aged 1 day (A), 1 week (B) and 2 weeks (C) at 25°C. One day old flies show a normal retinal phenotype whereas after one week (B) most of the mutant ommatidia contain some abnormal photoreceptors that also appeared decreased in size. Two weeks old homozygous tissue is severely degenerated and photoreceptors are hardly distinguished (C). **D-** Quantification of the level of degeneration in ds^{38} mutant clones aged one week (white column), or two weeks (grey columns) at

25°C and analyzed in blind. After one week of age, some clones show a low level of degeneration (20%) whereas most of them belong to the medium category (65%) and only few are severely degenerated (15%) (N=10 clones). After two weeks there is an increase in the severity of the phenotype and all ds^{38} clones observed are severely degenerated (N=10 clones).

One week-old mutant clones showed a decreased number of cells inside the clone and a strong decrease in the cell size of homozygous photoreceptors that sometimes made our interpretation more difficult (Fig. 5.9B). However, our analysis revealed that more than half of the clones observed belong to the medium category of degeneration (65%) whereas only few were severely degenerated (15%) (Fig. 5.9D). After two weeks the degenerative phenotype became worse and almost all mutant ommatidia lost most of their photoreceptors (Fig. 5.9C).

Like for the *ft* phenotype, degeneration of *ds* mutant clones did not spread into *wt* tissue, suggesting a cell-autonomous phenomenon.

We can conclude from these data that Ds takes part in the regulation of neuronal degeneration. The phenotype detected in *ds* mutant fly eyes suggests a neurodegenerative phenomenon stronger than the one observed in *ft* clones or mutants for the Hpo pathway. We cannot exclude the possibility that Ds prevents neurodegeneration through a signaling independent and parallel to the Ft-Hpo cascade (See discussion).

5.7 Genetic interaction between Ft and the Hpo pathway in preventing neurodegeneration

The transcriptional coactivator Yki is the major downstream effector of the Hpo-Wts kinase complex (Goulev, 2008; Wu, 2008; Zhang, 2008). Since Ft has been described as the most upstream activator of the machine which ultimately blocks Yki activity, we asked whether *ft* induced degeneration could be modified by partially blocking Yki activity. We thus

induced the formation of ft^{fd} homozygous clones, exclusively inside the retina, in mutant flies carrying a heterozygous background for either *ft* and *yki,* using the yki^{B5} null allele.

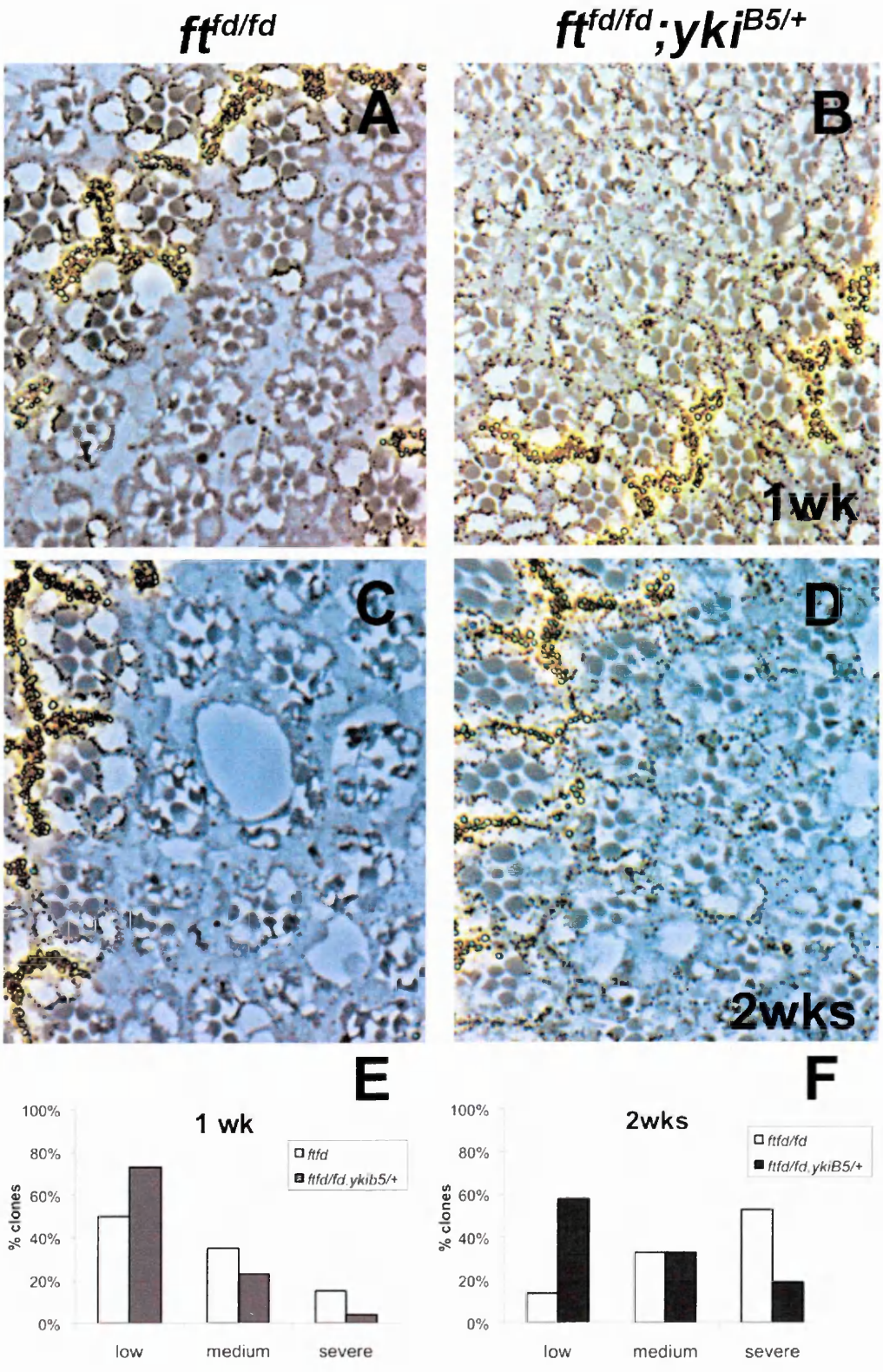

Figure 5.10 *ft* retinal degeneration is ameliorated by the reduction of *yki*

A,B- Tangential semithin sections of 1 week old $ft^{fd/fd}$ (A) and $ft^{fd/fd};yki^{B5/+}$ (B) clones from mutant flies aged at 29°C. In both the examples $ft^{fd/fd}$ homozygous ommatidia display a low level of degeneration with few abnormal or lost cells. **C,D**- Tangential semithin sections of 2 weeks old $ft^{fd/fd}$ (C) and $ft^{fd/fd};yki^{B5/+}$ (D) clones from mutant flies aged at 29°C. $ft^{fd/fd}$ homozygous clones in a *wt* background for *yki* (C) are severely degenerated, the ommatidia architecture is lost and the tissue is collapsed. On the contrary removing one copy of *yki* (D) results in a slowdown of $ft^{fd/fd}$ degenerative phenotype, the ommatidial shape is still recognizable and at least three photereceptors per ommatidium are normal. **E**- Quantification of the degeneration level in 1 week old $ft^{fd/fd}$ (white columns) and $ft^{fd/fd};yki^{B5/+}$ (grey columns) mutants analyzed in blind. Half of the $ft^{fd/fd}$ clones observed are low degenerated whereas 35% of them belong to the medium category and only few are severely degenerated (15%) (N=14 clones). The majority of $ft^{fd/fd}$ homozygous clones in a heterozygous background for *yki* are low (73%), some of them belong to the medium category (21%) and we found only one example (6%) of strong degeneration (N=15 clones). **F**- Quantification of the degeneration level in 2 weeks old $ft^{fd/fd}$ (white columns) and $ft^{fd/fd};yki^{B5/+}$ (grey columns) mutants analyzed in blind. After two weeks there is a significant increase in the severity of the phenotype in $ft^{fd/fd}$ homozygous clones that display few examples of low degeneration (10%) and more than half of the clones are severely degenerated (55%) (N=11 clones). On the contrary more than half of $ft^{fd/fd};yki^{B5/+}$ mutant retinae (58%) still belong to the lower category of degeneration whereas only few mutants (9%) are severely degenerated indicating a strong slowdown of $ft^{fd/fd}$ phenotype when removing one copy of *yki* (N=12 clones).

Most of the one week-old $ft^{fd/fd},yki^{B5/+}$ mutant flies (73%) showed some abnormalities in the photoreceptors inside the clone but the level of degeneration was on the whole low (Fig. 5.10B,E), similarly to $ft^{fd/fd}$ flies at the same age, although the percentage of low degenerated clones (50%) was minor (Fig. 5.10A,E). More than half of the two week-old $ft^{fd/fd},yki^{B5/+}$ mutant clones (58%) still displayed a low level of photoreceptors degeneration (Fig. 5.10D,F).

On the contrary, $ft^{fd/fd}$ clones with a *wt* background for *yki* presented a stronger phenotype, as already shown, with respect to $ft^{fd/fd},yki^{B5/+}$ mutants; only 10% of $ft^{fd/fd}$ clones were still low degenerated and more than half of the clones analyzed belonged to the severe category (55%) (Fig. 5.10C,F).

These results suggest that reduced dosage of yki slows down the *ft* degenerative phenotype consistent with their being an interaction between Ft signaling and the Hpo-Sav-Wts pathway.

One of the two models proposed to explain how Ft regulates the Hpo pathway describes the unconventional myosin Dachs as a crucial controller of Wts abundance which blocks the activation of the core and is inhibited by Ft. It is known that Dachs can rescue the overgrowth but not the planar polarity phenotype in *ft* mutants. For this reason we asked whether Dachs was also able to rescue *ft* degeneration.

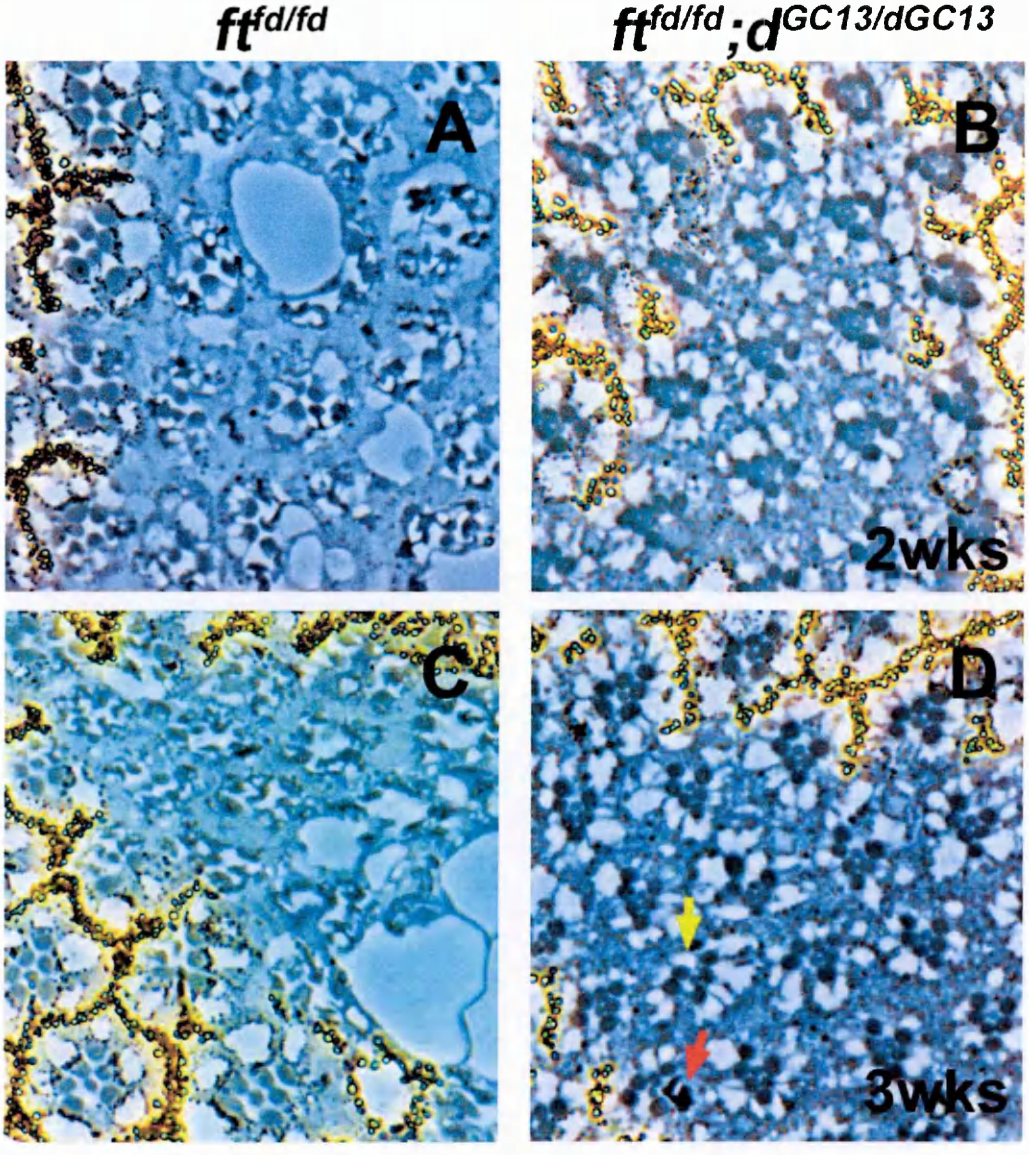

Figure 5.11 *ft* retinal degeneration is rescued by the lack of *dachs*
A,C- Semithin sections of $ft^{fd/fd}$ clones from mutant flies aged two (A) or three weeks (C) at 29°C. In both the examples mutant ommatidia are extremely degenerated and most of the *c* homozygous photoreceptors are abnormal. (N= 10 clones each genotype). **B,D-** Semithin sections of $ft^{fd/fd;}d^{GC13/GC13}$ double homozygous clones from mutant flies aged two (B) or three weeks (D) at 29°C. After two weeks the majority of the double mutant ommatidia are preserved (B) both in shape and content differently from the degenerated $ft^{fd/fd}$ single mutants (A). After three weeks $ft^{fd/fd;}d^{GC13/GC13}$ double mutants are almost entirely normal

and rarely one photoreceptor is lost (yellow arrow) or has degenerated (red arrow) suggesting a strong rescue of ft^{fd} retinal degeneration by removing *dachs*.

We generated double mutant clones for both *ft* and *dachs* by using ft^{fd} and d^{GC13} null alleles. Comparison between $ft^{fd/fd},d^{GC13/GC13}$ and $ft^{fd/fd}$ phenotype showed strong rescue of the retinal abnormalities for all time points analyzed.

As expected, the $ft^{fd/fd}$ phenotype increased to a severe degeneration after two or three weeks of age (Fig. 5.11A,C). On the contrary $ft^{fd/fd},d^{GC13/GC13}$ mutant retinae contained normal photoreceptors inside all the ommatidia belonging to the clone both after one and two weeks of age (Fig. 5.11B) and only in three weeks old double mutants very few photoreceptors degenerated (Fig. 5.11D).

Thus, loss of D results in a total rescue of the *ft* induced retinal degeneration, indicating that neurodegeneration in *ft* clones is indeed due to misregulation of the Hpo pathway, rather than a contribution of the Ft planar polarity signaling.

5.8 Genetic interaction between Ds and the Hpo pathway in preventing *ft* neurodegeneration

We have previously demonstrated that mutations of *ds* coding gene lead to a neurodegenerative phenotype comparable at least in part with the one observed in retinae mutant for *ft* and the components of the Hpo pathway. Since a link between Ds and Ft involvement in growth regulation via the Hpo cascade has been suggested (Rogulja et al, 2008; Willecke et al, 2008), we wondered whether *ds* interact genetically with the Hpo signaling to control retinal degeneration.

We thus induced the formation of clones homozygous for ds^{38} in a heteroygous background for yki^{B5} null allele, on one hand, and clones double mutants for ds^{38} and d^{GC13} on the other hand. If Ds is a suppressor of Yki activity, and behaves like Ft to monitor the Hpo central core signaling, we might expect that heterozygosity for *yki* would suppress degeneration in *ds* clones.

We compared the retinal phenotype of three distinct categories of mutant clones: $ds^{38/38}$, $ds^{38/38}$;$yki^{B5/+}$ and $ds^{38/38}$;$d^{GC13/GC13}$. One day after eclosion all the mutant flies showed apparently normal photoreceptors inside the clones. After ageing flies one week at 29°C, $ds^{38/38}$ mutant clones were severely degenerated (Fig. 5.12A,D) and also in a heterozygous background for the *yki* null allele (Fig. 5.12B,D). If there was an interaction between *yki* and *ds* it was too weak to be detected in this experiment (Fig. 3.21B). By contrast, clones double mutants for *ds* and *dachs*, $ds^{38/38}$,$d^{GC13/GC13}$, exhibited a weaker level of degeneration than $ds^{38/38}$ single clones when flies were aged one week at 29°C (Fig. 5.12C,D). In most mutant retinae isolated, the shape of the mutant ommatidia was recognizable and the photoreceptors cells became much more conserved both in aspect and number (Fig. 5.12C,D). Most of the double clones (70%) analyzed displayed only weak degeneration and none were severely affected.

The genetic analysis here presented demonstrates that *ds* retinal neurodegeneration is strongly rescued by the lack of D whereas partial block of Yki activity appears to not influence *ds* induced phenotype.

The rescue obtained from removing *d* in ft^{fd} clones was much stronger than for ds^{38} homozygous tissue, perhaps because the level of

degeneration of ds^{38} mutant photoreceptors was more severe than the ft^{fd} and thus more difficult to be ameliorated.

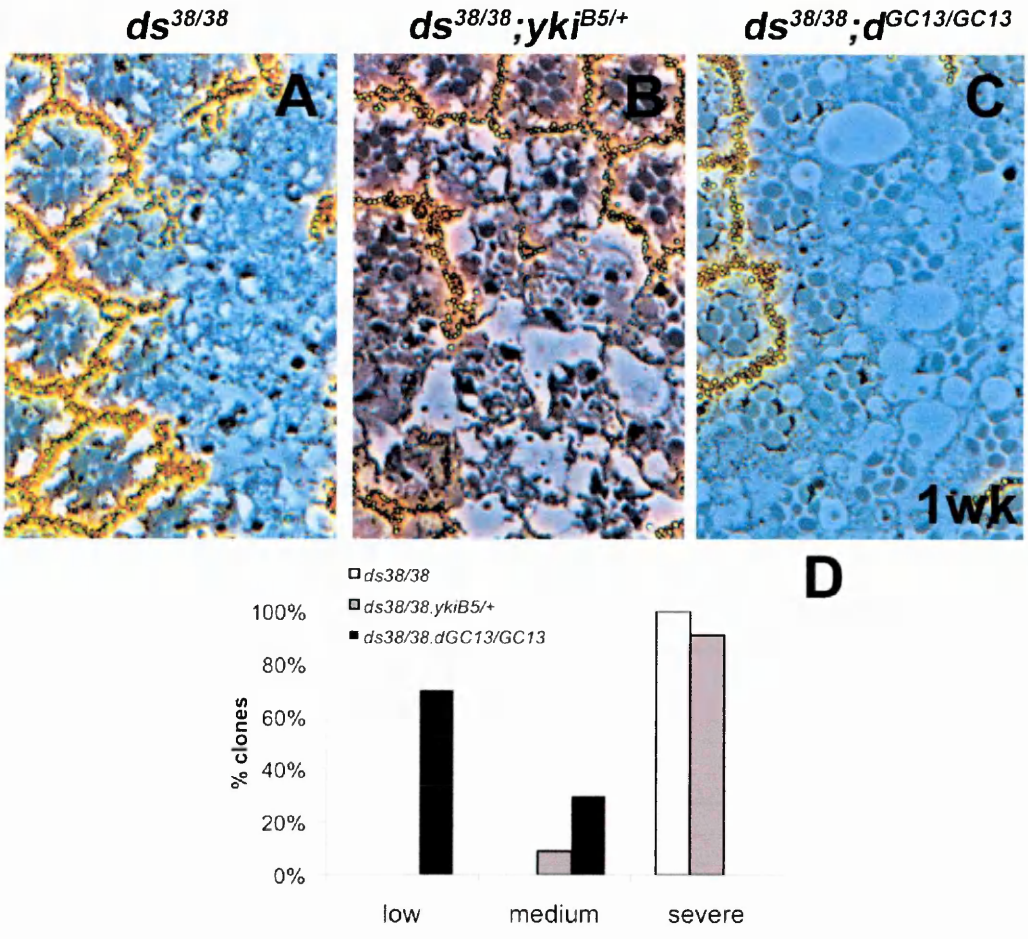

Figure 5.12 *ds* retinal degeneration is rescued by the lack of *d* but not by the reduction of *yki*
A,B,C- Semithin sections of $ds^{38/38}$ (A), $ds^{38/38};yki^{B5/+}$ (B) and $ds^{38/38};d^{GC13/GC13}$ clones from flies aged one week at 29°C. Mutant ommatidia inside $ds^{38/38}$ homozygous tissue are severely degenerated (A) and the level of degeneration is comparable to clones of *ds* in a heterozygous background for *yki* (B), although in this case the shape of mutant ommatidia is newly recognizable. On the contrary, $ds^{38/38};d^{GC13/GC13}$ double mutant clones show a strong amelioration of the *ds* phenotype and most of the mutant ommatidia contain at least four photoreceptors cells that have not degenerated suggesting a strong rescue of *ds* degeneration by the lack of *dachs*. **D-** Quantification of the degeneration level in 1 week old $ds^{38/38}$ (white columns), $ds^{38/38};yki^{B5/+}$ (grey columns) and $ds^{38/38};d^{GC13/GC13}$ mutants analyzed in blind. Both $ds^{38/38}$ and $ds^{38/38};yki^{B5/+}$ clones show a severe level of retinal degeneration whereas $ds^{38/38};d^{GC13/GC13}$ cause a strong rescue and more than half of the clones observed (70%) are low degenerated and only some of them belong to the medium category.

Similarly, it is likely that removing only one copy of *yki* in ds^{38} mutants is not enough to obtain an appreciable change of *ds* retinal phenotype. The scarce effect of *yki* heterozygosity on *ds* clones correlates with *yki* modest

rescue of ft^{fd} degeneration. This outcome results much lower than the strong rescue observed in *ds* clones by completely ablating *dachs*. However we cannot exclude that Dachsous cooperates with Fat and Dachs in a way that is parallel to the Fat-Hippo cascade.

5.9 DISCUSSION

In the first part of this work I have analyzed the role of Ft in retinal cells homeostasis. The evidence I obtained led us to propose a model in which Ft modulates neurodegeneration through a pathway which appear to include a number of unknown players.

Several papers published over the past few years described the interaction among the Hpo tumour suppressor pathway and Ft in distinct tissues (Bennett & Harvey, 2006; Cho et al, 2006; Willecke et al, 2006; Silva et al, 2006). Therefore we investigated whether this interaction occurs also in the retina. We discovered that most of the components of the Hpo signalling are linked to neuronal degeneration per se.

By preventing the activation of the Hpo cascade at distinct steps along the pathway, we obtained, in the majority of the cases, a common phenotype of photoreceptors alteration or loss. Intriguingly, the level of degeneration was different, in terms of severity and rapidity in the progression, depending on the hierarchical position occupied in the cascade by the mutated protein.

Mutations of the central components of the Hpo-Sav-Wts pathway, *sav* and *wts,* resulted in a comparable cell-autonomous degenerative phenotype that resembled the retinal abnormalities of *ft* mutant clones. The *sav/wts* phenotypes did not totally overlap *ft*-induced neurodegeneration,

especially in the rapidity of cell disappearance. Although our results about the number of degenerated photoreceptor cells were comparable, the number of mutant cells lost appeared higher in ft^{fd} clones than in sav^{3} or wts^{MGH1} homozygous tissues, as if *sav* or *wts* mutant cells were more resistant to death.

Exogenous hyper-activation of Yki, reported to mimic the removal of the main components of the central cassette (Bennett & Harvey, 2006; Cho et al, 2006; Willecke et al, 2006; Silva et al, 2006), also brought about a retinal degenerative event. However, the phenotype we observed by over-expressing Yki was weaker than in *ft* mutants.

A possible explanation for these distinct severity levels is linked to the difference in the modality by which Hpo-Sav-Wts and Ft pathways monitor organ size and tissue growth, the former restricting cell proliferation and promoting apoptosis, the latter being more involved in the regulation of cell proliferation but less or none in the Hpo-Sav-Wts induction of the apoptotic signaling. Another possibility is that the alleles we used carry mutations of different strengths, thus leading to different levels of degeneration. That is what in fact we observed for ft^{fd} compared to ft^{82} mutants, or for wts^{X1} and wts^{MGH1}.

Concerning the slow phenotype induced by the hyper-activation of Yki, it is likely that the presence of an exogenous Yki protein was sensed as toxic by the cell and induced a major activation of the endogenous Hpo-Sav-Wts signaling, thus causing the phosphorylation and inactivation of the exogenous Yki. Alternatively, over-expression of Yki induced with the combination of Gal4/UAS and Flp/FRT systems, was not sufficiently robust to block Hpo-Sav-Wts signaling completely.

Mer, Ex, Dachs and very recently Kibra molecules have been described as upstream direct regulators of the Hpo core (Baker & Yu, 2010; Baumgartner et al, 2010; Cho et al, 2006; Genevet et al, 2010; Hamaratoglu et al, 2006; McCartney et al, 2000). *ex* gene is considered to promote the activation of the cascade downstream of *ft*. Like *ft*, when mutated, it led to a retinal degenerative phenotype which progressed with age. The abnormalities appeared much later than in *ft* mutant fly eyes. This is not surprising and several explanation could justify the results we obtained from *ex* analysis.

First, ex^{e1} has been described as a LOF allele whose not completely known mutation gives rise to a deletion of the 5' UTR. It is not known whether Ex protein is affected at all (Boedigheimer et al, 1993a), suggesting the possibility that Ex function is retained. Second, it is likely that the downregulation of *ex* is partly compensated by its reported genetic redundancy with *mer* (Hamaratoglu et al, 2006; McCartney et al, 2000) or by the newly discovered *mer-kibra* complex (Baker & Yu, 2010; Baumgartner et al, 2010; Genevet et al, 2010). Finally, recent experiments have introduced a new perspective on Hpo regulation and raised the possibility of a more complex signaling involving different feedback loops (Badouel et al, 2009). Ex has been demonstrated to directly bind and inactivate Yki, the final target of the Hpo-Sav-Wts network, suggesting that Ex can regulate Yki activity not only upstream but also downstream or even independently of Wts. If this is the case, the down-regulation of *ex* would correspond to a double block of Yki function. Therefore we would have expected a stronger phenotype. The moderate neurodegeneration we detected in *ex* mutant photoreceptors could suggest that in the retinal tissue

Ex acts mainly upstream of the Hpo core and its absence is compensated by Mer or Kibra.

Mer, like Ex, is a membrane-associated FERM-domain protein, proposed to regulate the activation of the Hpo cascade (Hamaratoglu et al, 2006). Mutation of *Drosophila mer* on its own showed only minor effects on growth (McCartney et al, 2000). Thus, the very low level of abnormalities we found in *mer* mutant ommatidia and photoreceptors are not unexpected and correlate with the idea that Mer is involved in the regulation of Hpo-Sav-Wts activation less than Ex, thus affecting neuronal homeostasis less. Actually, both Ex and Mer are each capable of restricting cell growth and cell cycle progression. However, they also exert distinct functions. Studies on developing eye imaginal tissues, performed both in larvae and pupae, demonstrated that Ex has a clear role in regulating cell cycle exit, while Mer is more directly involved in monitoring apoptosis (Pellock et al, 2007).

Our hypothesis is that Ex and Mer act differentially in the maintenance of neuronal homeostasis in the adult retina, since our phenotypic analysis indicated that *mer* was less involved in photoreceptors maintenance than *ex*. In addition, both *kibra* and *ex* activities could be redundant and counterbalance the absence of *mer*.

D has an opposite role in the modulation of the Hpo pathway, since it has been proposed to block the activation of the Hpo core molecules by restricting Wts abundance (Cho et al, 2006). D had been previously described to be functionally linked to Ft in te regulation of cell overgrowth and cell affinity. The *d* phenotype had been shown to be epistatic of *ft*, as the *ft* mutant disc overgrowth was completely suppressed in cells homozygous for *d* (Cho & Irvine, 2004). Thus, the opposite effect of Ft and D on growth control could explain the opposite effect on neuronal

degeneration and why, within the first three weeks of adult life, *d* mutation did not cause neurodegeneration of the retinal tissue.

A second known interactor of Ft is the atypical cadherin Ds that was previously proposed to act as a ligand for Ft receptor in the regulation of the PCP signaling (Saburi & McNeill, 2005). Recent work has found Ds to be also involved in the Hpo-Sav-Wts signaling, although the molecular mechanism by which this binding can regulate tissue growth is complex and has not been well clarified (Rogulja et al, 2008; Willecke et al, 2008).

ds mutants singularly manifested strong neurodegeneration inside the homozygous mutant clones that was easily detectable starting from young fly ages. The phenomenon leading to *ds* abnormalities was not entirely comparable to the defects caused by *ft* or *sav/wts* mutants since it was much more rapid. Also, the results we obtained from our analysis are unexpected because they suggest a cell-autonomous phenomenon. This is against the proposed model of Ds binding *in-trans* the Ft protein present on the membrane of the neighbouring cell and supports instead a new model in which the two cadherins co-operate inside the same cell. Results present in the literature have indicated that both *ds* LOF and over-expression of Ds cause transcriptional induction of the Hpo-Sav-Wts target genes and that the effect is not restricted to the cells lacking or over-expressing Ds, indicating a complex way of regulating tissue growth (Willecke et al, 2008). Our data further stress the hypothesis of a more complex role of Ds in the pathway suggesting the possibility that Ds has another ligand, different from Ft, thus acting through a novel signaling. Alternatively, Ds could bind Ft within the same cell, *in-cis*, in a way similar to Delta-Notch ligand *in-cis*. In the literature, Delta and Notch have been described to encode cell surface proteins that function in a wide variety of cell fate specification events during

oogenesis, embryogenesis, and metamorphosis in *Drosophila*. The Delta ligand has been shown to have two activities: it transactivates Notch in neighbouring cells and *cis*-inhibits Notch in its own cell (Muskavitch, 1994). It is possible that Ds-Ft binding *in-cis* activates a signaling that regulates neuronal homeostasis differently from the PCP regulation monitored by their *trans*-interaction.

The link between Ft and Hpo-Sav-Wts signalings in preventing neurodegeneration is uncovered by the epistatic experiments we performed. The induction of the Hpo-Sav-Wts network by the reduced *yki* gene dosage on one hand, and the complete lack of *dachs* on the other hand, resulted sufficient to ameliorate *ft* induced phenotype, demonstrating a genetic interaction between Ft and the Hpo pathway. The fact that the rescue of *ft* retinal degeneration was obtained with both the two distinct genetic experiments, confirms the idea that Ft maintains the neuronal homeostasis both going through Yki but also through the D-Wts alternative way, independently of Yki. It is also not surprising that the rescue obtained by completely ablating *dachs* is stronger than the one arising from the reduction of only one of the two gene copies of *yki*.

Further epistatic experiments demonstrated that *ds*-induced retinal phenotype is ameliorated by inactivating *d* but not by partially blocking *yki*. Two main explanations justify these results. On one hand, it is possible that Ds is part of the Ft-Wts signalling regulating neuronal homeostasis, and that removing only one copy of *yki* gene is not sufficient to provide detectable rescue of the strong phenotype found in one week-old ds^{38} mutants. On the other hand, it is possible that Ds prevents neuronal degeneration collaborating with Ft and Dachs in a pathway that is parallel to the Hpo-Sav-Wts cascade.

Components of the Hpo-Sav-Wts signaling have also been implicated in a variety of other growth-unrelated processes, including the regulation of neural fate during early eye development (Maitra et al, 2006; Feng & Irvine, 2007; Pellock et al, 2007), photoreceptor cell type during later eye development (Mikeladze-Dvali et al, 2005), the correct Rhodopsin expression in R7/R8 photoreceptors cells and dendritic maintenance (Emoto et al, 2006).

Our results suggest that inactivation of the Hpo-Sav-Wts signalling also promotes the maintenance of neuronal integrity and support the existence of a mechanism in the adult retina that prevents activation of the transcritpion of the canonical Yki targets.

Interesting results from the group of Claude Desplan presented at the European *Drosophila* Research Conference (2009, Nice) come in support to our hypothesis of an involvement of the Hpo pathway in neuronal homeostasis. Although Wts was demonstrated to control the post-mitotic specification of R8 photoreceptor neuron subtypes, mutants for *wts* or over-expression of Yki in the fly eye were shown to activate the transcription of neither *diap1* nor *cycE* in the adult retina. In addition, Yki and Sd are required to activate Rhodopsin5 and repress Rhodopsin6 downstream of Wts, suggesting that they act in R8 as the transcriptional output of the Wts signaling, similar to their role in growth (Abstract #P121).

Neurodegeneration in Ft/Hpo mutants may arise as a consequence of inhibition of apoptosis, on one hand, and growth stimulation on the other hand. Both phenomena could put the cells under considerable metabolic stress because of an excessive need of energy and an inbalance of molecular components' synthesis and degradation. This outcome appeared consistent with the results from microarrays performed in the lab

(unpublished data) to check for genes regulated by Atro. These results identified *ft* as one of the main candidates and reported a repression of apoptosis and a stimulation of cell-cycle genes. However, the transcription of the canonical targets of the Hpo signalling cascade, such as *diap1* or *cycE*, identified during developmental growth control (Harvey et al, 2003; Pantalacci et al, 2003; Tapon et al, 2002; Wu et al, 2003), were not altered in the microarray analysis. The only Hpo target gene that resulted transcriptionally regulated in Atro microarrays was *dally-like*, that codifies for a proteoglycan required for the regulation of diffusible ligands, which is, like Wnt, involved in cell fate and patterning decisions (Baena-Lopez et al, 2008).

Further investigations will be required to test if some of the genes found transcriptionally altered in the microarray analysis may effectively represent targets of the Hpo-Sav-Wts pathway in this tissue, pushing neurons to re-enter the cell-cycle. To test whether transcription of genes involved in the cell-cycle and regulated by Atro, such as *string,* are really modified by the Hpo pathway, we could for example perform a microarray analysis or a quantitative RT-PCR in *sav* or *wts* mutant neuronal tissue. Alternatively, we can not exclude the possibility that the Ft/Hpo pathway regulates growth-independent events to maintain neuronal homeostasis.

Chapter 6

INVOLVEMENT OF ATROPHIN IN *ft* RETINAL DEGENERATION

The Ft cadherin is involved in the regulation of PCP (Fanto & McNeill, 2004; Saburi & McNeill, 2005). It has been initially proposed that Ft works upstream of the classical Frizzled signaling (Yang et al, 2002). Then, few years ago it was discovered that PCP control by Fat acts through a distinct way that includes both Atro (Fanto et al, 2003) and Ds (Casal et al, 2006).

Atrophins are transcriptional co-factors (Erkner et al, 2002; Zhang et al, 2002) and expansion of a CAG stretch in the human *atrophin-1* gene causes a polyQ neurodegenerative disease, the DRPLA (Nagafuchi et al, 1994a; Naito & Oyanagi, 1982).

To understand to what extent Atrophin transcriptional function was linked to neurodegeneration, a genome wide transcriptional profiling was performed in *Drosophila* models of the DRPLA generated in the lab (Nisoli et al., 2010). Intriguingly, the level of *ft* gene transcription was downregulated by the *wt* form of *Drosophila* Atro and expansion of polyQ stretches along Atrophin downregulated *ft* transcription even more.

Therefore, a twofold link between Ft and Atro functions emerges, both in transcriptional and PCP regulation.

6.1 *atro*$^{e46\text{-}2}$ mutations in the fly eye cause a weak neurodegeneration

In 2002 *Drosophila atro* gene was isolated and studied by two distinct groups in parallel, the Kerridge lab in France and the Xu lab in the USA (Erkner et al, 2002; Zhang et al, 2002).

Since it has been shown in the past that loss of *atrophin/grunge* (*atro* or *gug*) affected PCP both cell-autonomously and non-autonomously, in the same manner as *ft* (Fanto et al, 2003), we wondered whether the loss of *atro* function by itself could lead to develop any neuronal abnormality. For this reason, we induced the formation of clones homozygous for *atro* in the fly retina and compared the phenotype of four distinct *atro* mutant flies stocks based on two independent alleles, aged for different time points at 29°C.

We took advantage of the $atro^{e46\text{-}2}$ allele from the Xu lab and the gug^{35} allele coming from the Kerridge lab, since both have been described as null alleles (Erkner et al, 2002; Zhang et al, 2002). The $atro^{e46\text{-}2}$ allele is a deletion of around 3kb described to remove the first *atrophin* intron (Zhang et al, 2002). The original $atro^{e46\text{-}2}$ mutation was located on the third chromosome together with the *FRT2A* cassette, a genomic sequence that is a substrate for the FLP-mediated mitotic recombination.

The *FRT2A* cassette also contains an inserted P element which carries a truncated version of the *white* gene sequence, called the *mini-white* gene, and commonly used as a selectable marker in transformation constructs (Pirrotta, 1988). *white* expression is necessary for eye pigmentation and transformants carrying the *mini-white* gene shows a range of eye coloration from pale yellow to red, depending on the position of the *mini-white* insertion into the genome (Hazelrigg et al, 1984; Pirrotta et al, 1985). In the case of the *FRT2A,* the *mini-white* gene is expressed only weakly and homozygous clones generated in this genetic background are more difficult to be analyzed, since the weaker pigmentation makes it harder to distinguish between *wt* and mutant cells.

Thus, in parallel, we recombined the *atro*$^{e46\text{-}2}$ allele on a different chromosome carrying the *FRT80* cassette, instead of the *FRT2A*, which does not contain any *white* gene but a genetic sequence that confers resistance to the neomycine antibiotic. Flies heterozygous for *atro*$^{e46\text{-}2}$ were crossed with flies heterozygous for a P element carrying the *mini-white* gene sequence inserted upstream of another *FRT80* cassette. After mitotic Flp/FRT recombination, we thus obtained *atro*$^{e46\text{-}2}$ homozygous clones characterized by the absence of the red pigment.

Surprisingly we could not detect most of the abnormalities originally reported by the group of Xu (Zhang et al, 2002). We did not find any roughness in the mutant eyes, nor defects during the specification of photoreceptors, few PCP defects (Fig. 6.2B, white asterisks). Moreover, unlike the published data, most of the mutant ommatidia displayed a correct complement of the seven photoreceptors. Reasons for this discrepancy are discussed later in the section 6.4.

We thus compared the retinal phenotype of *atro*$^{e46\text{-}2}$*,FRT2A* and *atro*$^{e46\text{-}2}$*,FRT80* aged either one or three weeks at 29°C. In both genotypes, after one week of age, most of the mutant retinae were normal or displayed a very low level of degeneration inside the clone (Fig. 6.1A,C). Ommatidia coming from both sets of *atro*$^{e46\text{-}2}$ mutant clones were less disorganized in their aspect, if compared to mutant clones for *ft* or components of the Hpo pathway previously analyzed. Therefore, it was possible to perform a more detailed and quantitative analysis of the degenerative phenotype comparing the number of total photoreceptors per ommatidium in different mutant clones at distinct time points.

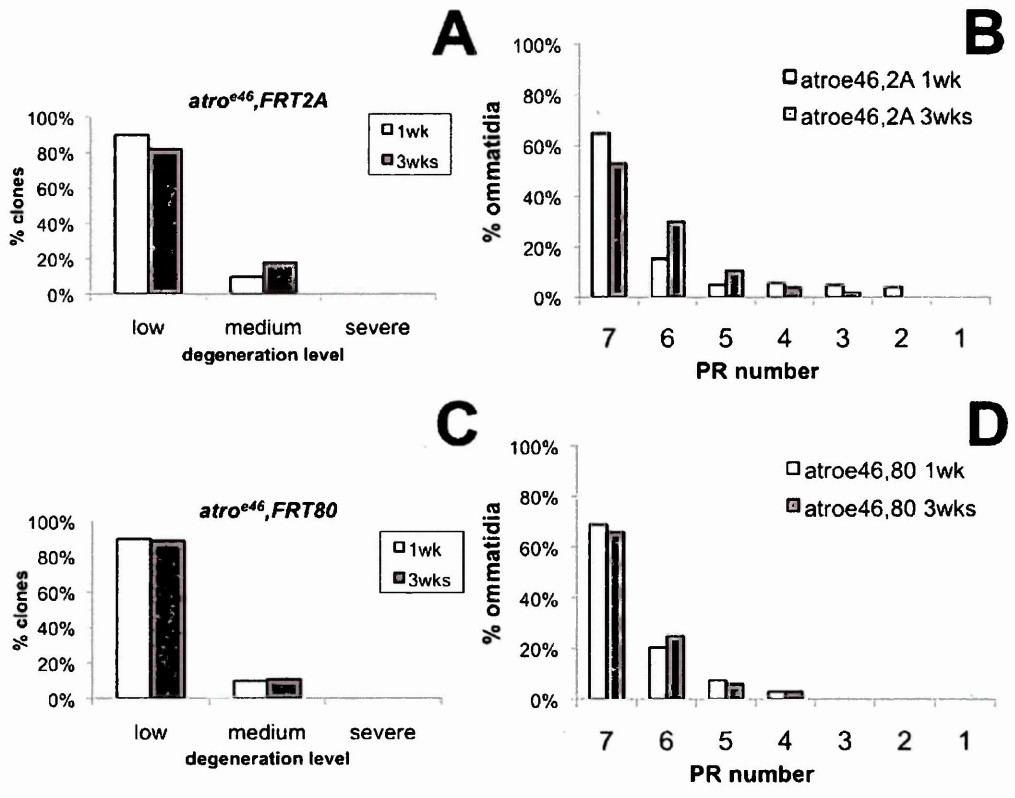

Figure 6.1 Level of degeneration and photoreceptor loss in *atro^{e46}* mutant clones of the fly retina

A- Quantification of the level of degeneration in *atro^{e46},FRT2A* mutant clones aged one week (white columns) or three weeks (grey columns) at 29°C and analyzed in blind. After one week of age, the majority of the *atro^{e46}* homozygous clones display a low level of degeneration (90%) whereas the other few clones belong to the medium category (N=10 clones). After three weeks there is a slow decrease of the low degenerated clones (82%) and a slow increase of the clones belonging to the medium category (N= 14 clones). **B-** Quantification of photoreceptors number in *atro^{e46},FRT2A* mutant clones aged one week (white columns) or three weeks (grey columns) at 29°C and analyzed in blind. After one week of age, the majority of the *atro^{e46}* mutant ommatidia contain a preserved number of photoreceptor cells (67%) or have lost one cell (15%) whereas only few ommatidia contain five or less cells (N= 241 ommatidia). After three weeks there is a decrease of preserved mutant ommatidia (53%) and a significant increase of ommatidia containing six (30%) or five (11%) photoreceptors (N=392 ommatidia, three independent experiments). Chi-square 21.5, $p<0.005$ for 6 degrees of freedom. **C-** Quantification of the level of degeneration in *atro^{e46},FRT80* mutant clones aged one week (white columns) or three weeks (grey columns) at 29°C and analyzed in blind. After one week of age, the majority of the *atro^{e46}* homozygous clones display a low level of degeneration (90%) whereas the other few clones belong to the medium category (N=10 clones). After three weeks the phenotype did not change and most of the clones still belong to the low category (89%) (N= 14 clones). **D-** Quantification of photoreceptor number in *atro^{e46},FRT80* mutant clones aged one week (white columns) or three weeks (grey columns) at 29°C and analyzed in blind. After one week of age, the majority of the *atro^{e46}* mutant ommatidia contain a preserved number of photoreceptor cells (69%) or have lost one cell (21%) whereas only few ommatidia contain five or less cells (N= 309 ommatidia). After three weeks there is a slow decrease of preserved mutant ommatidia (66%) but a non significant increase of ommatidia containing six (25%) or five (6%) photoreceptors (N=283 ommatidia, three independent experiments). Chi-square 1.41, $p>0.05$ for 6 degrees of freedom.

The quantification of the photoreceptor number in one week-old *atro*$^{e46-2}$ mutant tissues showed that most of the ommatidia contained the correct number of neuronal cells and only a few had lost one or two photoreceptors (Fig. 6.1B).

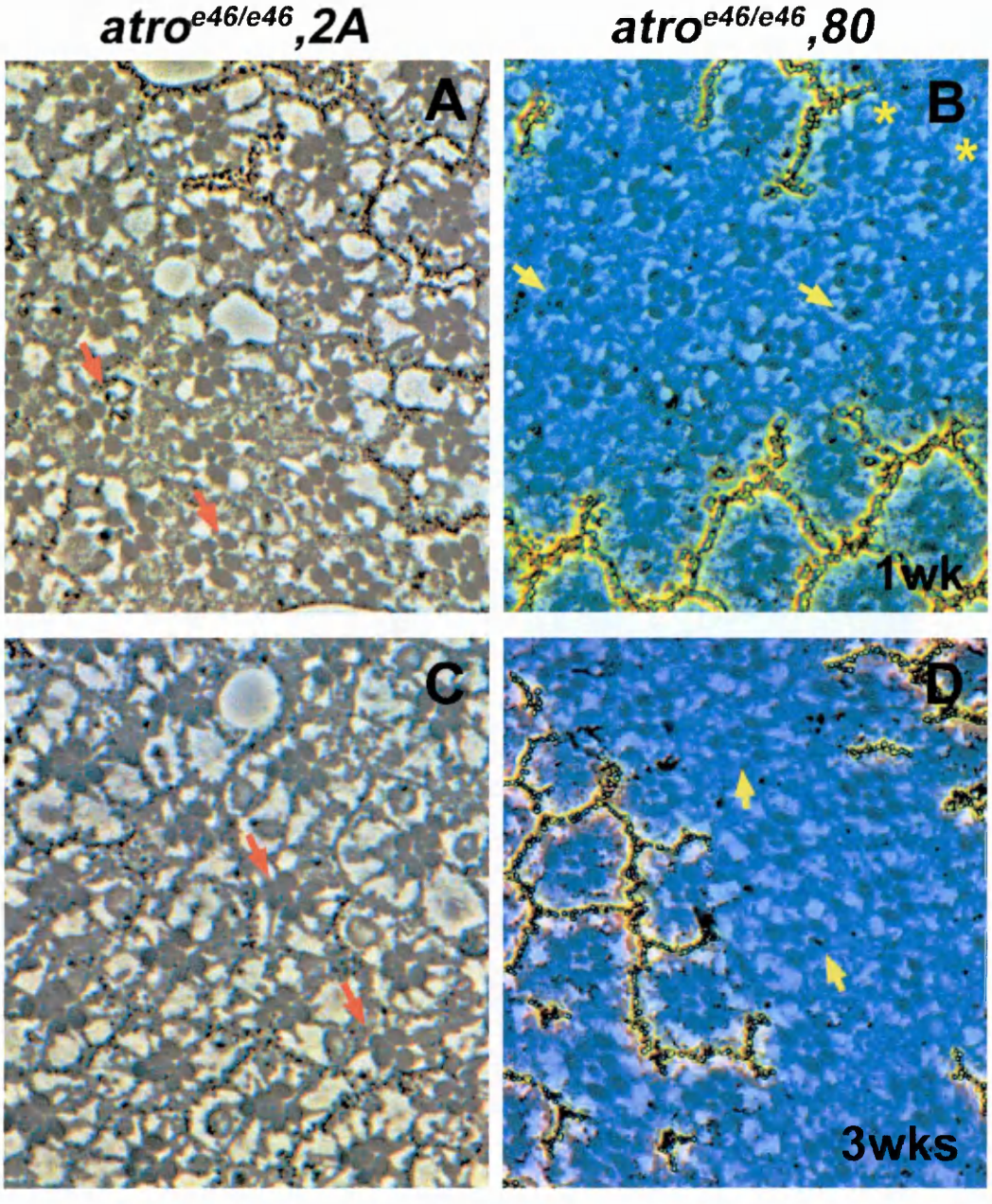

Figure 6.2 Low level of retinal neurodegeneration in *atro*^{e46} mutant clones
Semithin sections of *atro*^{e46},*FRT2A* (A,C) and *atro*^{e46},*FRT80* (B,D) mutant clones aged one week (A,B) or three weeks (C,D) at 29°C. In both time points there is only a low level of degeneration but the number of ommatidia that have one photoreceptor lost or degenerated is higher in *atro*^{e46},*FRT2A* (red arrows in A,C) with respect to *atro*^{e46},*FRT80* (yellow arrows in B,D). White asterisks in B indicate PCP defects.

After three weeks at 29°C, the level of abnormalities slowly progressed in *atro*$^{e46\text{-}2}$,*FRT2A* mutants, although most of the clones observed still belonged to the low category (Fig. 6.1A, 6.2A,B). There was a faint but significant ($p<0.005$) increase in the number of mutant ommatidia with reduced number of photoreceptors (Fig. 6.1B).

The quantification of the retinal phenotype in *atro*$^{e46\text{-}2}$,*FRT80* clones from three week-old flies showed a progress, although not statistically significant, in the neurodegeneration and photoreceptor loss (Fig. 6.1C,D).

In conclusion, the phenotypic analysis of *atro*$^{e46\text{-}2}$ mutant retinae indicates a weak neuronal degeneration more easily detectable in *atro*$^{e46\text{-}2}$,*FRT2A* mutants than in *atro*$^{e46\text{-}2}$,*FRT80* mutant clones.

To check that the *atro*$^{e46\text{-}2}$ was still present in the *FRT80,* we checked whether the new generated chromosome, *atro*$^{e46\text{-}2}$,*FRT80*, was able to complement the lethality of *atro*$^{e46\text{-}2}$,*FRT2A* original stock. No *atro*$^{e46\text{-}2}$,*FRT80/atro*$^{e46\text{-}2}$,*FRT2A* flies were recovered confirming the presence of the same lethal mutation on both the *FRT80* chromosome and on the starting *FRT2A* one. This implies that we had not lost the mutation. However, we cannot be sure that this mutation is *atro*$^{e46\text{-}2}$.

6.2 *gug*^{35} mutations in the fly eye cause a strong retinal degeneration

The second allele used for our study was the *gug*^{35} allele, described as an excision of the P inserted element carrying the *atro* sequence, that resulted in an imprecise deletion of the genomic DNA at the site of the insertion (Erkner et al, 2002). We used both *gug*^{35},*FRT2A* and *gug*^{35},*FRT80* flies (both from Kerridge lab) to compare their retinal phenotype with the one of *atro*$^{e46\text{-}2}$ mutants.

After one week at 29°C, the phenotype of *gug*^{35},*FRT2A* mutant clones was comparable to the one of *atro*$^{e46\text{-}2}$. Actually, the semithin sections were normal or displayed a low level of degeneration, with one photoreceptor abnormal or lacking per mutant ommatidium (Fig. 6.3A,B;Fig. 6.4A).

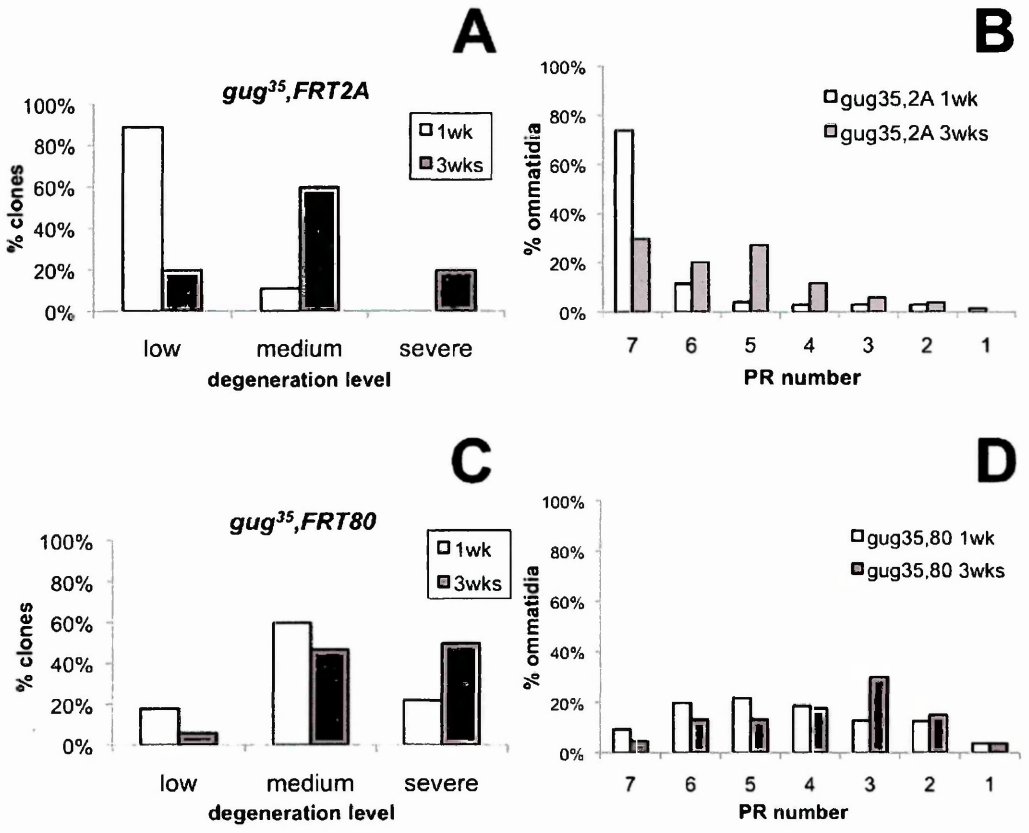

Figure 6.3 Level of degeneration and photoreceptor loss in *gug*^{35} mutant clones of the fly eye

A- Quantification of the level of degeneration in *gug*^{35},*FRT2A* mutant clones aged one week (white columns) or three weeks (grey columns) at 29°C. After one week of age, most of the *gug*^{35} homozygous clones display a low level of degeneration (89%) whereas the other few clones belong to the medium category (N=14 clones). After three weeks there is a strong decrease of the low degenerated clones (20%) and most of the clones observed belong to the medium category (60%) and some of them are severely degenerated (N=10 clones). **B-** Quantification of photoreceptors number in *gug*^{35},*FRT2A* mutant clones aged one week (white columns) or three weeks (grey columns) at 29°C. After one week of age, the majority of the *atro*^{e46} mutant ommatidia contain a preserved number of photoreceptor cells (74%) or have lost one cell (11%) whereas only few ommatidia contain five or less cells (N=357 ommatidia). After three weeks there is a highly significant decrease of preserved mutant ommatidia (30%) and a significant increase ($p<0.001$) of ommatidia containing six (20%), five (28%) or four (12%) photoreceptors (N=270 ommatidia, three independent experiments). Chi-square 201 for 6 degrees of freedom. **C-** Quantification of the level of degeneration in *gug*^{35},*FRT80* mutant clones aged one week (white columns) or three weeks (grey columns) at 29°C. After one week of age, only 18% of the *gug*^{35} homozygous clones were ckassified as low, whereas more than half belong to the medium category (60%) (N=14 clones). However the classification is failing to take into

account the strong developmental abnormalities at this stage. After three weeks there is an increase in the severity of the phenotype with a decrease of the low degenerated clones (6%) and most of the clones observed belong to the medium (47%) and severe category (50%) (N=16 clones). **D-** Quantification of photoreceptors number in *gug*^{35}*,FRT80* mutant clones aged one week (white columns) or three weeks (grey columns) at 29°C. After one week of age, a low number of *gug*^{35} mutant ommatidia contain a preserved number of photoreceptor cells (9.6%), many clones have lost at least one (20%), two (22%),three (19%) or four (13%) photoreceptors (N=293 ommatidia). After three weeks there is a significant increase of photoreceptor loss ($p<0.001$) especially ommatidia that have lost four (30%) or five (15%) photoreceptors (N=350 ommatidia, three independent experiments). Chi-square 31.5 for 6 degrees of freedom.

The outcome was different for *gug*^{35}*,FRT80* at the same time point, because very few mutant clones contained ommatidia with the correct number of neuronal cells. Importantly, this is the phenotype originally described for *gug*^{35} (Fanto et al, 2003). Most of the sections showed a medium level of degeneration, with two or more photoreceptors missing or degenerated inside the homozygous tissue (Fig. 6.3C,D;Fig. 6.4B).

Older *gug*^{35}*,FRT2A* mutant clones from flies aged three weeks at the same environmental conditions manifested a highly significant decrease ($p<0.001$) of the mutant photoreceptors inside the clone (Fig. 6.3B; Fig. 6.4C) and an increase in the level of degeneration (Fig. 6.3A; Fig. 6.4C).

The results obtained from same age *gug*^{35}*,FRT80* mutants matched the *gug*^{35}*,FRT2A* ones. After three weeks at 29°C actually most of *gug*^{35}*,FRT80* mutant clones belonged to the medium or severe category of degeneration (Fig. 6.3C; Fig. 6.4D), the tissue inside the clone was collapsed and most of the ommatidia had lost more than half of their photoreceptors (Fig. 6.3D; Fig. 6.4D).

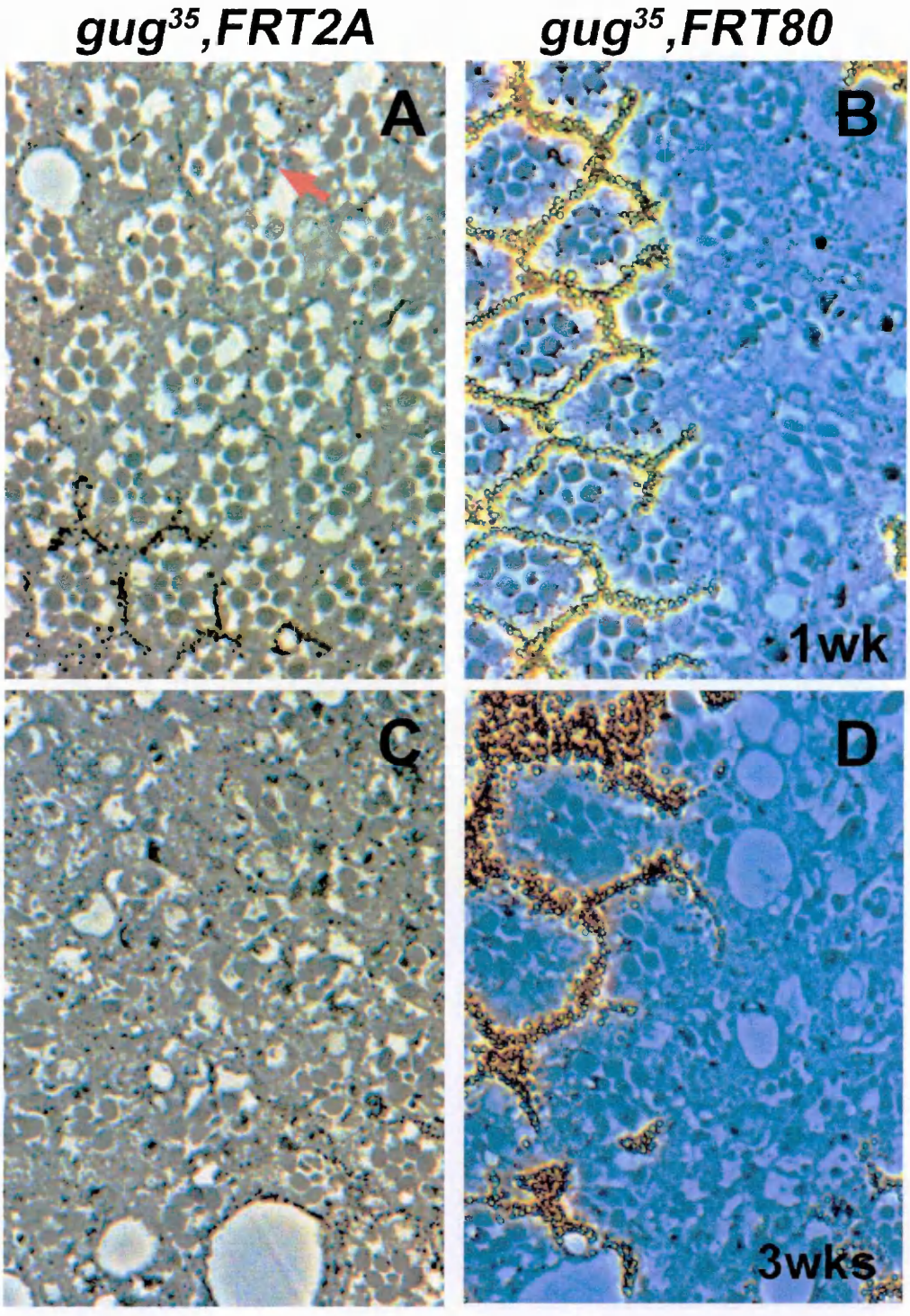

Figure 6.4 Progressive neurodegeneration in *gug*^{35} mutants of the fly retina
A,B- Semithin sections of *gug*^{35}*,2A* (A) and *gug*^{35}*,80* (B) mutant clones aged one weeks at 29°C. In *gug*^{35}*,2A* there is only a low level of degeneration and very few ommatidia have lost one photoreceptor (red arrow) whereas the phenotype in *gug*^{35}*,80* homozygous clones is much more stronger and the degeneration is more evident (example belonging to the medium category). **C,D-** Semithin sections of *gug*^{35}*,2A* (C) and *gug*^{35}*,80* (D) mutant clones aged three weeks at 29°C. In both the genotypes the severity of the phenotype is increased. More than half of *gug*^{35}*,2A* clones belong to the medium category like the semithin here shown (C) and half of the *gug*^{35}*,80* clones are severely degenerated like the example here shown (D).

Therefore, differently from the results of the *atro*$^{e46-2}$ analysis, both sets of *gug*^{35} mutant clones indicated a phenomenon of progressive neurodegeneration. The increase in the severity of *gug*^{35},*FRT2A* retinal phenotype was much stronger with respect to *gug*^{35},*FRT80.* However it should be considered that the latter started also from a highly irregular photoreceptor recruitment.

Since both alleles have been previously described to affect the same signaling in a comparable manner (Erkner et al, 2002; Zhang et al, 2002), these outcomes were unexpected. Our results indicate that *atro*$^{e46-2}$ and *gug*^{35} mutations do not induce similar lesions as reported.

One possibility is that the *gug*^{35},*FRT80* chromosome contains an additional mutation, which interacts with *atrophin* and gives rise to the strong loss of photoreceptors observed after one week of age, which is to be attributed to developmental defects (Fanto et al, 2003).

6.4 DISCUSSION

Our previous experiments demonstrated that Ft cooperates with the Hpo-Sav-Wts tumour suppressor signaling to prevent, at least in part, the neuronal degeneration. The Hpo cascade is not the only set of molecules functionally linked to Ft activity. Therefore, in order to better characterize the genetic signaling that links Ft to neurodegeneration, we have addressed our investigation towards the involvement of Atro, which had been shown to bind physically the Ft cytoplasmic domain and to collaborate in the regulation of the PCP signaling (Fanto et al, 2003).

We took advantage of the *atro*$^{e46\text{-}2}$ allele from the Xu lab and the *gug*^{35} allele from the Kerridge lab, since they have been both described in the literature as null alleles (Erkner et al, 2002; Zhang et al, 2002).

Unexpectedly, we were unable to detect most of the retinal abnormalities previously reported for *atro*$^{e46\text{-}2}$ homozygous clones in adult flies (Zhang et al, 2002). The only abnormality we could detect was the presence of a significant amount of misrotated ommatidia inside the mutant tissue. This resembled the PCP defects described in the paper of Zhang et al (2002).

Re-examinng the Zhang et al. paper (2002), we noticed that authors did not use the *atro*$^{e46\text{-}2}$ allele to induce the formation of homozygous clones in the fly eye. Rather, they described the retinal phenotype in *atro* mutant clones derived from the insertion of two distinct P transposons (P3 or P5) into the second *atro* intron, downstream of the site of *atro*$^{e46\text{-}2}$ mutation (Fig1F,G; Fig2A from (Zhang et al, 2002). In addition, the above alleles also carried a mutant allele of the *knirps* gene, the *radius interruptus* (*ri*) allele (Zhang et al, 2002), that was later discovered to be itself an *atro* target gene (Haecker et al, 2007). Actually, *Drosophila* Atro has been reported to interact with the transcriptional repressor Tailless (Moran & Jimenez, 2006; Pankratz et al, 1992; Yu et al, 1994) and to tether and repress the transcription of *knirps*, a segmentation gap gene known to be a direct target of Tailless (Zhang et al, 2006; Wang et al, 2006). A recent report has also revealed that Atro physically and genetically interacts with another nuclear protein, called Brakeless (Bks), to regulate *knirps* expression (Haecker et al, 2007).

By contrast *atro*$^{e46\text{-}2}$ was shown to be a mutant allele that derives from an imprecise excision of another P-element insertion (P1) inside *atro* first exon (Erkner et al, 2002).

Taken together, the different genetic backgrounds described above, indicate that it is reasonable that our analysis of *atro* phenotype results different from the one published.

We did not observe any significant retinal degeneration in the homozygous *atro*$^{e46\text{-}2}$ clones (Fig. 6.1;Fig. 6.2). Most of the clones aged three weeks, both for *atro*$^{e46\text{-}2}$*,FRT2A* and for *atro*$^{e46\text{-}2}$*,FRT80*, still displayed a low level of degeneration and more than 90% of the mutant ommatidia were preserved in their content or have lost one photoreceptor at most.

The simplest explanation for this faint retinal phenotype is that *atro*$^{e46\text{-}2}$ is a weak allele, differently from what has been described in the literature. Alternatively, it is possible that the mutation has been lost from our stock.

The second allele we used was *gug*^{35} loss of function allele from the Kerridge' lab (Erkner et al, 2002). In terms of rapidity and level of degeneration reached, the retinal phenotype induced by *gug*^{35}*,FRT2A* mutation was comparable to the one observed in *atro*^{e46}*,FRT2A* mutant clones. However, the increase in the severity of phenotype was much more significant in *gug*^{35}*,FRT2A* clones with respect to *atro*^{e46}*,FRT2A*, since more than half of the clones dissected acquired a medium level of degeneration and around half of the mutant ommatidia lost two or more photoreceptors. Homozygous clones derived from the mitotic recombination of the *gug*^{35}*,FRT80* chromosome also gave rise to a progressive and significant retinal neurodegeneration. These findings failed to confirm that *atro*^{e46} and *gug*^{35} are *atro* alleles of equivalent strength, as reported in the literature (Erkner et al, 2002; Zhang et al, 2002).

In addition, the *gug*^{35},*FRT80* phenotype was not comparable to the one of *atro*^{e46} or *gug*^{35},*FRT2A*. Actually half of the older *gug*^{35},*FRT80* homozygous clones observed displayed a severely degenerated phenotype that resulted much stronger than in *atro*^{e46},*FRT2A* or *gug*^{35},*FRT2A* mutants of the same age. The difference is likely the consequence of a different initial phenotype of *atro* mutant retina. In the case of the *gug*^{35},*FRT80* we actually found that young homozygous clones already displayed severe alterations inside the mutant tissue, very few ommatidia contained the conserved number of photoreceptor cells and, by contrast, many of them lost two or more cells.

The data obtained from this last analysis suggests that *gug*^{35},*FRT80* mutants gained some new features in their phenotype, that are likely to be independent of *atro* neurodegenerative phenomenon per se, but are probably responsible for the developmental defects. Our hypothesis is that the *gug*^{35},*FRT80* chromosome contains an additional mutation that gives rise to the highly irregular photoreceptor recruitment observed.

To explain the discrepancy among the *gug*^{35},*FRT2A* and the *gug*^{35},*FRT80* phenotype, I should perform a meiotic mapping of the *gug*^{35},*FRT80* chromosome, to find and remove the genomic region containing the hypothetical mutation. Secondly, I should perform again the phenotypic analysis of *gug*^{35} homozygous retinal clones taking advantage of the cleaned chromosome. However this would not help the analysis of the neurodegeneration, which is the focus of this project.

In conclusion, the two *atro/gug* alleles examined gave inconsistent clonal phenotypes in the adult retinae: *atro*^{e46} mutants result in a weak degenerative phenotype whereas *gug*^{35} lead to a strong degeneration.

The neuronal degeneration we observed with *gug*^{35} alleles was only partially comparable to the one observed in *ft* mutant retinae, especially for the rapidity in the appearance and progression of retinal abnormalities. This could be compatible with a model in which Atro is a non essential co-factor in this process.

As already demonstrated, the tumour suppressor Ft interacts physically with the transcriptional co-factor Atro (Fanto et al., 2003). It has been shown that some heteroallelic combinations of *ft* alleles were viable but, if one copy of *atro* was removed in this background, using the *gug*^{35}*,FRT2A* chromosome, lifespan was severely compromised. In addition, the flies that eclosed displayed age-related reduced motility (Fanto et al, 2003). Since one of the possible factors linked to such motor defects could be neuronal degeneration we should establish whether Ft and Atro maintain neuronal homeostasis along the same genetic way or in parallel signalings. In other words, we could induce the fomation of clones homozygous for *ft* mutation in a heterozygous background for *atro*^{e46} or *gug*^{35} alleles, and then investigate if the level of *ft*-induced neurodegeneration gets worse or is ameliorated by removing one copy of *atro*. This would indicate that Ft and Atro interact genetically to preserve cellular homeostasis in the nervous system. It is also possible that Ft would be able to compensate for Atro's absence through a different pathway, perhaps by regulating the Hpo pathway or that Atro-dependent degeneration kicks at a later stage, but further experiments would be necessary to reach a conclusion.

Chapter 7

CELLULAR MECHANISM AFFECTED IN *ft*- AND *hpo*-DEGENERATED NEURONAL CELLS

7.1 Morphological analysis of *ft* degenerated neuronal cells

We have previously excluded loss of adhesion and of cell polarity as the mechanism that induced deterioration of photoreceptors mutant for *ft* or components of the Hpo pathway. To better characterize the morphology of *ft* abnormal neurons and gain more insight into this form of cellular degeneration, we performed an electron microscopic analysis of adult *ft* mutant eyes.

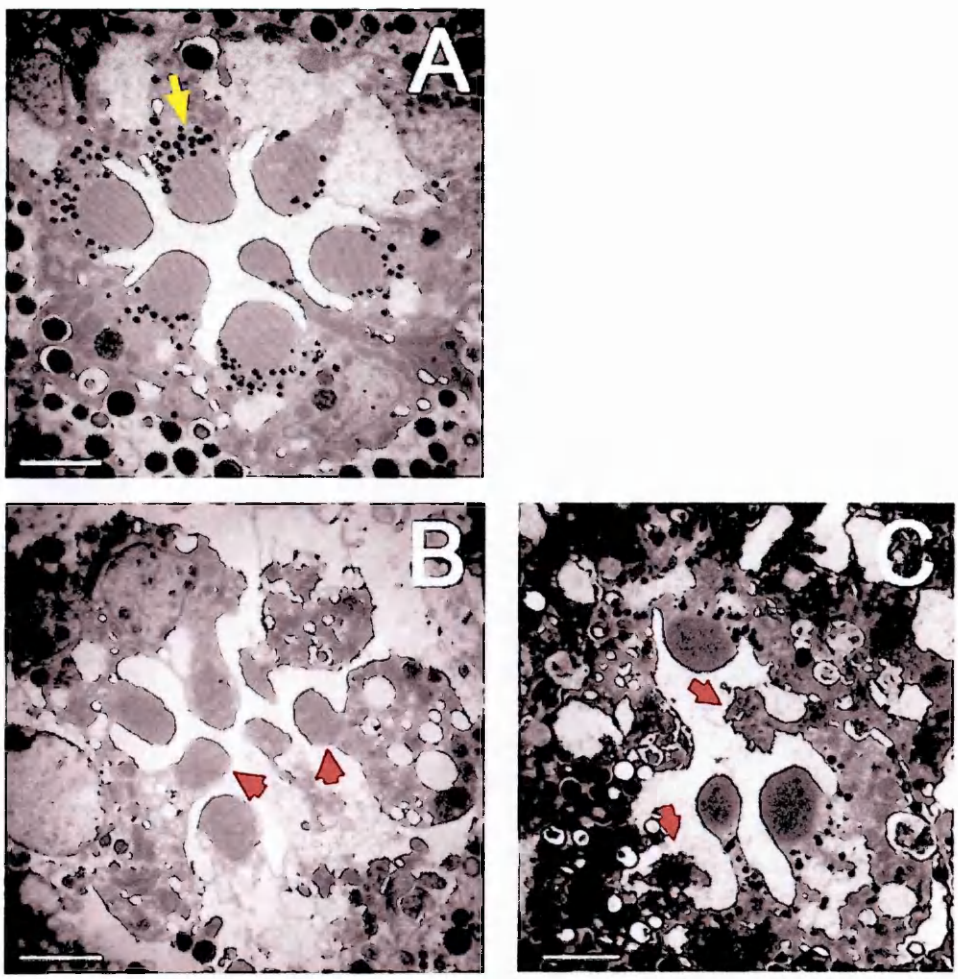

Figure 7.1 Altered morphology of ft^{fd} degenerated ommatidia
A- EM scan of a *wt* 2 weeks old ommatidium. All photoreceptors (R1-R7) position correctly to form the typical trapezoidal shape of the ommatidium. Pigments are

present at the basis of each rhabdomere (yellow arrow) indicating the cell is *wt*. **B,C-** EM scan of two ft^{fd} mutant ommatidia from 2 weeks old mutant flies. The left mutant ommatidium displays a conserved number of cells although most of them appear abnormal with more electron-dense structures inside the cytoplasm. Interestingly the morphology of their rhabdomeres (red arrows) is preserved.In the right mutant ommatidum, one photoreceptor is lost , three of the six remaining are degenerated with an altered morphology of both the cytoplasm and the rhabdomere (red arrows). Scale bars 1μm

Compared to ommatidia belonging to the *wt* tissue (Fig. 7.1A), altered photoreceptors displayed more electron-dense structures inside the cytoplasm (Fig. 7.1B) and were often decreased in size (Fig. 7.1C, arrows). Some abnormal photoreceptors exhibited rhabdomeres still correctly organized, with preserved microvilli architecture (Fig. 7.1B, arrows).

Inside the cytoplasm of *ft* mutant photoreceptors we noticed the presence of uncommon organelles that resembled the structure of double membrane vacuoles like autophagolysosomes (Fig. 7.2B,C), and multilamellar bodies (MLBs), both composed of concentric membrane layers and often sorrounding an electron-dense core (Fig. 7.2D). Sporadically we also observed some mitochondria that appeared with abnormal and less compact cristae (Fig. 7.2E).

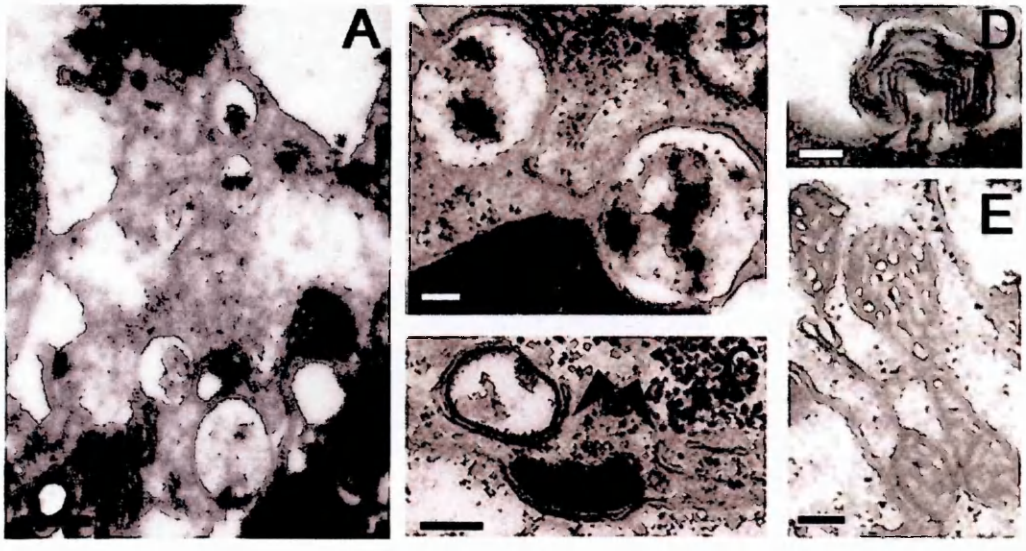

Figure 7.2 Morphology and cytoplasmic content of degenerated ft^{fd} photoreceptors
A- EM scan of a ft^{fd} degenerated photoreceptor (one week old) which has lost the correct morphology of the apical rhabdomere (on the top) and contains

several electron-dense structures inside the cytoplasm. **B-E** High magnification panels display autophagosomes with undigested debris (B), forming phagophores (C, arrowheads), multilamellar body (D) and damaged mitochondria (E) found in ft^{fd} mutant cells. Scale bars 0.5μm for the photoreceptor panel (A) and 0.2μm for zoom-in panels (B-E).

These organelles are part of a fundamental and conserved catabolic process, autophagy, necessary for the maintenance of the cellular homeostasis and the cell viability. Autophagy is an important source of energy for the cell, especially when it is under starvation, because it is involved in the removal of long-lived proteins, organelles and bulk cytoplasm present in the cell (Hariri et al, 2000). It has been also shown to be implicated in some neurodegenerative diseases, cancer and aging (Levine & Kroemer, 2008).

In conclusion, the electron microscopy suggests a possible modulation of the autophagic signaling in *ft*-induced neurodegeneration.

7.2 Increase in the abundance of autophagic organelles inside *ft* mutant photoreceptors

Autophagy is a highly conserved process from yeast to mammals described to begin with the formation of isolation membranes, called phagophores, at the phagophore assembly site. The phagophores then elongate and engulf a portion of the cytosol to form mature autophagosomes, which ultimately fuse with lysosomes to form the degradative autophagolysosomes (Xie & Klionsky, 2007).

My preliminary outcomes on the study of *ft* photoreceptors morphology have implicated autophagy in the regulation of *ft*-induced degeneration. To achieve a quantitation of autophagy in *ft* neuronal cells, we counted, at different time points, the autophagic organelles present inside the

cytoplasm of *ft* mutant photoreceptors in comparison to the nearby *wt* cells. If compared to the *wt* neurons, we could detect an increase in the number of autophagic vacuoles, filled with unstructured partially degraded material, inside *ft*-degenerated photoreceptors. The accumulation of these vacuoles was visible at each time point studied, one week, eleven days and two weeks (Fig. 7.3A,B and C).

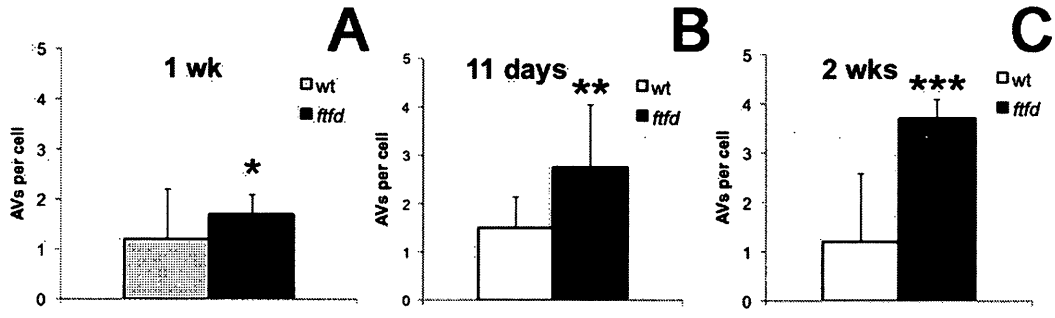

Figure 7.3 Accumulation of autophagic vacuoles in ft^{fd} mutant photoreceptors
A-C Graphs of the quantification of autophagic vesicles (AV) per photoreceptor found in EM sections of 1week (A), 11 days (B) and 2weeks (C) old ft^{fd} clones. Significant accumulation of AV is found in mutant cells (not pigmented) with respect to genotypically *wt* (pigmented) cells. *, $p<0.05$, **, $p<0.01$ and ***, $p<0.001$ in one tail t-test. N=12 pigmented cells vs. 20 not pigmented cells for the 1 week graph, N=12 pigmented cells vs. 16 not pigmented cells for the 11days graph and N=18 pigmented cells vs. 12 not pigmented cells for the 2 weeks graph.

The difference in the number of autophagic organelles between *wt* and ft^{fd} cells was statistically significant in all the three time points studied. Interestingly, the ratio deriving from the number of vacuoles in the two cells' groups increased with the time. Actually, the morphologic analysis of ft^{fd} mutant clones from two week-old flies showed that in *ft* mutant photoreceptors the average number of autophagic vacuoles per cell was three folds more than in *wt* cells (Fig. 7.3C). The presence of autophagic organelles inside two week-old *ft* mutant cells (Fig. 7.3C) was also higher if compared to their abundance in younger one week-old *ft* mutant cells (Fig. 7.3A).

We conclude that neurodegeneration caused by Ft mutation induces a moderate accumulation of autophagic vacuoles, suggesting that Ft preserves neuronal homeostasis by controlling the autophagic process.

7.3 Presence of the Atg8 autophagic marker in ft^{fd} mutant cells

Several membrane proteins are considered particularly useful in the study of autophagic organelles morphology and distribution. The best known mammalian protein that specifically associates with the autophagosome membrane is LC3, the mammalian ortholog of yeast Atg8p, commonly used as a highly specific marker for autophagic vacuoles (Kabeya et al, 2000).

Since the data obtained by EM experiments indicated the involvement of autophagy in *ft* degenerative mechanism, we decided to confirm our morphologic results with Atg8 as a molecular marker. Taking advantage of a GFP::Atg8a chimera, we constitutively over-expressed the *UAS-GFP::Atg8a* transgene via the *tubulinGal4* ubiquitous driver. We then induced the formation of $ft^{fd/fd}$ homozygous clones exclusively in the retinal tissue. Finally, we performed an immunofluorescent staining against GFP, to monitor autophagy by the presence of Atg8 in ft^{fd} mutant clones of the fly eye.

Results from whole mount stainings of one week old *ft* mutant retinae indicated the presence of some Atg8 positive dots both inside *ft* mutant photoreceptors cells but also nearby *wt* cells (Fig. 7.4A). In order to quantify whether there was a significant difference of green dots content among $ft^{fd/fd}$ and *wt* photoreceptors, we needed, first of all, to distinguish the $ft^{fd/+}$ heterozygous tissue from the $ft^{fd/fd}$ homozygous clones. The flies we used

for this experiment carried the ft^{fd} allele together with a *FRT* recombining cassette on one of the two second chromatids, and an *arm-LacZ* transgenic sequence, located nearby the same *FRT* cassette, on its homolog chromatid. After the Flp/FRT mitotic recombination, cells homozygous for ft^{fd} lost the *arm-LacZ* genomic sequence and resulted negative for the β̃galactosidase expression. We tried to use an antibody against β̃galactosidase (β-gal) to distinguish between the *wt* tissue and mutant clones. Unfortunately, our β̃gal staining was really weak and we could not use this criterion as the only way to select *wt* from non *wt* neuronal cells.

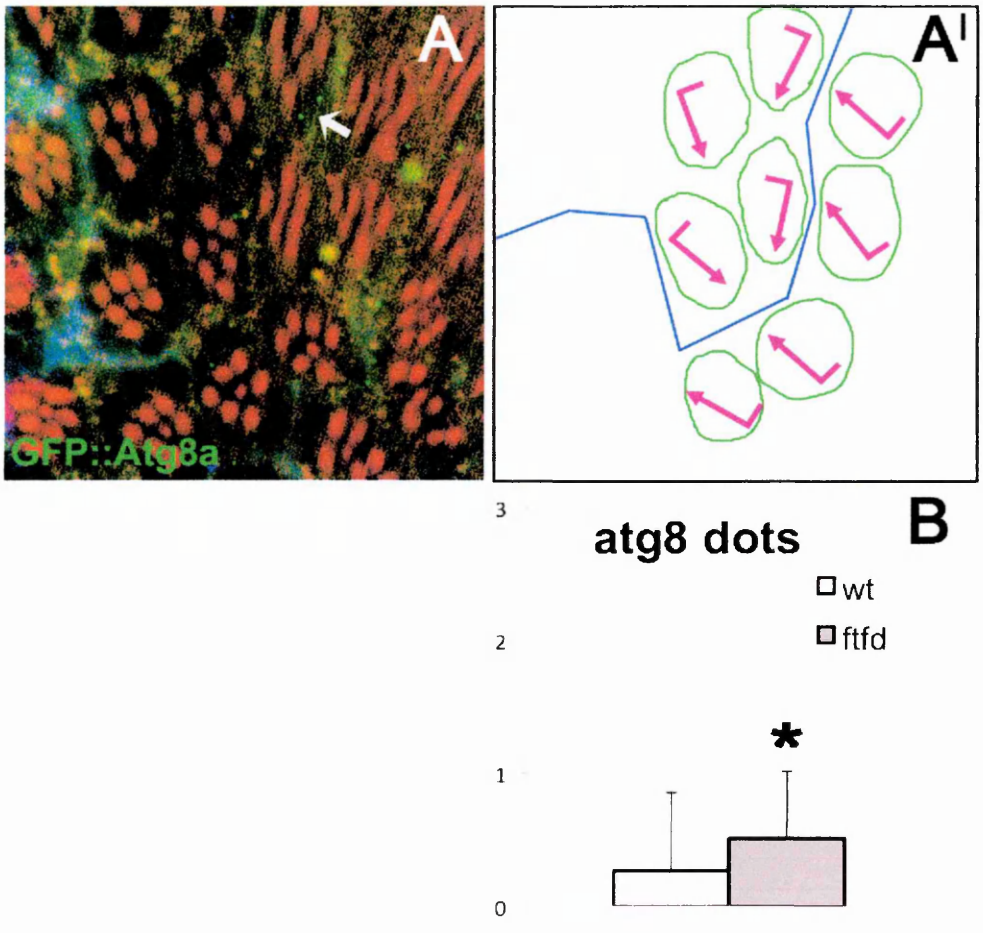

Figure 7.4 Abundance of Atg8 positive vacuoles in ft^{fd} mutant photoreceptors
A- Confocal picture of whole-mount retinae of a ft^{fd} clone aged one week at 29°C and expressing GFP::Atg8a throughout the eye with *Tub-Gal4* . Red is phalloidin marking rhabdomeres, green is GFP, the clone is marked by the absence of β-gal staining (blue). Small GFP::Atg8a dots accumulate specifically inside ft^{fd} mutant cells (arrow). **A^{I}-** Schematic representation of the pseudo-equator (blue line) and orientation of affected ommatidia. Only ommatidia present in the β-gal absent region and adjacent to the pseudo-

equator were considered as belonging to the homozygous clone and analyzed for the GFP::Atg8a presence **B-** Quantification of the number of green dots per photoreceptor in one week old ft^{fd} mutant clones indicates a modest increase of Atg8 presence in homozygous photoreceptor cells if compared to *wt* ones.*, $p<0.05$ in one tail t-test. N=175 *wt* photoreceptor cells vs.154 mutant photoreceptor cells.

We thus decided to take advantage of the known PCP defects displayed by *ft* homozygous clones (Casal et al, 2002; Fanto et al, 2003; Rawls et al, 2002). Mosaic analysis of *ft* mutant clones have demonstrated that PCP defects are not randomly distributed within *ft* clones; on the contrary, at the polar border of *ft* clones the polarity is much more affected rather than at the equatorial side, where the photoreceptors orientation is preserved (Rawls et al, 2002).

As a consequence of the biased distribution of *ft* mutant and non-mutant ommatidia, the delineation of an additional and imaginary inverted equator, also called pseudo-equator, has been described within the mutant clone, where ommatidia are oppositely oriented and face each other (Rawls et al, 2002). Based on this notions, we classified as belonging to the $ft^{fd/fd}$ clone those ommatidia that result adjacent to this pseudo-equator. We quantified the number of Atg8 green positive dots in several one week old ft^{fd} mutant clones and we obtained an average number of 0.51 positive dots per mutant photoreceptor cell out of 0.27 dots per *wt* photoreceptor (Fig. 7.4B). The result indicates a weak but significant increase ($p<0.05$) of Atg8 accumulation in $ft^{fd/fd}$ homozygous clones when compared to the content of *wt* tissue (Fig. 7.4A,B).

Our data from the immunofluorescent analysis of Atg8 suggests a moderate accumulation of positive autophagic vacuoles in *ft* mutant photoreceptors, in agreement with the EM outcomes. However, in order to conclusively demonstrate that autophagy is really involved in *ft*-induced

neurodegeneration, Atg8 outcomes need to be supported with further experiments.

7.4 Accumulation of the p62 autophagic marker in *ft* degenerated cells

The autophagy is one of the main systems that a cell uses for degrading cytoplasmic macromolecules to avoid the accumulation of abnormal proteins, such as ubiquitinated aggregates, in several neurodegenerative diseases.

Our morphologic analysis has highlighted the presence of autophagic vacuoles inside *ft*-degenerated photoreceptors that appeared not to be empty but rather filled with partially degraded material.

The scaffolding protein p62 is detected in polyubiquitinated aggregates destined to autophagic degradation (Bjorkoy et al, 2005) and it has also been shown to bind directly to the autophagic marker Atg8 (Pankiv et al, 2007). Since p62 is required for the degradation of aggregates by autophagy and is a marker of such aggregates (Moscat & Diaz-Meco, 2009), we wondered whether the presence of *Drosophila* p62 ortholog, called Ref(2)P, was modulated inside *ft* mutant photoreceptors.

We thus isolated the retinal tissue from one week-old ft^{fd} mutant flies and we performed a whole-mount immunofluorescence against endogenous p62 protein. The staining revealed the presence of many p62 positive aggregates (marked in blue) inside ft^{fd} null photoreceptors, marked by the absence of GFP antibody staining (Fig. 7.5 yellow arrows). As expected we also found some blue dots in completely *wt* tissue (Fig. 7.5 white arrows). We thus performed a quantitative analysis of p62 positive

dots comparable to the previous one carried for Atg8 marker, using the same phenotypic criteria to classify ommatidia as belonging to the *wt* tissue or the ft^{fd} homozygous clone. The number of p62 dots was calculated as an average of the number of blue spots per photoreceptor cell.

We observed a strong and significant increase in the abundance of p62 presence inside mutant ommatidia belonging to $ft^{fd/fd}$ homozygous clones with respect to *wt* regions (Fig. 7.5D).

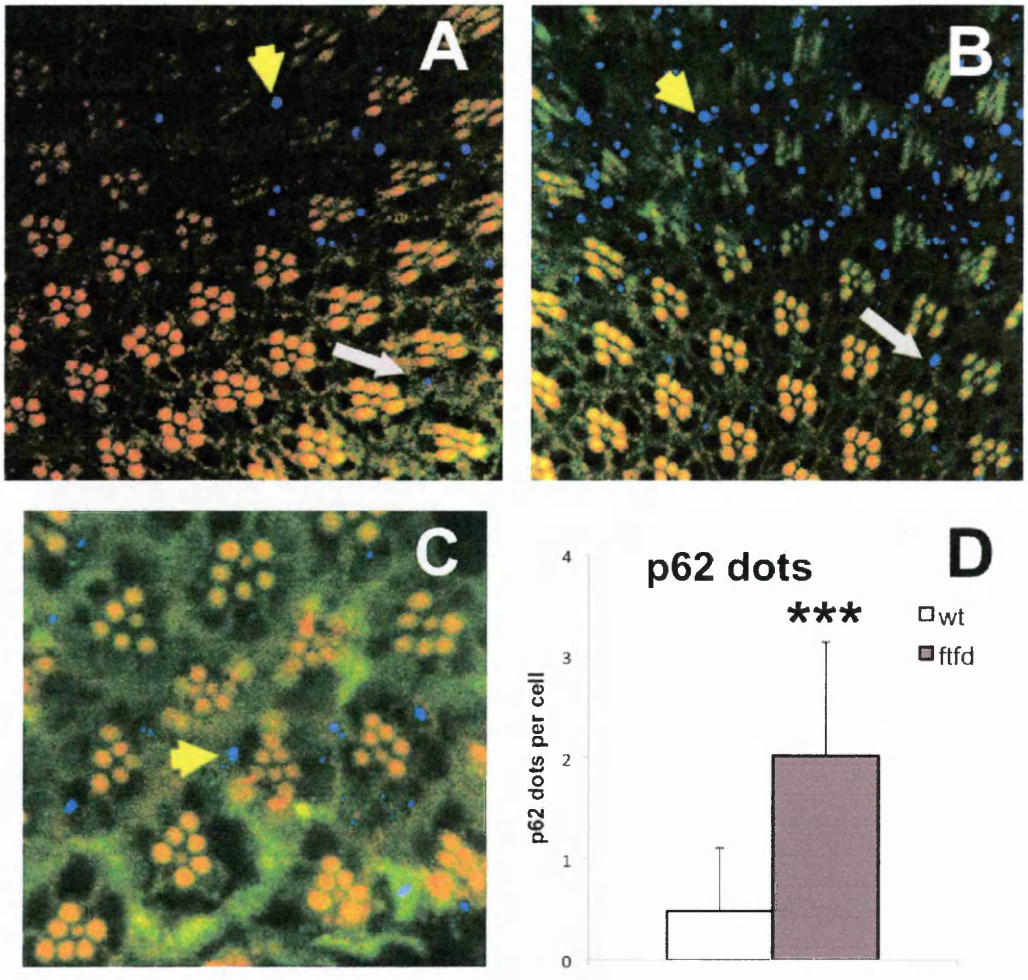

Figure 7.5 Accumulation of p62 in ft^{fd} mutant photoreceptors
A,B- Confocal pictures of whole-mount retinae of ft^{fd} homozygous clones from mutant flies aged 1 week at 29°C. Red is phalloidin marking rhabdomeres, blue is p62, the clone is marked by the absence of GFP staining (green) and the presence of PCP defects. In the left panel there is an example of low degenerated clone where most of the ommatidia contain a correct number of photoreceptors and p62 starts to gather in small dots specifically inside *ft* mutant cells (yellow arrow) but is observed also in *wt* tissue (white arrow). In the right panel an example of a more degenerated clone is shown where p62 is massively accumulated (yellow arrow) in the *ft* mutant clone, where many cells are degenerating. White arrow points to p62 dots inside the *wt* region. **C-** Enlargement of a confocal picture showing the region of the pseudo-equator where we quantified the number of p62 dots in ft^{fd} mutant

cells (yellow arrow). **D-** Quantification of the number of p62 blue dots per photoreceptor in one week old ft^{fd} mutant retinae indicates a significant increase of p62 in homozygous photoreceptor cells if compared to *wt* ones.***, $p<0.001$ in one tail t-test. N=350 *wt* photoreceptor cells vs. 406 mutant photoreceptor cells.

The average number of p62 presence, in neurons from flies aged one week at 29°C, was 2.1 blue dots per mutant photoreceptor cell versus 0.48 positive dots per *wt* cell being much lower than in *ft* mutant cells. Interestingly the number of p62 positive regions increased accordingly to the progression in the severity of the degenerative phenotype (Fig. 7.5B).

In conclusion, these results suggest the existence of massive protein aggregates inside *ft* mutant neuronal cells. This could be due to a block of the degradative process that contribute to the persistence of the material incorporated, including p62 positive aggregates.

7.5 Increase in the abundance of autophagic organelles inside *sav* mutant photoreceptors

Our previous genetic analysis revealed an interaction between Ft signaling and the Hpo-Sav-Wts pathway. Most of the components of the core, when mutated, induce a retinal degenerative phenotype (Fig. 5.2; Fig. 5.3; Fig. 5.4).

In order to understand the mechanism of degeneration in neuronal cells lacking one of the Hpo-Sav-Wts cascade molecules, and to compare this degeneration with the *ft* one, we performed an electron microscopy analysis of sav^3 mutant neuronal cells isolated from adult fly eyes.

Among the one week old sav^3 fly retinae, some mutant ommatidia displayed a decreased number of cells. Other ommatidia resulted normal in their content, although some of the mutant photoreceptors looked more electrondense, with a morphology of the cell completely disorganized (Fig.

7.6B) if compared to *wt* cells (Fig. 7.6A). It was hard to distinguish specific organelles inside the cytoplasm of these cells. However, less degenerated photoreceptors showed a cytoplasm dense in aberrant mitochondria and double membrane organelles very similar to the autophagic vacuoles detected in ft^{fd} mutant cells (Fig. 7.6D).

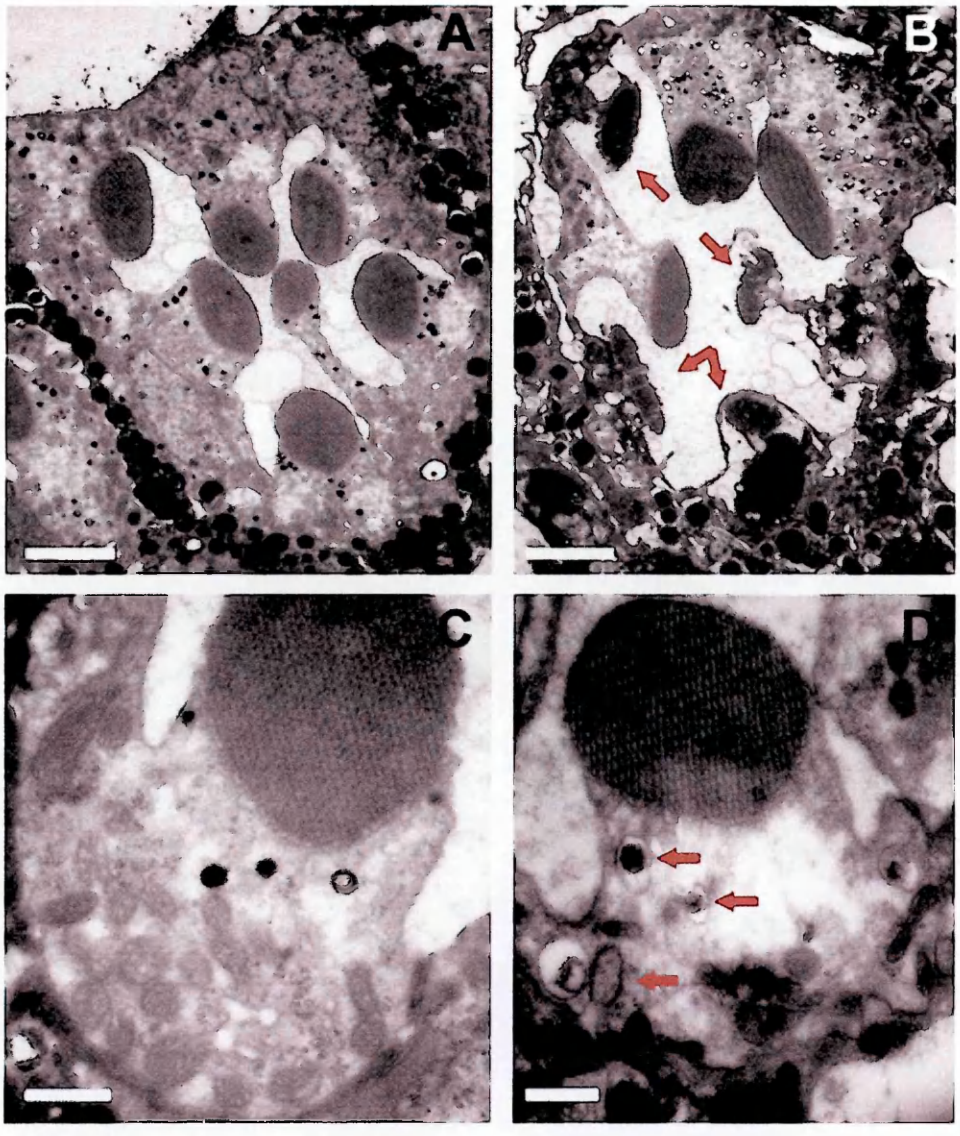

Figure 7.6 Altered morphology of sav^3 degenerated ommatidia
A- EM scan of a *wt* 1 week old ommatidium. Photoreceptors from R1 to R7 photoreceptors position correctly to form the typical trapezoidal shape of the ommatidium. Pigments are present at the basis of each rhabdomere indicating the cell is *wt*. **B-** EM scan of a ft^{fd} mutant ommatidium from 1 week old fly eye. The ommatidium displays a conserved number of cells although most of the cells appear highly degenerated (red arrows). **C,D-** Enlargement of a *wt* (C) and ft^{fd} mutant photoreceptors (D). The mutant cell maintains the correct morphology of the apical rhabdomere but contains several electrondense double-membrane structures inside the cytoplasm

(red arrows). Scale bars 1μm for the ommatidia, 0.5μm for the photoreceptors.

We thus decided to analyse in more detail the cytoplasm of *sav*^{3} mutant neuronal cells and to quantify the number of the autophagic vacuoles inside (Fig. 7.7A,B). Interestingly, *sav* mutant clones from flies aged one week at 29°C showed an accumulation of autophagic vacuoles different from the number of the same organelles inside *wt* cells (Fig. 7.6C). The average number of autophagic organelles in one week old *sav* mutant tissue was 2.1 per photoreceptor cell and the increase was statistically significant if compared to the average number in *wt* photoreceptors (0.8 per cell) (Fig. 7.7B).

In conclusion, morphologic analysis of neuronal cells mutants for one of the component of the Hpo-Sav-Wts pathway suggests that autophagy is deregulated when cells undergo neurodegeneration, very similarly to what we found in *ft* mutant clones.

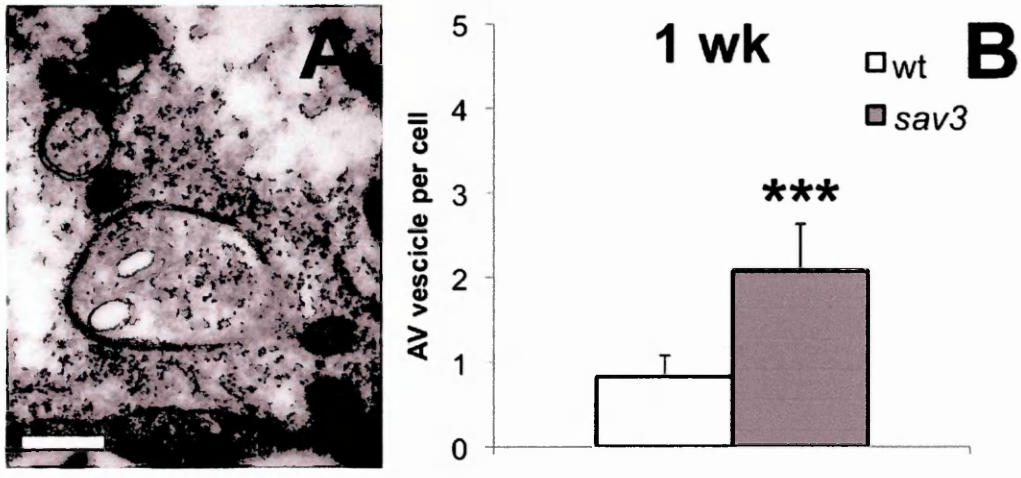

Figure 7.7 Accumulation of autophagic vacuoles in *sav*^{3} mutant photoreceptors
A- High magnification panel of a cell cytoplasm from a *sav* degenerated 1 week old photoreceptor cell where the presence of three distinct double membrane vescicles is evident. **B-** Graph of the quantification of autophagic vesicles (AV) per photoreceptor found in EM sections of 1 week old *sav*^{3} clones. Significant accumulation of AV is found in mutant cells (not pigmented) with respect to genotypically *wt* (pigmented) cells. ***, $p<0.001$ in one tail t-test. N=43 pigmented cells vs. 44 not pigmented cells. Scale bar is 0.2 μm.

7.6 Blocking autophagy enhances *ft* neurodegeneration

The process of autophagosome formation is driven by the activity of the autophagy-related (*Atg*) genes, which were identified through genetic screens in yeast and in several cases have been shown to promote autophagy in higher eukaryotes as well (Suzuki et al, 2007a). In *Saccharomyces cerevisiae*, the Ser/Thr kinase Atg1 appeared to play a role in initiating autophagosome formation in response to nutrient- and TOR-dependent signals (Matsuura et al, 1997). In *Drosophila*, a single *Atg1* gene was found and shown to act downstream of *Tor* to promote autophagy (Scott et al, 2007; Scott et al, 2004).

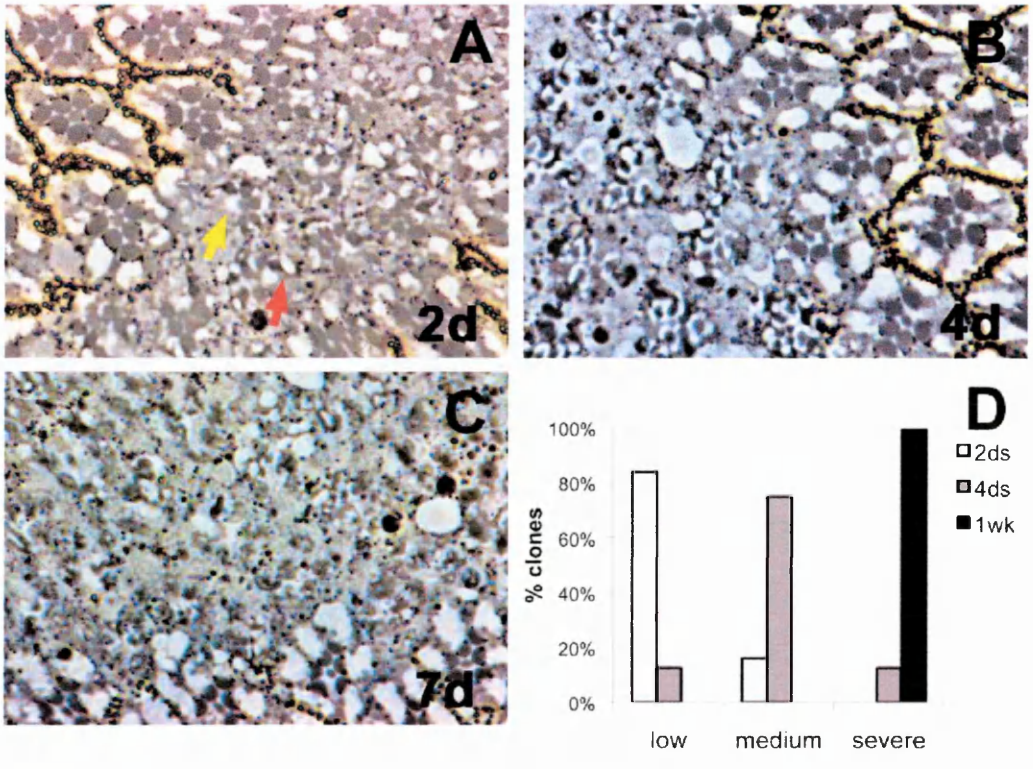

Figure 7.8 Enhancement of *ft* neuronal degeneration by blocking *atg1* in the fly eye
A,B,C- Semithin tangential sections of $ft^{fd/fd}$; $atg1^{\Delta 3D/\Delta 3D}$ double mutant clones from adult flies aged 2 days (A), 4 days (B) and 1 week (C) at 29°C. Two days after eclosure (A) almost all photoreceptors are intact and only few ommatidia displays one photoreceptor abnormal (red arrow) or missing (yellow arrow). After 4 days (B) many cells are lost or have degenerated and most of the clones observed belong to the medium category. After 1 week at 29°C all the double mutants dissected are severely degenerated an the structure of the ommatidia is completely lost. **D-** Quantification of the level of degeneration in $ft^{fd/fd}$; $atg1^{\Delta 3D/\Delta 3D}$ double mutant clones aged two days (white columns), four days (grey columns) and 1 week (black column) at 29°C. After two days of age, most of the clones

display a low level of degeneration (85%) whereas all the other clones observed belong to the medium category (N=10 clones). After four days there is an increase in the severity of the phenotype and only 10% of the clones observed is still low degenerated, whereas 75% belongs to the medium category (N= 12 clones). One week old double mutant clones are all severely affected and most of the photoreceptors have died (N=8 clones).

To investigate the function of autophagy in determining the *ft* phenotype, we examined the genetic signaling that regulates the pathway, we blocked its activation by using a mutant allele for *atg1*, one of the main regulators of the autophagy induction, and we generated clones homozygous for both ft^{fd} and $atg1^{\Delta 3D}$ loss of function alleles.

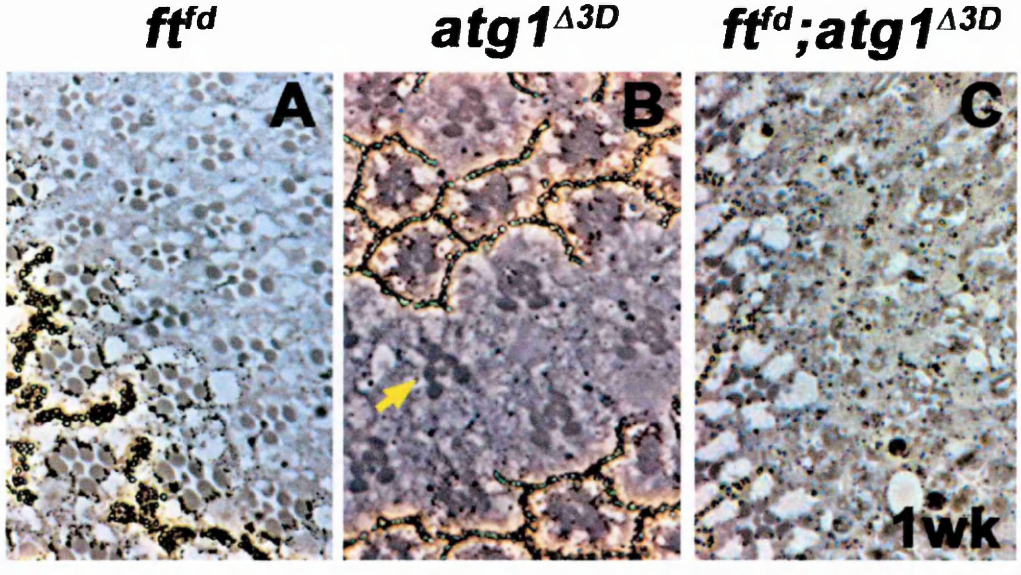

Figure 7.9 Stronger retinal degeneration in clones double mutants for *ft* and *atg1* compared to the single mutants
A,B,C- Semithin tangential sections of $ft^{fd/fd}$ (A), $atg1^{\Delta 3D/\Delta 3D}$ (B) single mutants and $ft^{fd/fd}$; $atg1^{\Delta 3D/\Delta 3D}$ double mutant clones (C) from adult flies aged 1 week at 29°C. Both single mutants display a low level of degeneration inside not pigmented regions, whereas the strong increase of retinal abnormalities in the double mutant clones is evident and the mutant tissue (right part of the section) is almost completely degenerated.

Soon after eclosion, we fixed the retinal tissue of double mutant flies. After ageing adult flies two days at 29°C, ft^{fd}; $atg1^{\Delta 3D}$ retinal double mutant clones already showed some mutant ommatidia with few abnormal or missing photoreceptors (Fig. 7.8A,D). The phenotype became more severe after four days at the same temperature and most of the double clones

isolated appeared with a medium level of degeneration (Fig. 7.8B,D). One week old ft^{fd}; $atg1^{\Delta 3D}$ double mutants displayed unequivocally a strong and severe phenotype and it was very hard to distinguish photoreceptors cells inside the clone (Fig. 7.8C,D).

Thus, comparing double mutant clones from flies aged one week at 29°C with $ft^{fd/fd}$ and $atg1^{\Delta 3D/\Delta 3D}$ single mutants at the same time point (Fig. 7.9) we could show that blocking autophagy, with $atg1^{\Delta 3D}$ allele, leads to a strong enhancement of *ft* retinal neurodegeneration.

In conclusion, these data support the idea that *ft* could be part of a signalling which cooperates with *atg1* to maintain the homeostasis of neuronal cells.

7.7 Blocking or activating Tor activity do not influence *ft* retinal degeneration

One of the key upstream regulators of autophagy is the TOR kinase (the target of rapamycin) which mediates inhibition of autophagic signalling by the presence of abundant nutrients or growth factors. The TOR kinase is conserved across species and it has been studied for a long time since it is a central effector of cell growth, involved in the control of several metabolic processes such as mRNA transcription, protein translation, cytoskeletal organization, autophagy and cell death (Wullschleger et al, 2006).

The induction of autophagy, that occurs when TOR activity is suppressed, has been suggested to benefit several neurodegenerative disorders like Huntington disease, both in mammals (Mizushima et al, 2008; Rubinsztein et al, 2007) and recently also in *Drosophila* (Wang & Levine, 2010).

Since our preliminary data suggested a modulation of autophagy by *ft* induced degeneration, we wondered whether the hyper-activation of autophagy, by blocking TOR activity, could influence the *ft* phenotype.

We blocked the TOR activity by using a mutant allele for *tor*, $tor^{\Delta P}$, described as a deletion resulting from an imprecise excision of the Tor^{EP2353} P-element which removes the Tor translation start site (Zhang, 2000). We then induced the formation of clones in the fly eye which were double mutants for ft^{fd} and $tor^{\Delta P}$ in a heterozygous background for both alleles.

As expected we obtained a strong inhibition of cell growth as a result of the TOR blockage (Fig. 7.10, arrows). Interestingly, we found also a decrease of the *ft* overgrowth phenotype. The size of the double mutant clones was actually very small and they basically corresponded with sporadic and isolated cells inside pigmented ommatidia (Fig. 7.10, arrows).

This kind of phenotype was comparable to the one of $tor^{\Delta P}$ single mutant clones (Fig. 7.10) and in contrast with the enormous size of ft^{fd} homozygous clone (Fig. 7.10). This result suggests a block of the cellular proliferation stimulated when *ft* tumor suppressor is mutated. We can infer that Fat requires Tor in the control of cell proliferation. However, our main purpose was the analysis of *ft* degenerative phenotype in a *Tor* mutant tissue. Unfortunately, the very small size of the mutant cells, together with the decrease dimension of the clone, prevented us from studying a possible modulation of *ft* neurodegenerative phenotype by *Tor*.

To overcome the problems faced by blocking Tor with $tor^{\Delta P}$ mutant allele, we used a dominant negative form of Tor, Tor^{TED}, described as a strong inducer of autophagy (Scott et al, 2004).

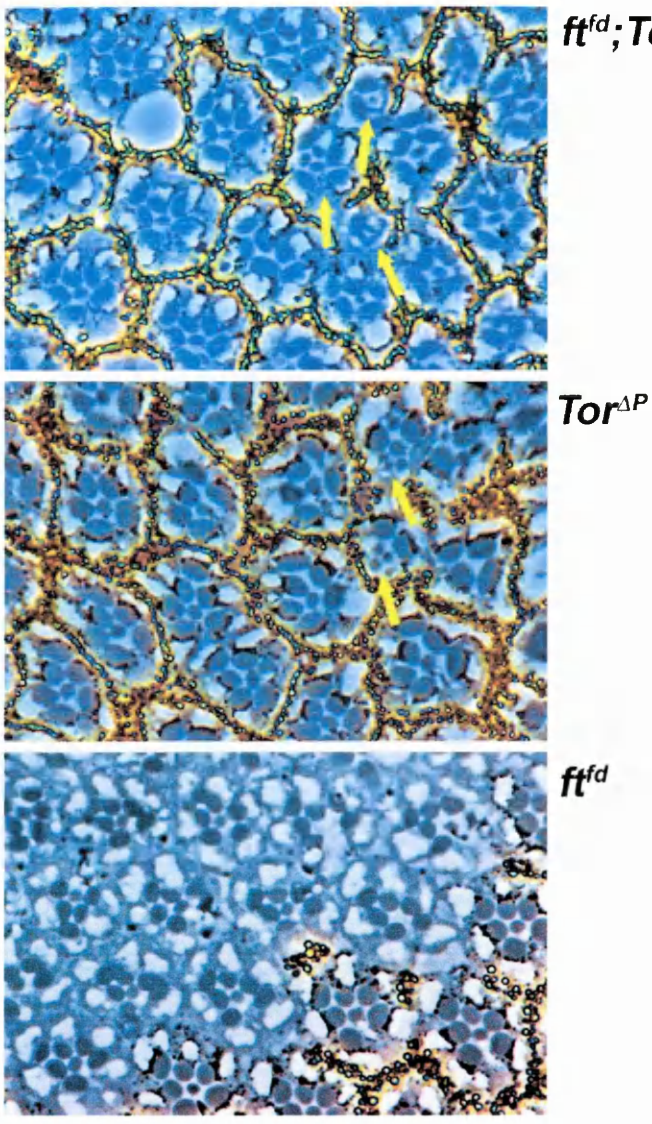

Figure 7.10 Tor is required to prevent *ft* overgrowth in the fly retina
Tangential sections of ft^{fd};$tor^{\Delta P}$ double mutants and $tor^{\Delta P}$ or ft^{fd} single mutants aged 1 week at 29°C. Double mutants' section displays a strong decrease of the clone overgrowth size and only few cells are double mutants (yellow arrows, absence of pigment at the base of the rhabdomere) similarly to the phenotype of $tor^{\Delta P}$ single mutant clones (middle panel) and in contrast to the overgrowth of ft^{fd} homozygous tissue (lower panel).

In parallel, we also decided to perform the opposite experiment, that is stimulating the TOR kinase by downregulating the activity of TSC2/TSC1 complex specifically in *ft* mutant clones. The protein complex consisting of TSC1 (or hamartin) and TSC2 (or tuberin) has emerged to be a

fundamental negative regulator of the TOR kinase (Huang & Manning, 2008). Studies of *Drosophila* Tsc1 and Tsc2 homologs have identified a specific function for TSC1-TSC2 complex in the control of cell growth, with loss of *Tsc1-Tsc2* resulting in increased cell size (Tapon et al, 2001). Further studies suggest that *Tsc1-Tsc2* inhibits the amino-acid-TOR signalling pathway, which normally couples amino-acid availability to translation initiation and cell growth (Zhang et al, 2003; Potter et al, 2001).

For our mosaic analysis, we took advantage of a genetic system, the mosaic analysis with a repressible cell marker (MARCM), that positively marks mutant cells (See Section 3.3). This genetic system combines the GAL80 repressor protein with the *Drosophila* Gal4-UAS binary system and the Flp/FRT system in order to genetically label clones (Lai & Lee, 2006; Lee & Luo, 1999).

We perfomed two distinct crosses in parallel, to understand whether blocking or activating Tor activity could modify *ft* retinal degeneration. Thanks to the MARCM strategy, after mitotic recombination, we obtained from the first cross clones of cells homozygous for ft^{fd} that also expressed the *UAS-Tor*^{TED} transgene, because they were GAL80 negative. From a parallel cross, we obtained clones of cells homozygous for ft^{fd} that expressed another transgene, the *UAS-Tsc1*^{IR}, which codifies for a *RNAi* sequence against Tsc1.

We compared the retinal phenotype of one week old ft^{fd} homozygous photoreceptors cells expressing the *Tsc1*^{IR} (Fig. 7.11A) with cells mutant for ft^{fd} and expressing *Tor*^{TED} (Fig. 7.11C) and ft^{fd} homozygous photoreceptors cells that lacked the *UAS* transgene but were in the same Gal80/Gal4 genetic background (Fig. 7.11E). After one week at 29°C, the level of degeneration we observed was comparable among the three distinct

genotypes and most of the mutant retinal tissues belonged to the medium category of degeneration (Fig. 7.11G).

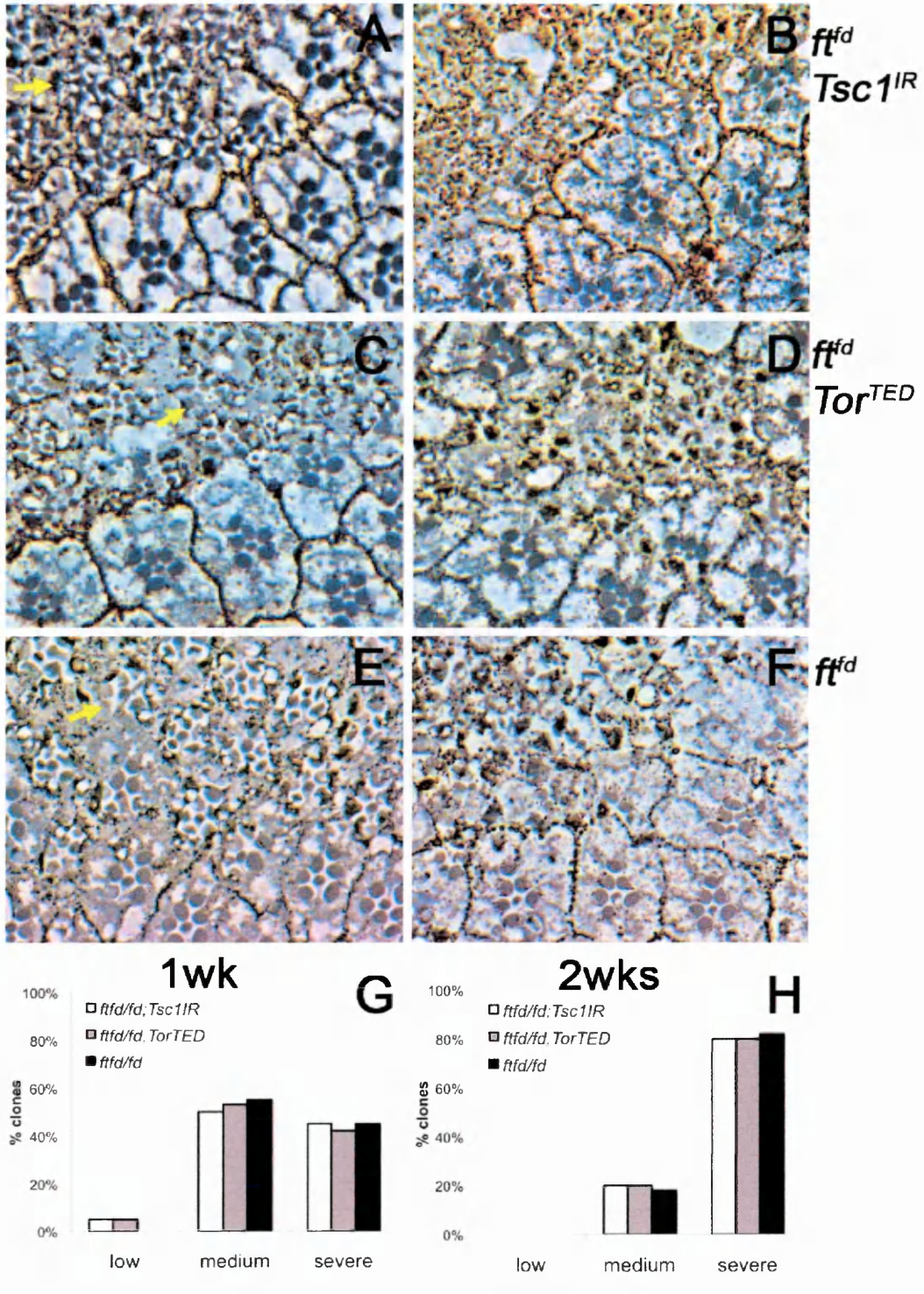

Figure 7.11 Blocking or activating Tor activity does not influence *ft* retinal degeneration

A-F Tangential section of ft^{fd},$Tsc1^{IR}$ mutants (A,B), ft^{fd},Tor^{TED} mutants (C,D) and ft^{fd} single mutants (E,F) aged 1 week (A,C,E) or two weeks (B,D,F) at 29°C. After 1 week the expression of *RNAi* against *Tsc1* in *ft* homozygous clones (A, top of the panel) gives rise to a retinal phenotype with many examples of abnormal photoreceptors (yellow arrow) and comparable to the phenotype of *ft* clones expressing Tor^{TED} (C, top of the panel) where also photoreceptor loss is

present. The phenotype is comparable to the one of *ft* homozygous clones without the expression of any transgene (E, top of the panel) where most of the mutant ommatidia display both degenerated photoreceptors and a decrease in their number (yellow arrow). After 2 weeks in both *ft* clones expressing $Tsc1^{IR}$ (B, top of the panel) or Tor^{TED} (D, top of the panel) and *ft* homozygous tissue *per se* (F, top of the panel) the majority of photoreceptors cells are severely degenerated or dead whereas the *wt* tissue is preserved. **G,H-** Quantification of the level of degeneration in $ft^{fd}, Tsc1^{IR}$ (white columns) mutants, ft^{fd}, Tor^{TED} mutant clones (grey columns) and ft^{fd} homozygous clones (black columns) aged one week (G) and two weeks (H) at 29°C and analyzed in blind. After one week of age, very few *ft* clones expressing $Tsc1^{IR}$ or Tor^{TED} inside *ft* homozygous clones display a low level of degeneration (5% for both) whereas half of the mutant retinae dissected belong to the medium category (50% for $Tsc1^{IR}$ expressing mutants and 53% for Tor^{TED} expressing mutants) and the other clones observed are severely degenerated (N=10 clones for $Tsc1^{IR}$ and 11 clones for Tor^{TED}). At the same age *ft* homozygous clones dissected do not show any example of low degeneration whereas more than half have a medium level of degeneration (55%) and the other are severely degenerated (N=10 clones). After two weeks the phenotype increases and most of all the *ft* clones analysed are severely degenerated (80% for $Tsc1^{IR}$ and also Tor^{TED} and 82% for *ft* clones without any transgenic expression) and only a minority belongs to the medium category of degeneration (N=10 clones for both $Tsc1^{IR}$ and also Tor^{TED} clones and 11 clones for *ft* clones).

Regions within the clone were characterized by a general disorganization of the mutant ommatidia and a decrease of the cell size (Fig. 7.11A,C,E). At this time point, we could already detect several degenerated mutant photoreceptors, even though the number of cells per ommatidium was almost conserved.

From a blind test analysis of the retinal phenotype, we noticed that there was a medium level of degeneration and $ft^{fd/fd}$ clones over-expressing Tor^{TED} or $Tsc1^{IR}$ displayed a phenotype comparable to $ft^{fd/fd}$ clones without any transgene' expression (Fig. 7.11G). After two weeks the retinal abnormalities became worse and most of the mutant photoreceptors were severely degenerated (Fig. 7.11H), both in ft^{fd} homozygous clones expressing Tor^{TED} or $Tsc1^{IR}$ (Fig 7.11B,D) and also inside the tissue mutant for *ft* but *wild-type* for *Tor* or *Tsc1* (Fig. 7.11F).

In conclusion, these outcomes do not give us any evidence that Tor kinase signaling modifies the retinal phenotype of *ft* mutant fly eyes.

Unexpectedly, we found that the level of degeneration of $ft^{fd/fd}$ mutant clones, induced in the MARCM genetic background, was excessively increased and much stronger with respect to the $ft^{fd/fd}$ phenotype previously analyzed in Flp/FRT mitotic clones at the same time points (Fig. 4.3). This effect could be a consequence of the different genetic background used, since in the first experiments was totally *wild-type* differently from the MARCM that was heterozygous for the Gal80-Gal4 drivers. This hypothesis appears unlikely because other people in the lab are using the MARCM technique without finding such background effects on degeneration. More likely, the unexpected higher level of degeneration of *ft* clones was due to the instability and uncontrollable changes in the temperature of the incubator where we left flies to age. This could have masked the real outcome of our experiments.

In conclusion, our data suggest that Tor activity does not influence advanced degeneration by *ft*. However we cannot rule out that blocking or activating Tor activity does not modulate *ft* retinal condition at an earlier stage of degeneration.

7.8 Stimulation of autophagy by Atg1 expression does not modify *ft* retinal degeneration

Our previous results had shown that *ft* induced neurodegeneration could not be rescued by modulating the upstream regulators of autophagy. One possibility is that blocking Tor activity is too strong and aspecific because it indirectly modulates several signalings such as transcription, translation and cell-cycle that could mask the real outcome of the analysis.

We then decided to test a more direct stimulation of autophagy downstream of Tor, by overexpressing the Atg1 *wt* protein. A weak *UAS-Atg1* construct, $Atg1^{GS}$, whose expression does not affect *per se* retinal consumption, has been shown to demonstrate that, by inducing autophagy, Atg1 inhibits cell growth and causes apoptotic cell death (Scott et al, 2007). As for the last set of experiments, we induced the formation of clones homozygous for ft^{fd} taking advantage of the MARCM system to express $Atg1^{GS}$ exclusively in the homozygous clone.

We observed that in one week old ft^{fd} mutant retinae, the expression of Atg1 (Fig. 7.12A) brought about a level of retinal degeneration that was faintly slower than ft^{fd} mutation alone (Fig. 7.12B), because we observed few clones with a low level of degeneration in the former case but not in the latter case (Fig. 7.12E). However we could not detect any significant rescue of the *ft* phenotype by Atg1 expression (Fig. 7.12E).

Older mutants aged two weeks at 29°C showed a more severe level of retinal abnormalities both in ft^{fd} mutants expressing the Atg1 transgene (Fig. 7.12C) and also in ft^{fd} homozygous clones with a *wild-type* background for Atg1 (Fig. 7.12D). Interestingly, we observed that both the organization and shape of ommatidia mutant for ft^{fd} and expressing *Atg1* appeared much more normal (Fig. 7.12C) if compared to the ommatidia inside ft^{fd} homozygous clones without the transgene (Fig. 7.12D) giving the impression of a slowdown in the phenotype, although in both the cases most of the photoreceptors were degenerated.

In conclusion, results from the genetic analysis of the autophagic signaling suggests that the progressive degeneration caused by the lacking of *ft* can be rescued neither by autophagy activation nor by expressing Atg1, one of the main components of the machinery.

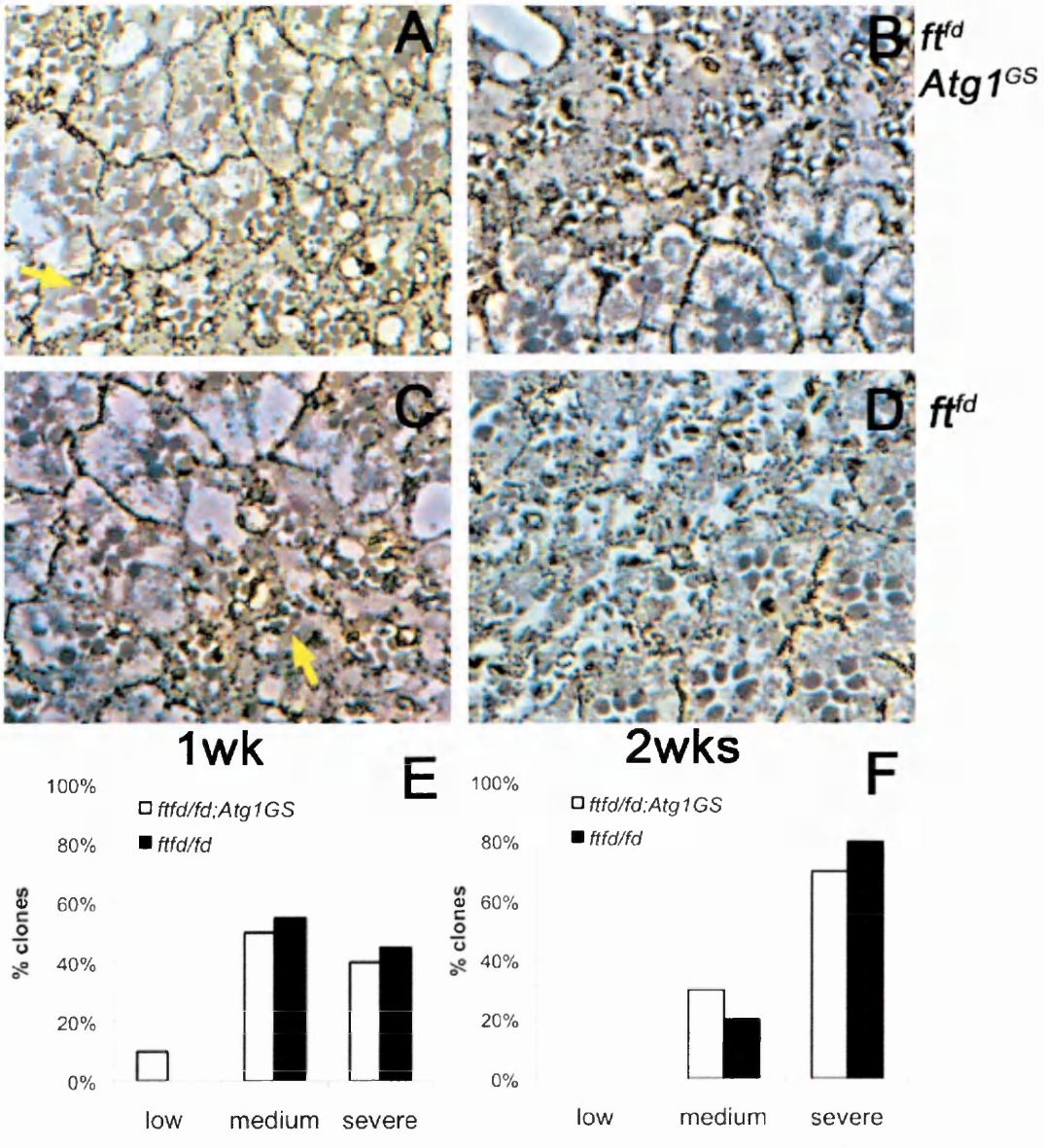

Figure 7.12 Stimulating autophagy with Atg1 faintly ameliorates *ft* retinal degeneration

A-D Tangential section of ft^{fd};$Atg1^{GS}$ mutants (A,B), and ft^{fd} single mutants (C,D) aged 1 week (A,C) or two weeks (B,D) at 29°C. After 1 week the expression of Atg1 in *ft* homozygous clones (A, bottom of the panel) gives rise to a retinal phenotype with some examples of abnormal photoreceptors (yellow arrow) that are overall comparable to the phenotype of *ft* clones *per se* (C) where also photoreceptor degeneration or loss is present (yellow arrow). After 2 weeks in *ft* clones expressing $Atg1^{GS}$ (B, top of the panel) we observe an increase in the level of degeneration since most of the cells are degenerated as in *ft* homozygous clones without $Atg1^{GS}$ (D, top of the panel). Interestingly mutant ommatidia of *ft* clones expressing *Atg1* are still distinguishable in their shape and content and the tissue in its complex appears less disorganized if compared to *ft* homozygous tissue *per se*.
G,H- Quantification of the level of degeneration in ft^{fd};$Atg1^{GS}$ (white columns) mutants and ft^{fd} homozygous clones (black columns) aged one week (E) and two weeks (F) at 29°C and analyzed in blind. After one week of age, few *ft* clones expressing *Atg1* display a low level of degeneration (10%) whereas half of the mutant retinae dissected belong to the medium category and the other clones observed are severely degenerated (N=10 clones). At the same age *ft* homozygous clones dissected do not show any

example of low degeneration whereas more than half (55%) have a medium level of degeneration and the others are severely degenerated (N=10 clones). After two weeks the number of *ft* homozygous clones expressing $Atg1^{GS}$ with a medium level of degeneration decreases (30%) and all the other clones analysed are severely degenerated (N=11 clones). The phenotype in *ft* clones, without any transgenic expression, was comparable (20% belong to the medium category and 80% to the severe one) to the clones expressing $Atg1^{GS}$ (N=10 clones).

These outcomes raise the possibility that the loss of *ft* leads to an alteration of the endogenous autophagic process downstream to the formation of the autophagosomes. It is thus likely that our exogenous induction of autophagy and the observed formation of more autophagosomes is not sufficient to solve this type of endogenous block because it is upstream of the defective step.

However because in the later experiments we experienced a markedly increased level of degeneration in control ft^{fd} clones, it remains to be established what would the outcome be in a condition in which the baseline of degeneration detected in ft^{fd} clones would be milder and more comparable to what we observed in the past experiments (Fig. 4.1).

7.9 DISCUSSION

Our knowledge of the cell death of *ft* mutant neurons was limited. We therefore investigated the cellular mechanism affected in *ft* mutant photoreceptor cells.

Autophagy is a physiologic catabolic process that occurs at basal levels in most tissues, contributes to the turnover of cytoplasmic components and maintains the cell homeostasis (Cecconi & Levine, 2008; Yang & Klionsky, 2009). It is also implicated in several disorders including many neurodegenerative diseases (Mizushima et al, 2008; Martinez-Vicente & Cuervo, 2007).

Previous work performed in the lab has reported that Atro and polyQ Atros cause neurodegeneration by blocking the autophagic flux (Nisoli et al., 2010). Both Hpo pathway and Atrophin have been described as critical molecules involved in autophagic digestion of salivary glands (Berry & Baehrecke, 2007; Dutta & Baehrecke, 2008; Martin et al, 2007).

Since autophagy is characterized by the formation of typical organelles such as the vacuoles that we observed in *ft* and *sav* mutant cells, we suspected a link between Ft-Hpo neurodegeneration and autophagy. From our morphologic analysis of *ft* and *sav* mutant clones, it appears that cytoplasmic membrane inclusions accumulate more in *ft* and *sav* degenerated photoreceptors than in *wt* cells. These organelles display the morphological hallmarks of autophagosomes, with membranous compartments containing undigested material. Impaired autophagy can lead either to an accumulation of autophagosomes, which contain material that is normally degraded after fusion with lysosomes, or to an accumulation of autophagolysosomes, if the fusion is correct but lysosomal proteolysis is disrupted (Klionsky, 2007).

Several neurodegenerative diseases have been described to strongly induce autophagy as a mechanism of defense against toxicity and death (Ravikumar et al, 2004). However, our morphologic outcome may result as well from a block in clearance, making it difficult to explain the reason why *ft* and *sav* accumulate autophagosomes in the cytoplasm, as it could be the consequence of both activating and blocking autophagy.

To gain more information about autophagy functioning in our Ft-Hpo model, we stained *ft* mutant retinae for the typical autophagic markers and we found that GFP-Atg8 increases, although moderately, in *ft* homozygous cells over *wt* photoreceptors, confirming the presence of autophagic

vacuoles in *ft* mutant cells. Interestingly, the immunofluorescence against another autophagic marker, Ref(2)P/p62, shows a strong accumulation of p62 dots, especially in more degenerated *ft* clones. Autophagy has been described as a pivotal process to avoid the accumulation of abnormal proteins, such as ubiquitinated aggregates, in several neurodegenerative diseases (Ross & Poirier, 2004). Since p62 is not only a direct interactor of Atg8, but it was originally described as a scaffolding protein required for the degradation of polyubiquitinated aggregates by autophagy (Bjorkoy et al, 2005), the result of p62 staining could indicate an abnormal accumulation of polyubiquitinated and potentially toxic proteins destined to be degraded by the lysosomal degradative system.

The presence of undigested material may suggest that autophagosomes are not able to fuse with lysosomes. Alternatively, the problem in *ft*-degenerated photoreceptors could be related to an impairment of early steps and not to a non correct or lacking fusion between autophagosomes and lysosomes. To establish whether a possible blockage of the autophagic flux is subsequent to the formation of autophagolysosomes and does not occur during their formation, we would first need to isolate *ft* mutant retinae and look for the co-localization of an autophagosomal marker, such as Atg8, and a lysosomal marker, such as Lysotracker staining. In addition, it would be desirable to measure the lysosomal degradation, although our *in vivo* system present many limitations to the study of the lysosomes functionality.

Our hypothesis does not exclude an initial stimulation of endogenous autophagy as a consequence of the fact that degenerated photoreceptors sense the cellular stressed condition and try to restore the physiological situation. It is likely that, at a later time, a block of the autophagic process

occurs and, since the cell cannot degrade toxic material, it is destined to die. This would explain the accumulation of autophagosomes both in *ft* and *sav* mutant cells as well the massive increase of p62 dots several fold more dramatic than the Atg8 accumulation, a pattern often correlated with a block in autophagic digestion. However, further experiments are required to understand the step(s) along the autophagic process that is(are) blocked or impaired in *ft* and *sav* degenerated neurons.

To better clarify the functional relevance of autophagy in the maintenance of Ft neuronal homeostasis, we attempted to rescue *ft* retinal degeneration by genetically modulating *Atg* signaling either by blocking or by stimulating the activation of autophagy. Autophagy has been indicated, by several authors, to exert a protective function in more and distinct neurodegenerative disorders (Mizushima et al, 2008; Martinez-Vicente & Cuervo, 2007; Sarkar et al, 2008). Consistent with these outcomes, we have observed that the induction of clones double mutant for *ft* and *atg1,* an inducer of autophagy initiation, with ensuring autophagy blockade in *ft* mutant retinae, strongly enhances the *ft*-caused neurodegeneration.Therefore, also in our model autophagy acts as a protective mechanism for the cell against death.

It is known from the literature that the TOR kinase, the target of rapamycin, is one of the key upstream regulators of autophagy, which inhibits the activation of the signalling in the presence of abundant nutrients or growth factors. We thus tested whether blocking TOR activity, with indirect stimulation of autophagy, could affect *ft* retinal phenotype. Conversely, we carried out the opposite genetic test by studying whether activating TOR activity, with indirect blocking of autophagy, could modulate *ft* neurodegeneration. Completely blocking TOR, with $tor^{\Delta P}$ mutant allele, led

to the inhibition of cell overgrowth (Fig. 7.10), but the very small size of the mutant cells, together with the decreased dimension of the clone, prevented us from studying a possible influence of Tor on *ft* neurodegenerative phenotype. So we tested partial loss of TOR activity, by expressing a dominant negative form of Tor, Tor^{TED}, and by hyperactivating the pathway by knocking down *Tsc1* RNA. What we observed was that neither blocking nor overactivating TOR, by blocking the TSC1/2 complex activity (Fig. 7.11), had significant effect on *ft* retinal degeneration.

These results contrast with previous work showing that induction of autophagy, by suppressing TOR activity, benefits several neurodegenerative disorders such as the Huntington disease, both in mammals (Mizushima et al, 2008; Rubinsztein et al, 2007) and recently also in *Drosophila* (Wang & Levine, 2010). However, Tor is not only involved in autophagy, it is a master regulator that, in addition to many other secondary catabolic and anabolic cellular processes, such as protein translation and cell-cycle progression, integrates the signals from nutrient and energy sensors to correctly coordinate cell growth and proliferation (Codogno & Meijer, 2005). Therefore although the absence of interaction could mean that Tor is not involved in *ft* neurodegeneration, an alternative hypothesis is that altered Tor activity could affect not only autophagy but also other processes, thus interfering with our analysis.

Another possibility is that the *ft* mutant blocks a stage that occurs after the initiation of autophagy and for this reason would not be affected by Tsc1/Tsc2 complex or Tor. For this reason we took advantage of a downstream and more direct stimulator of autophagy, Atg1 (Scott et al, 2007). Exogenous expression of Atg1 *wt* form, exclusively in the *ft*

homozygous retinal tissue, gave rise to a progressive neurodegeneration that was again comparable, although a bit slower, to *ft*-induced phenotype.

Although we did not obtain any significant rescue of the *ft*-induced degeneration with Atg1 over-expression, our results from the phenotypic analysis of double mutant clones for *ft* and *atg1* loss of function alleles suggest that Atg1 is necessary but not sufficient to modulate *ft* retinal degeneration.It is possible that the transgene we used is too weak to give a significant amelioration of the retinal condition. There is another transgene of Atg1, $Atg1^{68}$, but we did not use it because we observed that its expression in the retina causes retinal abnormalities *per se*.

Another reason why it is hard to reach a definitive conclusion from these experiments is that the level and timing of degeneration we detected in *ft* single mutants became irreproducible in later experiments. The retinal phenotype of *ft* mutants became much more severe probably because the 29°C incubator, where we left flies to age, uderwent uncontrollable changes of the temperature and the environmental conditions. They could be responsible for the excessive degeneration found in *ft* mutants aged for only a short period at 29°C, thus counterfeiting the real outcome. Unfortunately the high variability in the results prevented us to draw a model of the molecular autophagic machinery that contributes to prevent the Ft-Hpo neurodegeneration.

In conclusion, from our investigation of the cellular mechanisms affected in *ft* degenerated neuronal cells, we definitely found effects of autophagy on *ft*-induced neurodegeneration, although technical problems prevented us from following them up much further. The increased accumulation of organelles and typical autophagic markers detected by EM and immunofluorescence assays, together with the phenotypic analysis of

double mutant *ft,atg1* clones, support the protective nature of endogenous levels of autophagy for *ft*-induced degeneration. However, additional experiments are required to understand better the relationship between autophagy and the Ft-Hpo maintenance of the neuronal homeostasis. We need to clarify what happens inside the cell when they degenerate and what does not work correctly during autophagy degradation in *ft* neuronal cells. It would be also interesting to investigate whether mitochondria and their energy synthesis is altered in degenerated photoreceptors. On the other hand, we should expand the genetic epistasis to find whether and how autophagic signaling cascade interacts with the Ft-Hpo network.

Chapter 8

FINAL DISCUSSION

An overview of the evidence presented here indicates that the tumour suppressor Ft, together with the Hpo pathway, contributes to the signaling that partially protects retinal neurons from neurodegeneration.

Fat has also been demonstrated to be involved in the regulation of PCP together with the transcriptional co-factor Atro (Fanto et al, 2003). Both human and *Drosophila* Atrophins are linked to neurodegeneration (Nisoli et al, 2010). Experiments aimed at investigating the influence of *Drosophila* Atro transcriptional function on neurodegeneration have shown that the downregulation of *ft* transcription, a modulatory event specifically due to Atro itself, is enhanced by the expansion of polyglutamine regions along Atro sequence (unpublished, F. Napoletano).

It has also been demonstrated in the lab that *Drosophila* Atro and polyQ Atros cause neurodegeneration by blocking the autophagic flux (Nisoli et al, 2010). My data suggest that degeneration by *ft* is due to autophagic stress and phenocopies many, but not all, aspects of polyQ Atros toxicity. The effect of *ft* mutations is particularly similar to the overexpression of wt Atro. In both cases, at the ultrastructural level there is accumulation of autophagosomes but not of massive undigested autophagolysosomes (Nisoli et al, 2010). In addition, overexpression of the wt form of Atro, as for the loss of *ft*, leads to a great accumulation of the p62 with little increase in Atg8 punctae, whereas polyQ versions of Atrophins induce a much greater accumulation of the Atg8. This is consistent with a model in which Ft mediates an Atro-specific part of the toxicity, distinct from

the mere polyQ toxicity and yet significantly affected by polyQ expansion in Atro sequence.

An important difference between *ft*-induced degeneration and the wt Atro-caused phenotype is however the lack of lysotracker accumulation in *ft* mutant cells (data not shown) compared to photoreceptors overexpressing Atro wt (Nisoli et al, 2010). Lysotracker is a marker of correct acidification of autophagolysosomes and, an increase of its presence in degenerated cells, would imply a lysosomal storage effect, as observed by the expression of all Atro forms (Nisoli et al, 2010). This opposite outcome could be due to the difference between an overexpression phenotype (Atro wt), which loads the cell of unfolded proteins to be degraded in lysosomes, and a phenotype due to a loss of function as in *ft*, *wts* and *sav* mutants where autophagy needs to degrade endogenous components. Alternatively, there may be a real mechanistic difference between the two phenotypes, whose meaning and importance remains to be addressed.

The outcome of *atro* loss-of-function alleles in this system has also to be established, as the analysis of the different alleles and the interaction with *ft* was not conclusive. It is possible that some of the effects of polyQ Atro gain of function would be mimicked by *atro* loss-of-function, as already shown for other polyglutamine disorders, such as SCA1 or Huntington disease (Lim et al, 2008). Indeed, it has been reported that in Huntington disease, loss of mouse Huntingtin function worsen the neurodegeneration induced in transgenic models carrying the polyQ expanded protein (Auerbach et al, 2001; Van Raamsdonk et al, 2005), suggesting that polyglutamine expansion can cause both toxic gain of function and simultaneously loss-of-function of the disease-causing protein.

Furthermore, the Hpo pathway and Atro have both been described as critical molecules involved in autophagic digestion of salivary glands (Berry & Baehrecke, 2007; Dutta & Baehrecke, 2008; Martin et al, 2007). *Drosophila* salivary glands are an outstanding system for studying autophagic cell death during development (Berry & Baehrecke, 2007). Both caspases and autophagic network are highly active in dying salivary glands that occurs during the puparium step (Jiang et al, 1997; Lee & Baehrecke, 2001). *wts* mutants in salivary glands display an overgrowth phenotype with a decrease in apoptotic activity and a deregulation of the autophagy (Dutta & Baehrecke, 2008). In contrast, Yki over-expression, that should mimic *wts* LOF results, fails to inhibit salivary glands degradation (Dutta & Baehrecke, 2008). The opposite results suggest that the Hpo-Sav-Wts pathway here behaves differently from what previously described in developing fly tissues, such as eyes and wings imaginal discs (Cho et al, 2006; Huang et al, 2005).

Our data suggest that the retinal degeneration induced by *ft* and *hpo* mutants cause a modification of the autophagic process which phenocopies only in part the results from salivary glands and DRPLA fly model. Indeed, our morphologic study of autophagy involvement in *ft* and *sav* mutants gives an unequivocal and statistically significant accumulation of autophagosomes in *ft* and *sav* mutant cells. This suggests that the block in affected adult neurones is in clearance, rather than in induction, of autophagic vacuoles as it is in the salivary glands (Dutta & Baehrecke, 2008). This discrepancy is likely to reflect the different role and basal level of autophagy in the two tissues. Whereas in the salivary glands autophagy is massively induced as a cell killing mechanism, in post-mitotic neurons expressing polyQ Atrophins, autophagy is a rescue attempt which fails as suggested by the double *ft;atg1* mutant clones.

A model of how precisely each component of the canonical Hpo signalling cascade contributes to *ft*-induced retinal abnormalities remains to be developed. We have observed that over-expression of the final output Yki, which is shown in the literature to mimic the loss of the core components of the signalling in developmental growth control. This occurs in mutant developing larvae, leading to comparable heavy overgrowth phenotypes of both wing and eye imaginal discs. However, Yki overexpression leads to degeneration of photoreceptor neurons that is much milder than the phenotype obtained by mutations of *wts*, *sav* or *hpo* molecules. In addition, the weak rescue of the *ft*-induced retinal degeneration by the partial removal of *yki*, compared to the strong benefits on *ft* mutant photoreceptors by the removal of *dachs,* suggests a model that does entirely overlap neither with the one described for salivary glands, nor with the canonical signalling drawn studying developing imaginal discs.

Our outcomes of the Hpo pathway in the adult retina let us to hypothesize a model in which Ft, in order to preserve neuronal homeostasis, certainly requires the downstream Hpo-Sav-Wts core activation, which, in its turn, is mediated by Dachs. By contrast, the downstream effectors of this signalling remain unknown. Experiments done to unravel the genetic interation between Ft and Yki favour a model in which autophagy is regulated by Ft-Hpo-Sav-Wts signalling independently of Yki. However, Yki contributes, although weakly, to *ft-wts*-induced neurodegeneration. This, however, is likely not the exclusive or even the major final output of this cascade in photoreceptor neurones. The effect of Yki could reflect a contribution of the Hpo canonical pathway and the attempt to the cell-cycle re-entry. We cannot exclude that other unknown

factors may also modulate *ft* degenerative signalling downstream of Hpo-Sav-Wts core.

It remains also to be understood whether neurodegeneration in mutants of *ft* and components of the Hpo network is the consequence of an inappropriate stimulation of cell proliferation and tissue growth that would lead to a condition of deleterious cellular stress and autophagic dysfunction. Originally, the first transcriptional targets found to be regulated by the Hpo pathway in wings and eye imaginal discs were *diap1*, the *Drosophila* inhibitor of apoptosis, *cycE*, involved in cell-cycle progression (Harvey et al, 2003; Pantalacci et al, 2003; Tapon et al, 2002; Wu et al, 2003) and the micro-RNA molecule *bantam*, a positive regulator of imaginal discs growth (Nolo et al, 2006; Thompson & Cohen, 2006). We don't know whether the same applies for adult neurones. Further investigation on the genes transcripts modulated in mutants of *ft* and components of the Hpo core will help to better explain our model on neurodegeneration.

It is likely that any effect on autophagy by the Ft pathway would be of crucial importance also for its role in tumour suppression. Some evidence, such as the interaction among the oncogene BCL2 and Beclin1 (or Atg6), a PI3 kinase, that acts as an upstream regulator of autophagy (Liang et al, 1999), prompted researchers to link autophagy to cancer. These results suggested a more general idea of a block of autophagy by oncogenes and a stimulation of the process by tumour suppressors (Finkel et al.,2007). Hence, the precise role of autophagy during cancer progression and treatment is both tissue and context dependent (Chen & Debnath, 2010; Wang & Levine, 2010).

Increasing evidence also highlights the relevance of autophagy as a common mechanism shared by cancer and ageing (Finkel et al, 2007).

Scientists have long observed that the majority of cancers occur in older adults and that both cancer and ageing come from the accumulation of cellular damage. Aging is associated with a number of events at the molecular, cellular, and physiologic levels that influence carcinogenesis and subsequent cancer growth (Balducci & Ershler, 2005). The tumor suppressor gene, p53, in particular, has been proposed to influence both cancer development and the onset of aging (Tyner et al, 2002). Thus, our outcomes on *ft* neurodegeneration support a functional relationship between Ft-Hpo tumor suppressor cascade, neurodegeneration and ageing.

Finally, at least four Ft orthologues have been identified in mammals and are widely expressed throughout the mouse nervous system (Tanoue & Takeichi, 2005) and Fat-1 has recently been shown to interact with mouse Atrophins (Hou & Sibinga, 2009), indicating an evolutionarily conserved relation. It is thus possible that the regulation of Ft-like molecules and of the Hpo tumour suppressor cascade in mammals is important for neuroprotection and plays a key role in DRPLA in humans.

REFERENCES

Adler PN (2002) Planar signaling and morphogenesis in Drosophila. *Dev Cell* 2(5): 525-535

Anastasiadis PZ, Reynolds AB (2000) The p120 catenin family: complex roles in adhesion, signaling and cancer. *J Cell Sci* 113 (Pt 8): 1319-1334

Ashburner MT (1978) "The laboratory culture of Drosophila". *Ashburner M, Wright TRFThe genetics and biology of Drosophila* 2A: 1-81

Axe EL, Walker SA, Manifava M, Chandra P, Roderick HL, Habermann A, Griffiths G, Ktistakis NT (2008) Autophagosome formation from membrane compartments enriched in phosphatidylinositol 3-phosphate and dynamically connected to the endoplasmic reticulum. *J Cell Biol* 182(4): 685-701

Azad MB, Chen Y, Henson ES, Cizeau J, McMillan-Ward E, Israels SJ, Gibson SB (2008) Hypoxia induces autophagic cell death in apoptosis-competent cells through a mechanism involving BNIP3. *Autophagy* 4(2): 195-204

Badouel C, Gardano L, Amin N, Garg A, Rosenfeld R, Le Bihan T, McNeill H (2009) The FERM-domain protein Expanded regulates Hippo pathway activity via direct interactions with the transcriptional activator Yorkie. *Dev Cell* 16(3): 411-420

Baena-Lopez LA, Rodriguez I, Baonza A (2008) The tumor suppressor genes dachsous and fat modulate different signalling pathways by regulating dally and dally-like. *Proc Natl Acad Sci U S A* 105(28): 9645-9650

Baker NE, Yu SY (2001) The EGF receptor defines domains of cell cycle progression and survival to regulate cell number in the developing Drosophila eye. *Cell* 104(5): 699-708

Balducci L, Ershler WB (2005) Cancer and ageing: a nexus at several levels. *Nat Rev Cancer* 5(8): 655-662

Baumgartner R, Poernbacher I, Buser N, Hafen E, Stocker H (2010) The WW domain protein Kibra acts upstream of Hippo in Drosophila. *Dev Cell* 18(2): 309-316

Bennett EJ, Shaler TA, Woodman B, Ryu KY, Zaitseva TS, Becker CH, Bates GP, Schulman H, Kopito RR (2007) Global changes to the ubiquitin system in Huntington's disease. *Nature* 448(7154): 704-708

Bennett FC, Harvey KF (2006) Fat cadherin modulates organ size in Drosophila via the Salvador/Warts/Hippo signaling pathway. *Curr Biol* 16(21): 2101-2110

Berry DL, Baehrecke EH (2007) Growth arrest and autophagy are required for salivary gland cell degradation in Drosophila. *Cell* 131(6): 1137-1148

Bessa J, Gebelein B, Pichaud F, Casares F, Mann RS (2002) Combinatorial control of Drosophila eye development by eyeless, homothorax, and teashirt. *Genes Dev* 16(18): 2415-2427

Bilen J, Bonini NM (2005) Drosophila as a model for human neurodegenerative disease. *Annu Rev Genet* 39: 153-171

Bisceglia M, Galliani CA, Senger C, Stallone C, Sessa A (2006) Renal cystic diseases: a review. *Adv Anat Pathol* 13(1): 26-56

Bjorkoy G, Lamark T, Brech A, Outzen H, Perander M, Overvatn A, Stenmark H, Johansen T (2005) p62/SQSTM1 forms protein aggregates degraded by autophagy and has a protective effect on huntingtin-induced cell death. *J Cell Biol* 171(4): 603-614

Boedigheimer M, Bryant P, Laughon A (1993a) Expanded, a negative regulator of cell proliferation in Drosophila, shows homology to the NF2 tumor suppressor. *Mech Dev* 44(2-3): 83-84

Bonini NM, Fortini ME (2003) Human neurodegenerative disease modeling using Drosophila. *Annu Rev Neurosci* 26: 627-656

Brand AH, Perrimon N (1993) Targeted gene expression as a means of altering cell fates and generating dominant phenotypes. *Development* 118(2): 401-415

Brogiolo W, Stocker H, Ikeya T, Rintelen F, Fernandez R, Hafen E (2001) An evolutionarily conserved function of the Drosophila insulin receptor and insulin-like peptides in growth control. *Curr Biol* 11(4): 213-221

Bryant PJ, Huettner B, Held LI, Jr., Ryerse J, Szidonya J (1988) Mutations at the fat locus interfere with cell proliferation control and epithelial morphogenesis in Drosophila. *Dev Biol* 129(2): 541-554

Callebaut I, Courvalin JC, Mornon JP (1999) The BAH (bromo-adjacent homology) domain: a link between DNA methylation, replication and transcriptional regulation. *FEBS Lett* 446(1): 189-193

Campbell S, Inamdar M, Rodrigues V, Raghavan V, Palazzolo M, Chovnick A (1992) The scalloped gene encodes a novel, evolutionarily conserved transcription factor required for sensory organ differentiation in Drosophila. *Genes Dev* 6(3): 367-379

Casal J, Lawrence PA, Struhl G (2006) Two separate molecular systems, Dachsous/Fat and Starry night/Frizzled, act independently to confer planar cell polarity. *Development* 133(22): 4561-4572

Casal J, Struhl G, Lawrence PA (2002) Developmental compartments and planar polarity in Drosophila. *Curr Biol* 12(14): 1189-1198

Cattaneo E, Zuccato C, Tartari M (2005) Normal huntingtin function: an alternative approach to Huntington's disease. *Nat Rev Neurosci* 6(12): 919-930

Cecconi F, Levine B (2008) The role of autophagy in mammalian development: cell makeover rather than cell death. *Dev Cell* 15(3): 344-357

Chan EY, Longatti A, McKnight NC, Tooze SA (2009) Kinase-inactivated ULK proteins inhibit autophagy via their conserved C-terminal domains using an Atg13-independent mechanism. *Mol Cell Biol* 29(1): 157-171

Charroux B, Freeman M, Kerridge S, Baonza A (2006) Atrophin contributes to the negative regulation of epidermal growth factor receptor signaling in Drosophila. *Dev Biol* 291(2): 278-290

Chaudhuri A, Bowling K, Funderburk C, Lawal H, Inamdar A, Wang Z, O'Donnell JM (2007) Interaction of genetic and environmental factors in a Drosophila parkinsonism model. *J Neurosci* 27(10): 2457-2467

Chen JL, Lin HH, Kim KJ, Lin A, Forman HJ, Ann DK (2008a) Novel roles for protein kinase Cdelta-dependent signaling pathways in acute hypoxic stress-induced autophagy. *J Biol Chem* 283(49): 34432-34444

Chen N, Debnath J (2010) Autophagy and tumorigenesis. *FEBS Lett* 584(7): 1427-1435

Cheong H, Nair U, Geng J, Klionsky DJ (2008) The Atg1 kinase complex is involved in the regulation of protein recruitment to initiate sequestering vesicle formation for nonspecific autophagy in Saccharomyces cerevisiae. *Mol Biol Cell* 19(2): 668-681

Cho E, Feng Y, Rauskolb C, Maitra S, Fehon R, Irvine KD (2006) Delineation of a Fat tumor suppressor pathway. *Nat Genet* 38(10): 1142-1150

Cho E, Irvine KD (2004) Action of fat, four-jointed, dachsous and dachs in distal-to-proximal wing signaling. *Development* 131(18): 4489-4500

Clark HF, Brentrup D, Schneitz K, Bieber A, Goodman C, Noll M (1995) Dachsous encodes a member of the cadherin superfamily that controls imaginal disc morphogenesis in Drosophila. *Genes Dev* 9(12): 1530-1542

Codogno P, Meijer AJ (2005) Autophagy and signaling: their role in cell survival and cell death. *Cell Death Differ* 12 Suppl 2: 1509-1518

Coulom H, Birman S (2004) Chronic exposure to rotenone models sporadic Parkinson's disease in Drosophila melanogaster. *J Neurosci* 24(48): 10993-10998

Cuervo AM (2004) Autophagy: in sickness and in health. *Trends Cell Biol* 14(2): 70-77

Cuervo AM, Bergamini E, Brunk UT, Droge W, Ffrench M, Terman A (2005) Autophagy and aging: the importance of maintaining "clean" cells. *Autophagy* 1(3): 131-140

Cuervo AM, Dice JF, Knecht E (1997) A population of rat liver lysosomes responsible for the selective uptake and degradation of cytosolic proteins. *J Biol Chem* 272(9): 5606-5615

Daugherty RL, Gottardi CJ (2007) Phospho-regulation of Beta-catenin adhesion and signaling functions. *Physiology (Bethesda)* 22: 303-309

Deretic V, Levine B (2009) Autophagy, immunity, and microbial adaptations. *Cell Host Microbe* 5(6): 527-549

DiFiglia M, Sapp E, Chase KO, Davies SW, Bates GP, Vonsattel JP, Aronin N (1997) Aggregation of huntingtin in neuronal intranuclear inclusions and dystrophic neurites in brain. *Science* 277(5334): 1990-1993

Dong J, Feldmann G, Huang J, Wu S, Zhang N, Comerford SA, Gayyed MF, Anders RA, Maitra A, Pan D (2007) Elucidation of a universal size-control mechanism in Drosophila and mammals. *Cell* 130(6): 1120-1133

Dutta S, Baehrecke EH (2008) Warts is required for PI3K-regulated growth arrest, autophagy, and autophagic cell death in Drosophila. *Curr Biol* 18(19): 1466-1475

Edgar BA (2006) From cell structure to transcription: Hippo forges a new path. *Cell* 124(2): 267-273

Ellerby LM, Andrusiak RL, Wellington CL, Hackam AS, Propp SS, Wood JD, Sharp AH, Margolis RL, Ross CA, Salvesen GS, Hayden MR, Bredesen DE (1999) Cleavage of atrophin-1 at caspase site aspartic acid 109 modulates cytotoxicity. *J Biol Chem* 274(13): 8730-8736

Emoto K, Parrish JZ, Jan LY, Jan YN (2006) The tumour suppressor Hippo acts with the NDR kinases in dendritic tiling and maintenance. *Nature* 443(7108): 210-213

Erkner A, Roure A, Charroux B, Delaage M, Holway N, Core N, Vola C, Angelats C, Pages F, Fasano L, Kerridge S (2002) Grunge, related to human Atrophin-like proteins, has multiple functions in Drosophila development. *Development* 129(5): 1119-1129

Fanto M, Clayton L, Meredith J, Hardiman K, Charroux B, Kerridge S, McNeill H (2003) The tumor-suppressor and cell adhesion molecule Fat controls planar polarity via physical interactions with Atrophin, a transcriptional co-repressor. *Development* 130(4): 763-774

Fanto M, McNeill H (2004) Planar polarity from flies to vertebrates. *J Cell Sci* 117(Pt 4): 527-533

Feany MB, Bender WW (2000) A Drosophila model of Parkinson's disease. *Nature* 404(6776): 394-398

Feng Y, Irvine KD (2007) Fat and expanded act in parallel to regulate growth through warts. *Proc Natl Acad Sci U S A* 104(51): 20362-20367

Feng Y, Irvine KD (2009) Processing and phosphorylation of the Fat receptor. *Proc Natl Acad Sci U S A* 106(29): 11989-11994

Fernandez-Funez P, Nino-Rosales ML, de Gouyon B, She WC, Luchak JM, Martinez P, Turiegano E, Benito J, Capovilla M, Skinner PJ, McCall A, Canal I, Orr HT, Zoghbi HY, Botas J (2000) Identification of genes that modify ataxin-1-induced neurodegeneration. *Nature* 408(6808): 101-106

Fischer E, Legue E, Doyen A, Nato F, Nicolas JF, Torres V, Yaniv M, Pontoglio M (2006) Defective planar cell polarity in polycystic kidney disease. *Nat Genet* 38(1): 21-23

Furuta S, Hidaka E, Ogata A, Yokota S, Kamata T (2004) Ras is involved in the negative control of autophagy through the class I PI3-kinase. *Oncogene* 23(22): 3898-3904

Gallin WJ, Edelman GM, Cunningham BA (1983) Characterization of L-CAM, a major cell adhesion molecule from embryonic liver cells. *Proc Natl Acad Sci U S A* 80(4): 1038-1042

Garoia F, Grifoni D, Trotta V, Guerra D, Pezzoli MC, Cavicchi S (2005) The tumor suppressor gene fat modulates the EGFR-mediated proliferation control in the imaginal tissues of Drosophila melanogaster. *Mech Dev* 122(2): 175-187

Garoia F, Guerra D, Pezzoli MC, Lopez-Varea A, Cavicchi S, Garcia-Bellido A (2000) Cell behaviour of Drosophila fat cadherin mutations in wing development. *Mech Dev* 94(1-2): 95-109

Gatchel JR, Zoghbi HY (2005) Diseases of unstable repeat expansion: mechanisms and common principles. *Nat Rev Genet* 6(10): 743-755

Genevet A, Polesello C, Blight K, Robertson F, Collinson LM, Pichaud F, Tapon N (2009) The Hippo pathway regulates apical-domain size independently of its growth-control function. *J Cell Sci* 122(Pt 14): 2360-2370

Genevet A, Wehr MC, Brain R, Thompson BJ, Tapon N (2010) Kibra is a regulator of the Salvador/Warts/Hippo signaling network. *Dev Cell* 18(2): 300-308

Golic KG, Lindquist S (1989) The FLP recombinase of yeast catalyzes site-specific recombination in the Drosophila genome. *Cell* 59(3): 499-509

Gumbiner BM (2000) Regulation of cadherin adhesive activity. *J Cell Biol* 148(3): 399-404

Gusella JF, MacDonald ME (2000) Molecular genetics: unmasking polyglutamine triggers in neurodegenerative disease. *Nat Rev Neurosci* 1(2): 109-115

Haecker A, Qi D, Lilja T, Moussian B, Andrioli LP, Luschnig S, Mannervik M (2007) Drosophila brakeless interacts with atrophin and is required for tailless-mediated transcriptional repression in early embryos. *PLoS Biol* 5(6): e145

Halder G, Polaczyk P, Kraus ME, Hudson A, Kim J, Laughon A, Carroll S (1998) The Vestigial and Scalloped proteins act together to directly regulate wing-specific gene expression in Drosophila. *Genes Dev* 12(24): 3900-3909

Hamaratoglu F, Willecke M, Kango-Singh M, Nolo R, Hyun E, Tao C, Jafar-Nejad H, Halder G (2006) The tumour-suppressor genes NF2/Merlin and Expanded act through Hippo signalling to regulate cell proliferation and apoptosis. *Nat Cell Biol* 8(1): 27-36

Hara T, Nakamura K, Matsui M, Yamamoto A, Nakahara Y, Suzuki-Migishima R, Yokoyama M, Mishima K, Saito I, Okano H, Mizushima N (2006) Suppression of basal autophagy in neural cells causes neurodegenerative disease in mice. *Nature* 441(7095): 885-889

Hariri M, Millane G, Guimond MP, Guay G, Dennis JW, Nabi IR (2000) Biogenesis of multilamellar bodies via autophagy. *Mol Biol Cell* 11(1): 255-268

Harvey K, Tapon N (2007) The Salvador-Warts-Hippo pathway - an emerging tumour-suppressor network. *Nat Rev Cancer* 7(3): 182-191

Harvey KF, Pfleger CM, Hariharan IK (2003) The Drosophila Mst ortholog, hippo, restricts growth and cell proliferation and promotes apoptosis. *Cell* 114(4): 457-467

Hazelrigg T, Levis R, Rubin GM (1984) Transformation of white locus DNA in drosophila: dosage compensation, zeste interaction, and position effects. *Cell* 36(2): 469-481

Huang J, Manning BD (2008) The TSC1-TSC2 complex: a molecular switchboard controlling cell growth. *Biochem J* 412(2): 179-190

Huang J, Wu S, Barrera J, Matthews K, Pan D (2005) The Hippo signaling pathway coordinately regulates cell proliferation and apoptosis by inactivating Yorkie, the Drosophila Homolog of YAP. *Cell* 122(3): 421-434

Igarashi S, Koide R, Shimohata T, Yamada M, Hayashi Y, Takano H, Date H, Oyake M, Sato T, Sato A, Egawa S, Ikeuchi T, Tanaka H, Nakano R, Tanaka K, Hozumi I, Inuzuka T, Takahashi H, Tsuji S (1998) Suppression of aggregate formation and apoptosis by transglutaminase inhibitors in cells expressing truncated DRPLA protein with an expanded polyglutamine stretch. *Nat Genet* 18(2): 111-117

Inoki K, Li Y, Zhu T, Wu J, Guan KL (2002) TSC2 is phosphorylated and inhibited by Akt and suppresses mTOR signalling. *Nat Cell Biol* 4(9): 648-657

Inoki K, Zhu T, Guan KL (2003) TSC2 mediates cellular energy response to control cell growth and survival. *Cell* 115(5): 577-590

Ishikawa HO, Takeuchi H, Haltiwanger RS, Irvine KD (2008) Four-jointed is a Golgi kinase that phosphorylates a subset of cadherin domains. *Science* 321(5887): 401-404

Itakura E, Kishi C, Inoue K, Mizushima N (2008) Beclin 1 forms two distinct phosphatidylinositol 3-kinase complexes with mammalian Atg14 and UVRAG. *Mol Biol Cell* 19(12): 5360-5372

Jackson GR, Salecker I, Dong X, Yao X, Arnheim N, Faber PW, MacDonald ME, Zipursky SL (1998) Polyglutamine-expanded human huntingtin transgenes induce degeneration of Drosophila photoreceptor neurons. *Neuron* 21(3): 633-642

Jahreiss L, Menzies FM, Rubinsztein DC (2008) The itinerary of autophagosomes: from peripheral formation to kiss-and-run fusion with lysosomes. *Traffic* 9(4): 574-587

Jia J, Zhang W, Wang B, Trinko R, Jiang J (2003) The Drosophila Ste20 family kinase dMST functions as a tumor suppressor by restricting cell proliferation and promoting apoptosis. *Genes Dev* 17(20): 2514-2519

Johnson K, Grawe F, Grzeschik N, Knust E (2002) Drosophila crumbs is required to inhibit light-induced photoreceptor degeneration. *Curr Biol* 12(19): 1675-1680

Juhasz G, Erdi B, Sass M, Neufeld TP (2007) Atg7-dependent autophagy promotes neuronal health, stress tolerance, and longevity but is dispensable for metamorphosis in Drosophila. *Genes Dev* 21(23): 3061-3066

Juhasz G, Neufeld TP (2006) Autophagy: a forty-year search for a missing membrane source. *PLoS Biol* 4(2): e36

Jung CH, Jun CB, Ro SH, Kim YM, Otto NM, Cao J, Kundu M, Kim DH (2009) ULK-Atg13-FIP200 complexes mediate mTOR signaling to the autophagy machinery. *Mol Biol Cell* 20(7): 1992-2003

Justice RW, Zilian O, Woods DF, Noll M, Bryant PJ (1995) The Drosophila tumor suppressor gene warts encodes a homolog of human myotonic dystrophy kinase and is required for the control of cell shape and proliferation. *Genes Dev* 9(5): 534-546

Kabeya Y, Mizushima N, Ueno T, Yamamoto A, Kirisako T, Noda T, Kominami E, Ohsumi Y, Yoshimori T (2000) LC3, a mammalian homologue of yeast Apg8p, is localized in autophagosome membranes after processing. *EMBO J* 19(21): 5720-5728

Kamada Y, Funakoshi T, Shintani T, Nagano K, Ohsumi M, Ohsumi Y (2000) Tor-mediated induction of autophagy via an Apg1 protein kinase complex. *J Cell Biol* 150(6): 1507-1513

Kamada Y, Sekito T, Ohsumi Y (2004) Autophagy in yeast: a TOR-mediated response to nutrient starvation. *Curr Top Microbiol Immunol* 279: 73-84

Kanazawa I (1998) Dentatorubral-pallidoluysian atrophy or Naito-Oyanagi disease. *Neurogenetics* 2(1): 1-17

Kango-Singh M, Nolo R, Tao C, Verstreken P, Hiesinger PR, Bellen HJ, Halder G (2002) Shar-pei mediates cell proliferation arrest during imaginal disc growth in Drosophila. *Development* 129(24): 5719-5730

Kango-Singh M, Singh A (2009) Regulation of organ size: insights from the Drosophila Hippo signaling pathway. *Dev Dyn* 238(7): 1627-1637

Kankel MW, Duncan DM, Duncan I (2004) A screen for genes that interact with the Drosophila pair-rule segmentation gene fushi tarazu. *Genetics* 168(1): 161-180

Katoh Y, Katoh M (2006) Comparative integromics on FAT1, FAT2, FAT3 and FAT4. *Int J Mol Med* 18(3): 523-528

Kawamata T, Kamada Y, Kabeya Y, Sekito T, Ohsumi Y (2008) Organization of the pre-autophagosomal structure responsible for autophagosome formation. *Mol Biol Cell* 19(5): 2039-2050

Keller R (2002) Shaping the vertebrate body plan by polarized embryonic cell movements. *Science* 298(5600): 1950-1954

Kihara A, Noda T, Ishihara N, Ohsumi Y (2001) Two distinct Vps34 phosphatidylinositol 3-kinase complexes function in autophagy and carboxypeptidase Y sorting in Saccharomyces cerevisiae. *J Cell Biol* 152(3): 519-530

Klein T (2001) Wing disc development in the fly: the early stages. *Curr Opin Genet Dev* 11(4): 470-475

Klein T, Arias AM (1998) Different spatial and temporal interactions between Notch, wingless, and vestigial specify proximal and distal pattern elements of the wing in Drosophila. *Dev Biol* 194(2): 196-212

Klionsky DJ (2005) The molecular machinery of autophagy: unanswered questions. *J Cell Sci* 118(Pt 1): 7-18

Knight SP, Richardson MM, Osmand AP, Stakkestad A, Potter NT (1997) Expression and distribution of the dentatorubral-pallidoluysian atrophy gene product (atrophin-1/drplap) in neuronal and non-neuronal tissues. *J Neurol Sci* 146(1): 19-26

Koide R, Ikeuchi T, Onodera O, Tanaka H, Igarashi S, Endo K, Takahashi H, Kondo R, Ishikawa A, Hayashi T, et al. (1994) Unstable expansion of CAG repeat in hereditary dentatorubral-pallidoluysian atrophy (DRPLA). *Nat Genet* 6(1): 9-13

Komatsu M, Waguri S, Chiba T, Murata S, Iwata J, Tanida I, Ueno T, Koike M, Uchiyama Y, Kominami E, Tanaka K (2006) Loss of autophagy in the central nervous system causes neurodegeneration in mice. *Nature* 441(7095): 880-884

Kremerskothen J, Plaas C, Buther K, Finger I, Veltel S, Matanis T, Liedtke T, Barnekow A (2003) Characterization of KIBRA, a novel WW domain-containing protein. *Biochem Biophys Res Commun* 300(4): 862-867

Kretzschmar D, Hasan G, Sharma S, Heisenberg M, Benzer S (1997) The swiss cheese mutant causes glial hyperwrapping and brain degeneration in Drosophila. *J Neurosci* 17(19): 7425-7432

Kuusisto E, Salminen A, Alafuzoff I (2001) Ubiquitin-binding protein p62 is present in neuronal and glial inclusions in human tauopathies and synucleinopathies. *Neuroreport* 12(10): 2085-2090

La Spada AR, Wilson EM, Lubahn DB, Harding AE, Fischbeck KH (1991) Androgen receptor gene mutations in X-linked spinal and bulbar muscular atrophy. *Nature* 352(6330): 77-79

Lai SL, Lee T (2006) Genetic mosaic with dual binary transcriptional systems in Drosophila. *Nat Neurosci* 9(5): 703-709

LaJeunesse DR, McCartney BM, Fehon RG (1998) Structural analysis of Drosophila merlin reveals functional domains important for growth control and subcellular localization. *J Cell Biol* 141(7): 1589-1599

Lawrence PA, Struhl G, Casal J (2007) Planar cell polarity: one or two pathways? *Nat Rev Genet* 8(7): 555-563

Lee T, Luo L (1999) Mosaic analysis with a repressible cell marker for studies of gene function in neuronal morphogenesis. *Neuron* 22(3): 451-461

Liang J, Shao SH, Xu ZX, Hennessy B, Ding Z, Larrea M, Kondo S, Dumont DJ, Gutterman JU, Walker CL, Slingerland JM, Mills GB (2007) The energy sensing LKB1-AMPK pathway regulates p27(kip1) phosphorylation mediating the decision to enter autophagy or apoptosis. *Nat Cell Biol* 9(2): 218-224

Liang XH, Jackson S, Seaman M, Brown K, Kempkes B, Hibshoosh H, Levine B (1999) Induction of autophagy and inhibition of tumorigenesis by beclin 1. *Nature* 402(6762): 672-676

Lievens JC, Iche M, Laval M, Faivre-Sarrailh C, Birman S (2008) AKT-sensitive or insensitive pathways of toxicity in glial cells and neurons in Drosophila models of Huntington's disease. *Hum Mol Genet* 17(6): 882-894

Linder ME, Deschenes RJ (2007) Palmitoylation: policing protein stability and traffic. *Nat Rev Mol Cell Biol* 8(1): 74-84

Lum JJ, Bauer DE, Kong M, Harris MH, Li C, Lindsten T, Thompson CB (2005a) Growth factor regulation of autophagy and cell survival in the absence of apoptosis. *Cell* 120(2): 237-248

Ma D, Yang CH, McNeill H, Simon MA, Axelrod JD (2003) Fidelity in planar cell polarity signalling. *Nature* 421(6922): 543-547

Mahoney PA, Weber U, Onofrechuk P, Biessmann H, Bryant PJ, Goodman CS (1991) The fat tumor suppressor gene in Drosophila encodes a novel member of the cadherin gene superfamily. *Cell* 67(5): 853-868

Maitra S, Kulikauskas RM, Gavilan H, Fehon RG (2006) The tumor suppressors Merlin and Expanded function cooperatively to modulate receptor endocytosis and signaling. *Curr Biol* 16(7): 702-709

Mao Y, Rauskolb C, Cho E, Hu WL, Hayter H, Minihan G, Katz FN, Irvine KD (2006) Dachs: an unconventional myosin that functions downstream of Fat to regulate growth, affinity and gene expression in Drosophila. *Development* 133(13): 2539-2551

Martin DN, Balgley B, Dutta S, Chen J, Rudnick P, Cranford J, Kantartzis S, DeVoe DL, Lee C, Baehrecke EH (2007) Proteomic analysis of steroid-triggered autophagic programmed cell death during Drosophila development. *Cell Death Differ* 14(5): 916-923

Martinez-Vicente M, Cuervo AM (2007) Autophagy and neurodegeneration: when the cleaning crew goes on strike. *Lancet Neurol* 6(4): 352-361

Massey AC, Zhang C, Cuervo AM (2006) Chaperone-mediated autophagy in aging and disease. *Curr Top Dev Biol* 73: 205-235

Matakatsu H, Blair SS (2004) Interactions between Fat and Dachsous and the regulation of planar cell polarity in the Drosophila wing. *Development* 131(15): 3785-3794

Matakatsu H, Blair SS (2006) Separating the adhesive and signaling functions of the Fat and Dachsous protocadherins. *Development* 133(12): 2315-2324

Matakatsu H, Blair SS (2008) The DHHC palmitoyltransferase approximated regulates Fat signaling and Dachs localization and activity. *Curr Biol* 18(18): 1390-1395

Matsuura A, Tsukada M, Wada Y, Ohsumi Y (1997) Apg1p, a novel protein kinase required for the autophagic process in Saccharomyces cerevisiae. *Gene* 192(2): 245-250

McCartney BM, Kulikauskas RM, LaJeunesse DR, Fehon RG (2000) The neurofibromatosis-2 homologue, Merlin, and the tumor suppressor

expanded function together in Drosophila to regulate cell proliferation and differentiation. *Development* 127(6): 1315-1324

McClatchey AI (2003) Merlin and ERM proteins: unappreciated roles in cancer development? *Nat Rev Cancer* 3(11): 877-883

Mikeladze-Dvali T, Wernet MF, Pistillo D, Mazzoni EO, Teleman AA, Chen YW, Cohen S, Desplan C (2005) The growth regulators warts/lats and melted interact in a bistable loop to specify opposite fates in Drosophila R8 photoreceptors. *Cell* 122(5): 775-787

Mizushima N, Klionsky DJ (2007a) Protein turnover via autophagy: implications for metabolism. *Annu Rev Nutr* 27: 19-40

Mlodzik M (1999) Planar polarity in the Drosophila eye: a multifaceted view of signaling specificity and cross-talk. *EMBO J* 18(24): 6873-6879

Mohr (1923) Modifications of the sex-ratio through a sex-linked semilethal in Drosophila melanogaster (besides notes on an autosomal section deficiency). *In Studia Mendeliana: Ad Centesimum Diem Natalem Gregorii Mendelii a Grata Patria Celebrandum*:: 266-287

Moran E, Jimenez G (2006) The tailless nuclear receptor acts as a dedicated repressor in the early Drosophila embryo. *Mol Cell Biol* 26(9): 3446-3454

Moscat J, Diaz-Meco MT (2009) p62 at the crossroads of autophagy, apoptosis, and cancer. *Cell* 137(6): 1001-1004

Muchowski PJ (2002) Protein misfolding, amyloid formation, and neurodegeneration: a critical role for molecular chaperones? *Neuron* 35(1): 9-12

Muqit MM, Feany MB (2002) Modelling neurodegenerative diseases in Drosophila: a fruitful approach? *Nat Rev Neurosci* 3(3): 237-243

Muskavitch MA (1994) Delta-notch signaling and Drosophila cell fate choice. *Dev Biol* 166(2): 415-430

Nagafuchi S, Yanagisawa H, Ohsaki E, Shirayama T, Tadokoro K, Inoue T, Yamada M (1994a) Structure and expression of the gene responsible for the triplet repeat disorder, dentatorubral and pallidoluysian atrophy (DRPLA). *Nat Genet* 8(2): 177-182

Nagaoka U, Kim K, Jana NR, Doi H, Maruyama M, Mitsui K, Oyama F, Nukina N (2004) Increased expression of p62 in expanded polyglutamine-expressing cells and its association with polyglutamine inclusions. *J Neurochem* 91(1): 57-68

Naito H, Oyanagi S (1982) Familial myoclonus epilepsy and choreoathetosis: hereditary dentatorubral-pallidoluysian atrophy. *Neurology* 32(8): 798-807

Nisoli I, Chauvin JP, Napoletano F, Calamita P, Zanin V, Fanto M, Charroux B (2010) Neurodegeneration by polyglutamine Atrophin is not rescued by induction of autophagy. *Cell Death Differ*

Nucifora FC, Jr., Ellerby LM, Wellington CL, Wood JD, Herring WJ, Sawa A, Hayden MR, Dawson VL, Dawson TM, Ross CA (2003) Nuclear localization of a non-caspase truncation product of atrophin-1, with an expanded polyglutamine repeat, increases cellular toxicity. *J Biol Chem* 278(15): 13047-13055

Okamura-Oho Y, Miyashita T, Nagao K, Shima S, Ogata Y, Katada T, Nishina H, Yamada M (2003) Dentatorubral-pallidoluysian atrophy protein is phosphorylated by c-Jun NH2-terminal kinase. *Hum Mol Genet* 12(13): 1535-1542

Pandey UB, Nie Z, Batlevi Y, McCray BA, Ritson GP, Nedelsky NB, Schwartz SL, DiProspero NA, Knight MA, Schuldiner O, Padmanabhan R, Hild M, Berry DL, Garza D, Hubbert CC, Yao TP, Baehrecke EH, Taylor JP (2007) HDAC6 rescues neurodegeneration and provides an essential link between autophagy and the UPS. *Nature* 447(7146): 859-863

Pankiv S, Clausen TH, Lamark T, Brech A, Bruun JA, Outzen H, Overvatn A, Bjorkoy G, Johansen T (2007) p62/SQSTM1 binds directly to Atg8/LC3 to facilitate degradation of ubiquitinated protein aggregates by autophagy. *J Biol Chem* 282(33): 24131-24145

Pankratz MJ, Busch M, Hoch M, Seifert E, Jackle H (1992) Spatial control of the gap gene knirps in the Drosophila embryo by posterior morphogen system. *Science* 255(5047): 986-989

Pantalacci S, Tapon N, Leopold P (2003) The Salvador partner Hippo promotes apoptosis and cell-cycle exit in Drosophila. *Nat Cell Biol* 5(10): 921-927

Papandreou I, Lim AL, Laderoute K, Denko NC (2008) Hypoxia signals autophagy in tumor cells via AMPK activity, independent of HIF-1, BNIP3, and BNIP3L. *Cell Death Differ* 15(10): 1572-1581

Pattingre S, Bauvy C, Codogno P (2003) Amino acids interfere with the ERK1/2-dependent control of macroautophagy by controlling the activation of Raf-1 in human colon cancer HT-29 cells. *J Biol Chem* 278(19): 16667-16674

Pellikka M, Tanentzapf G, Pinto M, Smith C, McGlade CJ, Ready DF, Tepass U (2002) Crumbs, the Drosophila homologue of human CRB1/RP12, is essential for photoreceptor morphogenesis. *Nature* 416(6877): 143-149

Pellock BJ, Buff E, White K, Hariharan IK (2007) The Drosophila tumor suppressors Expanded and Merlin differentially regulate cell cycle exit, apoptosis, and Wingless signaling. *Dev Biol* 304(1): 102-115

Peng HW, Slattery M, Mann RS (2009) Transcription factor choice in the Hippo signaling pathway: homothorax and yorkie regulation of the microRNA bantam in the progenitor domain of the Drosophila eye imaginal disc. *Genes Dev* 23(19): 2307-2319

Pennuto M, Palazzolo I, Poletti A (2009) Post-translational modifications of expanded polyglutamine proteins: impact on neurotoxicity. *Hum Mol Genet* 18(R1): R40-47

Peters MF, Nucifora FC, Jr., Kushi J, Seaman HC, Cooper JK, Herring WJ, Dawson VL, Dawson TM, Ross CA (1999) Nuclear targeting of mutant Huntingtin increases toxicity. *Mol Cell Neurosci* 14(2): 121-128

Pirrotta V (1988) Vectors for P-mediated transformation in Drosophila. *Biotechnology* 10: 437-456

Pirrotta V, Steller H, Bozzetti MP (1985) Multiple upstream regulatory elements control the expression of the Drosophila white gene. *EMBO J* 4(13A): 3501-3508

Plaster N, Sonntag C, Schilling TF, Hammerschmidt M (2007) REREa/Atrophin-2 interacts with histone deacetylase and Fgf8 signaling to regulate multiple processes of zebrafish development. *Dev Dyn* 236(7): 1891-1904

Polesello C, Huelsmann S, Brown NH, Tapon N (2006) The Drosophila RASSF homolog antagonizes the hippo pathway. *Curr Biol* 16(24): 2459-2465

Potter CJ, Huang H, Xu T (2001) Drosophila Tsc1 functions with Tsc2 to antagonize insulin signaling in regulating cell growth, cell proliferation, and organ size. *Cell* 105(3): 357-368

Ravikumar B, Duden R, Rubinsztein DC (2002) Aggregate-prone proteins with polyglutamine and polyalanine expansions are degraded by autophagy. *Hum Mol Genet* 11(9): 1107-1117

Ravikumar B, Vacher C, Berger Z, Davies JE, Luo S, Oroz LG, Scaravilli F, Easton DF, Duden R, O'Kane CJ, Rubinsztein DC (2004) Inhibition of mTOR induces autophagy and reduces toxicity of polyglutamine expansions in fly and mouse models of Huntington disease. *Nat Genet* 36(6): 585-595

Rawls AS, Guinto JB, Wolff T (2002) The cadherins fat and dachsous regulate dorsal/ventral signaling in the Drosophila eye. *Curr Biol* 12(12): 1021-1026

Reddy BV, Irvine KD (2008) The Fat and Warts signaling pathways: new insights into their regulation, mechanism and conservation. *Development* 135(17): 2827-2838

Reggiori F, Shintani T, Nair U, Klionsky DJ (2005) Atg9 cycles between mitochondria and the pre-autophagosomal structure in yeasts. *Autophagy* 1(2): 101-109

Reiter LT, Potocki L, Chien S, Gribskov M, Bier E (2001) A systematic analysis of human disease-associated gene sequences in Drosophila melanogaster. *Genome Res* 11(6): 1114-1125

Riley BE, Orr HT (2006) Polyglutamine neurodegenerative diseases and regulation of transcription: assembling the puzzle. *Genes Dev* 20(16): 2183-2192

Rock R, Schrauth S, Gessler M (2005) Expression of mouse dchs1, fjx1, and fat-j suggests conservation of the planar cell polarity pathway identified in Drosophila. *Dev Dyn* 234(3): 747-755

Rogina B, Benzer S, Helfand SL (1997) Drosophila drop-dead mutations accelerate the time course of age-related markers. *Proc Natl Acad Sci U S A* 94(12): 6303-6306

Rogulja D, Rauskolb C, Irvine KD (2008) Morphogen control of wing growth through the Fat signaling pathway. *Dev Cell* 15(2): 309-321

Rong YS, Golic KG (2000) Gene targeting by homologous recombination in Drosophila. *Science* 288(5473): 2013-2018

Ross CA (1995) When more is less: pathogenesis of glutamine repeat neurodegenerative diseases. *Neuron* 15(3): 493-496

Rubinsztein DC (2006) The roles of intracellular protein-degradation pathways in neurodegeneration. *Nature* 443(7113): 780-786

Rubinsztein DC, Gestwicki JE, Murphy LO, Klionsky DJ (2007) Potential therapeutic applications of autophagy. *Nat Rev Drug Discov* 6(4): 304-312

Rusten TE, Lindmo K, Juhasz G, Sass M, Seglen PO, Brech A, Stenmark H (2004) Programmed autophagy in the Drosophila fat body is induced by ecdysone through regulation of the PI3K pathway. *Dev Cell* 7(2): 179-192

Saburi S, Hester I, Fischer E, Pontoglio M, Eremina V, Gessler M, Quaggin SE, Harrison R, Mount R, McNeill H (2008) Loss of Fat4 disrupts PCP signaling and oriented cell division and leads to cystic kidney disease. *Nat Genet* 40(8): 1010-1015

Saburi S, McNeill H (2005) Organising cells into tissues: new roles for cell adhesion molecules in planar cell polarity. *Curr Opin Cell Biol* 17(5): 482-488

Sanchez-Garcia I, Rabbitts TH (1994) The LIM domain: a new structural motif found in zinc-finger-like proteins. *Trends Genet* 10(9): 315-320

Sarkar S, Krishna G, Imarisio S, Saiki S, O'Kane CJ, Rubinsztein DC (2008) A rational mechanism for combination treatment of Huntington's disease using lithium and rapamycin. *Hum Mol Genet* 17(2): 170-178

Saudou F, Finkbeiner S, Devys D, Greenberg ME (1998) Huntingtin acts in the nucleus to induce apoptosis but death does not correlate with the formation of intranuclear inclusions. *Cell* 95(1): 55-66

Schilling G, Wood JD, Duan K, Slunt HH, Gonzales V, Yamada M, Cooper JK, Margolis RL, Jenkins NA, Copeland NG, Takahashi H, Tsuji S, Price DL, Borchelt DR, Ross CA (1999) Nuclear accumulation of truncated atrophin-1 fragments in a transgenic mouse model of DRPLA. *Neuron* 24(1): 275-286

Schweitzer R, Shilo BZ (1997) A thousand and one roles for the Drosophila EGF receptor. *Trends Genet* 13(5): 191-196

Scott JA, Yap AS (2006) Cinderella no longer: alpha-catenin steps out of cadherin's shadow. *J Cell Sci* 119(Pt 22): 4599-4605

Scott RC, Juhasz G, Neufeld TP (2007) Direct induction of autophagy by Atg1 inhibits cell growth and induces apoptotic cell death. *Curr Biol* 17(1): 1-11

Scott RC, Schuldiner O, Neufeld TP (2004) Role and regulation of starvation-induced autophagy in the Drosophila fat body. *Dev Cell* 7(2): 167-178

Settembre C, Fraldi A, Rubinsztein DC, Ballabio A (2008) Lysosomal storage diseases as disorders of autophagy. *Autophagy* 4(1): 113-114

Shen Y, Lee G, Choe Y, Zoltewicz JS, Peterson AS (2007) Functional architecture of atrophins. *J Biol Chem* 282(7): 5037-5044

Shilo BZ (2003) Signaling by the Drosophila epidermal growth factor receptor pathway during development. *Exp Cell Res* 284(1): 140-149

Shintani T, Klionsky DJ (2004) Autophagy in health and disease: a double-edged sword. *Science* 306(5698): 990-995

Silva E, Tsatskis Y, Gardano L, Tapon N, McNeill H (2006) The tumor-suppressor gene fat controls tissue growth upstream of expanded in the hippo signaling pathway. *Curr Biol* 16(21): 2081-2089

Simmonds AJ, Liu X, Soanes KH, Krause HM, Irvine KD, Bell JB (1998) Molecular interactions between Vestigial and Scalloped promote wing formation in Drosophila. *Genes Dev* 12(24): 3815-3820

Simon MA (2004) Planar cell polarity in the Drosophila eye is directed by graded Four-jointed and Dachsous expression. *Development* 131(24): 6175-6184

Simons M, Mlodzik M (2008) Planar cell polarity signaling: from fly development to human disease. *Annu Rev Genet* 42: 517-540

Sisodia SS (1998) Nuclear inclusions in glutamine repeat disorders: are they pernicious, coincidental, or beneficial? *Cell* 95(1): 1-4

Sopko R, McNeill H (2009b) The skinny on Fat: an enormous cadherin that regulates cell adhesion, tissue growth, and planar cell polarity. *Curr Opin Cell Biol* 21(5): 717-723

Sopko R, Silva E, Clayton L, Gardano L, Barrios-Rodiles M, Wrana J, Varelas X, Arbouzova NI, Shaw S, Saburi S, Matakatsu H, Blair S, McNeill H (2009a) Phosphorylation of the tumor suppressor fat is regulated by its ligand Dachsous and the kinase discs overgrown. *Curr Biol* 19(13): 1112-1117

Strano S, Monti O, Pediconi N, Baccarini A, Fontemaggi G, Lapi E, Mantovani F, Damalas A, Citro G, Sacchi A, Del Sal G, Levrero M, Blandino G (2005) The transcriptional coactivator Yes-associated protein drives p73 gene-target specificity in response to DNA Damage. *Mol Cell* 18(4): 447-459

Strutt H, Mundy J, Hofstra K, Strutt D (2004) Cleavage and secretion is not required for Four-jointed function in Drosophila patterning. *Development* 131(4): 881-890

Strutt H, Strutt D (2005) Long-range coordination of planar polarity in Drosophila. *Bioessays* 27(12): 1218-1227

Suzuki K, Kirisako T, Kamada Y, Mizushima N, Noda T, Ohsumi Y (2001) The pre-autophagosomal structure organized by concerted functions of APG genes is essential for autophagosome formation. *EMBO J* 20(21): 5971-5981

Suzuki K, Kubota Y, Sekito T, Ohsumi Y (2007a) Hierarchy of Atg proteins in pre-autophagosomal structure organization. *Genes Cells* 12(2): 209-218

Tamura T, Sone M, Yamashita M, Wanker EE, Okazawa H (2009) Glial cell lineage expression of mutant ataxin-1 and huntingtin induces developmental and late-onset neuronal pathologies in Drosophila models. *PLoS One* 4(1): e4262

Tanida I, Minematsu-Ikeguchi N, Ueno T, Kominami E (2005) Lysosomal turnover, but not a cellular level, of endogenous LC3 is a marker for autophagy. *Autophagy* 1(2): 84-91

Tanoue T, Takeichi M (2005) New insights into Fat cadherins. *J Cell Sci* 118(Pt 11): 2347-2353

Tapon N, Harvey KF, Bell DW, Wahrer DC, Schiripo TA, Haber DA, Hariharan IK (2002) salvador Promotes both cell cycle exit and apoptosis in Drosophila and is mutated in human cancer cell lines. *Cell* 110(4): 467-478

Tapon N, Ito N, Dickson BJ, Treisman JE, Hariharan IK (2001) The Drosophila tuberous sclerosis complex gene homologs restrict cell growth and cell proliferation. *Cell* 105(3): 345-355

Tepass U, Gruszynski-DeFeo E, Haag TA, Omatyar L, Torok T, Hartenstein V (1996) shotgun encodes Drosophila E-cadherin and is preferentially required during cell rearrangement in the neurectoderm and other morphogenetically active epithelia. *Genes Dev* 10(6): 672-685

Tepass U, Truong K, Godt D, Ikura M, Peifer M (2000) Cadherins in embryonic and neural morphogenesis. *Nat Rev Mol Cell Biol* 1(2): 91-100

Teter SA, Eggerton KP, Scott SV, Kim J, Fischer AM, Klionsky DJ (2001) Degradation of lipid vesicles in the yeast vacuole requires function of Cvt17, a putative lipase. *J Biol Chem* 276(3): 2083-2087

Thompson BJ, Cohen SM (2006) The Hippo pathway regulates the bantam microRNA to control cell proliferation and apoptosis in Drosophila. *Cell* 126(4): 767-774

Thoreen CC, Kang SA, Chang JW, Liu Q, Zhang J, Gao Y, Reichling LJ, Sim T, Sabatini DM, Gray NS (2009) An ATP-competitive mammalian target of rapamycin inhibitor reveals rapamycin-resistant functions of mTORC1. *J Biol Chem* 284(12): 8023-8032

Tomlinson A (1988) Cellular interactions in the developing Drosophila eye. *Development* 104(2): 183-193

Tyner SD, Venkatachalam S, Choi J, Jones S, Ghebranious N, Igelmann H, Lu X, Soron G, Cooper B, Brayton C, Hee Park S, Thompson T, Karsenty G, Bradley A, Donehower LA (2002) p53 mutant mice that display early ageing-associated phenotypes. *Nature* 415(6867): 45-53

Udan RS, Kango-Singh M, Nolo R, Tao C, Halder G (2003) Hippo promotes proliferation arrest and apoptosis in the Salvador/Warts pathway. *Nat Cell Biol* 5(10): 914-920

Venkatachalam K, Long AA, Elsaesser R, Nikolaeva D, Broadie K, Montell C (2008) Motor deficit in a Drosophila model of mucolipidosis type IV due to defective clearance of apoptotic cells. *Cell* 135(5): 838-851

Venkatraman P, Wetzel R, Tanaka M, Nukina N, Goldberg AL (2004) Eukaryotic proteasomes cannot digest polyglutamine sequences and release them during degradation of polyglutamine-containing proteins. *Mol Cell* 14(1): 95-104

Wallingford JB (2004) Closing in on vertebrate planar polarity. *Nat Cell Biol* 6(8): 687-689

Wang L, Rajan H, Pitman JL, McKeown M, Tsai CC (2006) Histone deacetylase-associating Atrophin proteins are nuclear receptor corepressors. *Genes Dev* 20(5): 525-530

Wang RC, Levine B (2010) Autophagy in cellular growth control. *FEBS Lett* 584(7): 1417-1426

Wei X, Shimizu T, Lai ZC (2007) Mob as tumor suppressor is activated by Hippo kinase for growth inhibition in Drosophila. *EMBO J* 26(7): 1772-1781

Willecke M, Hamaratoglu F, Sansores-Garcia L, Tao C, Halder G (2008) Boundaries of Dachsous Cadherin activity modulate the Hippo signaling pathway to induce cell proliferation. *Proc Natl Acad Sci U S A* 105(39): 14897-14902

Williams A, Jahreiss L, Sarkar S, Saiki S, Menzies FM, Ravikumar B, Rubinsztein DC (2006) Aggregate-prone proteins are cleared from the cytosol by autophagy: therapeutic implications. *Curr Top Dev Biol* 76: 89-101

Wong LL, Adler PN (1993) Tissue polarity genes of Drosophila regulate the subcellular location for prehair initiation in pupal wing cells. *J Cell Biol* 123(1): 209-221

Wu S, Huang J, Dong J, Pan D (2003) hippo encodes a Ste-20 family protein kinase that restricts cell proliferation and promotes apoptosis in conjunction with salvador and warts. *Cell* 114(4): 445-456

Wullschleger S, Loewith R, Hall MN (2006) TOR signaling in growth and metabolism. *Cell* 124(3): 471-484

Xu T, Rubin GM (1993) Analysis of genetic mosaics in developing and adult Drosophila tissues. *Development* 117(4): 1223-1237

Xu T, Wang W, Zhang S, Stewart RA, Yu W (1995) Identifying tumor suppressors in genetic mosaics: the Drosophila lats gene encodes a putative protein kinase. *Development* 121(4): 1053-1063

Yagi T, Takeichi M (2000) Cadherin superfamily genes: functions, genomic organization, and neurologic diversity. *Genes Dev* 14(10): 1169-1180

Yanagisawa H, Bundo M, Miyashita T, Okamura-Oho Y, Tadokoro K, Tokunaga K, Yamada M (2000) Protein binding of a DRPLA family through arginine-glutamic acid dipeptide repeats is enhanced by extended polyglutamine. *Hum Mol Genet* 9(9): 1433-1442

Yang CH, Axelrod JD, Simon MA (2002) Regulation of Frizzled by fat-like cadherins during planar polarity signaling in the Drosophila compound eye. *Cell* 108(5): 675-688

Yang Z, Klionsky DJ (2009) An overview of the molecular mechanism of autophagy. *Curr Top Microbiol Immunol* 335: 1-32

Yazawa I, Nukina N, Hashida H, Goto J, Yamada M, Kanazawa I (1995) Abnormal gene product identified in hereditary dentatorubral-pallidoluysian atrophy (DRPLA) brain. *Nat Genet* 10(1): 99-103

Yorimitsu T, Nair U, Yang Z, Klionsky DJ (2006) Endoplasmic reticulum stress triggers autophagy. *J Biol Chem* 281(40): 30299-30304

Yoshida C, Takeichi M (1982) Teratocarcinoma cell adhesion: identification of a cell-surface protein involved in calcium-dependent cell aggregation. *Cell* 28(2): 217-224

Yu J, Zheng Y, Dong J, Klusza S, Deng WM, Pan D (2010) Kibra functions as a tumor suppressor protein that regulates Hippo signaling in conjunction with Merlin and Expanded. *Dev Cell* 18(2): 288-299

Yu J, Poulton J, Huang YC, Deng WM (2008) The hippo pathway promotes Notch signaling in regulation of cell differentiation, proliferation, and oocyte polarity. *PLoS One* 3(3): e1761

Yu RT, McKeown M, Evans RM, Umesono K (1994) Relationship between Drosophila gap gene tailless and a vertebrate nuclear receptor Tlx. *Nature* 370(6488): 375-379

Zatloukal K, Stumptner C, Fuchsbichler A, Heid H, Schnoelzer M, Kenner L, Kleinert R, Prinz M, Aguzzi A, Denk H (2002) p62 Is a common component of cytoplasmic inclusions in protein aggregation diseases. *Am J Pathol* 160(1): 255-263

Zeidler MP, Perrimon N, Strutt DI (1999) The four-jointed gene is required in the Drosophila eye for ommatidial polarity specification. *Curr Biol* 9(23): 1363-1372

Zeng X, Kinsella TJ (2008) Mammalian target of rapamycin and S6 kinase 1 positively regulate 6-thioguanine-induced autophagy. *Cancer Res* 68(7): 2384-2390

Zhang S, Xu L, Lee J, Xu T (2002) Drosophila atrophin homolog functions as a transcriptional corepressor in multiple developmental processes. *Cell* 108(1): 45-56

Zhao B, Lei QY, Guan KL (2008) The Hippo-YAP pathway: new connections between regulation of organ size and cancer. *Curr Opin Cell Biol* 20(6): 638-646

Zhao B, Wei X, Li W, Udan RS, Yang Q, Kim J, Xie J, Ikenoue T, Yu J, Li L, Zheng P, Ye K, Chinnaiyan A, Halder G, Lai ZC, Guan KL (2007) Inactivation of YAP oncoprotein by the Hippo pathway is involved in cell contact inhibition and tissue growth control. *Genes Dev* 21(21): 2747-2761

Zoghbi HY, Botas J (2002) Mouse and fly models of neurodegeneration. *Trends Genet* 18(9): 463-471

Zoltewicz JS, Stewart NJ, Leung R, Peterson AS (2004) Atrophin 2 recruits histone deacetylase and is required for the function of multiple signaling centers during mouse embryogenesis. *Development* 131(1): 3-14